GEOELECTRIC STUDIES OF THE CRUST AND UPPER MANTLE IN NORTHERN SCOTLAND

By

Ebong Willie Mbipom

Thesis presented for the degree of

Doctor of Philosophy of the

University of Edinburgh in the Faculty of Science

1980

DECLARATION

I hereby declare that the work presented in this thesis is my own unless otherwise stated in the text and that the thesis has been composed by myself.

Ebong Willie Mbipom

ABSTRACT

A brief review of regional geoelectric studies around the North Atlantic is given. The theoretical basis for both magneto-telluric (MT) and geomagnetic deep sounding (GDS) methods are discussed and modelling procedures for one-, two- and three-dimensional Earth structures are reviewed. A description of the diakoptic program for two-dimensional induction studies (Brewitt--Taylor and Johns, 1977) and its use in the geoelectric modelling in this study are given.

The digital recording system used is described and the fieldwork logistics adopted are also presented.

Measurements of five components of MT field variations in the period band 10 - 1200s have been made at twenty sites across the Moine Thrust and the Great Glen along a NW-SE traverse in Northern Scotland. Three of the sites lay along the length of the Glen.

By means of power spectral and standard two-dimensional MT analysis techniques, Earth response parameters have been obtained for the region.

Apart from the complex geology and tectonic history of the region, the adjacent seas have a considerable effect on the induction parameters in Northern Scotland. Using experimental data from sites on the Lewisian Foreland and numerical modelling, a method has been found for minimising coast effects on interpreted geoelectric structure.

The first two-dimensional geoelectric model for the crust and the upper mantle across Northern Scotland is presented. The model is complex but agrees well with surface geology.

Zones of large resistive bodies which extend to 10-20 km in

the geoelectric model correlate well with known granitic bodies in the region. On the shield fragment, a depth of 30 km found for the geoelectric interface also agrees with the depth to the Moho from seismic refraction studies.

There are significant lateral variations in the conductivity structure along the Great Glen around which both the crust and upper mantle are conducting.

Under the metamorphic zone, the lower crust and the uppermost mantle are conducting. Hydrated rocks and partial melting are the likely cause of the low resistivities of 50-500 ohm m detected below the upper crust.

The good conductor in the Great Glen and the widespread resistive zones of large granitic bodies north of the Highland Boundary Fault may be related to the past tectonic activities in Northern Scotland. The region merits further study and various suggestions for such work are given.

ACKNOWLEDGEMENTS

I thank my supervisor, Dr. R. Hutton who made me interested in solid Earth problems in Nigeria and also suggested the project in Northern Scotland. Her advice, encouragement and hospitality to me and my wife were very invaluable. I am also grateful to Dr. D. Rooney, her former research student who helped me during the execution of the first phase of the fieldwork in 1977.

My gratitude also goes to the Federal Government of Nigeria for a postgraduate scholarship and to the Department of Geophysics for study and research facilities.

I thank Mr. G. Dawes for computing advice and especially for cassette data processing programs. My thanks also go to Drs. C. Brewitt-Taylor, J. Sik, B. Hobbs, D. Summers and J. Weaver for various discussions and reprints on different aspects of induction studies. I am particularly indebted to Dr. Brewitt-Taylor for his two-dimensional modelling program.

Mrss. D. McKirdy and M. Ingham, my colleagues are also thanked for various discussions and good companionship in our office and in the field. The technical help and support from Mrss. I. McDonald and A. Jackson are gratefully acknowledged and I am also thankful to Mrs. J. Whan who typed the tables in this thesis. My thanks go too to various final year Geophysics undergraduates who helped during the fieldwork.

Discussions with Dr. M.R.W.Johnson and other geologists in the University Geology Department and in the I.G.S. Highland Unit are also gratefully acknowledged. I am also grateful to the staff of I.G.S. Geomagnetism Unit for data transcription done in their laboratory at the initial phase of this study.

I thank various landowners, factors and farmers on whose

fields the measurements were made. Their hospitality and friendliness are gratefully remembered.

I would also like to express my gratitude to our friends, Dr. and Mrs. D. Beamish who provided a home in Edinburgh for me and my family for a greater part of the study period.

Finally, my thanks go to my wife, Grace whose love and patience made the long absence for this study possible.

C O N T E N T S

	Page
INDEX OF FIGURES	1
LIST OF TABLES	5
CHAPTER 1. INTRODUCTION	6
1.1 Electromagnetic induction studies of the Earth	6
1.2 The resistivity of rocks	7
1.3 Results of some North Atlantic geoelectric studies	10
1.3.1 The Canadian Shield	12
1.3.2 Southern Scotland	16
1.3.3 Comparison with geoelectric models from other Precambrian regions	20
1.4 Previous induction studies in Northern Scotland	22
1.5 The geology and geophysical data for Northern Scotland	26
1.5.1 Geology	26
1.5.2 Some geophysical models for the region	28
1.6 The aim of the geoelectric study	32
CHAPTER 2. THEORY RELEVANT TO ELECTROMAGNETIC INDUCTION STUDIES	35
2.1 Electromagnetic wave propagation in the Earth	35
2.1.1 Maxwell's equations	37
2.2 Application to geoelectric studies	38
2.2.1 Cagniard apparent resistivity	38
2.2.2 Cagniard's assumptions	40
2.3 Theory for a two-dimensional Earth	42
2.3.1 Tensor relations and analysis	43

Page

2.4 The GDS method 48

2.4.1 The GDS transfer function 48

2.4.2 Bank's maximum and minimum responses 50

2.4.3 Hypothetical event contour plots 51

2.4.4 Hz/Hy amplitude ratios 52

2.5 Modelling and interpretation procedures 56

2.5.1 One-dimensional models 57

2.5.2 Two-dimensional models 60

2.5.3 The two-dimensional modelling program 61

2.5.4 Calculation of surface response functions 67

2.5.5 Some model results 70

2.5.6 Perturbation of regional two-dimensional conductivity structure by local inhomogeneities 74

2.6 Three-dimensional modelling 76

2.6.1 The choice of a three-dimensional numerical method 76

2.6.2 Analogue modelling 81

CHAPTER 3. MT FIELD MEASUREMENT 84

3.1 The MT instrument system

3.1.1 The magnetic field sensors 84

3.1.2 The electric field measurement 86

3.1.3 The recorders 87

3.2 Instrument system calibration 91

3.2.1 The telluric system 91

3.2.2 The magnetic system 92

3.3 Fieldwork logistics 93

3.3.1 Preparation 96

3.3.2 Data acquisition 97

Page

3.3.3 Data quantity and quality 99

3.3.4 Sites occupied 99

CHAPTER 4. DATA ANALYSIS 104

4.1 Data transcription 104

4.1.1 Event selection 106

4.2 Single event analysis 107

4.2.1 Spectral analysis 107

4.2.2 Precautions 111

4.2.3 Cross spectra and coherence analysis 113

4.2.4 Analysis program for single events 115

4.3 Mean response functions 117

4.3.1 The averaging program 117

4.3.2 Effect of sequential sampling 120

CHAPTER 5. RESULTS 122

5.1 Individual station results

5.1.1 The Lewisian Foreland 122

5.1.2 The Lairg region 127

5.1.3 The Great Glen region 134

5.1.4 Others 141

5.2 Regional results 147

5.2.1 Azimuth of the major impedance 147

5.2.2 Geoelectric pseudosections 153

5.2.3 Induction vector maps 156

5.2.4 Bank's GDS response functions 160

5.3 Qualitative conclusions from the results 160

CHAPTER 6. INTERPRETATION OF RESULTS 164

Page

6.1 General problems of geoelectric data interpretation 164

6.1.1 Source field effect 165

6.1.2 Complex geology 166

6.1.3 Surface distortion 169

6.1.4 Conductive channelling of induced currents 172

6.1.5 The effect of adjacent seas 174

6.1.6 Conclusions on the general problems of interpretation 182

6.2 GDS amplitude ratio profiles 185

6.3 Resistivity models for the crust and upper mantle

6.3.1 One-dimensional models 187

6.3.2 Two-dimensional model 190

6.3.3 An estimate of the bounds of acceptable models 197

6.4 Evidence from other geophysical models 200

CHAPTER 7. CONCLUSIONS AND SUGGESTIONS 206

7.1 Conclusion 206

7.2 Suggestions for future studies 207

APPENDIX 209

REFERENCES 212

INDEX OF FIGURES

Page

1.1 P-T diagram of the metamorphic facies and temperature curves in the Earth's crust. 9

1.2 North Atlantic terrains showing previous geoelectric study areas 13

1.3 Preferred resistivity-depth distribution in Wisconsin 15

1.4 Comparison of interpreted resistivity-depth profile for the lower crust in the Canadian shield with Brace's (1971) model 15

1.5 Resistivity model for the crust and upper mantle for Eastern Canada 17

1.6 GDS and MT sites and resistivity model for Southern Scotland 19

1.7 Comparison of crustal and upper mantle geoelectric models for different stable regions 21

1.8 Long period GDS measurement sites in Scotland 23

1.9 Results of previous GDS studies in Northern Scotland 25

1.10 A simplified geological map of Northern Scotland 29

1.11 LISPB profile and schematic cross-section through the crust and uppermost mantle of N.Britain 31

1.12 Heat flow values in Northern Scotland 33

2.1 a) Amplitudes of induction source field variations 36

b) Corresponding amplitudes of induced electric field

2.2 Coordinate axes 36

2.3 Rotated impedance tensor elements 46

2.4 Hypothetical event contour maps for Northern Scotland 53

2.5 Model Hz/Hy profile for a buried conducting prism 55

2.6 a) A three-layer resistivity model 58

b) Apparent resistivity phase master curves

Page

c) Apparent resistivity master curves

2.7 Scheme for two-dimensional modelling procedure 66

2.8 The grid for the two-dimensional modelling 66

2.9 Some two-dimensional model profiles

a) A buried conductor 71

b) A valley with a conductive infill 72

c) A resistive intrusion 73

2.10 Results of Haak's model calculations for 'preferred' directions of the electric field 75

2.11 Domains for three-dimensional modelling and the thin sheet model 78

2.12 General three-dimensional model results of Jones and Pascoe 79

2.13 Simplified analogue model map of the British Isles 82

3.1 A block diagram of the MT system 85

3.2 The N.E.R.C. Geologger 89

3.3 a) A block diagram for the telluric system calibration set-up 95

b) The response of the telluric system

3.4 a) A block diagram for the magnetic system calibration set-up 95

b) The response of the magnetic system

3.5 Replot of MT record sections 100

a) Night-time bay-type variation with Pi's

b) General variation with early morning Pc's

c) General variation in the afternoon

d) A noisy record

3.6 MT sites in Northern Scotland 101

4.1 Block diagram of the MT data editing and processing system 105

Page

4.2 Event time distribution 108

4.3 Data and corresponding spectral windows 110

a) The rectangular or box-car data window

b) The spectral window for the rectangular window

c) The cosine taper data window

d) The cosine taper spectral window

4.4 Scheme for single event analysis 116

4.5 Scheme for the averaging program 118

5.1 MT results for sites on the Lewisian Foreland 123

5.2 MT results for Lairg region 128

5.3 MT results for the Great Glen region 135

5.4 MT results for other sites 142

5.5 Maps of the azimuth of the major impedance 151

5.6 Geoelectric pseudo-sections 154

5.7 Induction vector maps 157

5.8 Bank's maximum response arrows 161

6.1 a) Latitudinal variations of the magnetic field components D, H and Z 167

b) Time variation of the ratio of the vertical to the horizontal field component for geomagnetic latitude relevant to N. Scotland 167

6.2 Results of impedance rotation analysis

a) Two-dimensional sites 170

b) Complex sites 171

6.3 Results of numerical model coast effect studies 176

a) Apparent resistivity

b) GDS amplitude ratio profile

6.4 a) MT response data for sites in the Foreland 178

b) One-dimensional resistivity models for the Foreland 178

Page

6.5 Two-dimensional GDS response for a buried conductor in an elongated island 180

6.6 A comparison of three-dimensional analogue model with two-dimensional numerical results 181

6.7 Comparison of two-dimensional numerical model with experimental data 183

6.8 GDS Hz/Hy amplitude ratio profiles across N.Scotland 186

6.9 Regional one-dimensional models for the crust and upper mantle 188

6.10 Two-dimensional resistivity model for Northern Scotland 191

6.11 Two-dimensional model responses and data compared for 95s 193

6.12 Two-dimensional model responses and data compared for 819s 195

6.13 Resistivity as a function of temperature for samples of granitic rocks and the range for the Scottish lower crust resistivity 201

6.14 Geoelectric and seismic upper mantle structures around the Great Glen 204

LIST OF TABLES

	Page
1.1 Generalised resistivity ranges for rocks of different lithology and age	11
2.1 Some two-dimensional numerical modelling studies	62
3.1 Helmholtz coils response	94
3.2 Scaling factors and -3db points for the MT system response	94
3.3 1977 - 78 MT sites	102
5.1 Summarised results of single station analysis	148
6.1 Bounds of acceptable models	198

CHAPTER 1

INTRODUCTION

1.1 Electromagnetic Induction Studies of the Earth

In the last few decades there has been increasing interest in the Earth's interior and its relationship to regional and large scale features of the Earth's surface. The magnetotelluric (MT) and the geomagnetic deep sounding (GDS) methods are two complementary electromagnetic induction techniques for studying the electrical conductivity structure of the Earth's crust and upper mantle.

Natural geomagnetic field variations of external origin are the primary source of the electric currents induced in the Earth. Such telluric currents were first detected as early as 1849 by Barlow. He observed irregular currents of much higher intensity than the artificial ones used for communication on English telegraph lines. Tikhonov (1950) in the U.S.S.R. seems to be one of the first workers to point out that geomagnetic field variations could be used for geoelectric studies of the Earth's interior.

For such studies, it is necessary to measure the three components of the magnetic field variations and two corresponding components of the induced electric field. One satisfactory technique of field measurements is described later in Chapter Three. By means of Maxwell's equations, inversion of the data and numerical modelling, as reviewed in Chapter Two, the conductivity structure in the region of interest can be obtained from the geoelectric data.

Geoelectric models can provide information on the deep geology and possible geothermal areas within the region. Studies of regional conductivity anomalies may also aid the reconstruction of the tectonic history of a region (Law and Riddihough, 1971).

1.2 The Resistivity of Rocks

A rock is an assemblage of minerals and its electrical properties will therefore depend on the constituent minerals, the interrelation between them as well as other factors like temperature, water content and pressure.

The resistivity of rocks in the upper few kilometers of the crust is controlled by the solution filling the pore spaces in the rocks except in areas where there are conducting minerals like graphites and magnetites. For water bearing rocks, the resistivity depends on the porosity, the amount of void space in the rock and the salinity of the fluid. The conduction is mainly electrolytic. An empirical formula known as Archie's law is often used to express the relation between ρ_t, the bulk resistivity of a rock, ρ_w, the resistivity of the pore fluid and S, the porosity expressed as a fraction per unit volume of the rock. The relation is given by

$$\rho_t = k\rho_w S^{-m}$$

where k and m are constants to be determined experimentally. The exponent m is usually between 1 and 2 from most observations (Keller and Frischknecht, 1966).

Below about 5 km, it is believed that most or all of the

cracks in the rock are closed due to overburden pressure. Pore fluid controlled conductivity should therefore become less significant in the lower crust at depths of 10 - 25 km. In a normal continental region with lower crustal temperatures below an upper limit of 600 - 700 deg.C, resistivities should be over 1000 ohm m (Berdichevsky et al, 1972). However, if water is present either in free state or as water of hydration in the constituent minerals in the lower crust, laboratory studies have shown that partial melting can occur at normal crustal temperatures. This gives rise to low resistivities. From laboratory studies on serpentinised peridotites (Zablocki, 1964) and serpentines (Berdichevsky et al, 1972) a tenfold increase in electrical conductivity has been shown to occur in the temperature range of 400 - 600 deg.C due to the release of water of hydration by the minerals. Berdichevsky et al also pointed out that under natural conditions of greater pressures, the increase in conductivity could be considerably greater. If hydrated minerals are present in the lower crust, low resistivities can therefore be expected.

The possibility of free water being present in the lower crust is much more problematic. Wyllie (1971) has postulated that an aqueous pore fluid could exist in equilibrium with any known crustal rock if conditions of pressure and temperature are suitable. In regions with past tectonic histories of down-going slabs of crustal materials, one can speculate that water saturated sediments carried down into the lower crust may partly account for some free water at depth. Geotherms for different rock types as function of depth in the Earth's crust are shown in Fig.1.1.

Near abnormal regions like tectonic plate margins and active

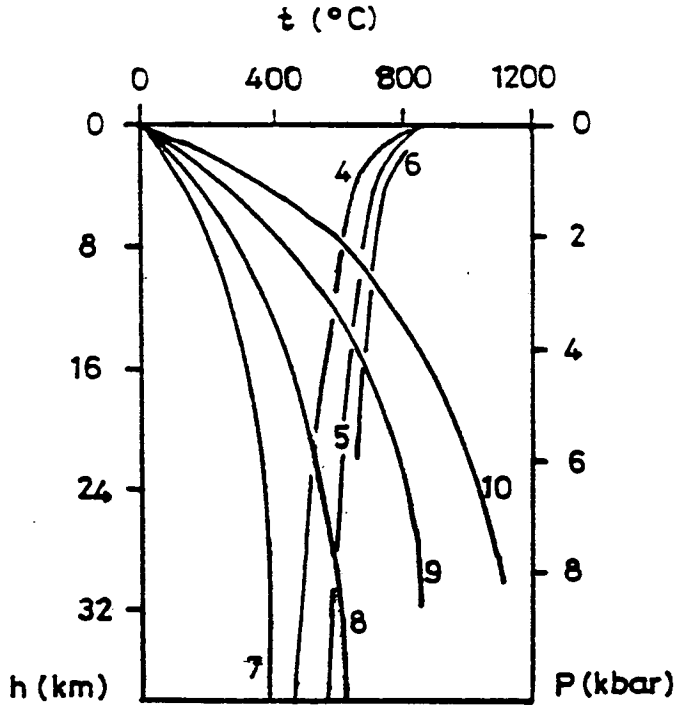

Fig.1.1 P-T diagram of the metamorphic facies and temperature curves in the Earth's crust.
Temperature of the beginning of melting of schists and granites : 4 - granites in the presence of water, 5 - schists, 6 - granites.
Temperature curves : 7 - shields and old platforms, 8 - Palaeozoic platforms, 9 - area of Mesozoic activation, 10 - eugeosynclines, island arcs and rifts.
(Berdichevsky et al, 1972).

zones of the Earth, the temperature of the crust may be considerably over 700 deg.C. A low resistivity in the crust will depend mostly on the temperature and the melt fraction of the crustal rocks (Stegena, 1976; Hutton, 1976; Stanley et al, 1977).

At mantle depths, high temperatures and partial melting of constituent rocks which are mostly of olivine composition (Ringwood, 1969; Kennedy and Higgins, 1972) are believed to be responsible for observed low resistivities in the upper mantle. At such depths, pressure effects on conductivity may also become considerably significant (Duba et al, 1974).

However, many of the published results of laboratory studies on the factors that affect conductivity of rocks and minerals need to be used with caution as laboratory conditions may not truly simulate the conditions prevailing in the Earth (Duba, 1976). Generalised resistivity ranges for rocks of different lithology and geological age are shown in Table1.1.

1.3 Results of Some North Atlantic Geoelectric Studies

The results of many regional induction studies of the crust and upper mantle around the world have been published in the last twenty years. Induction studies in stable shield areas (Kovtun, 1976) and in rifts and active zones (Hutton, 1976) are two excellent reviews on such studies. More recently, Fournier (1978) has tabulated the main results of published MT results from different countries and Singh (1978) has also discussed some of the conductivity anomalies in the lower crust and upper mantle from GDS studies. These reviews with the references therein are valuable sources of information on the techniques, results and data interpretation of induction studies that have been carried

Table 1.1

Generalised Resistivity Ranges for rocks of different lithology and age.

Age	Marine Sedimentary Rocks	Terrestial Sedimentary Rocks	Extrusive rocks (basalts, rhyolite)	Intrusive rocks (granite, gabbro)	Chemical precipitates (limestone, salt)
Quaternary and Tertiary (0 - 65 Ma)	1 - 10	15 - 50	10 - 200	500 - 2000	50 - 5000
Mesozoic (65 - 225 Ma)	5 - 20	25 - 100	20 - 500	500 - 2000	100 - 10,000
Carboniferous Paleozoic (225 - 395 Ma)	10 - 40	50 - 300	50 - 1000	1000 - 5000	200 - 100,000
Early Paleozoic (395 - 600 Ma)	40 - 200	100 - 500	100 - 2000	1000 - 5000	10,000 - 100,000
Precambrian (600 - 3000 Ma)	100 - 2000	300 - 5000	200 - 5000	5000 - 20,000	10,000 - 100,000

Resistivity in Ohm m; Keller and Frischknecht (1966).

out in different regions of the Earth.

In this section, results of geoelectric studies which have provided quantitative information for the conductivity structure of the crust and upper mantle in areas around the Northern Atlantic are reviewed. The regions studied are marked on the map in Fig.1.2 which also shows the most satisfactory computer aided reassembly of the continental land masses on the borders of the Northern Atlantic. It is hoped that this regional review will help to highlight the crustal and upper mantle geoelectric structures of Northern Atlantic terrains to which Northern Scotland belongs as well as the potentialities of electromagnetic induction method as an efficient tool for studying the tectonically-associated deep geology of continents.

1.3.1 The Canadian Shield

i) The Southern Extension

MT measurements in the period band 0.1 - 1000s were made at sixteen stations across the Precambrian region in Northern Wisconsin by Dowling (1970). Results from five stations labelled 1 to 4 and 10 in his paper were interpreted using one-dimensional models. From the models, the upper crust had a relatively high resistivity of 1000 - 10000 ohm m while there was a striking decrease in resistivity by an order of magnitude in the lower crust below about 12 km. Near the crust-mantle interface, the resistivity increased to values comparable to those of the upper crust. The resistivity models for Wisconsin are shown in Fig 1.3.

The MT models were compared with known seismic section for the area as shown in Fig.1.3. A close agreement between a 5.4 km/s velocity layer and the resistive upper crust and between the

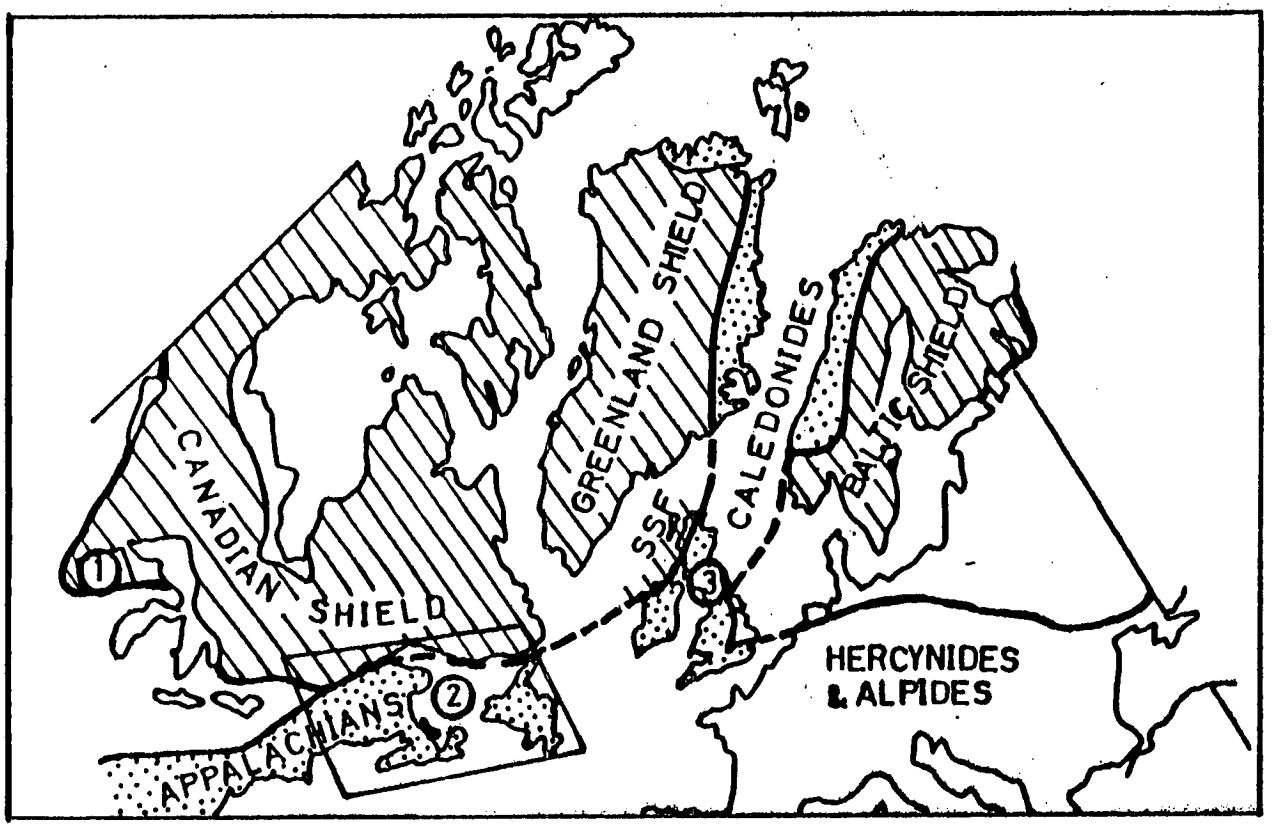

Fig.1.2 North Atlantic terrains (redrawn from Read and Watson, 1975) and showing previous geoelectric study areas. (SSF - Scottish Shield Fragment).
1 - Wisconsin
2 - E. Canada
3 - S. Scotland

conducting lower crust and a 6.51 km/s velocity layer that extended to the base of the crust was found at four of the five sites. This correlation gave support to a two layer crustal model and the difference in resistivity between the upper and lower crust was thought to be caused by a change in the composition of the constituent rocks.

Sternberg (1979) used direct current dipole-dipole and electromagnetic transient methods to study the crustal structure of the same area of the extension of the Canadian Shield. His best estimate of a four-layer resistivity structure for the area had the following features

a) A thin surface layer of glacial till of a few hundred ohm m resistivity.

b) A layer at a depth of 4.5 to 11 km with a resistivity in the range 3000 - 7000 ohm m which was thought to be compatible with the resistivities of wet crustal rocks.

c) a layer at the depth range 14 - 22 km with resistivities greater than 10^5 ohm m. These high resistivities were attributed to relatively dry rocks.

d) a lower crustal layer of resistivity in the range 50 - 1500 ohm m.

The low resistivities could not be explained by postulated models for the temperature and composition of the lower crust. A comparison of his resistivity-depth profile for the lower crust with Brace's (1971) model from a compilation of laboratory measurements is shown in Fig.1.4. In Brace's laboratory model, resistivity decreased at depths below about 25 km due to increased conduction at elevated temperature. Sternberg pointed out that as his model, below 15 - 20km, showed resistivities

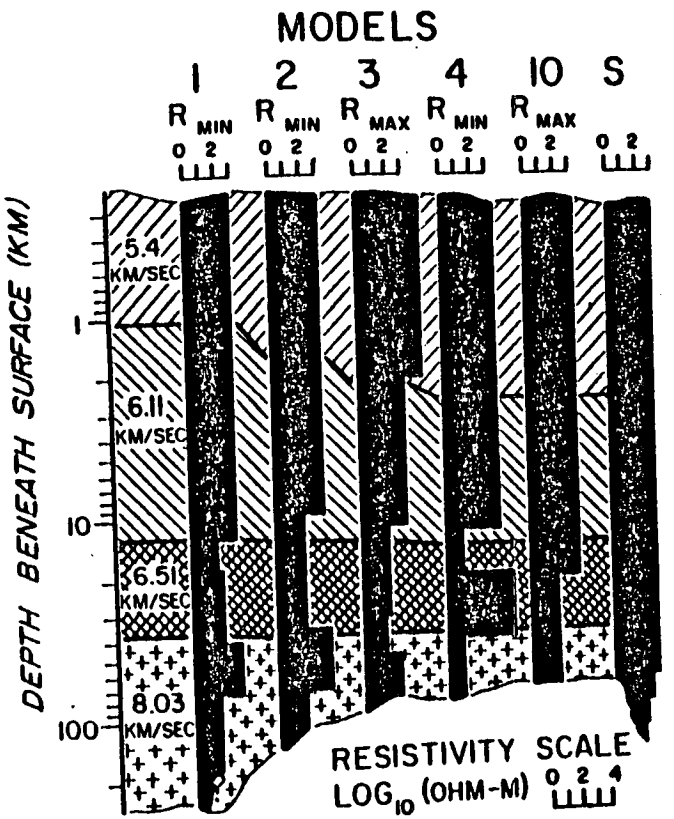

Fig.1.3 Preferred resistivity-depth distribution in Wisconsin.
S - postulated profile.
(Dowling, 1970).

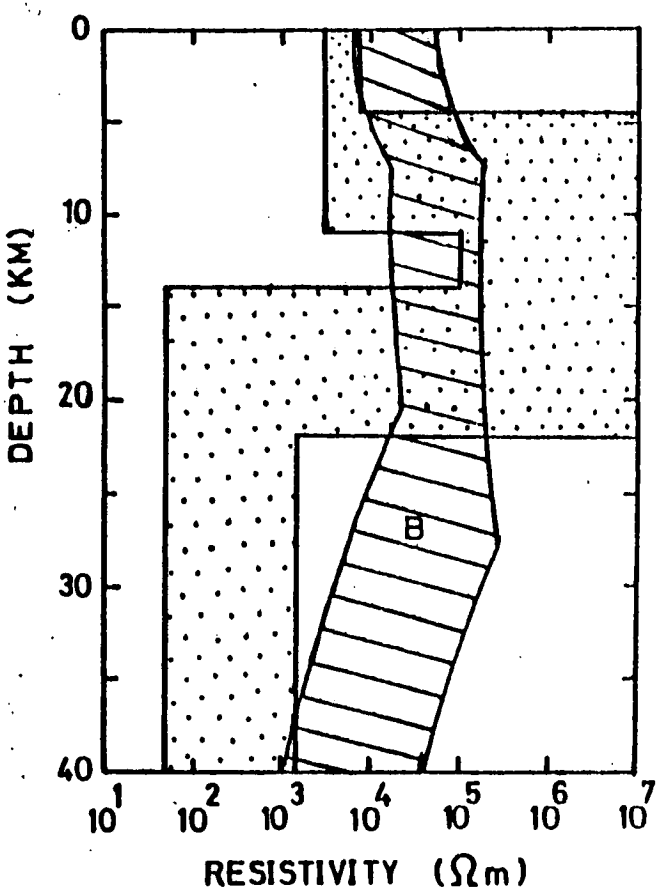

Fig.1.4 Comparison of interpreted resistivity-depth profile for the lower crust in the Canadian shield with Brace's (1971) model, B.
(Sternberg, 1979).

which were much lower than the laboratory based profile, models of the lower crust not based on temperature increase only were necessary in order to explain his observations. Rocks with water of hydration in the lower crust or temperatures higher than normal values for a stable shield were needed to explain his resistivity model.

ii) The Grenville Province of the Canadian Shield and the Appalachians

Kurtz and Garland (1976) made MT measurements in the period band 15 to 10000s at 16 sites in the region around the St. Lawrence River in Eastern Canada. The project sought to examine the conductivity structure of the Appalachian system to the south--east and the Grenville province of the Canadian Shield north--west of the St. Lawrence River.

A generalised resistivity cross-section in a NW-SE traverse across the two regions from their MT data is shown in Fig.1.5. The authors pointed out that in the shield, the lower crust was conducting while the upper crust was resistive. In the Appalachian region, the reverse was the case. They suggested that the location of the change in the geoelectric structure might be related to the line of closure of the proto-Atlantic ocean which was believed to exist in Atlantic Canada in Precambrian times. They also pointed out that hydrated rocks which were invoked to explain seismic results in the shield region could also explain their observation.

1.3.2 Southern Scotland

Jones and Hutton (1979a) made MT measurements similar to

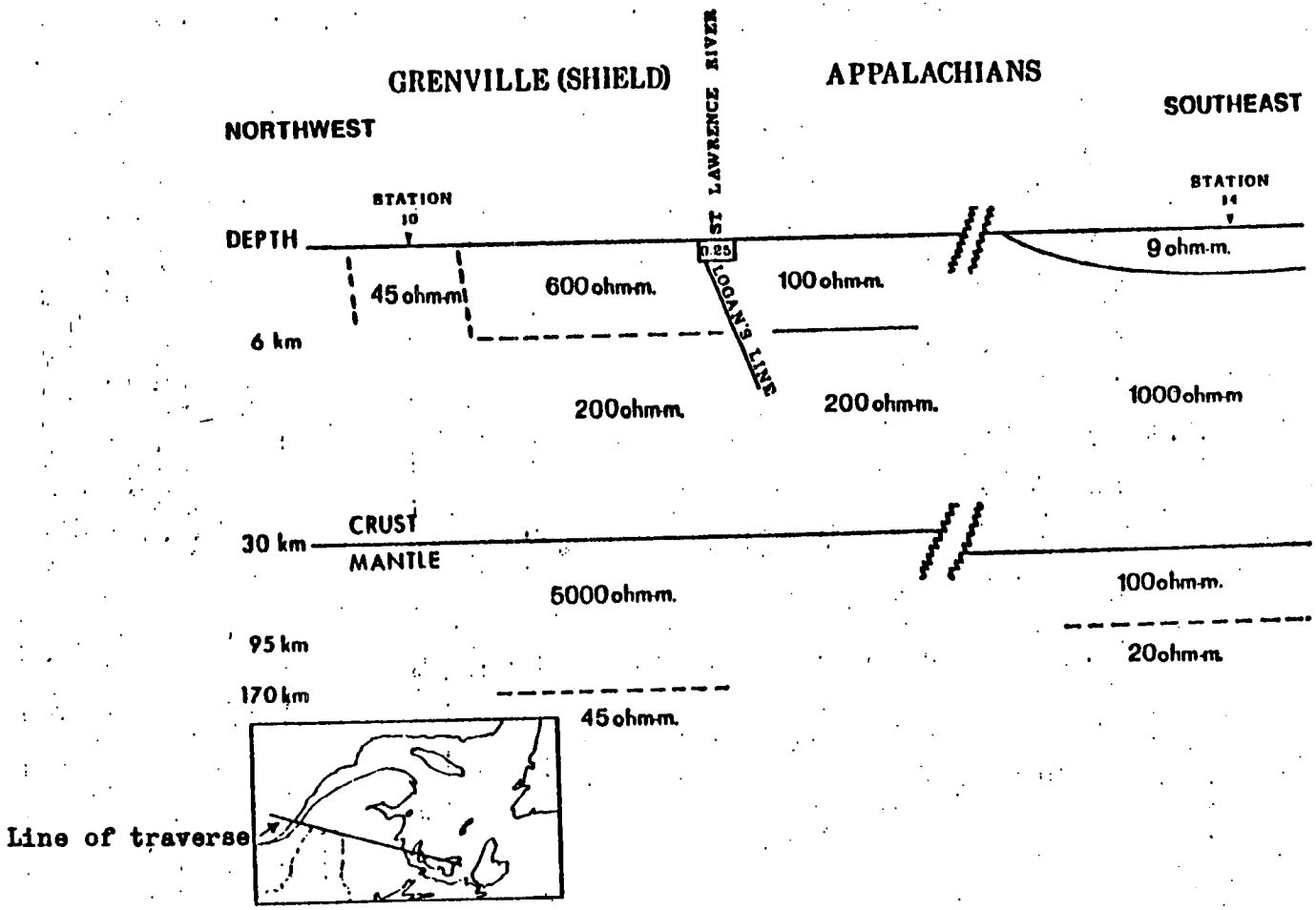

Fig.1.5 Resistivity model for the crust and upper mantle for Eastern Canada. (Kurtz and Garland, 1976)

those described later in Chapter Three at 13 locations in Southern Scotland along lines perpendicular and parallel to the strike of a major conductivity anomaly detected by GDS studies in the region (Osemeikan and Everett, 1968; Edwards et al, 1971; Bailey and Edwards, 1976; Hutton and Jones, 1978). The GDS and MT sites of Hutton and Jones (1978) are shown in Fig.1.6a.

Some of the main conclusions from their studies were as follows

a) North of the Southern Uplands Fault, there was a layer of conductivity in the range 0.02 - 0.05 S/m from a depth of about 10 to 45-65 km.

b) In the Southern Uplands, the whole of the crust was resistive and the upper mantle conducting to a depth of 40 - 70 km.

c) At one site, TOW, there was a very good conductor of conductivity about 0.5 S/m in the upper crust.

d) The marked lateral variation in electrical conductivity structure a few kilometers south of the Southern Uplands Fault occured in a region where the top of the 6.4 km/s seismic refractor dipped sharply and where there was a well-defined gravity low.

e) The GDS data located two narrow belts which separated the region into three zones. One belt was parallel to the Fault but slightly south of it and the other was near to the Scottish-English border and had an east-west strike. The three zones were the Midland Valley, the Southern Uplands and Northern England.

In order to interprete the MT data from six of the sites which were representative of the three zones delineated by the GDS studies, Jones and Hutton (1979b) developed a Monte-Carlo inversion procedure for one-dimensional modelling of the data. The geoelectric sections are shown in Fig.1.6b.

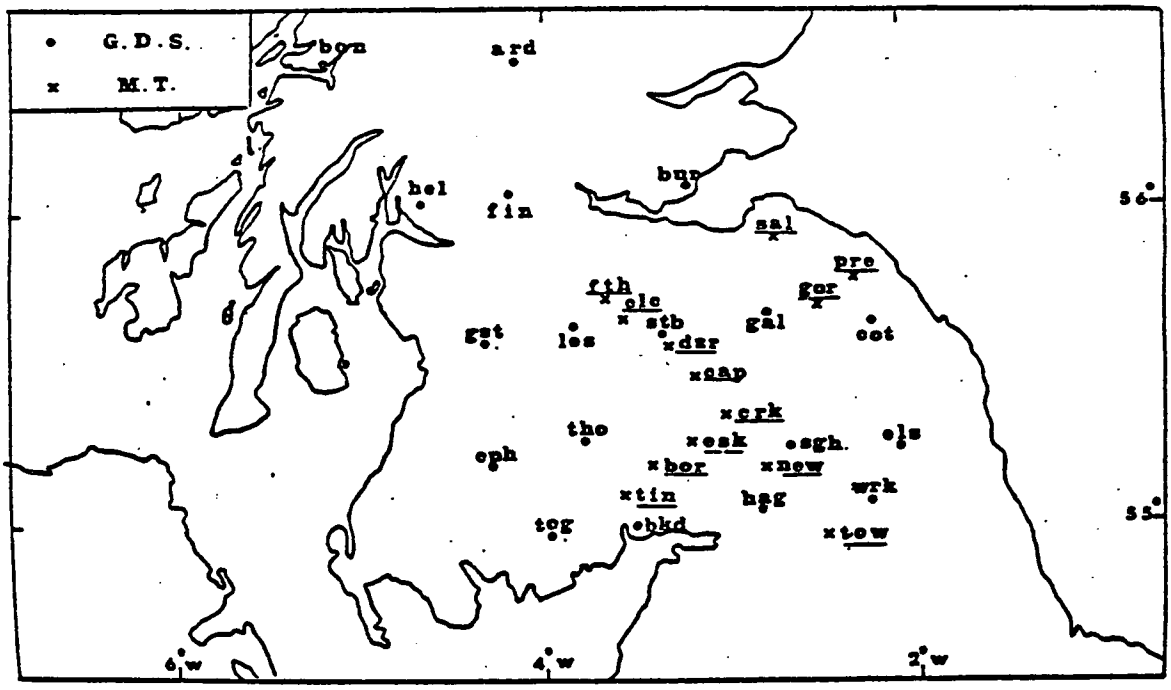

(a)

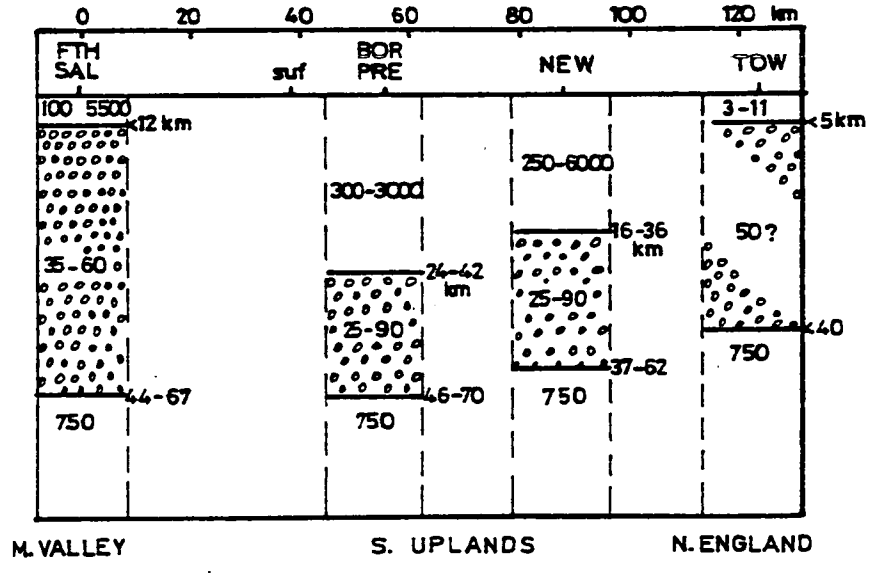

(b)

Fig.1.6 GDS and MT sites - (a) and resistivity model - (b) for Southern Scotland.

In the Midland Valley, the upper crust was resistive down to a depth of less than about 12 km while the lower crust had low resistivities between 35 and 60 ohm m.

In the Southern Uplands, the lower crust and the upper mantle were conducting.

Under Northern England, there was a high conducting zone near the surface which was attributed to conducting sediments in the Northumberland Basin.

The good conductor found in the lower crust and upper mantle was thought to be due to hydration and partial melting.

On comparing their geoelectric models with those of Eastern Canada (Kurtz and Garland, 1976) they found a strong correlation between the results for the shield region and the Midland Valley and between the Appalachian region and the Southern Uplands. They therefore suggested that the proto-Atlantic suture zone was represented by the Southern Uplands.

Ingham and Hutton (personal communication) are currently carrying out both MT and audio-magnetotelluric (AMT) studies in the region. These studies will provide a better resolution for the crustal structure and the lateral conductivity variation. Their preliminary two-dimensional results (Hutton et al, 1980) confirm the existence of a very good conductor under the Southern Uplands from a depth of about 24 to 90 km as reported by Jones and Hutton (1979a, b).

1.3.3 Comparison with Geoelectric Models from other Precambrian Regions

On both sides of the Atlantic Ocean, two major crust-mantle geoelectric structures can be identified from the results of

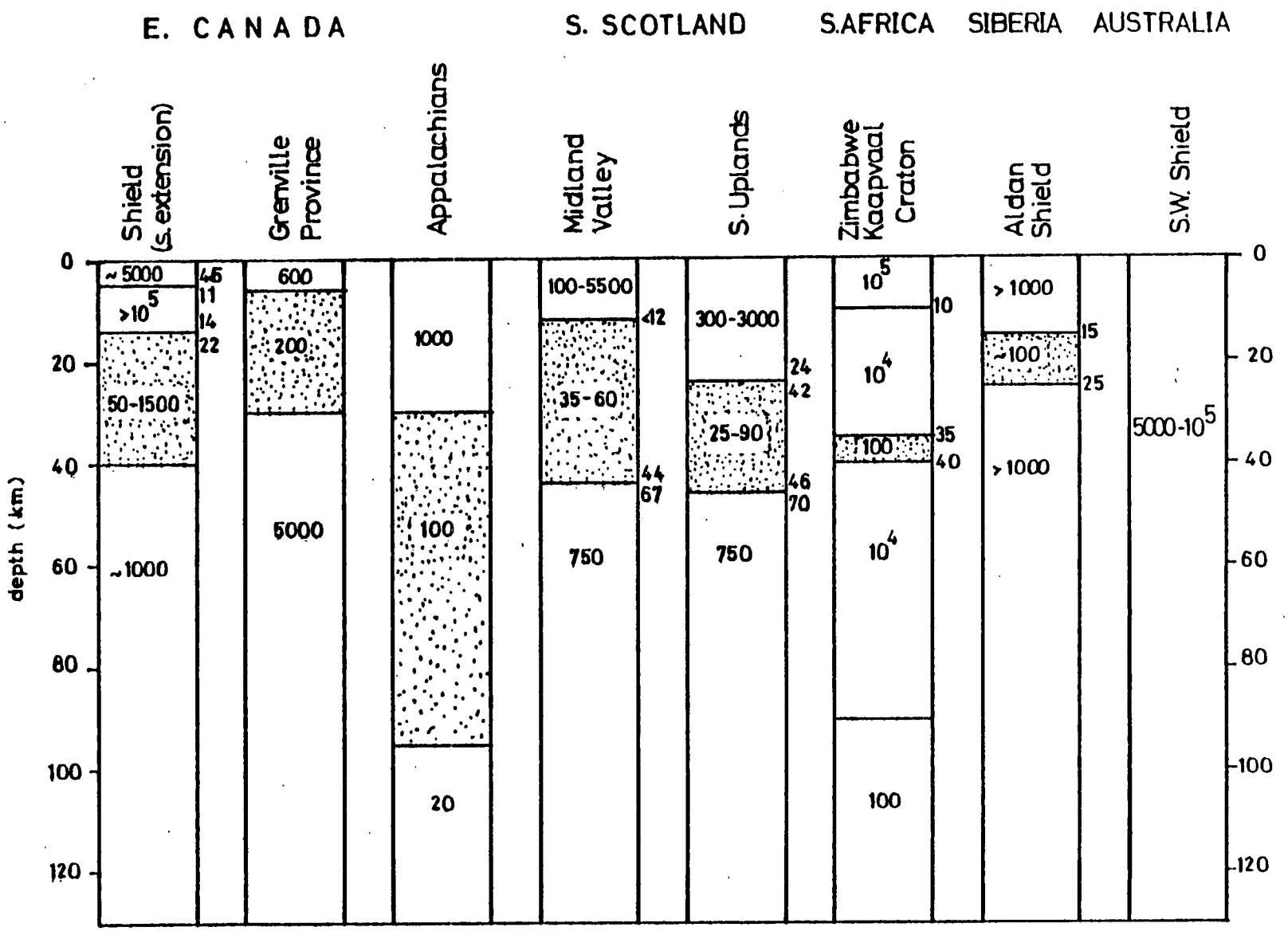

Fig.1.7 Comparison of crustal and upper mantle geoelectric models for different stable regions.

induction studies. One structure corresponds to a stable shield and has a resistive crust, a conducting lower crust and a resistive upper mantle. In the second structure which is typical of the Appalachian region in the Canada and the Southern Uplands in Scotland, the whole crust is resistive while the uppermost mantle is conducting.

The geoelectric models obtained for the crust and the upper mantle from Northern Atlantic studies are compared schematically in Fig.1.7 with results from Southern Africa (van Zijl and Joubert, 1975; Blohm et al,1977), South-western Australia (Everett and Hyndman, 1967a) and the Vilyuisk Syncline-Aldan Shield region in the U.S.S.R. (Berdichevsky et al, 1972). In Southern Africa, the ultra-deep geoelectric soundings were carried out using very large electrode spacings between 30 and 1250 km and the Cabora Bassa power line. It is interesting to note that hydrated rocks is the common explanation usually given for a conducting lower crust in these regions by most of the workers.

1.4 Previous Induction Studies in Northern Scotland

i) Magnetometer Array Studies

The first major induction study in Northern Scotland was initiated in 1973 when an array of twenty Gough-Reitzel magnetometers was operated for about three months (Sik and Hutton, 1977;Hutton et al, 1977a). In 1976 and 1977 more GDS measurements were made at fourteen additional sites in the region using fluxgate magnetometers (Hutton et al, 1980). The site locations for the long period GDS studies are shown in Fig.1.8.

From the analysis of the data in the period band 5-120 minutes, the main conclusions from their studies were

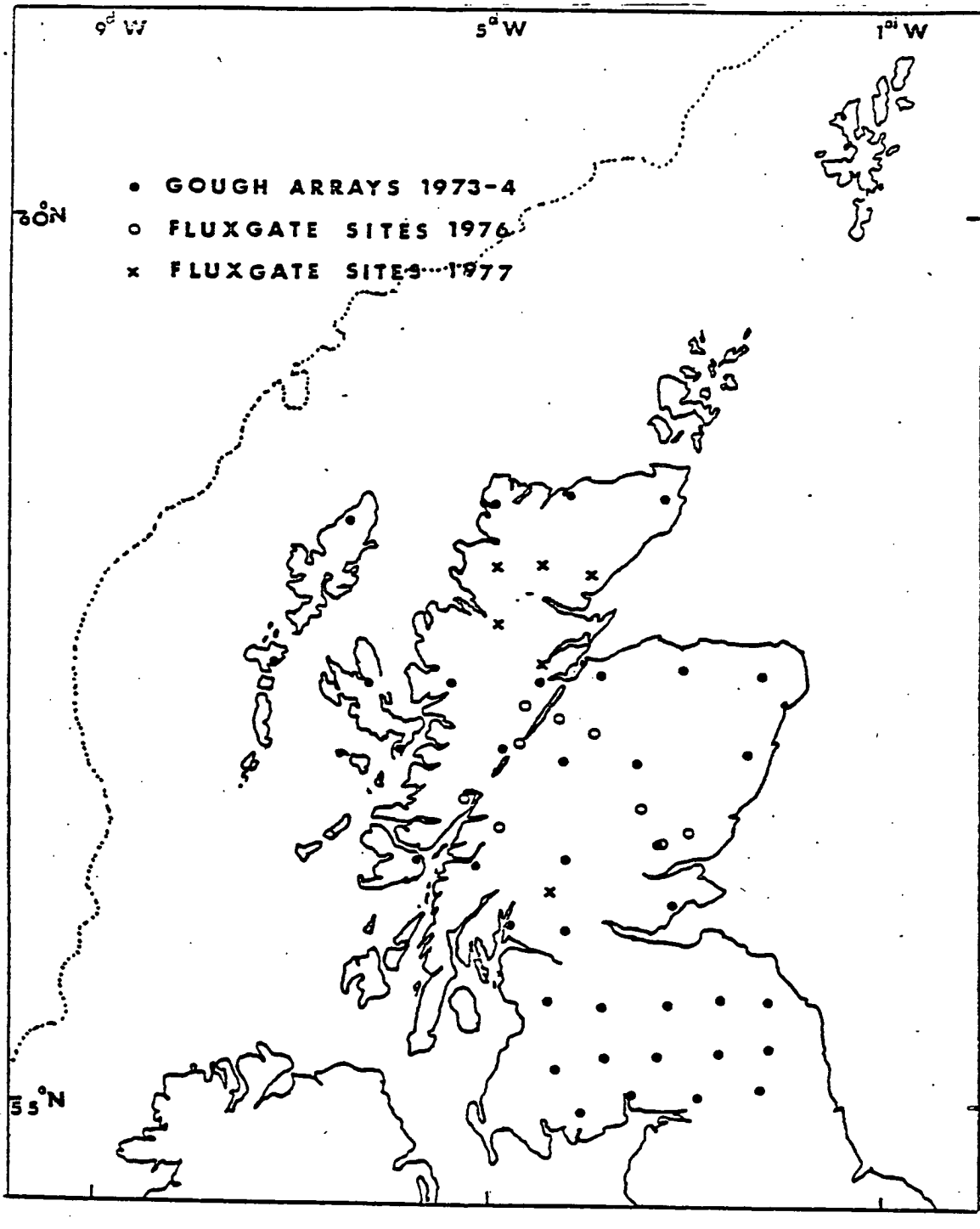

Fig.1.8 Long period GDS measurement sites in Scotland.

a) The behaviour of the induction parameters at periods between 10 and 80 min. was complex.

b) Both the Atlantic Ocean and the adjacent seas had considerable influence on the induction parameters in the region.

c) Superimposed on the complex pattern of induction due to the conducting seas were local induction anomalies. The most outstanding of these was a conductivity anomaly associated with the Great Glen. Induction vectors which point towards anomalous current concentrations in their GDS technique are shown in Fig.1.9a for 26 and 85 min. period.

ii) Induction in the Seas around the Orkney Islands

In 1974, GDS measurements were made at four sites on the northernmost region of the Scottish mainland and at four sites on the perimeter of the Orkney Islands (Robinson, 1977). The aim of the study was the investigation of the anomalous induction effects caused by the ocean surrounding a small group of islands close to mainland Scotland. Measurements for periods greater than 5 min. were made with Askania magnetometers. His induction vector plots are shown in Fig.1.9b.

From his results, three main induction effects were identified.

a) 5 - 30 min. period

Induction vectors at sites near the coast were large and normal to the coastline indicating a local coast effect. This gave rise to a large concentration of current in the channel between the Scottish mainland and the Orkney Island as shown by the large open arrows in the figures. The effect decreased considerably at sites on the mainland interior.

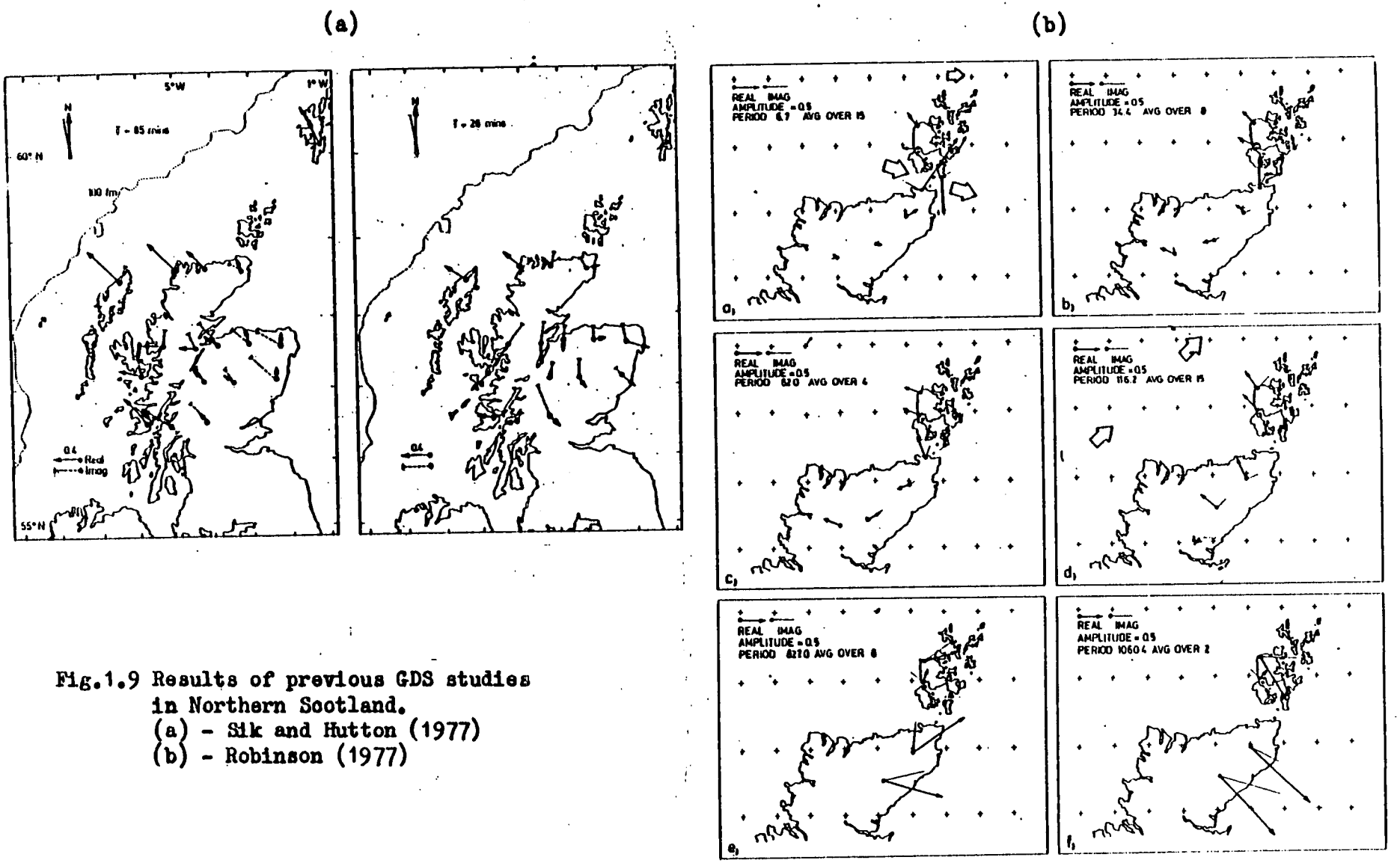

Fig.1.9 Results of previous GDS studies in Northern Scotland.
(a) - Sik and Hutton (1977)
(b) - Robinson (1977)

b) 30 min.- 3 hr. period

For periods longer than an hour the vectors pointed strongly towards the north-west with a very uniform amplitude of 0.4 over the region. This behaviour of the induction arrows was associated with the effects of the Atlantic continental edge about 150 km away in a direction perpendicular to the vectors.

c) 8 - 24 hr. period

For these periods, the author speculated that the direction of the vectors might be controlled by the regional source field.

iii) Conclusions

The considerable influence of the ocean and the adjacent seas on the induction parameters are highlighted by the results of the two GDS studies which have been briefly reviewed. Superposed on these effects are local induction anomalies.

In order to obtain the conductivity structure on the Scottish mainland, it is therefore essential to obtain an estimate of the coast effect on induction response functions using both MT and GDS techniques.

1.5 The Geology and Geophysical Data for Northern Scotland

In this section, the main geological units into which Northern Scotland can be divided are discussed briefly. The main geophysical section for the deep structure from LISPB, the Lithospheric Seismic Profile in Britain (Bamford et al, 1976) is presented. Results and the deductions from the few heat flow and gravity field studies are also discussed.

1.5.1 Geology

Scotland can be divided into four main geological blocks each separated by a fault. The four zones are the Lewisian Foreland, west of the Moine Thrust; the Caledonian metamorphic zone north of the Highland Boundary Fault; the Midland Valley and the non-metamorphic zone south of the Southern Uplands Fault. From plate tectonic models, geological and geophysical data, it is believed that a proto-Atlantic ocean called Iapetus (Harland and Gayer, 1972) divided Scotland from Northern England in late Precambrian times (Wilson, 1966). The closure of the proto-Atlantic is thought to have taken place by the end of the lower Palaeozoic time (600-395Ma). Although it is still a matter of controversy, the suture zone in Britain is believed to be south of the Southern Uplands (Phillips et al, 1976).

Northern Scotland is made up of the two zones north of the Highland Boundary Fault. The Lewisian Foreland is the North Atlantic shield fragment in Britain as illustrated in Fig.1.2 and consists of a Precambrian basement of crystalline gneiss which has remained stable since 1600 million years ago. Parts of the region are traversed by numerous dykes which are mainly of olivine and pyroxene composition. The dykes have a W-N-W or N-W strike direction (Read and Watson, 1975 p.40).

The Foreland is bound on the east by the Moine Thrust belt which is a few kilometers wide but about 150 km long. East of the Moine Thrust are rocks which were metamorphosed and deformed during a major tectonic episode known as the Caledonian orogeny which ended about 400 Ma ago. Recent isotopic evidence (Watson, 1978) suggests that most of the underlying rocks in the metamorphic zone were modified by the Grenville Orogeny which affected parts of Eastern Canada about 1000-800 Ma ago presumably when

Northern Scotland was closer to Canada and Greenland before the closure of the Iapetus. The Moine rocks which cover most of the area are metamorphosed schists and shales with occasional outcrops of the Lewisian basement which is believed to extend as far as the Great Glen. Near the Highland Boundary, the rocks are mainly of Dalradian group. The Great Glen Fault divides the metamorphic zone in Northern Scotland into the North-west Highlands and the Grampian Highlands. The fault traverses about 160 km of the Highlands in a north-easterly direction also the main strike direction of other less significant faults in the region. Kennedy (1946) was the first person to postulate a horizontal displacement of 104 km along the fault's length in the pre-Carboniferous time by matching Strontian and Foyers granite across the fault zone. Kennedy's matching has been has been questioned by several authors and the movement along the fault remains a matter of controversy (Harris et al, 1978).

During the Devonian time (395-345Ma) the crust of the metamorphic zone underwent increasing stabilization following the end of subduction and the closure of the proto-Atlantic ocean. The period was marked by volcanics, syn- and post-tectonic granitic intrusions. An interesting subdivision of these granites has been made recently by Brown and Locke (1979). Uplift and erosion of the Moine and Dalradian rocks led to the formation of basins in which Devonian sandstones accumulated and several faults on the Highlands were initiated or activated. A simplified geological map of the region is shown in Fig.1.10.

1.5.2 Some Geophysical Models for the Region

Although continuous geological mapping of most parts of

Fig.1.10 A simplified geological map of Northern Scotland.

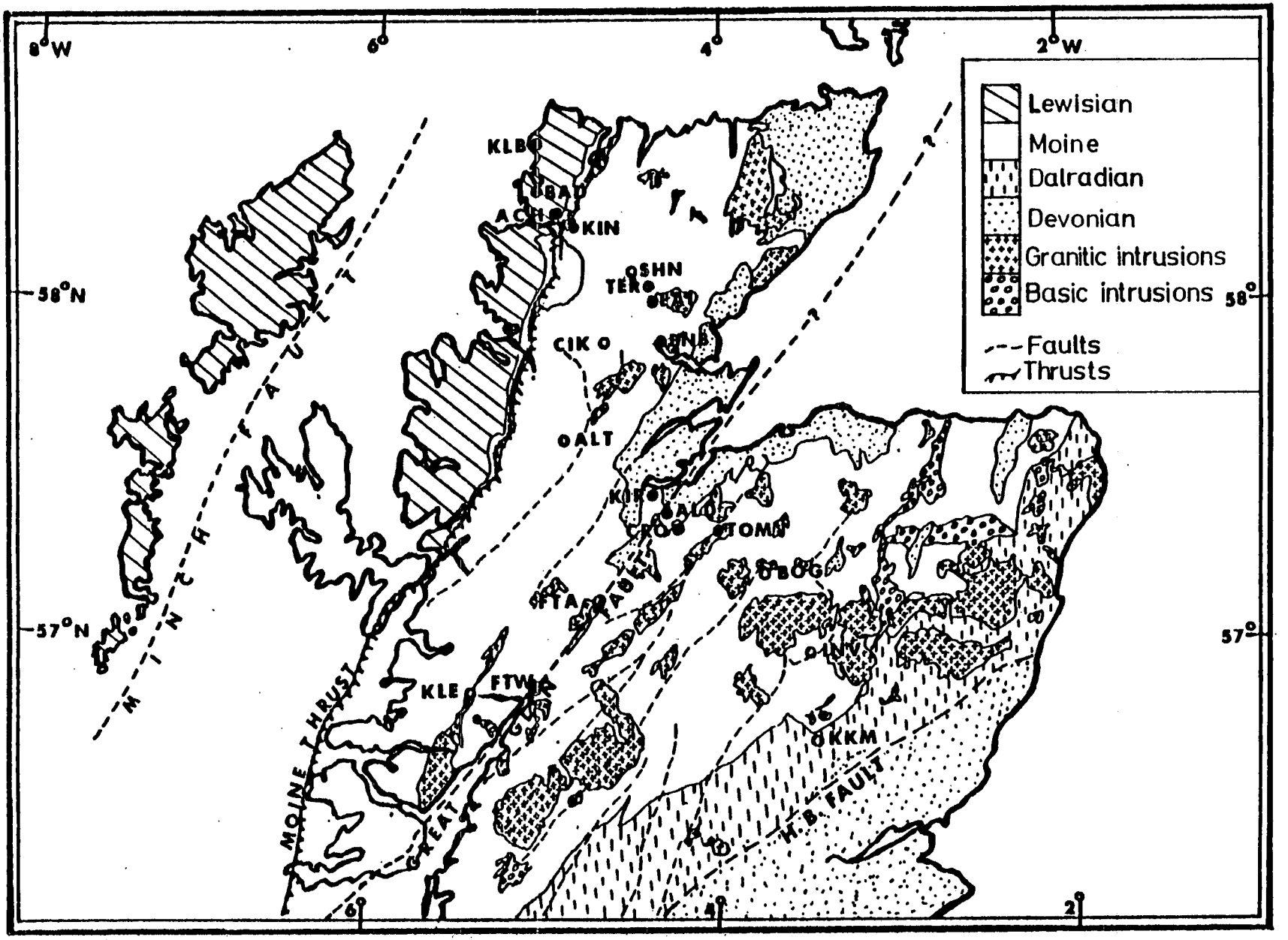

Northern Scotland has been carried out in the last 120 years, significant geophysical studies of the deeper structures were initiated only about five years ago. The major seismic experiment, LISPB, has been described by Bamford et al (1976). Their Alpha-profile which crosses the region in a NW-SE direction is marked in Fig.11a. From their interpretation, a model for the crustal and upper mantle structure of Northern Britain is shown in Fig.1.11b. The region north of the Highland Boundary Fault had the following features (Bamford et al, 1978; Faber and Bamford, 1979).

i) A superficial layer which includes upper Paleozoic and more recent sediments. Surface geology indicates the presence of Devonian sediments around the Moray Firth region and the Great Glen. The geometry of the seismic superficial layer shown around the Great Glen area however should be taken with caution as the resolution of the LISPB data for the uppermost 3 km is unreliable (Faber and Bamford, 1979).

b) An upper crustal layer with velocities of 6.1-6.2 km/s which they related to Caledonian metamorphic rocks. South of Loch Tay north of the Highland Boundary Fault, the velocities for the corresponding layer was 5.8-6.0 km/s which was thought to represent the lower Paleozoic sequence.

c) The next layer had velocities of 6.48 ± 0.06 and was associated with the pre-Caledonian basement. The depth of the layer varied between 6 and 14 km.

In view of the tectonic history associated with the region, it is interesting that the seismic model suggests a continuation of the layer into the Midland Valley with a termination near the Southern Uplands Fault.

b) Schematic cross-section through the crust and uppermost mantle of N. Britain
(Bamford et al, 1978)

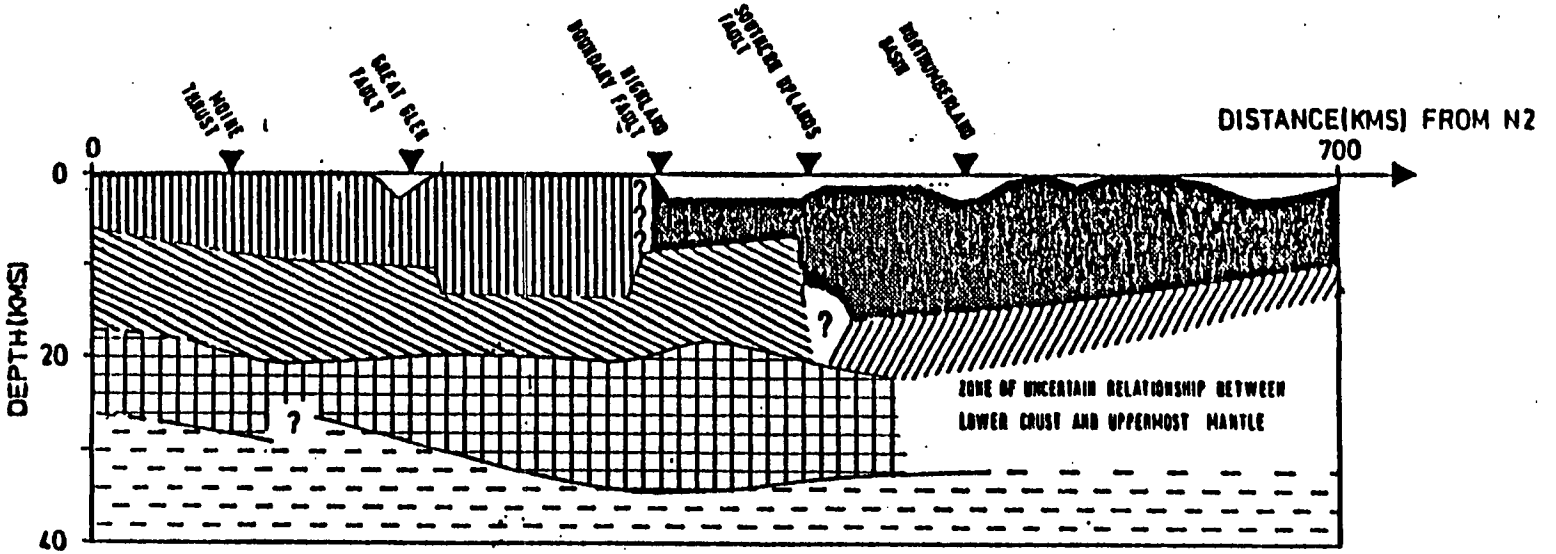

KEY

- Superficial layer
- Caledonian belt metamorphics (5.1-6.2 km/s)
- Lower Palaeozoic (5.6-6.8 km/s)
- Pre-Caledonian basement (~6.4 km/s)
- Pre-Caledonian basement (~6.3 km/s)
- Lower crust (~7 km/s)
- Upper mantle (~8 km/s)
- ? Uncertain structure

a) LISPB PROFILE

Fig.1.11

d) A lower crustal layer of velocity about 7 km/s at a depth of about 20 km.

e) The Moho interface between the lower crust and the upper mantle was at about 30 km on the Foreland and steepened slightly to about 35 km near the Highland Boundary. The upper-most mantle had a velocity of 8 km/s. Considerable lateral variations in the velocities at mantle depths between 45 and 69 km were found beneath the Great Glen and the Grampian Highlands (Faber and Bamford, 1979).

A gravity model has been contructed recently along the LISPB Alpha-profile (Dimitropoulos and Donato, personal communication). The negative gravity anomalies in the region were attributed to widespread granitic bodies. From their model studies, a granitic belt 7 to 19 km deep between the Great Glen Fault and Loch Tay Fault was required to fit the observed gravity anomaly in the region.

The few heatflow measurements made in Northern Scotland (Oxburgh et al, 1980) are shown in Fig.1.12. Pugh (1977) made detailed heatflow measurements along Loch Ness in the Great Glen and found a significant regional variation within the range 40-83 mWm^{-2} with an increase in the south-west direction and locally high values near the Foyers granite. The gradient of heatflow along the loch was thought to be related to the amount of radiogenic material at depth.

1.6 The Aim of the Geoelectric Study

The surface geology of most parts of Northern Scotland has been well studied and is known to be complex. From the long period GDS array measurements, the deep structures across the

Fig. 1.12 Heat flow values (mWm^{-2}) in Northern Scotland.

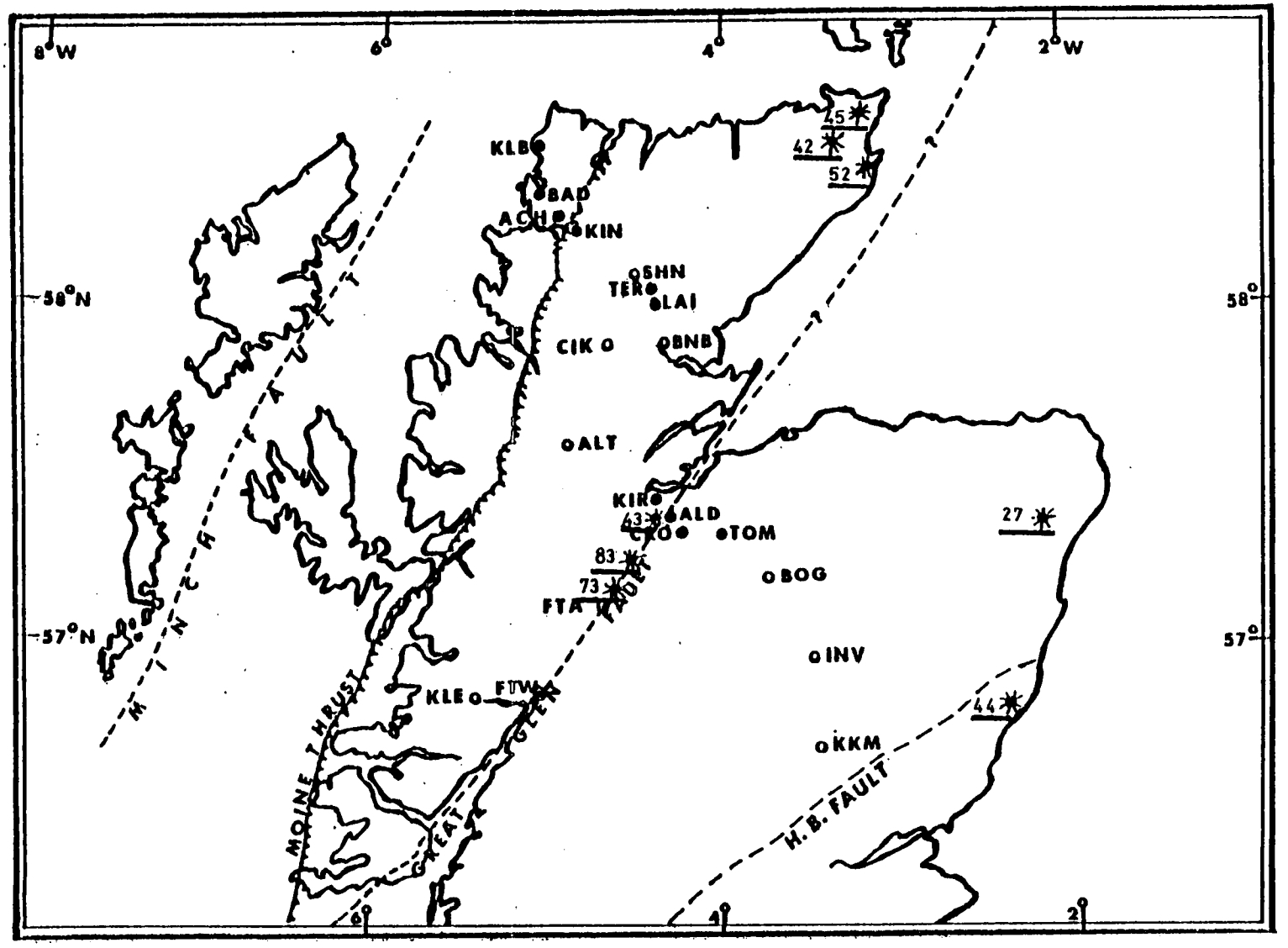

region appeared to be complex although no quantitative models for the regional crustal and upper mantle geoelectric structures were given.

It was therefore decided to carry out simultaneous MT and GDS measurements in the region using short period field variations in the period band 10-1200s to supplement the long period data. This study sought to

i) examine the geoelectric structure of the crust and upper mantle across known major geological features like the Moine Thrust and the Great Glen.

ii) obtain a reliable and quantitative geoelectric model for the crust and upper mantle by a combined use of MT and GDS techniques.

iii) provide an independent geophysical model to complement the model from the LISPB experiment which was until then the only model for the deep structures across the region.

It was hoped that the geoelectric study would thereby contribute to our understanding of the deep geology and tectonic history of Scotland.

CHAPTER 2

THE THEORY RELEVANT TO ELECTROMAGNETIC INDUCTION STUDIES

The use of natural electromagnetic field variations for geoelectric studies of the Earth has stimulated the interest of geophysicists in the last thirty years. Some results of regional geoelectric studies have been reviewed briefly in Chapter One. It would be both difficult and unrealistic to present here all the developments in the theory since the publication of the first main papers on the basic theory of magnetotelluric investigation of the Earth by Tikhonov (1950) and Cagniard (1953).

In this chapter, a simple theory of natural electromagnetic wave propagation in a model earth is given. Following this, the relevant theories which form the basis of the GDS and MT data analysis in this thesis are reviewed. The theoretical basis for the interpretation of the results for one- and two- dimensional geoelectric structures are also discussed. For the latter, a method of calculating GDS and MT response functions from outputs of the computer program for the diakoptic solution of induction problems (Brewitt-Taylor and Johns, 1977) is given. The few model studies of three-dimensional structures are also reviewed.

2.1 Electromagnetic Wave Propagation in the Earth

The source field which induces currents in the Earth is of external origin and its spectrum is shown in Fig.2.1a. The source field varies over a broad band of frequencies which extends from audio to extra-low frequencies. This permits geoelectric studies over several decades of frequencies. Maxwell's equations are used to describe the geoelectric fields due to induction by these

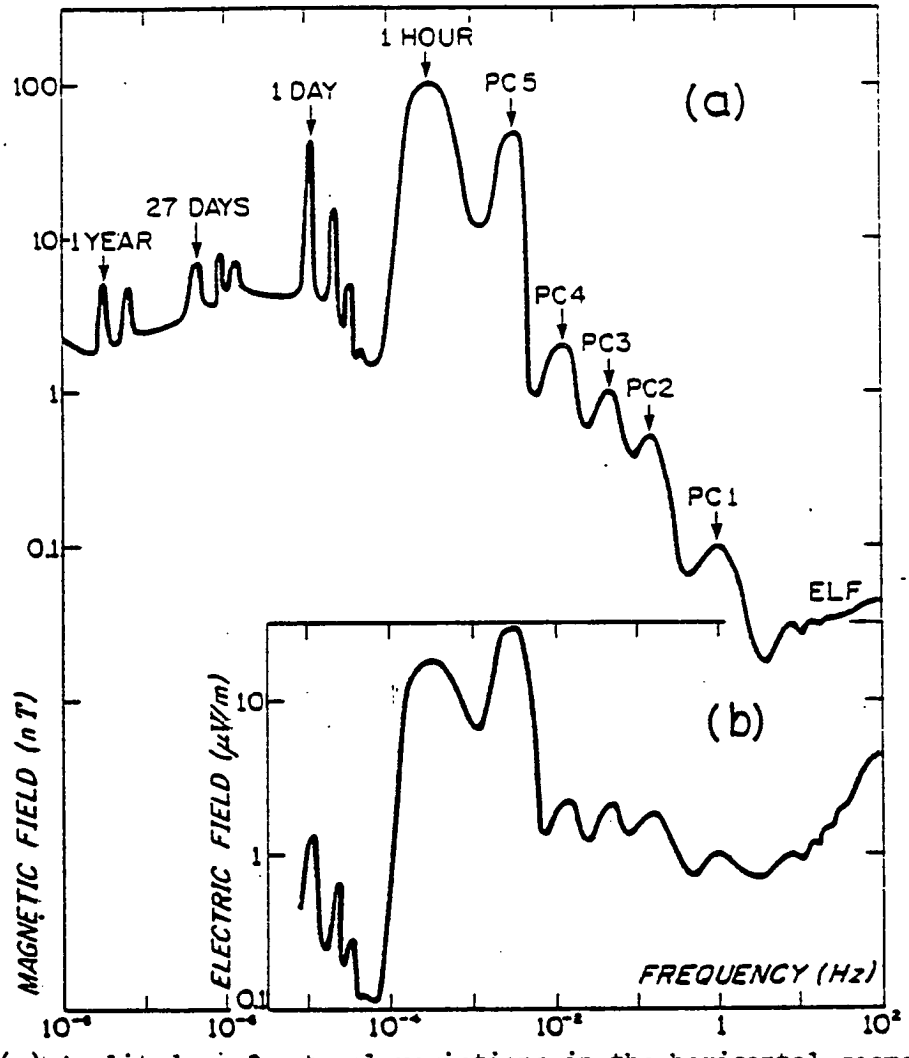

Fig.2.1(a) Amplitudes of natural variations in the horizontal geomagnetic field useful in induction research.
(b) Corresponding amplitudes in the earth-electric field, computed for a model earth of uniform resistivity 20 ohm-m.(Serson,1973).

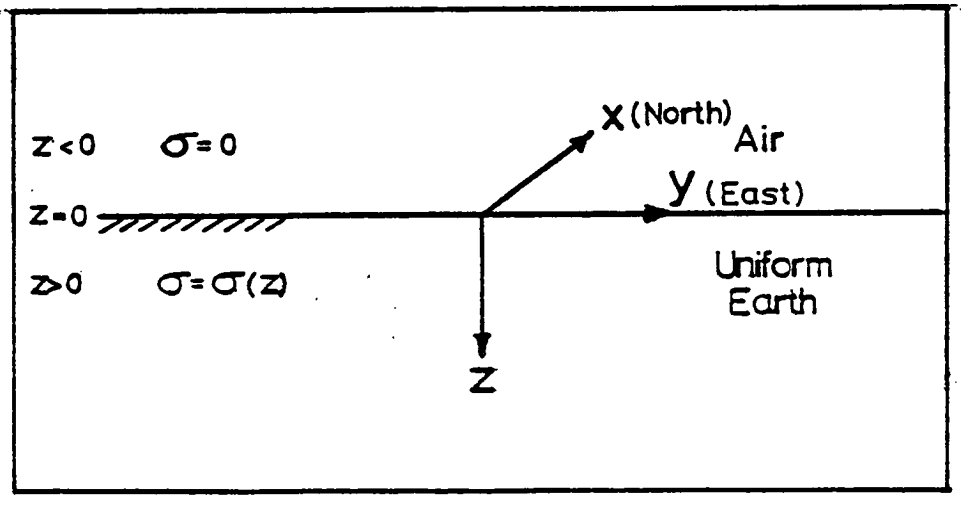

FIG·2·2 COORDINATE AXES

external electromagnetic field variations.

2.1.1 Maxwell's Equations

Consider a right handed coordinate axes x, y, z and let the Earth be the half-space $z > 0$ in Fig.2.2. Further, let field quantities vary with time as exp(iwt), where w is the angular frequency of the source field.

Maxwell's basic equations are

$$\text{Curl } \underline{E} = -\partial \underline{B}/\partial t \qquad 2.1$$

$$\text{Curl } \underline{H} = \underline{J} + \partial \underline{D}/\partial t \qquad 2.2$$

$$\text{div } \underline{B} = 0 \qquad 2.3$$

$$\text{div } \underline{D} = 0 \qquad 2.4$$

where $\underline{E}$, $\underline{H}$ and $\underline{B}$ are the electric, magnetic and induction field vectors respectively and $\underline{D}$ is the electric displacement vector.

The constitutive relations,

$$\underline{D} = \epsilon \underline{E} \qquad 2.5$$

$$\underline{B} = \mu \underline{H} \qquad 2.6$$

and

$$\underline{J} = \sigma \underline{E} \qquad 2.7$$

$$\rho = 1/\sigma \qquad 2.8$$

where ϵ, μ and σ are the permittivity, permeability and the conductivity of the medium.

It can be shown that in a uniform isotropic medium, both E and H satisfy the wave equation,

$$\nabla^2 \underline{F} = \sigma\mu \partial \underline{E}/\partial t + \epsilon\mu \partial^2 \underline{F}/\partial t^2 \qquad 2.9$$

For induction problems, the boundary conditions usually applied are

i) Tangential $\underline{E}$ is continous across the boundary between two media

i) Tangential $\underline{H}$ is continous across the boundary and

iii) The component of $\underline{B}$ normal to the boundary is continous across the boundary.

2.2 Application to Geoelectric Studies

For geoelectric studies, equation 2.9 is solved for different models of the Earth with necessary simplifying assumptions about its structure and geometry and about the inducing source field. The first substantial paper on the problem by Cagniard (1953) provided a simple theory for a one-dimensional earth. Some of his simplifying assumptions about the source field were examined by Wait (1954) and by Price (1962). In the last decade, the anisotropic nature of induction response functions has stimulated workers to consider more realistic earth models. In this section, we review briefly the simple theory which forms the basis of the MT method of geoelectric studies.

2.2.1 Cagniard Apparent Resistivity

For a homogeneous Earth, the solution of equation 2.9 is of the form

$$F = A\exp(iwt+nz) \qquad 2.10$$

where $$n = \pm (iw\mu\sigma - \epsilon\mu w^2)^{\frac{1}{2}} \qquad 2.11$$

For geoelectric studies which are described in this thesis, w is between $2\pi/10$ and $2\pi/1000$. Assuming that ϵ and μ for the Earth do not change appreciably from their free space values of $1/36\pi * 10^{-9}$ Fm^{-1} and $4\pi * 10^{-7}$ Hm^{-1} respectively, it can be shown by substitution in equation 2.11 that the term $\epsilon\mu w^2$ is negligible

compared to $\mu w\sigma$ for typical continental rocks. This implies that displacement current effects are negligible in the propagation and equation 2.11 becomes

$$n = \frac{1+i}{\sqrt{2}} (\mu w\sigma)^{\frac{1}{2}}$$
$$= \pm (\mu w\sigma/2)^{\frac{1}{2}} + i(\mu w\sigma/2)^{\frac{1}{2}} \qquad 2.12$$

i) Apparent Resistivity

The wave impedance of a homogeneous medium is defined by

$$Z = Ex/Hy = Ey/Hx \qquad 2.13$$

For an infinite half space, using equations 2.10 and 2.12, it can be shown that

$$Z = iw\mu/n = iw\mu/(iw\mu\sigma)^{\frac{1}{2}} = (iw\mu/\sigma)^{\frac{1}{2}}.$$

The apparent resistivity ρ_a is given by

$$\rho_a = 1/\sigma = -iZ^2/w\mu = (1/w\mu)|\underline{E}/\underline{H}|^2 \qquad 2.14$$

with a constant phase difference of 45 deg. between $\underline{E}$ and $\underline{H}$.

ii) Units

In an MT survey, the magnetic and the electric field variations are usually measured in nT and mV/km respectively. The formula for the apparent resistivity from equation 2.14 thus becomes

$$\rho_a = 0.2T|\underline{E}/\underline{H}|^2 \qquad 2.15$$

ii) Penetration Depth

The skin depth is defined as the depth in a uniform Earth in

which the amplitude of the field decreases to 1/e of its surface value and from equation 2.12 is given by

$$d = (2/\omega\mu\sigma)^{\frac{1}{2}} = 503(T\rho_a)^{\frac{1}{2}} m \qquad 2.16$$

For a uniform continental region of $\sigma = 0.001\ Sm^{-1}$, the skin depth for a wave of period 40s would therefore be about 100 km.

2.2.2 Cagniard's Assumptions

The simple theory outlined above is based on the following assumptions made by Cagniard in his theory for the MT technique.

a) The source field is a plane electromagnetic wave of infinite wave length.

Wait (1954) and Price (1962) were among those who objected to the plane wave assumption and they pointed out the errors that can be introduced in the computed earth response functions when the horizontal wavelengths are finite. Price (1962) developed a general theory of the MT method which included the source field parameter. The parameter had a maximum value equal to the Earth's circumference and a minimum value equal to about four times the height of the predominant source field currents. Thus for electrojet sources, the minimum value of the source field parameter was about 400 km for sites below the auroral and equatorial electrojets. Srivastava (1965) produced some model curves for the interpretation of MT data for different source wavelengths. Madden and Nelson (1964) in their defence of the Cagniard MT method pointed out that the effects on MT interpretation of lateral variations in the conductivity and the resulting tensor nature of the impedance can be much more serious than that of the plane wave assumption. Peltier and Hermance (1971)

investigated the problem further by using in their solution of the induction problem, a model electrojet as the source field of finite extent. They came to the conclusion that the plane-wave source field assumption led to a correct interpretation of the subsurface conductivity distribution for periods shorter than 10000s provided there was an increase in the conductivity with depth. As the longest period of interest in the present study of Northern Scotland is about 1000s, it is felt that finite source field effects on the data are probably not significant although more consideration will be given to the possibility of such effects in Chapter Six.

b) The second assumption was that the earth was plane and stratified rather than spherical.

Provided the depths of interest are smaller than the Earth's radius, Wait (1962) has shown that the effect of this assumption on MT results is negligible.

c) In the simple model, the Earth was also assumed to be homogeneous and electrically isotropic.

As already pointed out, Madden and Nelson (1964) in their support of the Cagniard formulation, agreed that the effect of conductivity inhomogeneities within the Earth can complicate the interpretation of MT results. Since then, many studies have been done on half-space models with lateral conductivity variations. In his review of analytical solutions to electromagnetic induction in the Earth, Hobbs (1975) has summarised the various investigations of the two-dimensional problem for a non-uniform half-space. Dawson and Weaver (1979a) have more recently studied conductivity inhomogeneities near the Earth's surface by using the thin-sheet approximation. Numerical modelling (Jones, 1973;

Praus, 1975) and laboratory modelling (Dosso, 1973) have also been used in studies of the induction response of a non-uniform Earth.

2.3 Theory for a Two-dimensional Earth

As was discussed in the last section, the homogeneous plane layered Earth model is inadequate for the interpretation of induction data. The inhomogeneous nature of the Earth is often revealed by apparent resistivity anisotropy and the presence of a vertical component of the magnetic field due to induction. Swift (1967) is one of the first workers to study anisotropic resistivity data. He interpreted the anisotropic data from South-western United States in terms of an inhomogeneous earth structure and derived expressions for the tensor apparent resistivities. His approach forms the basis of the routine MT analysis program used in this study and is presented briefly.

For a two-dimensional model Earth, let the variations in the conductivity be confined to the y and z directions where the half space is as defined in 2.1.1. Let $\underline{E}$ = (Ex, Ey, Ez) and $\underline{H}$ = (Hx, Hy, Hz). From Maxwell's equations in 2.1.1,

$$\partial Ez/\partial y - \partial Ey/\partial z = -i\omega\mu Hx \qquad 2.17$$

$$\partial Ex/\partial z = -i\omega\mu Hy \qquad 2.18$$

$$\partial Ex/\partial y = i\omega\mu Hz \qquad 2.19$$

$$\partial Hz/\partial y - \partial Hy/\partial z = \sigma Ex \qquad 2.20$$

$$\partial Hx/\partial z = \sigma Ey \qquad 2.21$$

$$-\partial Hx/\partial y = \sigma Ez \qquad 2.22$$

These equations separate into two distinct cases because equations 2.18, 2.19 and 2.20 involve only Ex, Hy and Hz, whereas the others involve Ey, Hx and Ez. The first case is known as the E-polarisation case for which the electric field, Ex is everywhere parallel to the strike of the discontinuities in the conductivity and there is an anomalous vertical component of the magnetic field, Hz. The second mode is the H-polarisation case for which the magnetic field is everywhere parallel to the strike direction of the conductivity discontinuity.

In a two-dimensional case, it is therefore necessary to define two impedances as follows :

$$Z_{//} = Ex/Hy \quad \text{(for the E-polarisation case)} \qquad 2.23$$

$$Z_{\perp} = Ey/Hx \quad \text{(for the H-polarisation case)} \qquad 2.24$$

In general, Ex and Ey measured along axes which do not correspond to the strike direction will each depend on both Hx and Hy and this new relationship gives rise to the tensor nature of the measured MT impedances.

2.3.1 Tensor Relations and Analysis

The relationship between Ex, Ey, Hx and Hy can be expressed in the following manner :

$$Ex = ZxxHx + ZxyHy \qquad 2.25$$

$$Ey = ZyxHx + ZyyHy \qquad 2.26$$

where Zxy and Zyx are known as the principal impedances. Zxx and

Zyy represent additional impedances due to the contribution from parallel components of the magnetic fields. For a homogeneous layered Earth which corresponds to the Cagniard model,

$$Zxx = Zyy = 0$$

and $$Zxy = -Zyx$$

Data obtained with the measurement axes at some arbitrary orientation to a two-dimensional structure can be rotated into the strike direction in the following manner.

In the matrix form, equations 2.25 and 2.26 can be written as

$$\begin{pmatrix} Ex \\ Ey \end{pmatrix} = \begin{pmatrix} Zxx & Zxy \\ Zyx & Zyy \end{pmatrix} \begin{pmatrix} Hx \\ Hy \end{pmatrix} \qquad 2.27$$

For a new set of axes x', y', at an angle θ to the x-axis in Fig.2.2, the field components $E'x$, $E'y$, $H'x$ and $H'y$ are given by

$$\begin{pmatrix} E'x, & H'x \\ E'y, & H'y \end{pmatrix} = \begin{pmatrix} \cos\theta & \sin\theta \\ -\sin\theta & \cos\theta \end{pmatrix} \begin{pmatrix} Ex, & Hx \\ Ey, & Hy \end{pmatrix} \qquad 2.28$$

Using equation 2.27,

$$M^{-1} \begin{pmatrix} E'x \\ E'y \end{pmatrix} = \begin{pmatrix} Zxx & Zxy \\ Zyx & Zyy \end{pmatrix} M^{-1} \begin{pmatrix} H'x \\ H'y \end{pmatrix} \qquad 2.29$$

where $M = \begin{pmatrix} \cos\theta & \sin\theta \\ -\sin\theta & \cos\theta \end{pmatrix}$

$$\begin{pmatrix} E'x \\ E'y \end{pmatrix} = M \begin{pmatrix} Zxx & Zxy \\ Zyx & Zyy \end{pmatrix} M^{-1} \begin{pmatrix} H'x \\ H'y \end{pmatrix} \qquad 2.30$$

$$\text{and } Z' = M \begin{pmatrix} Zxx & Zxy \\ Zyx & Zyy \end{pmatrix} M^{-1} \qquad 2.31$$

Z thus represents the impedance tensor for the new measuring coordinates. It can be determined as follows :-

$$Z' = \begin{pmatrix} \cos\theta & \sin\theta \\ -\sin\theta & \cos\theta \end{pmatrix} \begin{pmatrix} Zxx & Zxy \\ Zyx & Zyy \end{pmatrix} \begin{pmatrix} \cos\theta & -\sin\theta \\ \sin\theta & \cos\theta \end{pmatrix} \qquad 2.32$$

since $M = \sin^2\theta + \cos^2\theta = 1$.

Expressing Z' as $\begin{pmatrix} Z'xx & Z'xy \\ Z'yx & Z'yy \end{pmatrix}$, it can be shown from equation 2.32 that

$$2Zxx = (Zxx+Zyy) + (Zxx-Zyy)\cos2\theta + (Zxy+Zyx)\sin2\theta \qquad 2.33$$

$$2Zxy = (Zxy-Zyx) + (Zxy+Zyx)\cos2\theta + (Zyy-Zxx)\sin2\theta \qquad 2.34$$

$$2Zyx = (Zyx-Zxy) + (Zyx+Zxy)\cos2\theta + (Zyy-Zxx)\sin2\theta \qquad 2.35$$

$$2Zyy = (Zyy+Zxx) + (Zyy-Zxx)\cos2\theta - (Zxy+Zyx)\sin2\theta \qquad 2.36$$

The principal directions are defined by the directions, θ_s and $\theta_s + \pi/2$ which maximise Zxy and minimise Zyx respectively. These directions can be determined numerically by computer rotation of the impedance using small increments in e.g. 5 degrees or less. This is expensive in computer time although the resulting impedance plots present useful visual information on the degree of structural complexity at each site. Fig.2.3 illustrates the behaviour of tensor impedance elements at a two-dimensional site (Station 14) and at a complex site (Station 12) respectively. Swift (1967) has used an analytical approach to determine the

COMPLEX 2 SITE

STATION 12

AMPLITUDE OF TENSOR ELEMENTS

PERIOD= 96.1 SEC N EST= 16

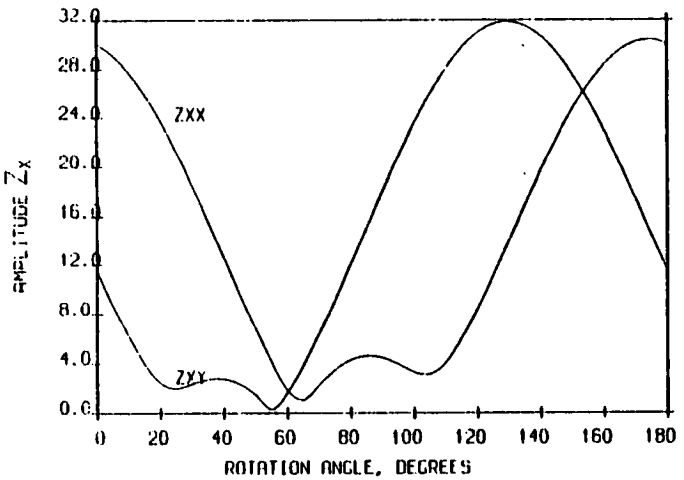

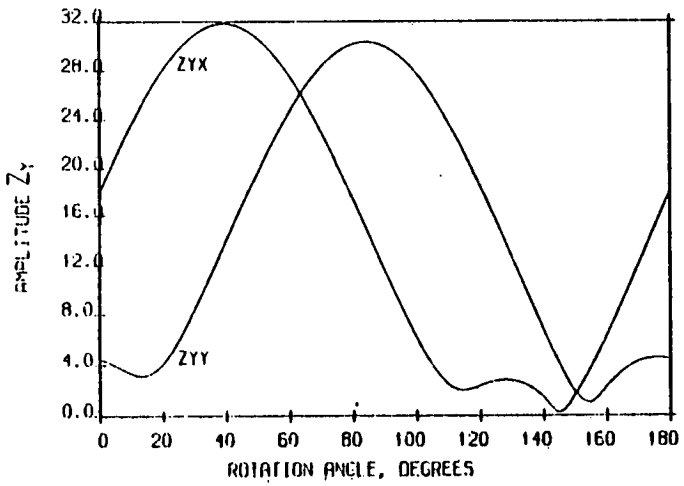

TWO-DIMENSIONAL SITE

STATION 14

AMPLITUDE OF TENSOR ELEMENTS

PERIOD= 95.3 SEC N EST= 25

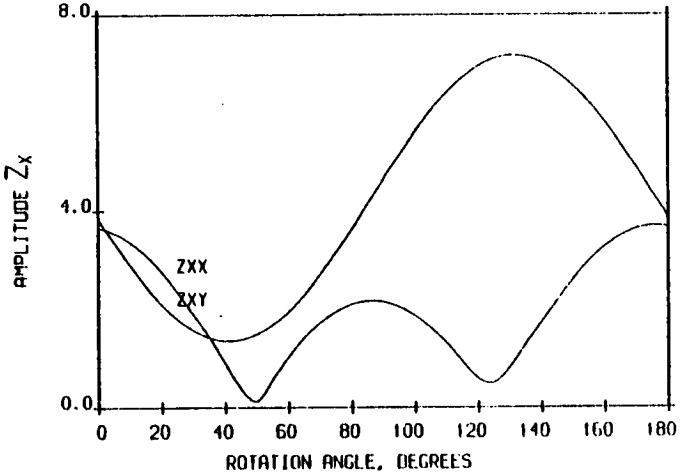

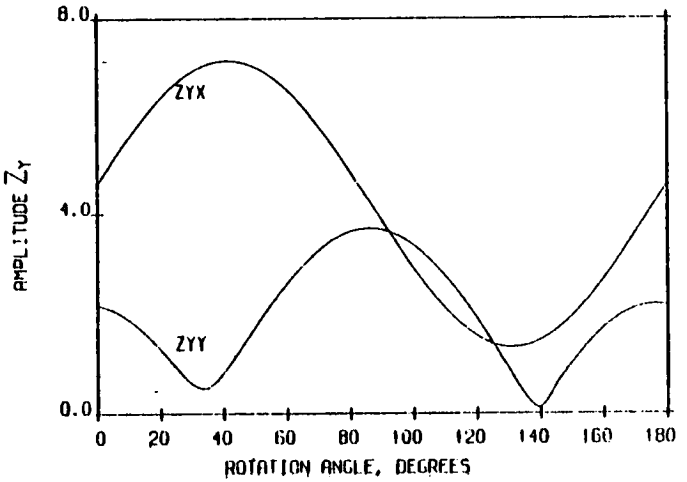

angle at which $(|Z'xy|^2 + |Z'yx|^2)$ is maximised. He showed that

$$\tan 4\theta_s = \frac{(Zxx-Zyy)(Zxy+Zyx)^* + (Zxx-Zyy)^*(Zxy+Zyx)}{|Zxx-Zyy|^2 - |Zxy+Zyx|^2} \qquad 2.37$$

At this angle, Zxx and Zyy should reduce to zero over an ideal two-dimensional structure. The computer program which was used in the MT data processing adopted equation 2.37 for the determination of the principal directions at each site.

Equation 2.14 can be used to calculate the two apparent resistivities max and min

where $\rho_{max} = 0.2T|Zxy|^2$ 2.38

and $\rho_{min} = 0.2T|Zyx|^2$ 2.39

The ratio $\rho_{max} : \rho_{min}$ is a measure of the non-uniformity of the structure, i.e. the anisotropy at the site. In the two-dimensional case, the anisotropy increases rapidly as the position of the discontinuity in the structure is approached. The model responses in Fig.2.9 illustrate this feature

Another dimensionality indicator is the skewness factor. This is independent of the direction of measurement and was defined by Swift (1967) as

$$\text{Skew} = |Zxx + Zyy|/|Zxy - Zyx| \qquad 2.40$$

For one- and two-dimensional structures, the skew should be zero. This is seldom so. An assessment of the degree of two-dimensionality is best made by study of (a) the ρ_{max}, ρ_{min} profiles, (b) the anisotropy, (c) skew factor and (d) the induction vectors from GDS analysis.

2.4 The GDS Method

The geomagnetic deep sounding method evolved historically from study of magnetic observatory recordings of the elements Hz, Hx and Hy and the relationship between these elements. From this relationship, it can be shown that some qualitative deductions can be made about the electrical conductivity distribution in the crust and upper mantle. On combining the GDS and the MT observations together, a reliable quantitative information on the geoelectric structure for the region under survey can be obtained.

2.4.1 The GDS Transfer Function

In the two-dimensional problem Hz, the anomalous vertical component of the magnetic field is present in the E-polarisation case. Hz is used in the GDS method through the transfer function concept which was developed by Schmucker (1964, 1970) and Everett and Hyndman (1967b) among others.

A simplified relationship between the three magnetic field components at a measurement site is given by

$$Hz = AHx + BHy + e \qquad 2.41$$

where e represents a noise term due to a residual part of Hz that does not correlate with the horizontal field, the measurement noise or both.

A number of simplifying assumptions are implicit in the relation in equation 2.41, namely

a) The normal vertical component of the inducing source field is

small compared with Hz and therefore can be ignored.

b) The normal vertical component does not correlate with Hx and Hy.

c) Any horizontal fields due to the anomaly are negligible compared to the corresponding normal horizontal fields.

Banks (1973) has discussed the validity of these assumptions and has indicated that they are probably adequate for induction studies in mid-latitudes. Caution is, however, needed in the application of this simple formula to single station measurements as the characteristics of a particular source field structure can change the value of the transfer function significantly. At mid-latitudes, Beamish (1979) has suggested that estimates of A and B are best determined from a weighted mean which takes into account the effect of the normal vertical field.

At any given site, the quantities in equation 2.41 are frequency dependent and A and B are complex. They can be evaluated in the frequency domain by the spectral analysis technique discussed in Chapter Four. The transfer functions A and B can be expressed as

$$A = Ar + Ai \qquad 2.42$$

$$B = Br + Bi \qquad 2.43$$

where r and i denote real and imaginary parts. Amplitudes R and I can be defined by means of the expressions

$$R^2 = Ar^2 + Br^2 \qquad 2.44$$

$$I^2 = Ai^2 + Bi^2 \qquad 2.45$$

with corresponding directions by

$$\theta_r = \tan^{-1}(Br/Ar) \qquad 2.46$$

$$\theta_i = \tan^{-1}(Bi/Ai) \qquad 2.47$$

$(R,\theta r)$ and $(I,\theta i)$ are known as the real and imaginary induction vectors. They provide a useful way of displaying transfer function amplitude and azimuth information on maps. The real, or in-phase vector, lies in a preferred plane and when reversed in direction (Parkinson, 1962; Edwards et al, 1971 ; Gough et al, 1973) points towards anomalous electric currents in a two-dimensional structure. The real vector is usually larger than the imaginary vector when the conductive body is large and deep. The imaginary or the quadrature vector tends to be large when surface conductors are present. Induction vectors can therefore provide quick qualitative information on the possible location of simple conductivity anomalies in a region under survey.

2.4.2 Bank's Maximum and Minimum Responses

Banks and Ottey (1974) suggested another way of presenting the information in equation 2.41 and expressed it as

$$Hz = GpH1 + G_l H2 \qquad 2.48$$

where 1 and 2 denote a new set of axes such that the Hz response is a maximum along 1 and a minimum along 2. The noise term e has been neglected and Gp and G_l are complex. The relationships between Gp and G_l and A and B are given by

$$Gp = A\cos\theta + B\sin\theta \qquad 2.49$$

and

$$G_l = B\cos\theta + A\sin\theta \qquad 2.50$$

The value of θ for which Gp is maximum or minimum is given by

$$\tan 2\theta_p = (AB^* + A^*B)/(|A|^2 - |B|^2) \qquad 2.51$$

In a strictly two-dimensional situation, G_l will be zero and Hl will be normal to the strike of the conductor. In geoelectric studies, G_l is seldom zero but where it is small compared with Gp, an interpretation in terms of a two-dimensional model may be justified. The GDS maximum-minimum response technique was incorporated into the analysis program in this study for the interpretation of the GDS response functions in Northern Scotland. The results are discussed in Chapter Five.

2.4.3 Hypothetical Event Contour Plots

In their report on the interpretation of electrical conductivity anomalies in Eastern Canada, Bailey et al (1974) proposed another method of presenting GDS transfer function data. The method known as the hypothetical event analysis seeks to calculate the vertical anomalous magnetic field, Hz at all stations in the region from an assumed inducing source field which has a uniform horizontal field H of specified polarisation. The hypothetical Hz is calculated from equation 2.41 (neglecting e) using the estimated values of A and B at a given period and then contoured on a regional map. Since the assumed inducing field is uniform, calculated variations in Hz are due to conductivity anomalies which can then be interpreted qualitatively. Apart from the inherent assumptions in transfer function estimates already discussed, a justification for the additional assumption of uniformity of the regional hypothetical field of any polarisation needs consideration as it is well known that real horizontal

fields can be non-uniform in some regions. The authors have considered the problem posed by this assumption and they felt that the errors in this method were of the same order of magnitude as the errors due to the assumption of a uniform field for actual events. They also suggested that in the worst case of non-uniformity, one could still use the change in the sign of hypothetical Hz to infer conductivity distributions since, they argued, a sign change in the horizontal field due to a local anomaly is unlikely.

The main advantages of the method appear to be that

i) it permits the use of non-simultaneous data in regional induction studies

ii) a uniform source field rather than the natural source field of unknown complex geometry can be used in the analysis

iii) it allows the polarisation of the hypothetical source to be varied and thereby a more detailed study of the structure can be made.

The hypothetical event technique has been used in Scotland by Hutton et al (1977, 1980). Fig. 2.4 illustrates typical hypothetical Hz contours for 30min and 5min period obtained by Hutton et al (1980) using all available Gough magnetometer array and flugate magnetometer data in Northern Scotland. A comparison of the deductions made by the use of this technique with those obtained by the methods used in this study is presented in Chapter Six.

2.4.4 Hz/Hy Amplitude Ratios

When GDS measurements lie on a traverse, equation 2.41 can be used to determine A and B. The value of the complex ratio of

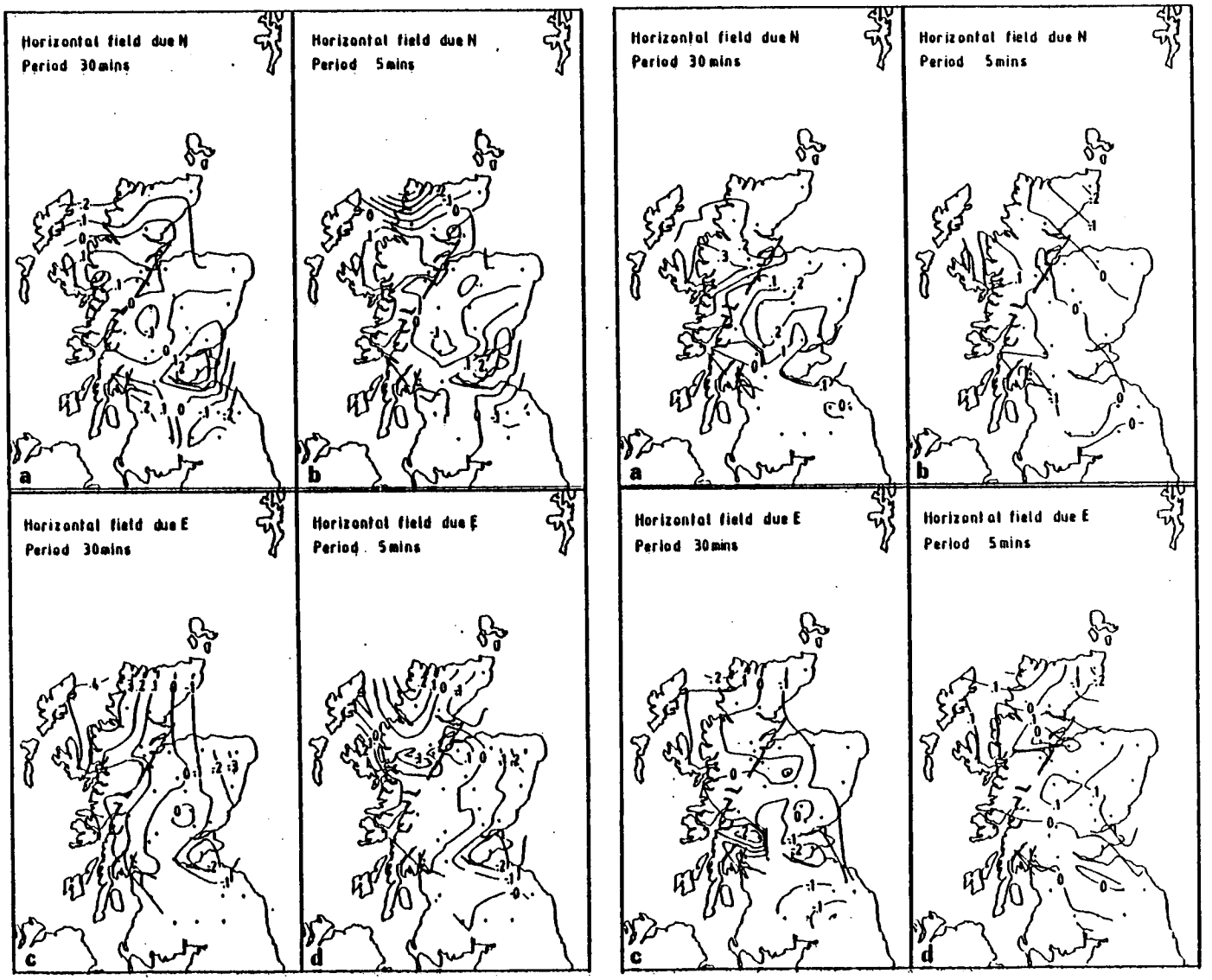

Fig.2.4 Hypothetical event contour maps for Northern Scotland.

the vertical to the horizontal component of the magnetic field can be calculated for any direction of the inducing field by axes rotation. When the traverse data are not simultaneous, a hypothetical source field can be assumed for regional induction since by means of rotation, the response function can be obtained for specific source field polarisations.

In a two-dimensional situation where the strike of the main tectonic or geologic features in the region is known, a plot of the amplitude ratio, Hz/Hy against y, where y is in a direction perpendicular to the strike is often used for both qualitative and quantitative interpretation of conductivity anomalies.

Fig.2.5 shows a model Hz/Hy profile over a conducting prism of resistivity 100 ohm m about a tenth of a skin-depth below the surface of a continental half-space of resistivity 2000 ohm m. The response was computed using a two-dimensional modelling program for diakoptic solution of induction problems (Brewitt-Taylor and Johns, 1977). For experimental data, we should therefore expect the real part of the ratio to be small with a sign reversal over the axis of a conducting anomaly. At distances of several skin-depths from the centre of the anomaly, the ratio becomes small. Quantitative information about a region can thus be obtained by comparing the experimental profile with such model solutions. An inadequate fit will reflect the shortcomings of the simplifying assumptions inherent in transfer function estimates, the uncertainty in any assumed regional strike as well as the general non-two-dimensional nature of the real Earth. The use of both magnetic component amplitude ratio and apparent resistivity profiles in the search for the best model proved quite useful in the interpretation of the results of this study as will be

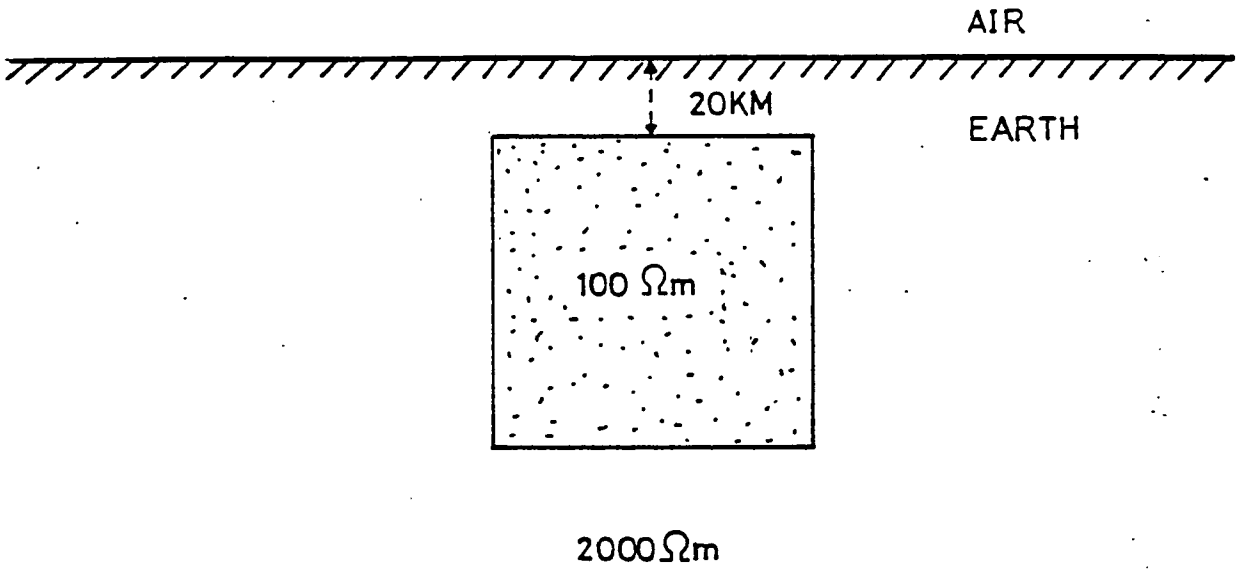

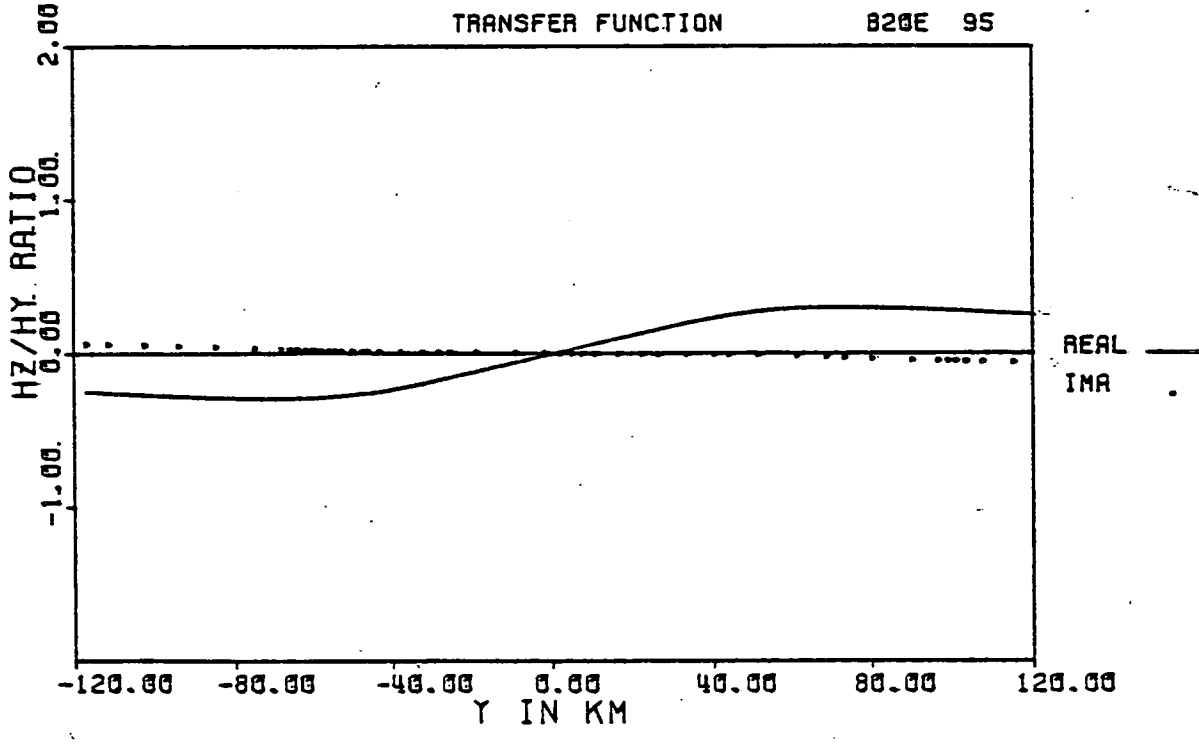

Fig.2.5 Model Hz/Hy profile for a buried conducting prism.

discussed in Chapter Six.

2.5 Modelling and Interpretation Procedures

From a preliminary study of the results of either MT or GDS analysis using some of the methods outlined in the preceding sections, a qualitative interpretation of field data can be made. It is more reliable if such interpretation satisfies both MT and GDS data. For quantitative interpretation, however, modelling of the data is necessary.

Interpretation of MT data usually starts with the simple approach of forward modelling. In its simplest form, this is the curve-matching technique in which experimental data are compared with curves of computed responses for known Earth models. By trial and error a best fitting model is obtained. One serious defect of all forward modelling methods is that there is no way of quantifying the non-uniqueness of the solution. Inversion techniques which seek to obtain conductivity models directly from experimental data are fairly well developed for one-dimensional plane layered structures. As a result of the work of Backus and Gilbert (1967, 1968, 1970), it is possible to determine, in the modelling technique, the space of acceptable models. This provides a measure of the non-uniqueness of the solution. However, there is need for caution in the use of one-dimensional models for interpretation especially where dimensionality factors suggest a considerable departure from the simple one-dimensional case. Unfortunately, the inversion of two-dimensional conductivity data (Weidelt, 1975) is not yet well developed.

In this section, a description is given of the three-layer curve-matching technique which was used as the starting model for

application of a one-dimensional inversion program. Descriptions of this one-dimensional program, the two-dimensional modelling program and the programs which were developed for the construction of the MT and GDS response profiles are also discussed. Computed responses are presented for typical two-dimensional models.

2.5.1 One-dimensional Models

i) The Forward Solution

In this method, the interpretation involves the comparison of apparent resistivity and phase data curves with a set of model response curves drawn on the same scale. The model curves are computed for simple geological structures (Fig.2.6a) and when a close fit between data and theoretical curves are found, the model resistivities and layer depths may be used as estimates of the real Earth parameters. Cagniard (1953), Yungul (1961) and Srivastava (1967) have published master curves for the interpretation of MT apparent resistivity and phase data for a one-dimensional layered Earth. Srivastava's three-layer master curves were used in this study.

The procedure used for the application of the MT curve matching technique was as follows :

First, using a Calcomp Plotter, the apparent resistivity, ρ_a and phase, ϕ data are plotted against period, T on the same log scale as the model curves (Figs.2.6b and c).

For a three-layer Earth model with resistivities ρ_{1m} , ρ_{2m} , ρ_{3m} and layer thickness h_{1m} , h_{2m}, let the corresponding quantities for the real Earth be ρ_1 , ρ_2 , ρ_3 and h_1 and h_2 at a given period, T.

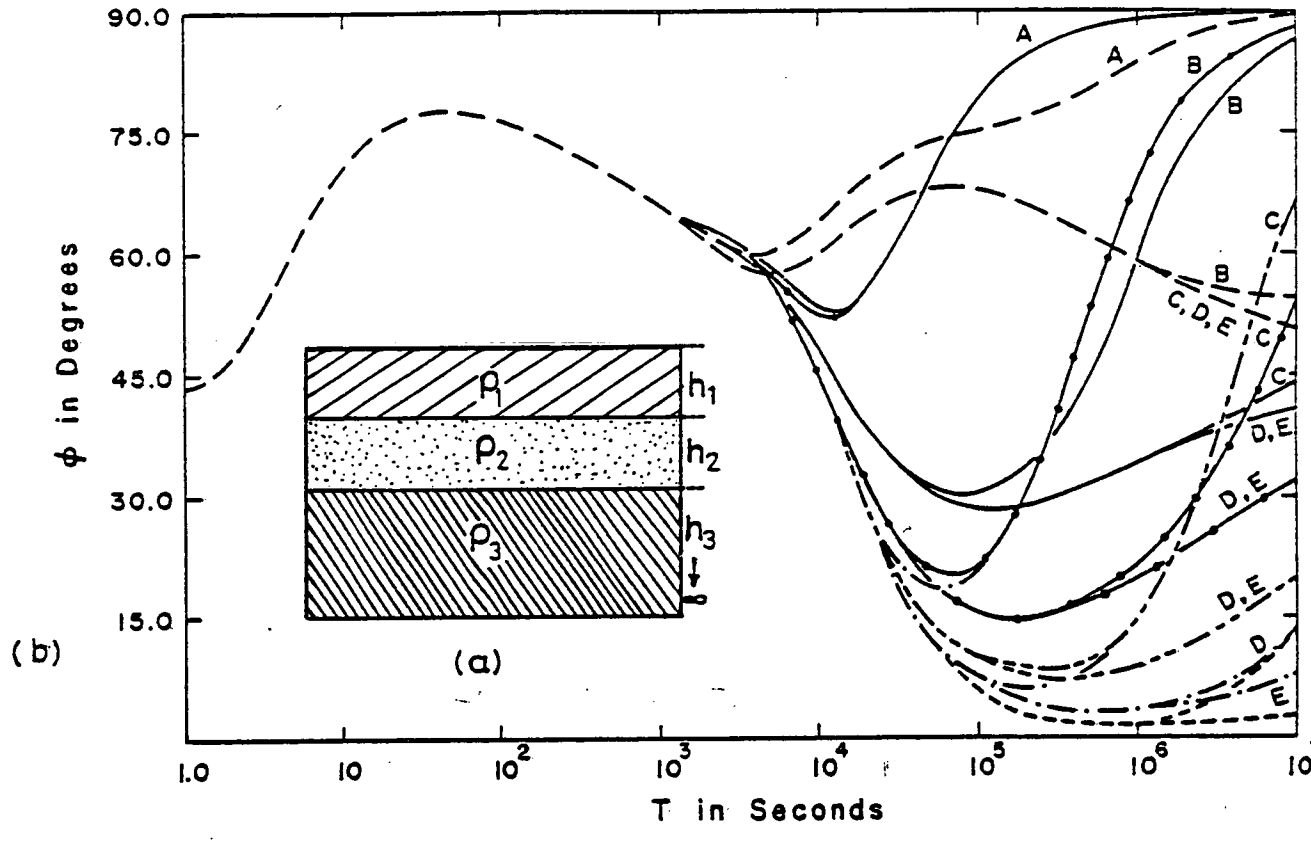

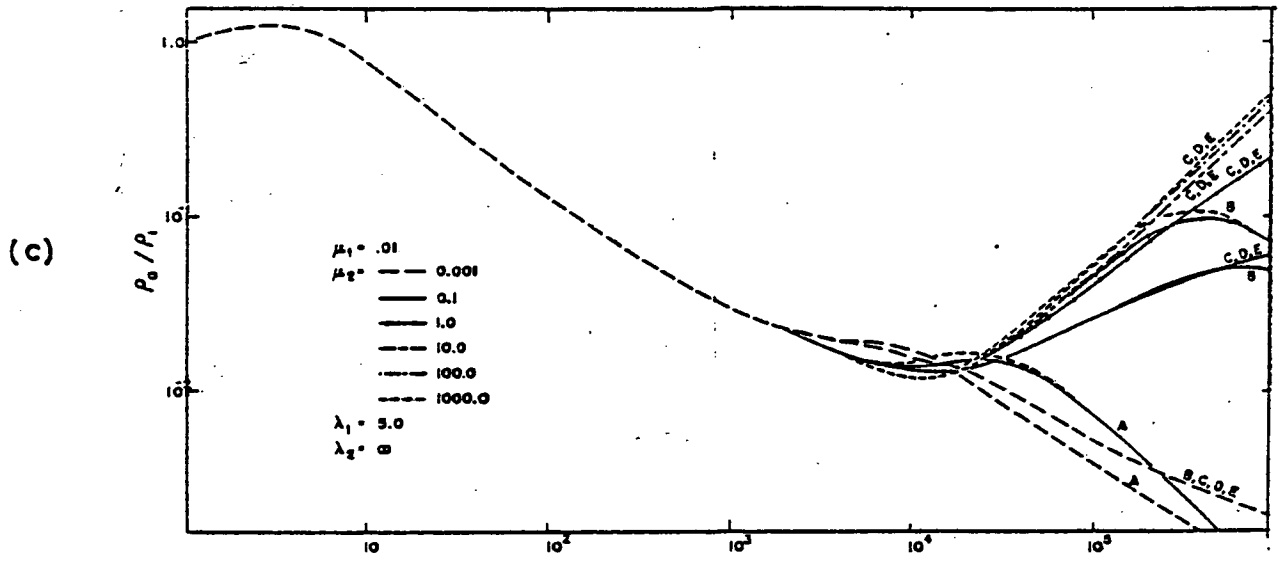

Fig.2.6 (a) - A three layer resistivity model.
(b) - Apparent resistivity phase master curves.
(c) - Apparent resistivity master curves.
(Srivastava, 1967)

The model curves are plotted as ρ_a / ρ_1 against T, where ρ_1 is set to unity. Hence, for a match between the two curves, the intercept of the line $\rho_a / \rho_1 = 1$ on the experimental curve yields the top layer resistivity, ρ_1. The intercept of the model curve axis, T = 1, on the experimental curve T-axis gives the period shift, T_1. The thickness, h_1 of the first layer is given by

$$h_1^2 = \rho_1 * T_1$$

The thickness of the next layer is $h_2 = \lambda_1 h_1$ and the resistivity, $\rho_2 = \mu_1 \rho_1$. The resistivity of the third layer $\rho_3 = \mu_2 \rho_1$. The factors λ_1, μ_1, μ_2 for different master curves are stated on the curves.

ii) One-dimensional Inversion

A procedure for one-dimensional inversion of MT data was developed by Schmucker (1970) for the two layer case of a resistive layer underlain by a conductor. The depth and the conductivity which are obtained by this method are therefore for a uniform substitute conductor at each period of interest. Weidelt (1972), Hermance and Grillot (1974) and Summers (1976) among others have also studied the problem of one-dimensional inversion of MT data. Jones and Hutton (1979b) used the Monte-Carlo inversion scheme for the interpretation of their MT data from Southern Scotland. This latter formalism was also adopted in the present study as the method gives a range of acceptable models and thus a measure of the non-uniqueness of the solution obtained. The method has been very well described by Jones and Hutton and will not be repeated here. The few minor changes to their computer program were considered necessary. These are now discussed.

Following the withdrawal of G05ADF from the E.R.C.C. Systems

Library, a new equivalent random number generator, G05DDF with the necessary sequence setter, G05CCF was substituted. The mean and the standard deviation parameters required by G05DDF were set at 0 and 1 respectively for a random sequence.

The starting model parameters for each data set were obtained by curve-fitting using Srivastava's (1967) three-layer master curves. For realistic models to result from the inversion scheme this was found to be necessary. An additional constraint was introduced at the model plotting stage so that about ten best models were plotted. They satisfied the conditions that $\sum(\log \hat{\rho}(f)-\log\rho_m(f))^2$ and $\sum(\hat{\phi}(f)-\phi_m(f))^2$ respectively, as defined by Jones and Hutton (1979b) were minimised. This one-dimensional inversion formed part of the preliminary data analysis irrespective of the complexity of the structure of the observation site. An initial analysis in terms of three-layer Earth models was considered adequate from the appearance of the apparent resistivity and phase curves from most sites.

2.5.2 Two-dimensional Models

Since direct inversion techniques for two-dimensional conductivity anomalies are difficult, many workers have used the less elegant but simpler model solution method for quantitative interpretation of geoelectric data.

As in the one-dimensional forward modelling principle, a fit between data and model two-dimensional response provides a solution to the problem. The numerical techniques for obtaining models have improved greatly in the last decade and have been reviewed by Jones (1973) and by Praus (1975). The methods which have been most commonly used in geoelectric studies are the

finite element, finite difference and the the transmission line analogy. A summary of some of these numerical model studies is presented in Table 2.1.

2.5.3 The Two-dimensional Modelling Program

The program written by Brewitt-Taylor for a diakoptic solution of induction problems was used in this study for two-dimensional modelling. The method of solution uses the anology between Maxwell's equations and the equations which relate the voltage and current in a transmission line or surface. Components of the network outline rectangles in each of which the conductivity is constant. The new finite difference formulation of the general two-dimensional induction problem (Brewitt-Taylor and Weaver, 1976) was used for setting up the equations involved. The formulation is considered outside the scope of this study and the reader is referred to their excellent discussion of the method. The numerical equations are solved by the method of diakoptics which is particularly suited to electrical network formulation. An essential characteristic of the method is the division of the network into a number of subnetworks which are then analysed and described separately by means of a corresponding number of matrices. In the final stage of the solution, the network is reassembled by means of the matrices. A full description of the formulation has been given by Brewitt-Taylor and Johns (1977).

In addition to a correct formulation of the finite difference problem without the errors which were noted in the Jones and Pascoe (1971) method, the other advantages of the Brewitt--Taylor program are

Table 2.1

Some Two-dimensional Numerical Model Studies

Method	Worker	Comments
1. Finite Difference	Jones and Price (1970)	Induction response over model continental-oceanic interface. E and H-polarisation cases.
	Jones and Pascoe (1971)	Induction response over a general conductivity structure for E & H-polarisation cases. Computer programs published.
	Williamson et al. (1974)	Stated the corrections required for variable grid spacing in Jones and Pascoe (1971) formulation.
	Losecke and Muller (1975)	E & H-polarisation responses for overhanging high-resistivity structures. Model geoelectric sections constructed.
	Brewitt-Taylor and Weaver (1976)	A new finite-difference formulation presented with corrections for the errors in Jones and Pascoe (1971) formulation. Method thus suitable for both uneven grid and general conductivity variations. Model response over an embedded anomaly compared with results using Williamson et al (1974) and Jones and Pascoe (1971) method.

Table 2.1 (continued)

Some Two-dimensional Numerical Model Studies

Method	Worker	Comments
	Praus (1976)	Model response over dipping conductivity boundaries. E and H-polarisation cases.
2. Finite Element	Reddy and Rankin (1973)	Model response over sloping conductivity interface, E and H-polarisation cases.
	Kisak et al (1975, 1977)	Both E and H-polarisation responses obtained for a vertical fault model.
	Kaikkonen (1977)	Both E- and H-polarisation responses over dipping conducting sheet with and without conductive overburden, Audio-frequencies used.
3. Transmission Line Analogy	Swift (1967)	Model studies of resistivity anisotropy in S.W. United States were carried out. Theoretical apparent resistivity curves over a vertical contact presented.

Table 2.1

Some Two-dimensional Numerical Model Studies

Method	Worker	Comments
	Wright (1969, 1970)	Model E- and H-polarisation apparent resistivities arising from inhomogeneities were calculated. A model for the Rhine Grabben was presented and the need to combine both E and H-polarisation data for a realistic interpretation was stressed.
	Peeples and Rankin (1973)	Model studies of a buried graben in West Canadian sedimentary basin used for the interpretation of MT results. Model principal apparent resistivities and pseudo-sections presented.
	Brewitt-Taylor and Johns (1977)	The two-dimensional induction problem was first formulated by means of equivalent electrical network and solutions to the numerical equations involved were obtained by the method of diakoptics. The results obtained for an embedded anomaly were the same as in Brewitt-Taylor and Weaver (1976) but there was a considerable saving in computer time and storage.

i) The reduction in program array size as the problem is not tackled as a whole but through division into subnetworks.

ii) The ability to store subnetwork results for repeated use in subsequent problems which contain the same subnetwork. Depending on the nature of the problem, this may result in a considerable time saving.

A description of the program commands and their execution is given in PROGRAM INPT, an unpublished program manual written by Brewitt-Taylor.

Essentially, the diakoptic program consists of two parts, the preparation program, INPT and the arithmetic program, ARITH as shown schematically in Fig. 2.7.

Program INPT was used for the preparation of the problem specification file. This contained the commands for the execution by ARITH, the second program. Some of the important specifications and commands were

a) The selection of the mode (E or H-polarisation) of the problem.

b) The specification of the period, the field components, the unit and the geometry of the grid and media properties - relative permittivity and permeability and conductivity.

c) The boundary conditions

d) The Section command which specified the limits of the diakoptic sections and caused a note to be made of corresponding solutions and their disc file locations. The correctness of the sectioning was also checked by this command.

e) The Solution command caused all diakoptic sections to be assembled together and provided the solution of the field equations.

f) The Print command caused some or all of the field solutions to

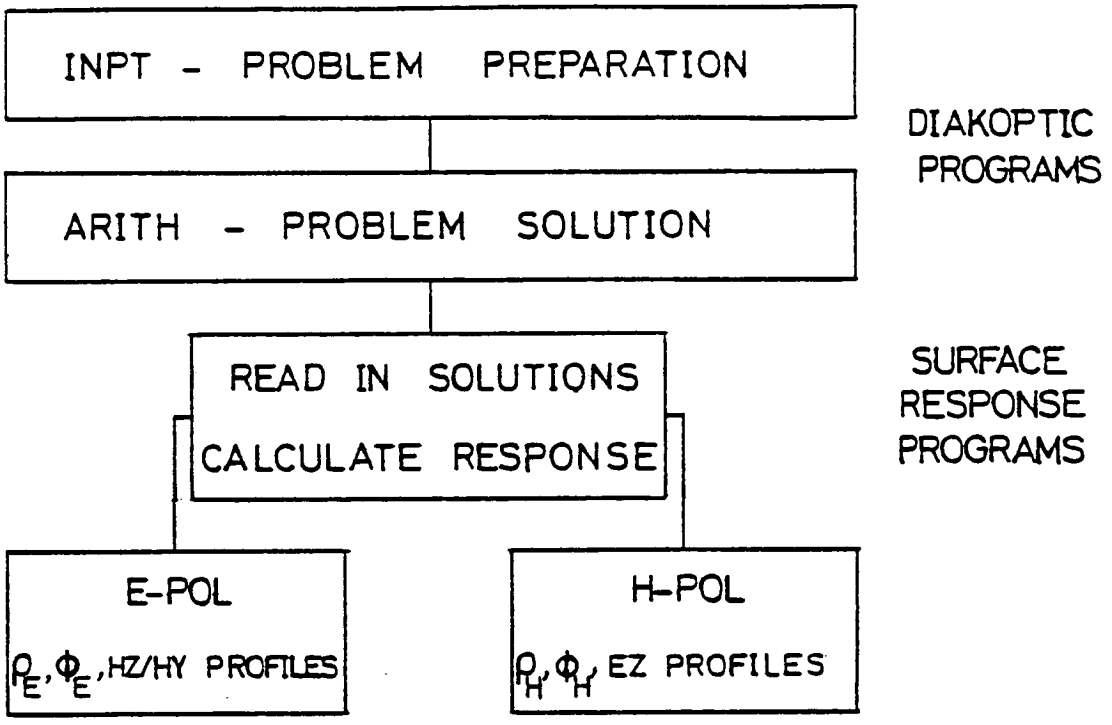

Fig.2.7 Scheme for two-dimensional modelling procedure.

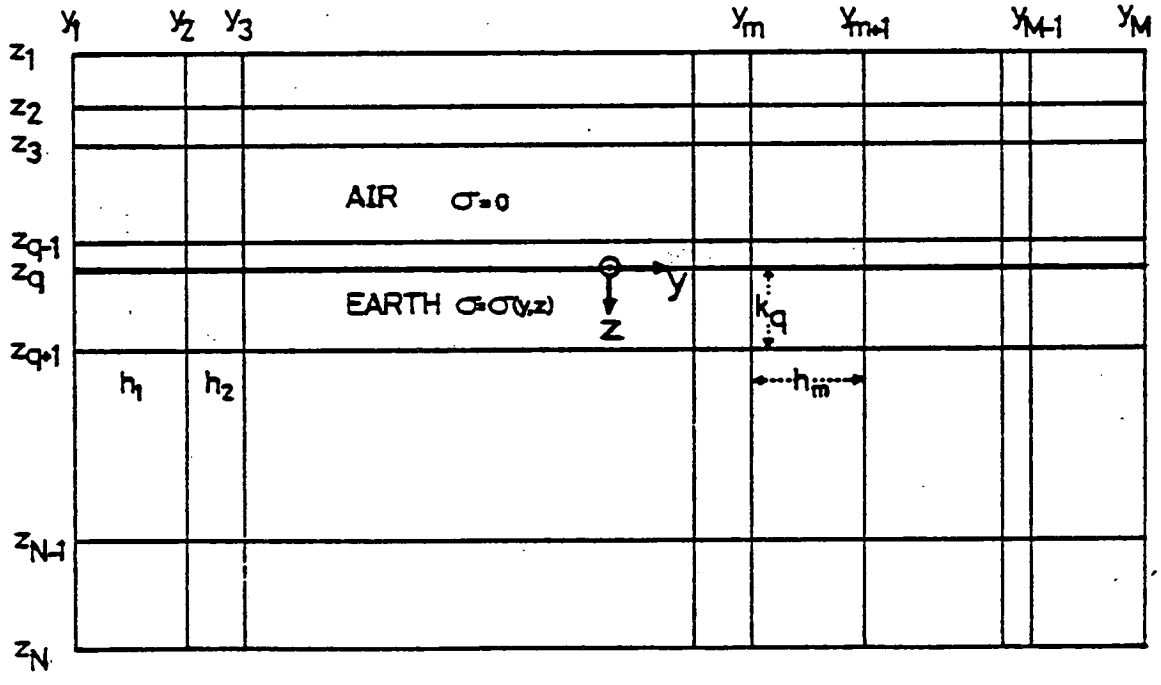

Fig.2.8 The grid for Two-dimensional modelling.

be printed out as complex numbers or as amplitudes and phases.

Program INPT could also be used to read in problem specifications and commands which were accepted in a previous run and also had facilities for copying, deleting or altering the specifications to produce a new command file. This was useful in the modelling exercise since re-entry was not required each time the problem was altered slightly. The second program ARITH accepted the commands from INPT and checked that the specified sections cover the entire problem without overlap before execution could continue. It also printed out the field values.

2.5.4 Calculation of Surface Response Functions

i) The Conductivity Model and Grid

In order to extract field quantities from the output of the two-dimensional program and calculate the surface response, it was necessary to understand the way the conductivity model and grid had been set up in the Brewitt-Taylor and Weaver (1976) formulation. The latter is now discussed briefly using the same notation as in the reference to that work.

The problem area is a rectangular cuboid with sides formed by the x, y, z coordinates as defined in Section 2.1. In each coordinate direction, a series of grid planes divide up the problem area into elementary rectangular cuboids. The relative permittivity, ϵ_r and permeability, μ_r and the conductivity, σ of the material are specified for each of these elements. In the two-dimensional problem, these properties do not vary in the x-direction. The grid planes need not be evenly spaced. Fig. 2.8 shows the yz-plane and a mesh of M*N nodes with the corresponding grid planes going into the paper.

Variable node spacings are defined by

$$h_m = y_{m+1} - y_m$$

$$k_n = z_{n+1} - z_n \qquad (1 \leqslant m \leqslant M-1,\ 1 \leqslant n \leqslant N-1)$$

Further, z_q is assumed to be zero so that the nodes corresponding to q are on the Earth's surface. The region $z<0$ is free space where $\epsilon_r = \mu_r = 1$ and $\sigma = 0$.

The conductivity values are specified at the centres of the rectangular elements of the mesh so that $\sigma_{m+\frac{1}{2},n+\frac{1}{2}}$ is the conductivity at the point

$y = y_m + h_m/2$ and $z = z_n + k_n/2$ for $1 \leqslant m \leqslant M-1$ and $q \leqslant n \leqslant N-1$.

ii) E-polarisation Mode

The field components involved are Ex, By and Bz. The first component, Ex is calculated and printed out by the diakoptic program. From equations 6.9 and 6.10 of the Brewitt-Taylor and Weaver's paper , Bz at the Earth's surface is given by

$$(B_z)_{m+\frac{1}{2},q} = (E_{m+1,q} - E_{m,q})/iwh_m \qquad 2.52$$

and $(By)_{m,q} = To[T1 - T2 - (T3 + T4)T5]$ 2.53

where $To = ik_q k_{q-1}/w(k_q + k_{q-1})$; $T1 = E_{m,q+1}/k_q^2$

$T2 = E_{m,q-1}/k_{q-1}^2$; $T3 = 1/k_q^2 - 1/k_{q-1}^2$

$T4 = iK_{m,q+\frac{1}{2}}$; $T5 = E_{m,q}$

and $K = w\mu\sigma$

Using equation 2.14, the apparent resistivity $\rho_{//}$ and its phase can be calculated. The real and imaginary parts of Hz/Hy profile across the model can also be calculated.

iii) The H-polarisation Case

The field components involved are Ey, Bx and Ez. For this case, equation 2.12 in the paper shows that on the Earth's surface,

$$B_{m,1} = 1, \text{ a constant.} \qquad 2.54$$

Hx is calculated and printed out by the diakoptic program. Ey and Ez are calculated in the following manner.

From equation 7.9 in the paper, Ey is given by

$$(Ey)_{m,1} = T6(H_{m,2} - 1) - T7 \qquad 2.55$$

where $T6 = 1/(\sigma_{m,1}\ k_1)$ and $T7 = \frac{1}{2}iwk_1^*1$

From equation 7.8 in the paper, the vertical component of the electric field is given by

$$(Ez)_{m+\frac{1}{2},n+\frac{1}{2}} = (H_{m,n+1} + H_{m,n} - H_{m+1,n+1} - H_{m+1,n})/2h_m\sigma_{m+\frac{1}{2},n+\frac{1}{2}} \qquad 2.56$$

Brewitt-Taylor and Weaver have discussed in detail the difficulties and errors that can arise in the finite difference formulation of a problem which involves the most general configuration of conductivity boundaries of the type considered by Jones and Pascoe (1971). The authors pointed out that more useful and correct information is provided by application of the central-difference formulae away from regions of possible sharp variations in the conductivity. For this reason, the magnetic field component in the E-polarisation case and the electric fields in the H-polarisation mode are evaluated at the points (m+1/2,n+1/2) rather than at the nodes (m,n).

To supplement these Brewitt-Taylor programs, two computer programs were written by the author to evaluate and plot the profiles of the two apparent resistivities with their phases and the ratio Hz/Hy. The complete two-dimensional modelling procedure, used in this study, is illustrated schematically in

Fig.2.7.

2.5.5 Some Model Results

The procedure outlined in Section 2.5.4 has been used to calculate induction responses over some geological structures of types expected in Northern Scotland. In each of these models, the half-space extends from y=-500 to 500km and z=0 to 800km. The strikes of the anomalies are infinite along the x-axis. In the figures, only the profiles between ±120km have been plotted. For Figs.2.9a and b, this horizontal distance corresponds to about halve a skin-depth and about four skin-depths in Fig.2.9c. These model responses indicate the following points.

a) The H-polarisation MT response delineates the vertical boundaries of the anomaly better than the corresponding E-polarisation parameter. This is so because Ey varies discontinuously across conductivity boundaries while Ex is continuous.

b) Both the apparent resistivity and phase data are complementary and should be used together as far as possible for interpretation.

c) The Hz/Hy amplitude ratio is also sensitive to the vertical boundaries of the anomaly and should be used together with the resistivity data for interpretation.

Both the real and imaginary parts of the Hz/Hy ratio vanish on the axis of the anomaly. They can thus provide information on the strike of the anomaly.

For deeper conductors e.g. Fig.2.9(a), the real part is larger than the imaginary part of the ratio. For surface anomalies (Figs2.9b and c) the imaginary part is nearly as large as the real part of the ratio over the anomaly and both vanish at

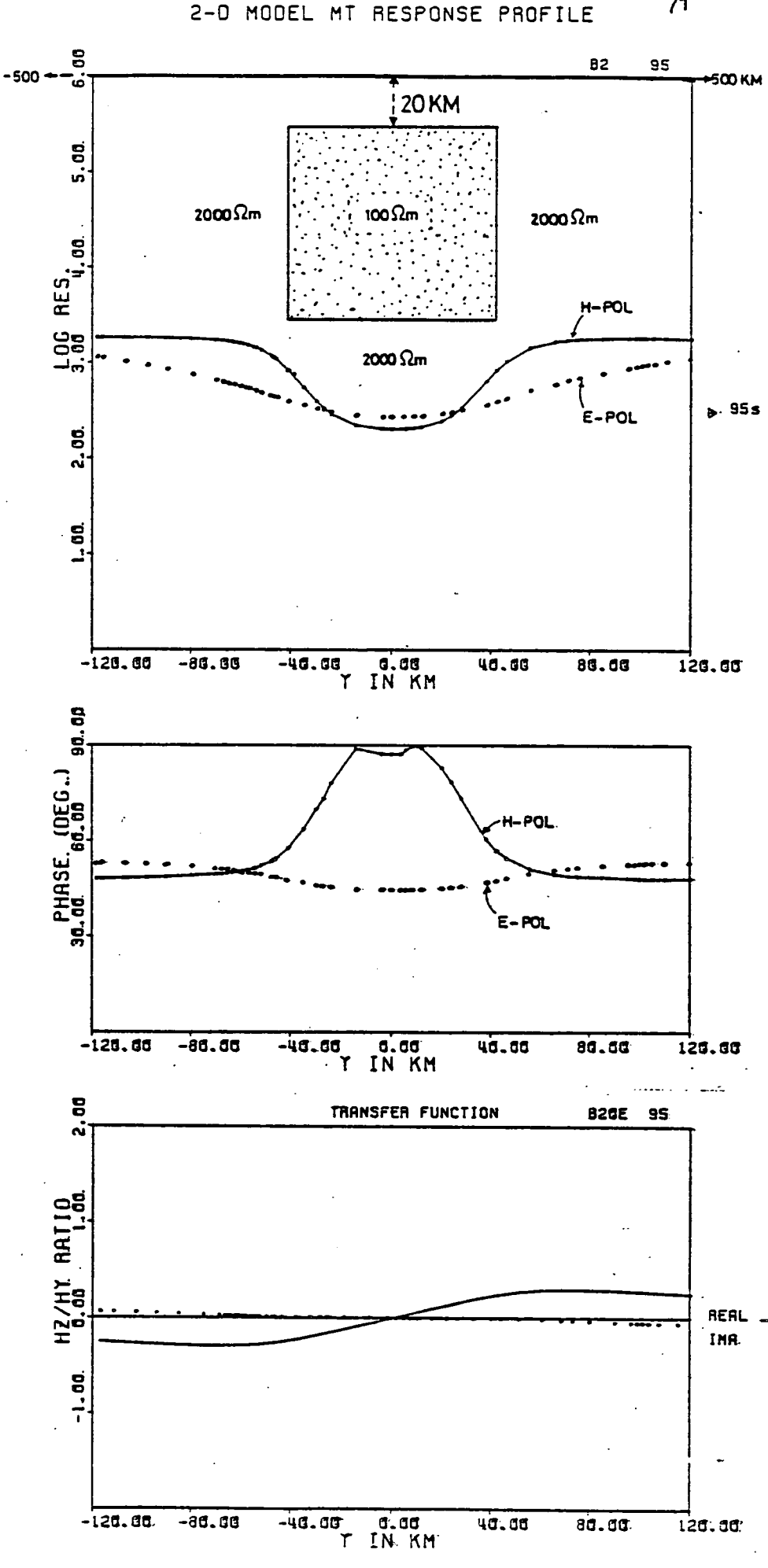

Fig.2.9 Some two-dimensional model profiles (a) - A buried conductor.

T = 95 s

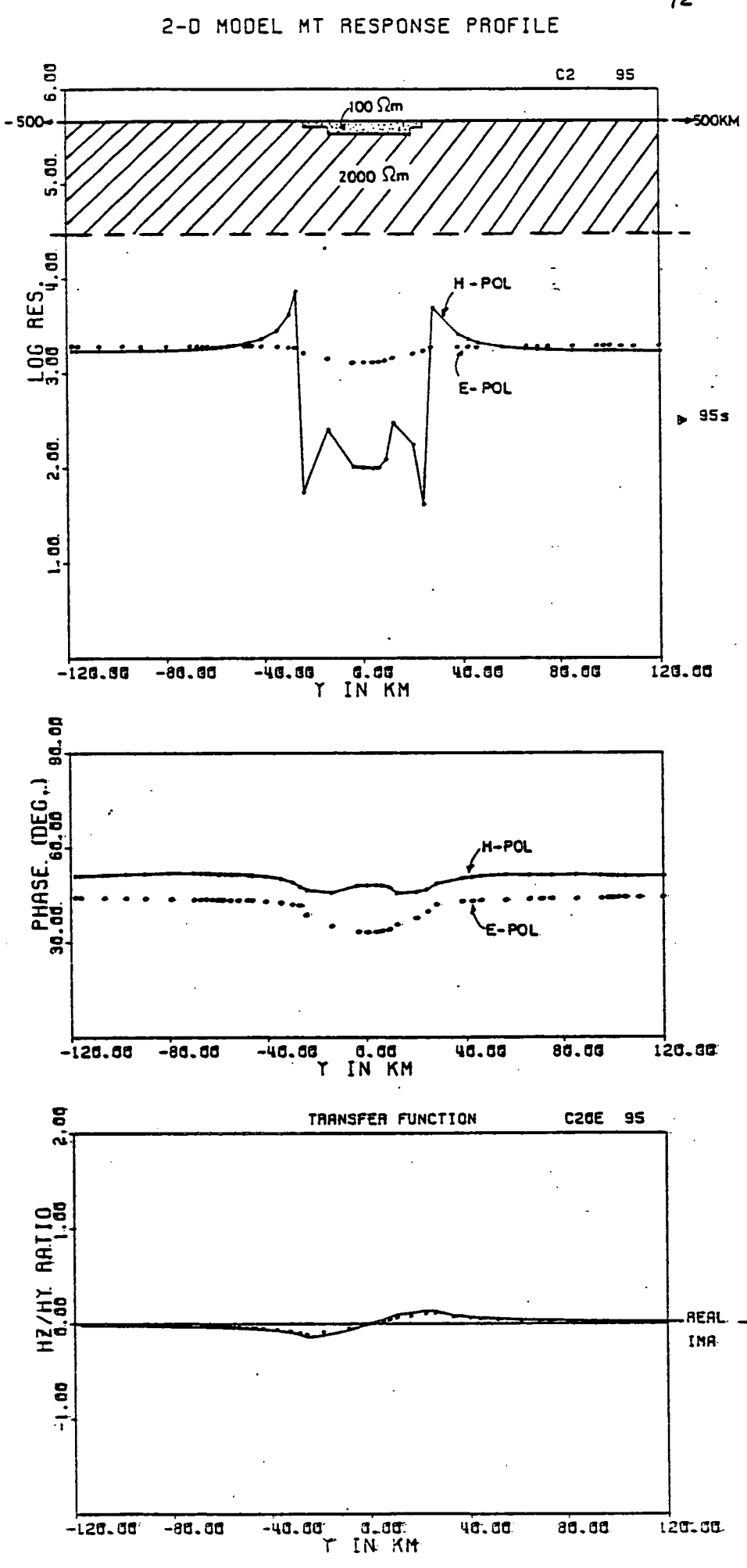

Fig.2.9b A valley with a conductive infill.
T = 95 s

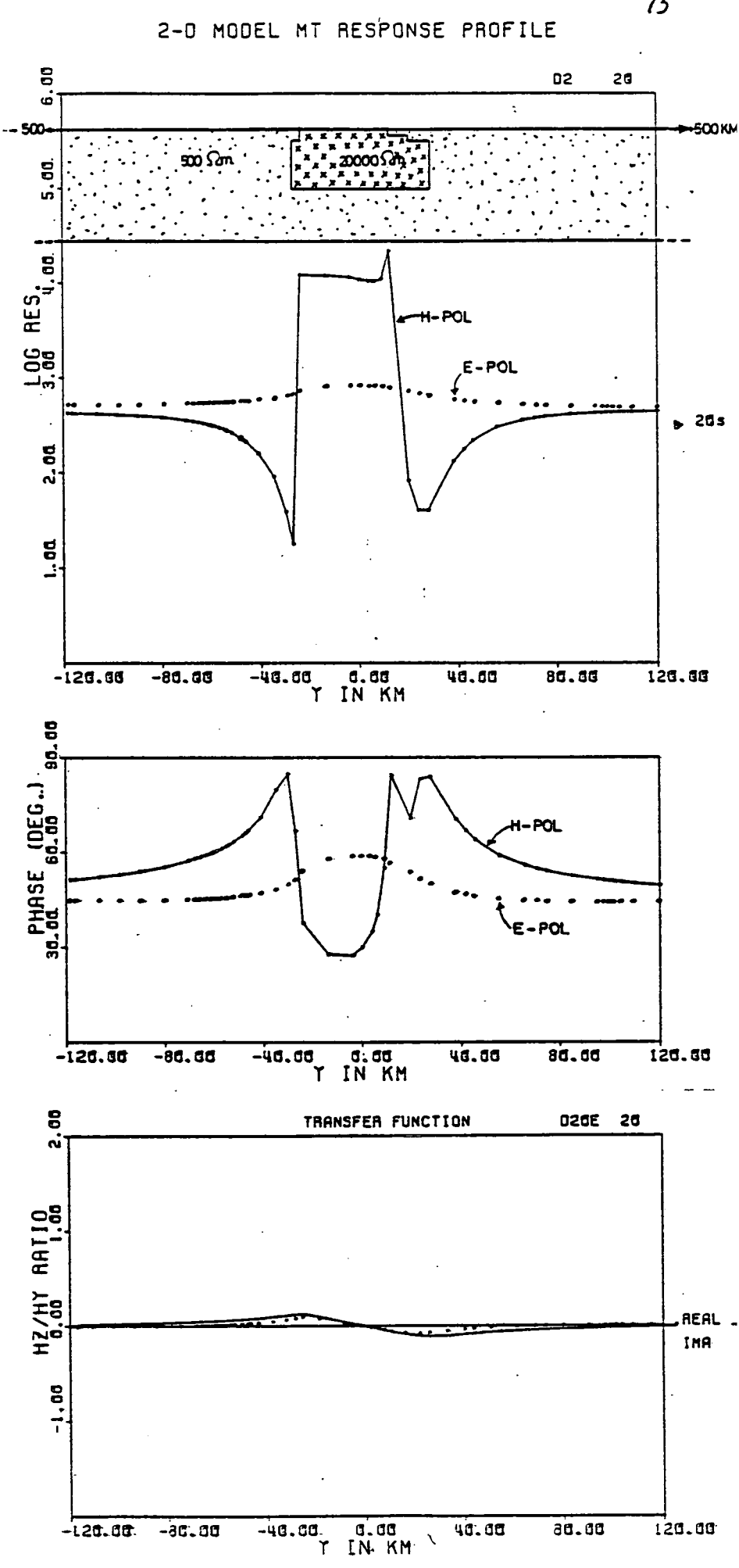

Fig.2.9c A resistive intrusion.
T = 20 s

a few skin-depths from the anomaly.

2.5.6 Perturbation of Regional Two-dimensional Conductivity Structure by local Inhomogeneities

Haak (1972) has suggested that some observed distortions of magnetotelluric response functions in two-dimensional geoelectric structures may be due to the diversion of regional induced currents by small local inhomogeneities near the measurement site. He further suggested that such distortions can be studied by the following analysis.

i) The measured electric field components Ex and Ey are rotated numerically till directions are found for which there is minimum correlation between the two components.

ii) Two directions α and β, for which the correlations between Ex and Hy and between Ey and Hx maximise, are then determined by rotating Hx and Hy numerically. For a two-dimensional structure,

$$\alpha \sim \beta = \pi/2$$

Where there is distortion by local anomalous bodies, α and β will no longer be orthogonal. The analysis is referred to as Haak's Min-Max analysis in the scheme for event analysis in Fig.4.4.

Haak (1978) has considered further the relationship between the azimuth of the electric field and thin conductivity inhomogeneities of different geometries near the Earth's surface. Figs.2-.10a, b, c and d illustrate the results of his model calculations. These diagrams demonstrate how the 'preferred direction' of the electric field or the azimuth of the major impedance from closely-spaced MT sites can be used to delineate qualitatively the boundaries of a local anomalous conductivity structure.

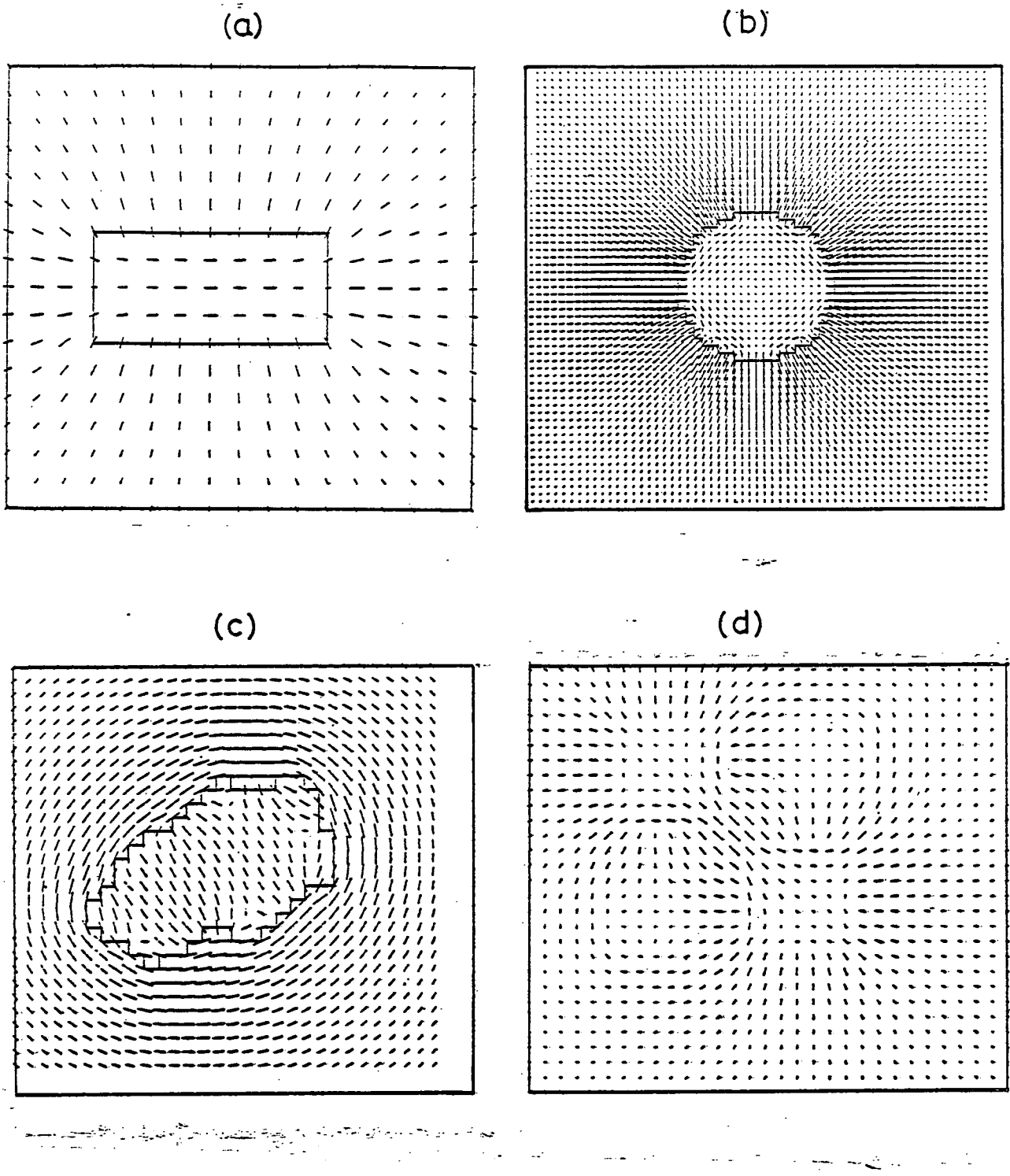

Fig.2.10 Results of Haak's model calculations for 'preferred' directions of the electric field.
(a) - Embedded rectangular plate
(b) - Circular disc
(c) - A poorly conducting insert
(d) - Four embedded squares - two more conducting and two less conducting than the host medium.
(Haak, 1978).

2.6 Three-dimensional Modelling

The two-dimensional modelling methods in Table 2.1 assume that the conductivity structure has a strike direction along which there are no changes in the electrical properties of the structure. In addition, idealised shapes for conductivity anomalies are often assumed to facilitate numerical solutions. Although useful information about regional conductivity anomalies have been provided by such models, large magnetometer array studies and closely-spaced MT surveys have shown that for most regional induction studies, three-dimensional structures are encountered. A realistic interpretation of regional geoelectric data must therefore include some consideration of the pertubation of a regional two-dimensional structure by localised inhomogeneities and the three-dimensional nature of real anomalies. In this section, a review of the few three-dimensional numerical and analogue modelling studies of conductivity anomalies is given.

2.6.1 The Choice of a Three-dimensional Numerical Method

Weidelt (1975) has rightly observed that the paucity of numerical solutions to the three-dimensional induction problem is not due to difficulties with the mathematical formulation but to the large computer storage and the time required for the solution. These two factors must therefore be considered in the choice of a method for three-dimensional modelling.

As in the two-dimensional case, the induction response of a finite three-dimensional conductivity anomaly embedded in a uniform half-space can be studied by solving Maxwell's equations subject to certain boundary conditions which require the anomalous field to vanish at infinity. There are four main approaches

in the literature for the numerical solution of the three-dimensional problem, the fourth method being particulary suitable for thin anomalies near the Earth's surface. The four methods with the corresponding domains over which the problem is solved are illustrated schematically in Figs.2.11a,b,c and d.

In the first method (Fig.2.11a), the problem domain includes free space and the edges of the rectangular cuboid are placed as far away as possible from the anomaly. Jones et al (1972, 1978) and Lines and Jones (1973) have used this approach.

In their finite difference formulation, the domain was divided by a three-dimensional grid mesh and Maxwell's equations were then solved by iteration. Because of the large domain, the storage and computer time requirement for this method are prohibitive. The general three-dimensional model considered by Jones and Pascoe (1972) and the model responses are shown in Fig.2.12a,b and c.

In the second method, there is a reduction in the domain as shown in Fig.2.11b. Only the cuboid which contains the anomaly is considered. Fields outside this cuboid are expressed as a surface integral in terms of the tangential component of the anomalous electric field along rs and ut. At the vertical boundaries, ru and st, approximate boundary conditions are applied and Maxwell's equations are then solved in the same manner as in the first method. Weidelt (1975) has presented an outline of this approach to the solution of three-dimensional problems.

Fig.2.11c illustrates the drastic reduction of the problem domain in the third method. Maxwell's equations are reduced to an integral equation for the electric field. The volume integrals are taken over the anomalous domain only. The method is particu-

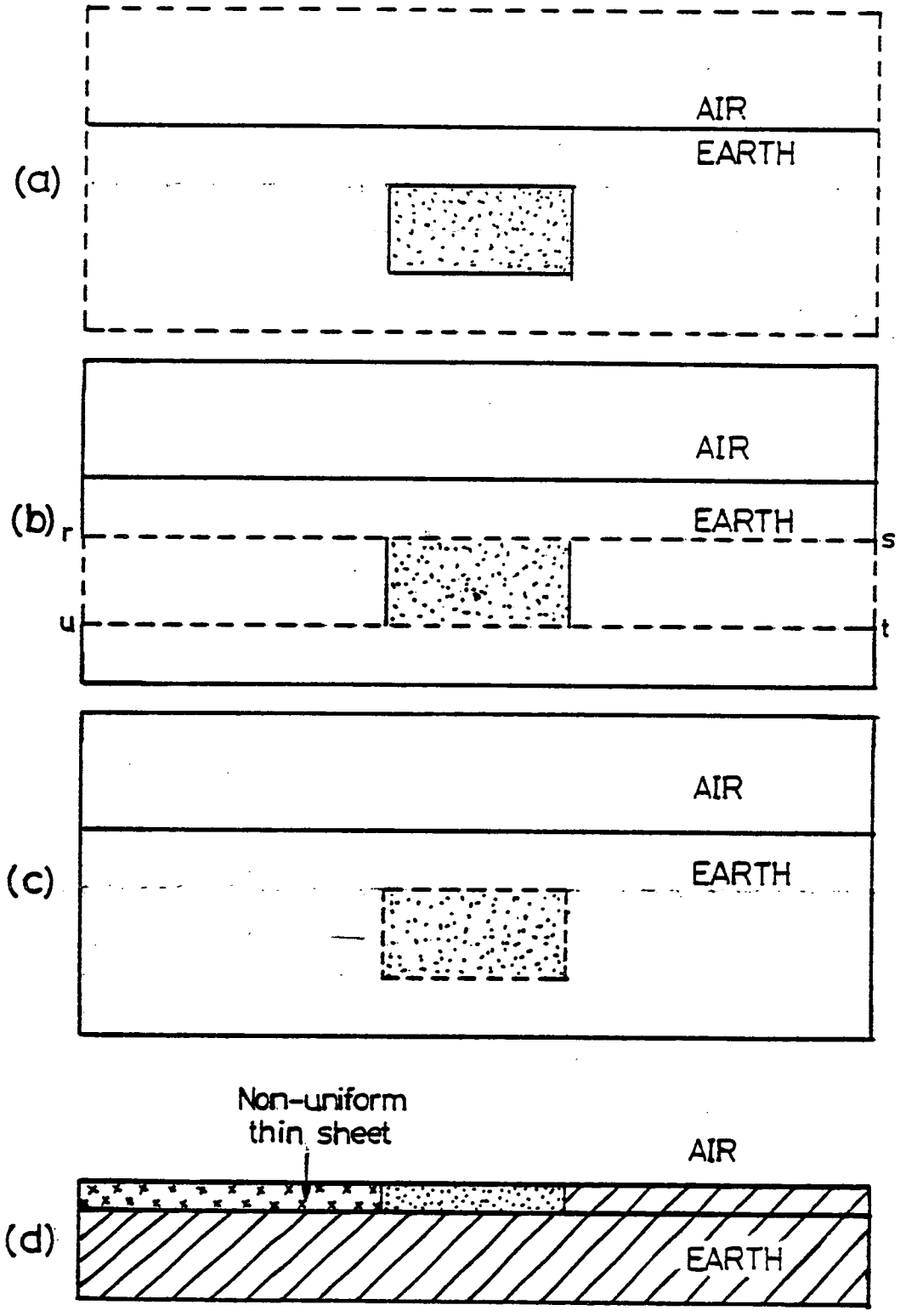

Fig.2.11 Domains for three-dimensional modelling.
(a) - Domain used by Jones and Pascoe (1972)
(b) - Domain dicussed by Weidelt (1975)
(c) - Domain used by Weidelt (1975).
(Broken lines indicate the problem domain)
(d) - The thin sheet model

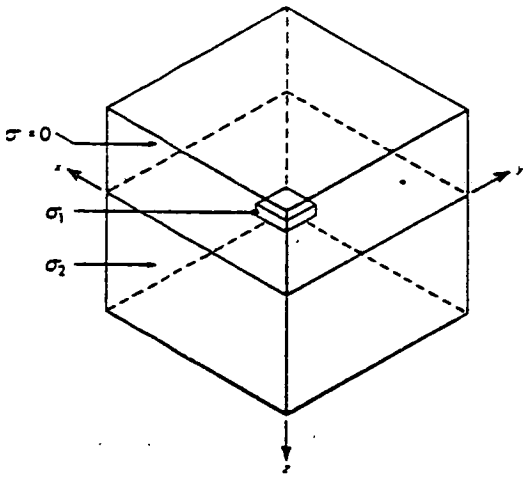

(a) The general three-dimensional model. $\sigma = 0$ represents free space.

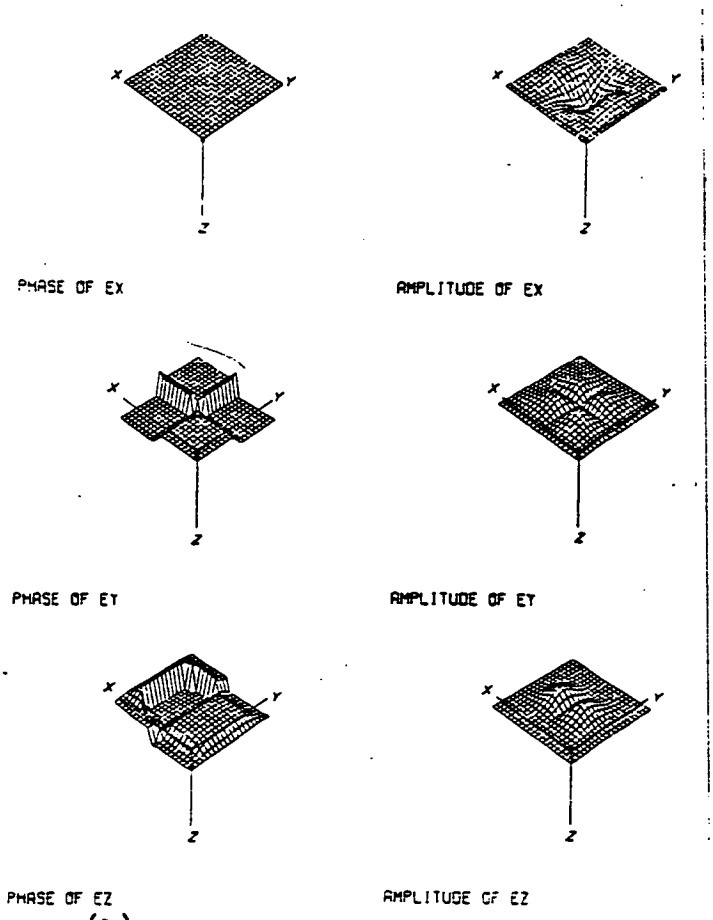

(b) ($\sigma_1 > \sigma_2$). Electric field component amplitudes and their phases.

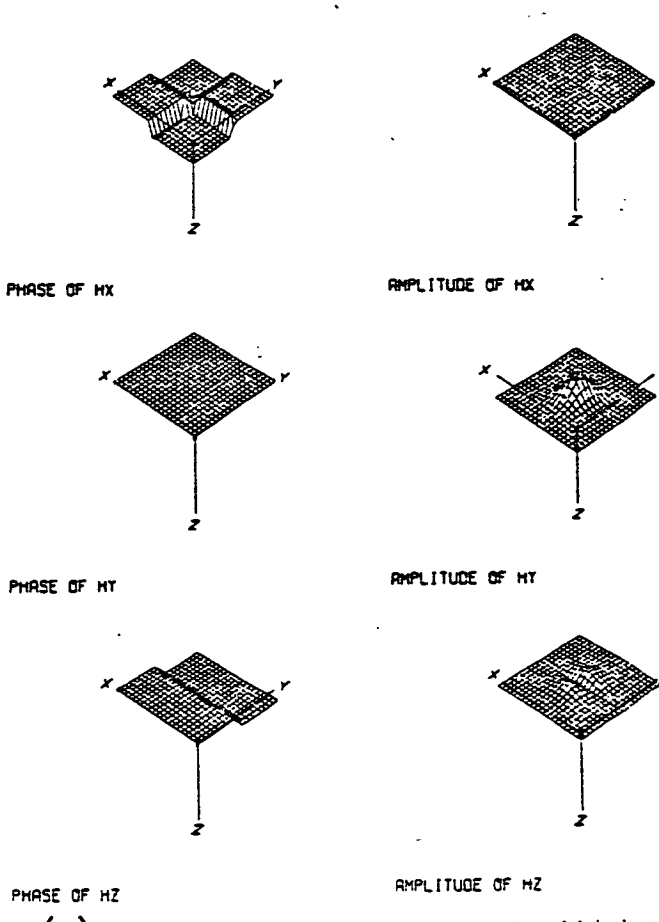

(c) ($\sigma_1 > \sigma_2$). Magnetic field component amplitudes and their phases.

Fig.2.12 General three-dimensional model results of Jones and Pascoe (1972).

larly suitable for small anomalous bodies as the solutions to the integral equations involved require considerable computer time. The method was developed for a finite three-dimensional anomaly in a three-layer medium by Raiche (1974). Weidelt(1975) has also used the method to study the response of a rectangular anomalous body of dimension 50*25*10 km and resistivity 1 ohm m embedded just below the surface of a uniform half-space of resistivity 10 ohm m.

If the anomalous zone is confined to a surface layer, it is possible to construct a model Earth which is made up of a uniform conducting half-space overlain by a thin sheet of variable integrated conductivity representing the anomalous domain. This approach is therefore known as the Thin Sheet Approximation and is the fourth method currently used for three-dimensional modelling. The advantages of the approximation in three-dimensional modelling includes the much desired reduction of the dimensions of the numerical grid as well as the reduction of the electric field components used in the calculations from three to two. The thin sheet formulation was first introduced by Price (1949) for studies of induction in the oceans. For regional induction studies, Vasseur and Weidelt (1977) adapted the method for use in their model studies of the Northern Pyrenean conductivity anomaly. From their study, the anomaly was attributed to a conductive channel between the Atlantic Ocean and the Mediterranean Sea.

A similar formulation has been used by Ranganayaki and Madden (1980) but their 'generalised thin sheet' is a compound sheet made up of a resistive thin sheet under the conductive thin sheet.The resistive sheet represents a resistive coupling of the

surface layer to the mantle of a real Earth.

Weaver (1979) and Dawson and Weaver (1979b) have presented a new formulation of the thin sheet method. Their formulation can be used for studies of all types of conductivity model subject to the conditions required for the thin sheet approximation to be valid as discussed by Weaver (1979). Field equations are solved analytically above and below the non-uniform sheet. The domain over which numerical methods are applied is the sheet itself (Fig.2.11d). This method will be used for three-dimensional model studies of the British Isles (Weaver, personal communication).

2.6.2 Analogue Modelling

Geophysical parameters can be simulated in the laboratory using certain scaling conditions (Dosso, 1973) for the study of electromagnetic induction response of three-dimensional structures. The scaling conditions require a typical continental land of conductivity 0.00063 S/m to be represented by saturated salt solution of conductivity 21 S/m while sea water of conductivity 3.6 S/m is represented by graphite of conductivity 120000 S/m. A uniform inducing source field of period 300s can be simulated by alternating current of frequency 30 kHz in two parallel wires suspended above the salt solution. A typical model description for the study of induction in the British Columbia coastal region including Vancouver Island has been published recently by Nienaber et al (1979).

In analogue models, apart from the advantage over numerical models, of using an artificial source of known geometry, three-dimensional anomalous bodies of intricate shapes can be simulated in some detail. There is however the problem of a limited number

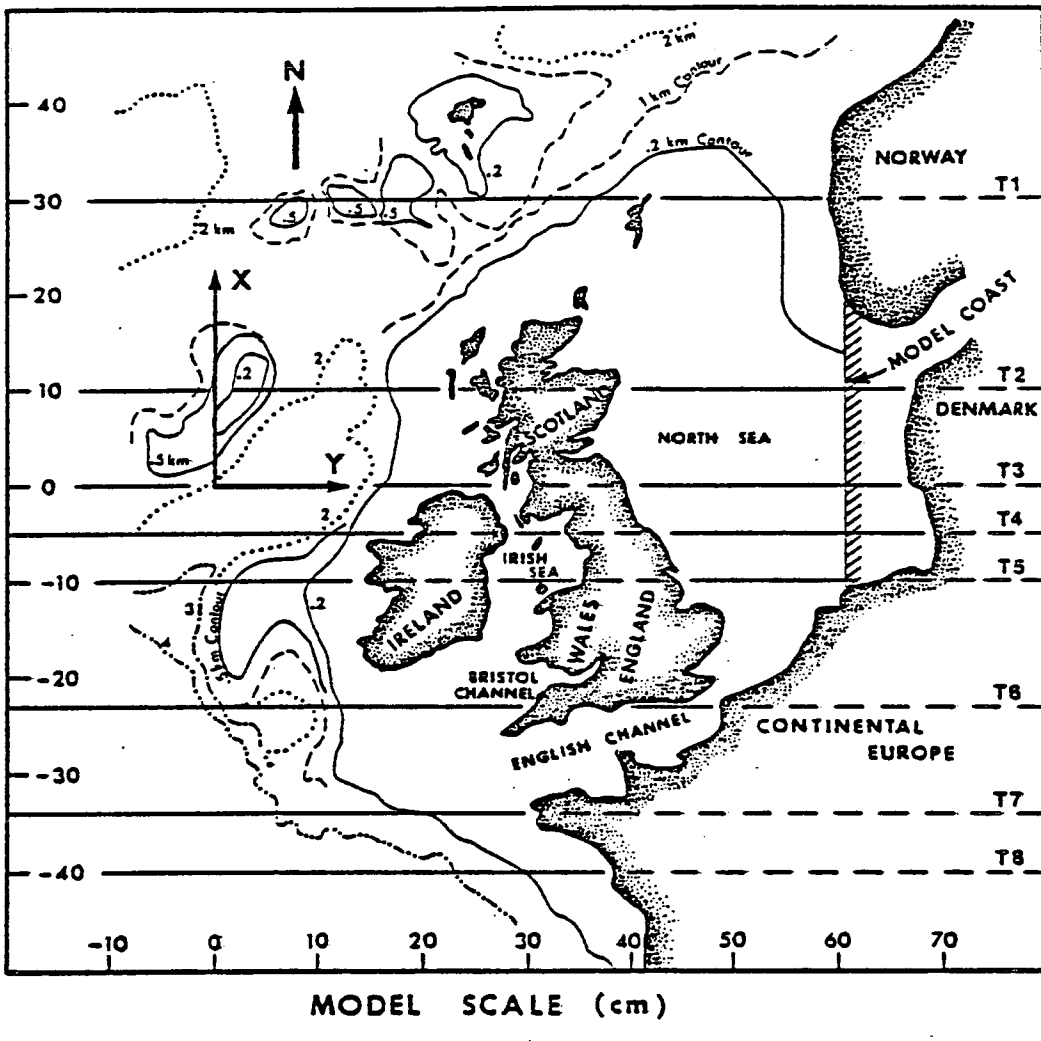

Fig.2.13 Simplified analogue model map of the British Isles. (Dosso et al, 1980).

of model materials suitable for the simulation of the known conductivities of rocks.

Dosso et al (1980) have carried out an analogue model study of induction around the British Isles. Their analogue model map is shown in Fig.2.13. The conductivity values used were the same as the typical values already stated for land and sea water and the period of source field variation was equivalent to about 30 min. The results of traverse T2 across Northern Scotland is compared with numerical and experimental results for the region in Chapter Six.

CHAPTER 3

MT FIELD MEASUREMENT

In this section a brief description of the component units of the MT measurement system which was used in Northern Scotland will be given. The calibration of the system and the logistics for the fieldwork are discussed and a map showing the location of the measurement sites is given.

3.1 The MT Instrument System

A block diagram of the measurement system is shown in Fig.3.1 and a brief description of the main units is given.

3.1.1 The Magnetic Field Sensors

The magnetometer which was used for the magnetic field measurements was designed by J. Jolivet and was produced by Societie Eca, Paris. The subsequent modification of the sensor to its present form has been described by Albouy et al. (1971).

It is essentially a suspended magnet instrument with the moving part immersed in a liquid of the same density as the magnetic needle. This protects the suspension against shock. In addition, a feedback device, with a compact optical system which includes a photoresistor, is built into the sensor for field variation detection. From its design, a field change of 1nT across the sensor is expected to produce 0.5mV output from variations of periods greater than about 5 seconds.

The setting up of each sensor for the measurement of the three magnetic field components during a survey has been described by Rooney (1976). Prior to the fieldwork in Northern Scotland, the sensors were usually buried in a box just below the

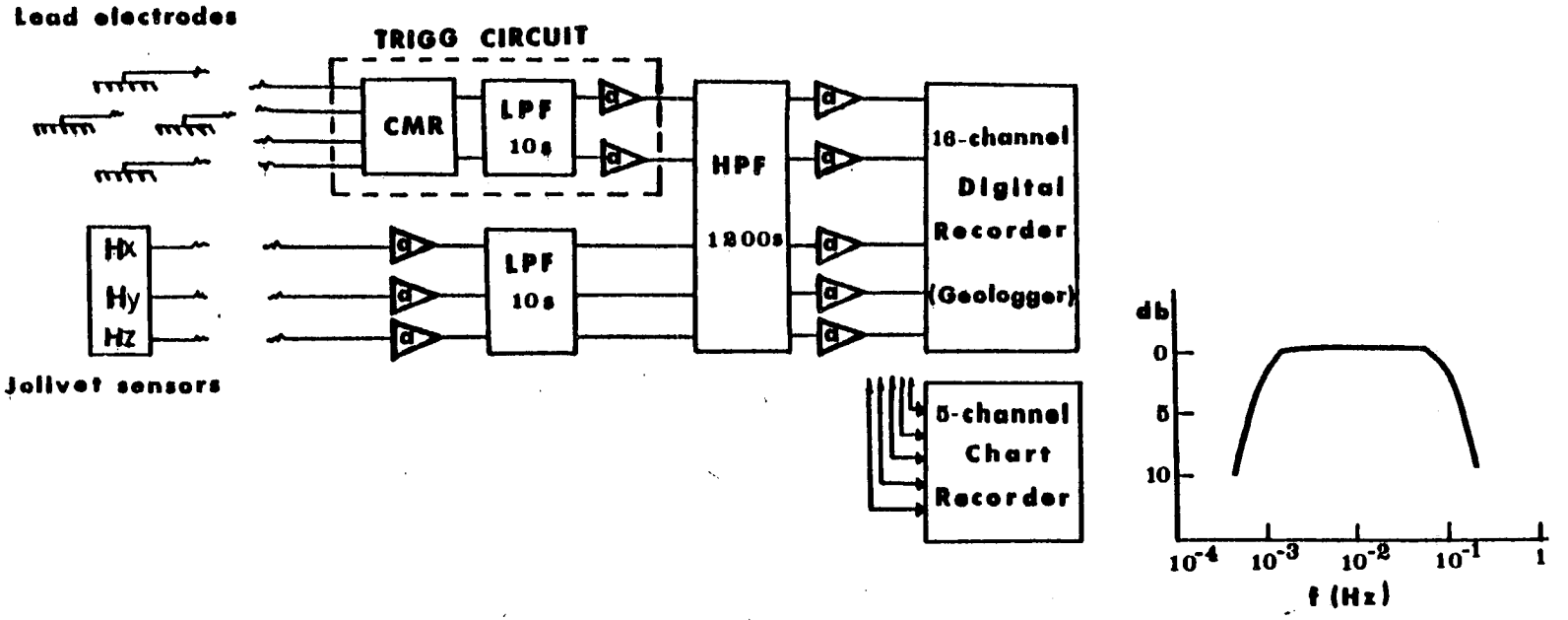

Fig.3.1 A block diagram of the MT system.

earth's surface for protection against wind, noise and temperature gradient. At sites where the surface geology makes digging trenches difficult, as in some parts of the present study, burying three sensors would require additional labour with loss of data acquisition time and increased retrieval time . Therefore during the pre-fieldwork testing of the MT system, a new method of insulation which did not involve burying was tried out.A sensor was placed in a wooden box which was carefully lined and covered with thick layers of polystyrene. Additional insulation and protection against wind and animals was provided by covering the insulated system with a large fibreglass cistern which was firmly pegged to the ground. A second sensor was insulated by burying and then operated in parallel for comparison with the former. The resulting records of field variation were similar from visual examination indicating that the new method of insulation was satisfactory.

The output signal from the sensor was amplified ten times usually using a Keithley microvoltmeter. The signal was then filtered using a band-pass filter designed for -3db points near 10 and 1200 seconds. A second stage of amplification (1 - 100) was added for accurate recording on the Geologger digital recorder. The signal was monitored simultaneously on a chart recorder.

3.1.2 The Electric Field Measurement

Hollow cylindrical lead electrodes designed in the manner described by Jones (1977) were used for the electric field measurements. The electrodes were buried so that their tops were at about 0.5m below the surface of the earth in order to avoid

significant temperature variations. A cross-shaped array was used at all sites except at two sites where the available area made an L-shaped array more expedient. The electrodes were usually aligned in the magnetic NS and EW directions, located by means of a magnetic compass. Electrode separation of 50m to 100m was found to be adequate. The signal cables were made of heavy duty 3-core mains flex and all connections were carefully insulated with several layers of lasotape to avoid unwanted earthing of the leads.

The telluric signals from the electrodes were amplified and band-pass filtered using a circuit originally designed by Trigg (1972). The filters were designed to have -3db points near 10 and 1200 seconds as in the magnetic system. The essential parts of the electronic circuit in the system have been described by Rooney (1976). A second stage of amplification (1 - 100) was added in order to facilitate accurate digital recording .

3.1.3 The Recorders

Both analogue and digital recording on cassette tape were made simultaneously at each site. A 5-channel Watanabe potentiometric recorder was used for the analogue recording. A medium chart speed of 7.5mm/min. was commonly used especially during the second phase of the fieldwork in 1978 by which time the digital records had been found to be satisfactory. As chart recording was undertaken primarily for monitoring purposes attention was concentrated on the acquisition of digital records.

The N.E.R.C. Geologger (Valiant, 1976) was used for the digital recording on cassette tapes.The Geologger consists of a 16 channel Datel logger with the necessary interfacing and

interconnections carried out by Valiant. Channel 0 is ignored, channels 1 - 4 have sensitivities ± 10V and the remaining 11 channels have sensitivities of ±5V. Channel 15 is used for recording hour time marks which are internally generated by a quartz crystal timing chain. The Geologger runs on a 50 Hz mains but it also has a 12V, 1.5AHr lead acid gelled internal battery which automatically powers the recorder when there is a mains failure. The recorder and its front panel controls are shown in Fig.3.2. A detailed and excellent description of the Geologger, operating instructions, the theory and the design of the electronic circuitry are given in the Technical Handbook by Valiant and will not be repeated here; rather, the specifications and the precautions which were adopted in using the instrument for MT data acquisition will be given.

(a) The Tape

Cassette tapes specially recommended for reliable operation on Datel tape transport and cassette reader were used throughout. Both used and unused cassette tapes were kept in their holders far away from the bulk eraser especially when the latter was activated for use.

The option of 64 words per block of the tape was used throughout for recording. This means 64*4*4 bits binary digits per block. The first three bytes of the word represent the input signal and the fourth byte indicates the channel number. Hence a single data point on a channel is completely represented by a 16 bit word. In order not to lose information from this 64-word block, it was necessary to record on 8 channels of the tape in the following order :

channel 1, 6 : Hz

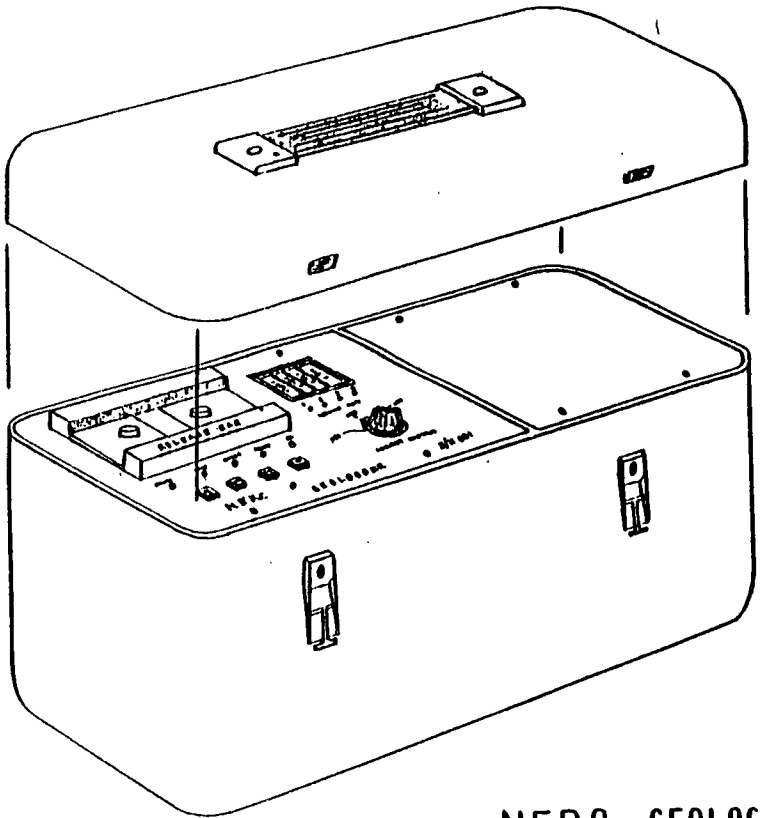

N.E.R.C. GEOLOGGER.

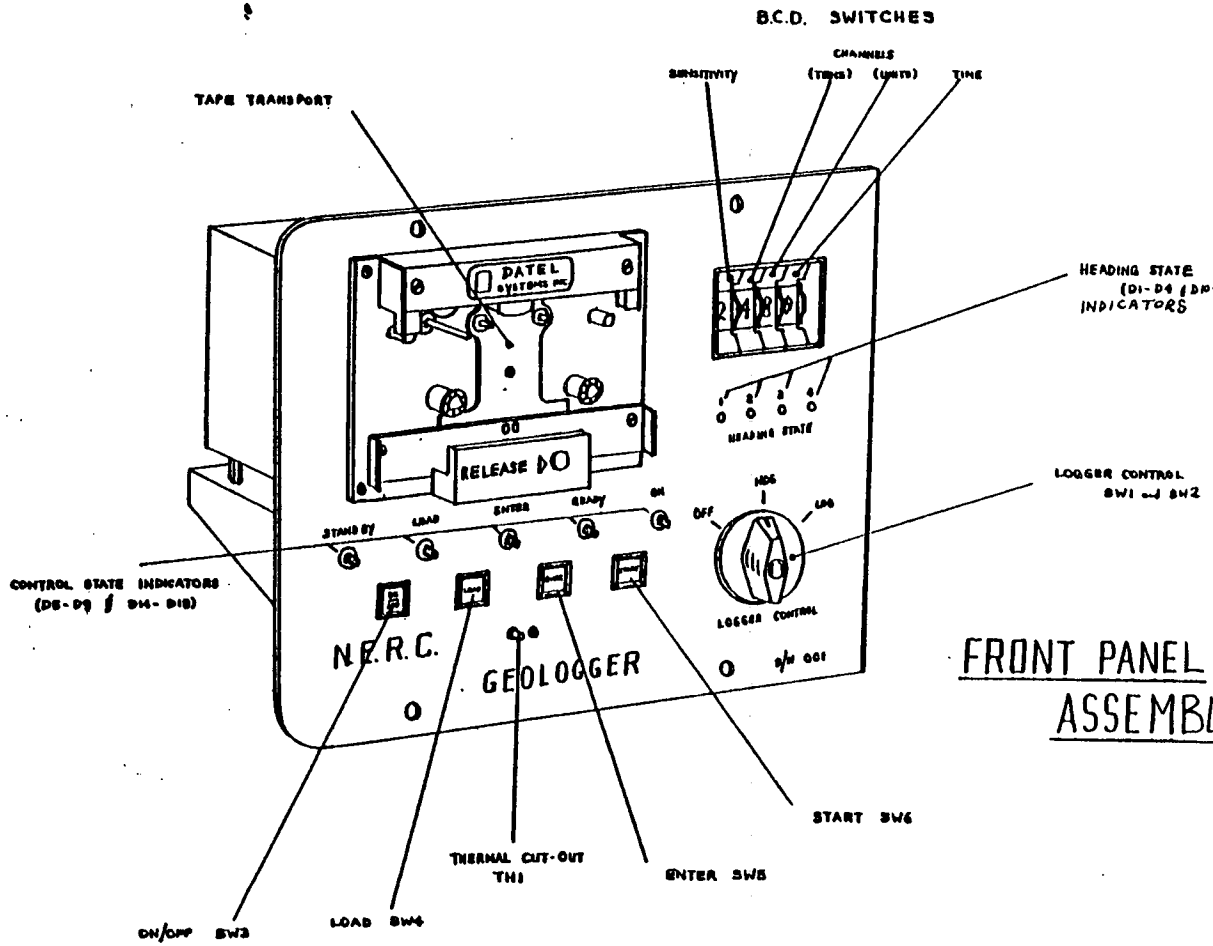

FRONT PANEL
ASSEMBL

Fig.3.2 The N.E.R.C. Geologger. (Valiant, 1976).

2, 7 : Hy

3, 8 : Hx

4 : Ey

5 : Ex

This order was strictly adhered to at all sites. With this arrangement, magnetic variations were recorded at two different sensitivities, ±10V and ±5V and thus small variations could be more accurately retrieved from the more sensitive channels 6, 7 and 8, if necessary. The second advantage of this arrangement was that large variations which would otherwise have overloaded the sensitive channels were still within range on the less sensitive channels 1 , 2, 3 and 4 and thus no information was lost during high magnetic activity. The incoming data was sampled sequentially and written to the channels beginning with channel 1 and the transitional time taken between any two consecutive channels was 0.14s. After successful transfer of the data to storage on computer discs, each cassette tape was bulk erased for use again.

(b) Tape Heading

Four sets of information were written on to the tape while the logger control was on 'ENTER' mode as shown below.

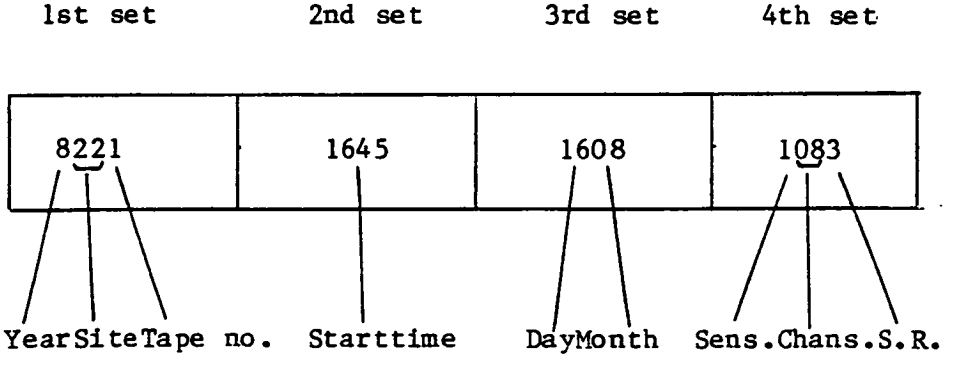

The 4th set of information was very important as it controlled the operation of the logger on 'LOG' mode. It dictated to the memory the number of tape channels and the sampling rate required. Seven sampling rates of 1, 2.5, 5, 10, 30, 60 and 150 seconds were available. A sampling rate of 5 seconds was used throughout. At this sampling rate, each tape lasted for about 20 hours. A visual check was always made to ensure visually that sampling and tape advancement were functioning normally for the first few minutes before the Geologger lid was replaced.

3.2 Instrument System Calibration

The measurement systems used for the telluric and magnetic fields were not absolute instruments systems. It is therefore necessary to calibrate the MT system before and after each field trip. During several weeks of field work, occasional check of the filter-amplifier response was also essential. A brief description of the calibration procedure is given below.

3.2.1 The Telluric System

The telluric system was set up as for field measurements but in place of the inputs from the lead electrodes, a sinusoidal signal of about 1.3mV amplitude from a stable output signal generator (Model HP 3310B) was fed into the two telluric channels as shown in Fig.3.3a. The input signal was measured with a digital voltmeter (Model 7040) and also monitored continuously on one channel of the analogue recorder in order to check on the constancy of the input throughout the calibration.

The frequency was varied between 0.4 and 0.0005 Hz (2.5 to

2000 seconds) and the output from the two telluric channels were obtained for about twenty different frequency settings. For each frequency, an adequate number of complete waves was obtained to limit the uncertainty of the mean amplitude of the output to about 1%. The ratios of the output to input signal for each channel was calculated and the resulting response functions were plotted as shown in Fig.3.3b.

The -3db points for the system were read off the response curves. Further, the gain of the system was deduced from the ratio of the amplitude of the output to input signal and from this ratio, the correction factor for the marked gain of each channel was calculated. Table 3.2 summarises the results for the telluric system characteristics as obtained from these calibration measurements.

3.2.2 The Magnetic System

(a) Calibration of the Helmholtz Coils

Magnetic field variations for the calibration of the magnetic system were produced in the laboratory by using a signal generator and a system of Helmholtz coils. It was therefore necessary to calibrate the coils first before using them. The system consisted of three pairs of X, Y and Z coils with two members of each pair connected in series. Each coil consisted of 144 turns of SWG22 insulated copper wire wound on a wooden square frame. The field produced by the coils was contant in a small cube of side about 10 cm at the centre of the system and was also frequency-independent.

Using a D.C. supply, the field produced by each coil for a given voltage was measured with a Forster Oersted meter (Model

1.104). This was repeated for eight different values between 0 and 8V, the polarity of the voltage was reversed in each case so that two calibration lines were obtained in each case. The output (Table 3.1) of each pair of coils was then obtained from the mean least-square slope.

(b) Calibration of the magnetometer system

The magnetic system was set up in the usual way.The Jolivet magnetometer was set up in its insulating box within the Helmholtz coil system and carefully levelled so that the sensor lay within the cube of constant field at the centre of the coil system. The sinusoidal input voltage to the coils was monitored with a digital voltmeter and also recorded directly on an analogue recorder. The direct output voltage of the magnetometer was measured using a solid state Keithley electrometer (Model 602) and the filtered amplified signal was also recorded. During the calibration exercise, care was taken to use the same system channel and Jolivet magnetometer as was used for field measurements.

As the magnetic system was very sensitive to noise (moving magnetic objects) and vibration, the calibration of the system was done at night and at weekends when the laboratory was not used by many people. As for the telluric system calibration, an adequate number of complete cycles was obtained for each frequency setting to give a mean amplitude with a measurement uncertainty of about 1%. The system response is shown in Fig.3.4b.

3.3 Field Work Logistics

The data collection in this project involved going away from

TABLE 3.1. HELMHOLTZ COILS RESPONSE

COIL	OUTPUT (nT/mV)
X	4.72 ± 0.03
Y	4.05 ± 0.03
Z	3.48 ± 0.03

TABLE 3.2 SCALING FACTORS AND -3dB POINTS

COMPONENT	JOLIVET SENSOR NO.	SCALING FACTOR	-3dB POINTS (S)
HZ	3	1.66 nT/mV	10.0 - 1180
HY	1	1.55 nT/mV	11.0 - 1200
"	5	1.70 nT/mV	"
HX	2	1.54 nT/mV	12.0 - 1180
EY	-	1.00	11.0 - 1200
EX	-	1.00	11.0 - 1200

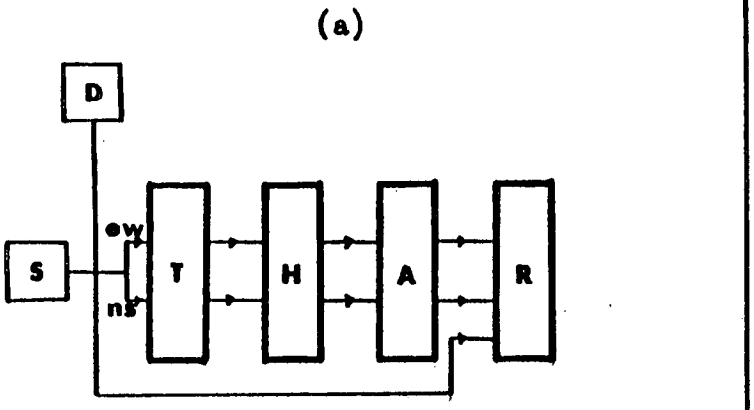

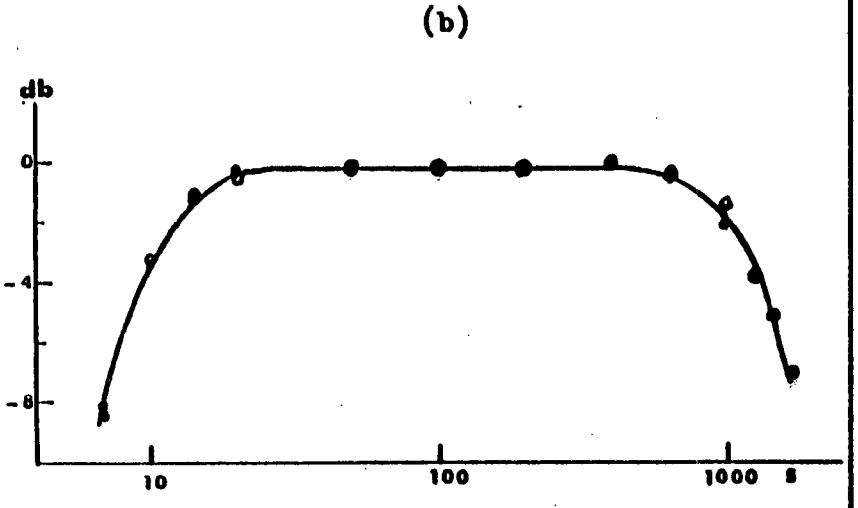

Fig.3.3 (a) A block diagram for the telluric system calibration set-up.
(b) The response of the telluric system.
(ew - o , ns - •)

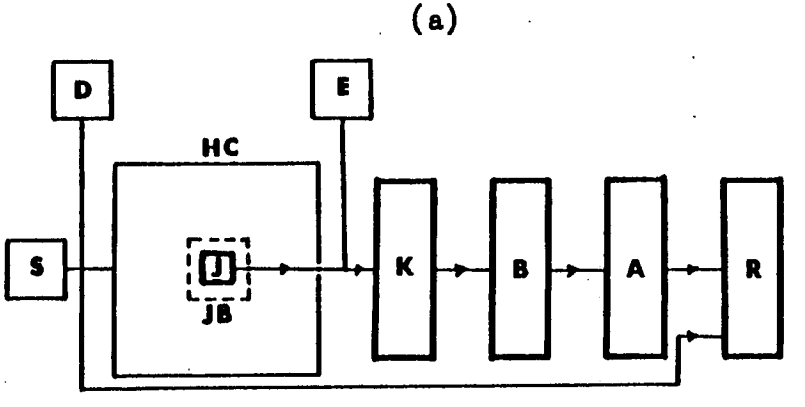

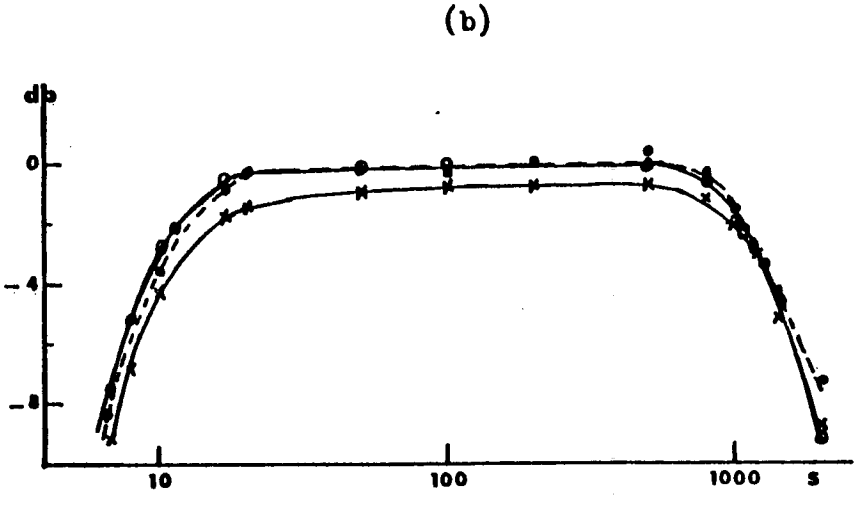

Fig.3.4 (a) A block diagram for the magnetic system calibration set-up.
(b) The response of the magnetic system.
(Hx - × , Hy - • , Hz - o)

S - signal generator; D - digital voltmeter; T - Trigg unit; H - high-pass filter; A - 2nd stage amplifier; R - recorder; HC - Helmholtz coils; J - Jolivet sensor; JB - wooden box; E - electrometer; K - Keithley amplifier; B - band-pass filter.

Edinburgh for several weeks to some areas which were over 200 km away. Hence it was necessary to plan carefully all aspects of the fieldwork beforehand. Under this section, essential aspects of such planning before the trip and the data acquisition, data quality and quantity check and control during the fieldwork period will be given.

3.3.1 Preparation

Once the location of the main MT traverse was chosen with the help of results of previous studies and the geological reports as reviewed in Chapter 1, a tentative time-table was prepared several weeks before the field trip. Trips were planned for the summer period when conditions in Northern Scotland are suitable for MT fieldwork. This time-table included dates, approximate location on a one inch map of the sites to be occupied, addresses, telephone numbers, personel, possible accommodation and the facilities which were expected at or near the sites. It was essential to go out,chose and obtain permission for the use of the land for the first site several days before the field trip. This ensured a convenient start at a location near other possible sites for which permission could then be sought while recording was in progress. The whole system was tested at sites near Edinburgh several days before the field trip to check the satisfactory functioning of component units.

The equipment could just be contained in a long-wheel base landrover. Keeping track of all the items during and after the fieldwork was a problem, hence a checklist (Appendix 1) was prepared after the first field trip in 1977. The list was thereafter found to be very useful. Care was taken to take

adequate estimated stock of consumables like cassettes, charts,-bulbs for magnetometers to avoid loss of days while in the field. It is hoped that this list will be updated from time to time when new MT equipment becomes available.

In 1978, a caravan was acquired. This provided accommodation for three people as well as acting as a field laboratory. It enabled the electronic units to be permanently rack-mounted in the caravan and thus there was considerable time saving in site installation and packing up. However, special care was needed in towing the caravan from site to site in the Highlands in summer. Delicate instruments like the Jolivet magnetometers and the recorders had to be packed and handled carefully during transportation.

3.3.2 Data Acquisition

In this section, the procedure used for setting up an MT site is described. The order of activities was as follows :

(i) Marking of electrode position and digging of the holes for the electrodes; examination of the electrodes; check of the continuity and insulation of the telluric lines; burying the electrodes and laying out of telluric lines; making connections to the different channels.

(ii) Marking out and levelling the locations for the insulating wooden boxes for the magnetic sensors; setting up, aligning and levelling of the magnetometers; checking the insulation and continuity of the magnetic lines.

(iii) Checking all amplifier, filter and power supply connections and connecting the outputs to the chart recorder and the geologger.

(iv) Connecting up the magnetic lines to their channels on the electronic rack.

(v) Connecting up the power source (±6V, with due attention to signs) to the Jolivet magnetometers; 'zeroing' the magnetometers and monitoring of the outputs on the chart recorder.

(vi) Making enteries in the diary. Such enteries included the following :

(a) Date, site name and number

(b) Name, address and telephone number of the site owner and the facilities which were available.

(c) Sketch of the electrode configuration, position of the magnetometers and recording equipment.

(d) The channel numbers or colour of ink used for specific field components; filter bandwidths, amplification factors, f.s.d. and chart speed; tape number and start-time of all recordings. Whenever a subsequent change was made, this was also noted.

(vii) Carrying out a polarity check on the magnetic field channels using a bar magnet of known polarity.

Following these steps, if the preliminary monitoring of the field components on the chart looked satisfactory and the system seemed to be functioning properly, a labelled cassette was loaded on the geologger and digital recording started.

The MT site was then operational. It is pertinent to state at this point that the operations which have been described so far can be carried out successfully by a minimum of two people, one of whom must be familiar with the MT method and the Edinburgh system, in particular. Usually, two or three people could install a site in about 2 to 4 hours depending on the subsoil and the weather conditions at the site.

3.3.3 Data Quantity and Quality

In order to collect adequate and good quality data in as many sites as possible during each field trip, it was essential to examine the analogue record and assess the number of events available for analysis . Such assessment was usually done after about two days of recording depending on the source field activity. About ten events of two hour duration were usually considered adequate for subsequent analyses. Thus, a site was normally occupied for about 3 - 7 days depending on the level of geomagnetic activity and the problems at the site.

Attention was also given to the quality of the MT data during acquisition on site. For this, the analogue recording was essential as there was no other way of monitoring the digital data while in the field. From the analogue record it was easy to see which channels were faulty, noisy, insensitive or overloaded and the necessary corrective measure taken before continuing the recording. Where the site was clearly noisy and unsuitable, it was advantageous to discontinue operation at that site as soon as possible and to move to a new location.

As a precaution, the chosen sites were usually located away from busy roads, high voltage power lines and transformers. The magnetic sensors were set up away from tall trees in order to avoid vibrations during windy conditions. Livestock could also create problems hence fields in which animals were grazing were not very suitable as sites. Typical MT records obtained during the field measurements in Northern Scotland are shown in Fig.3.5.

3.3.4 Sites Occupied

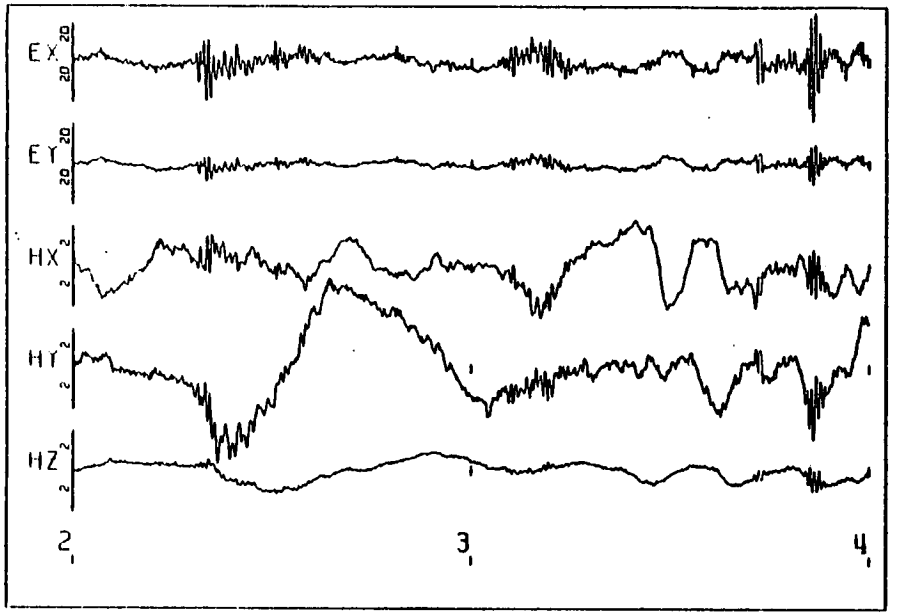

Fig.3.5 (a) Night-time bay-type variation with Pi's.

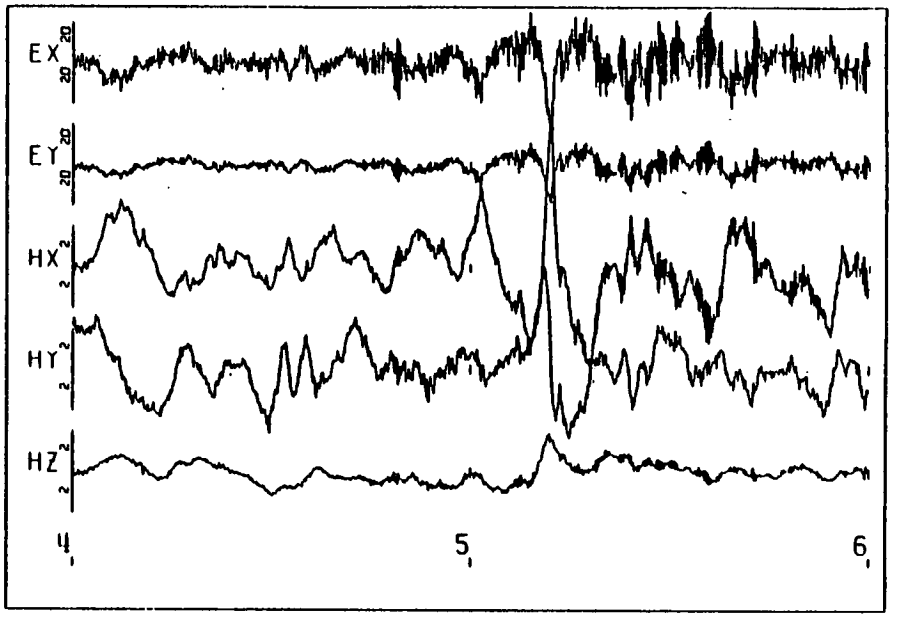

(b)General variation with early morning Pc's.

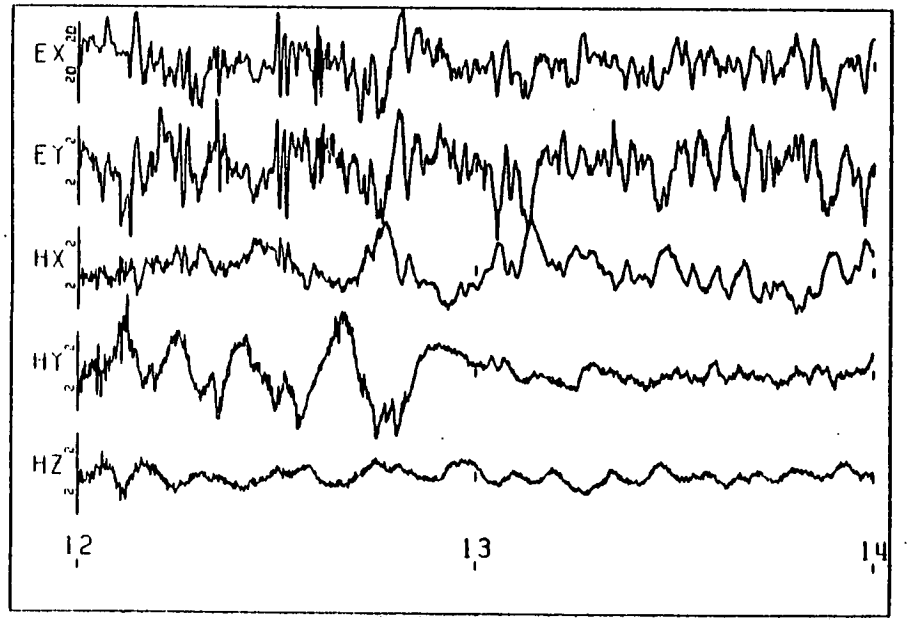

Fig.3.5 (c) A general variation in the afternoon.

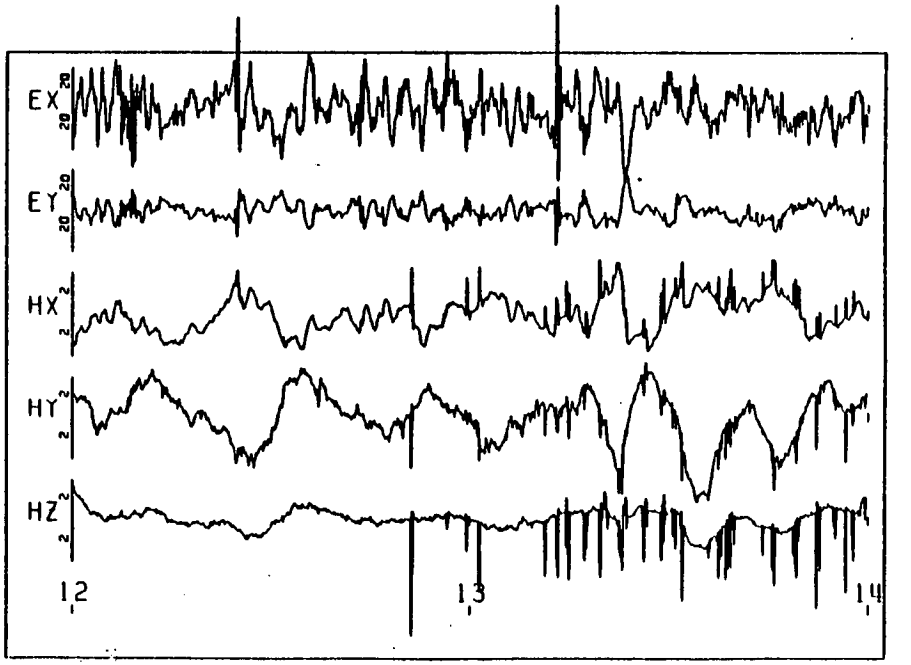

(d) A noisy record

Fig.3.6 MT sites in Northern Scotland.

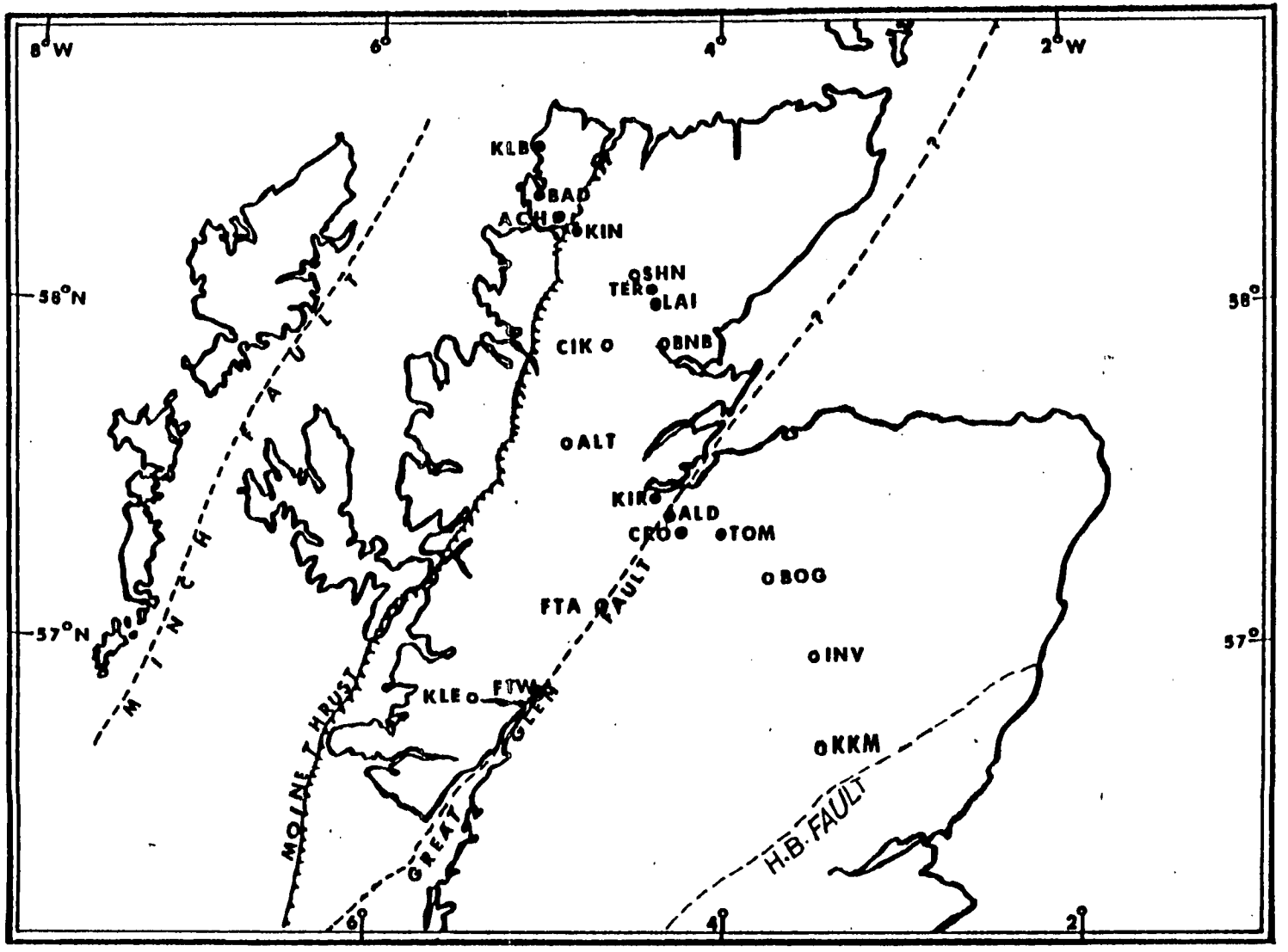

TABLE 3.3 1977-78 MT SITES

SITES		GEOGRAPHIC COORDINATES		DATES
Name	No.	Lat.	Long.	
KIRKHILL (KIR)	02	57.46	-4.40	17 - 21.8.77
BADNABAY (BAD)	03	58.37	-5.05	22 - 27.8.77
KINLOCHBERVIE (KLB)	04	58.48	-5.07	27.8 - 3.9.77
ACHFARY (ACH)	05	58.31	-4.91	5 - 12.9.77
KINLOCH (KIN)	06	58.27	-4.82	9 - 14.9.77
ALDOURIE (ALD)	07	57.40	-4.32	16 - 21.9.77
CROACHY (CRO)	08,10	57.32	-4.25	15 - 21.9.77
TOMATIN (TOM)	09	57.31	-3.99	21 - 23.9.77
LAIRG (LAI)	11	58.01	-4.36	24.9 - 1.10.77
TERRYSIDE (TER)	12	58.07	-4.43	3 - 7.10.77
INVEREY (INV)	13	56.99	-3.52	17 - 22.6.78
KIRKMICHAEL (KKM)	14	56.72	-3.43	24 - 27.6.78
KINLOCHEIL (KLE)	15	56.86	-5.34	28.6 - 2.7.78
FORT WILLIAM (FTW)	16	56.88	-5.04	3 - 5.7.78
FORT AUGUSTUS (FTA)	17	57.14	-4.67	6 - 9.7.78
ACHANALT (ALT)	18	57.61	-4.91	9 - 13.7.78
WEST SHINNESS (SHN)	19	58.10	-4.49	14 - 18.7.78
BONAR BRIDGE (BNB)	20	57.91	-4.31	19 - 21.7.78
CROICK (CIK)	21	57.90	-4.54	21 - 25.7.78
BOAT OF GARTEN (BOG)	22	57.24	-3.74	25 - 28.7.78

The MT sites occupied in 1977 and 1978 are shown in Fig.3.6. Both mains power and a shelter for the equipment were needed at or near the locations of the ten sites occupied in 1977. In 1978, the shelter requirement was unnecessary due to the acquisition of the caravan but field operation still depended on access to mains power supply. This was found to be very reliable throughout the study region. The sites occupied, dates of operation and coordinate reference are given in Table 3.3.

CHAPTER 4

DATA ANALYSIS

In this chapter, we shall be mainly concerned with the processing of the five component electromagnetic field variation data which were collected in the manner described in Chapter Three. A description of the transcription of the cassette tape data into computer compatible format, spectral and coherence analysis will be given. The method adopted for estimating response functions from different events at each site will also be discussed. The primary results of the data analysis will be presented in Chapter Five. Further analysis of these primary results are necessary for a correct interpretation of the data and a more quantitative conclusion on the conductivity-depth structure across the region. The discussion of such additional analysis will be found in Chapter Six which will also deal with data interpretation.

4.1 Data Transcription

The raw digital data were obtained on cassette tapes. For computer processing, it was necessary to transcribe the data into a suitable format. The Edinburgh Multi Access System, EMAS ICL 4-75 computer system was used for the analysis in this study. The different stages involved and the peripheral systems which were used in the processing are shown in the block diagram of Fig.4.1.

The data were read into a PDP11 computer which interfaced into EMAS. On EMAS, the data were edited into store-map files which are compact in structure and also permit fast data access for event selection and replot. Dawes (1978) has described the computer programs which were used for the cassette data transcri-

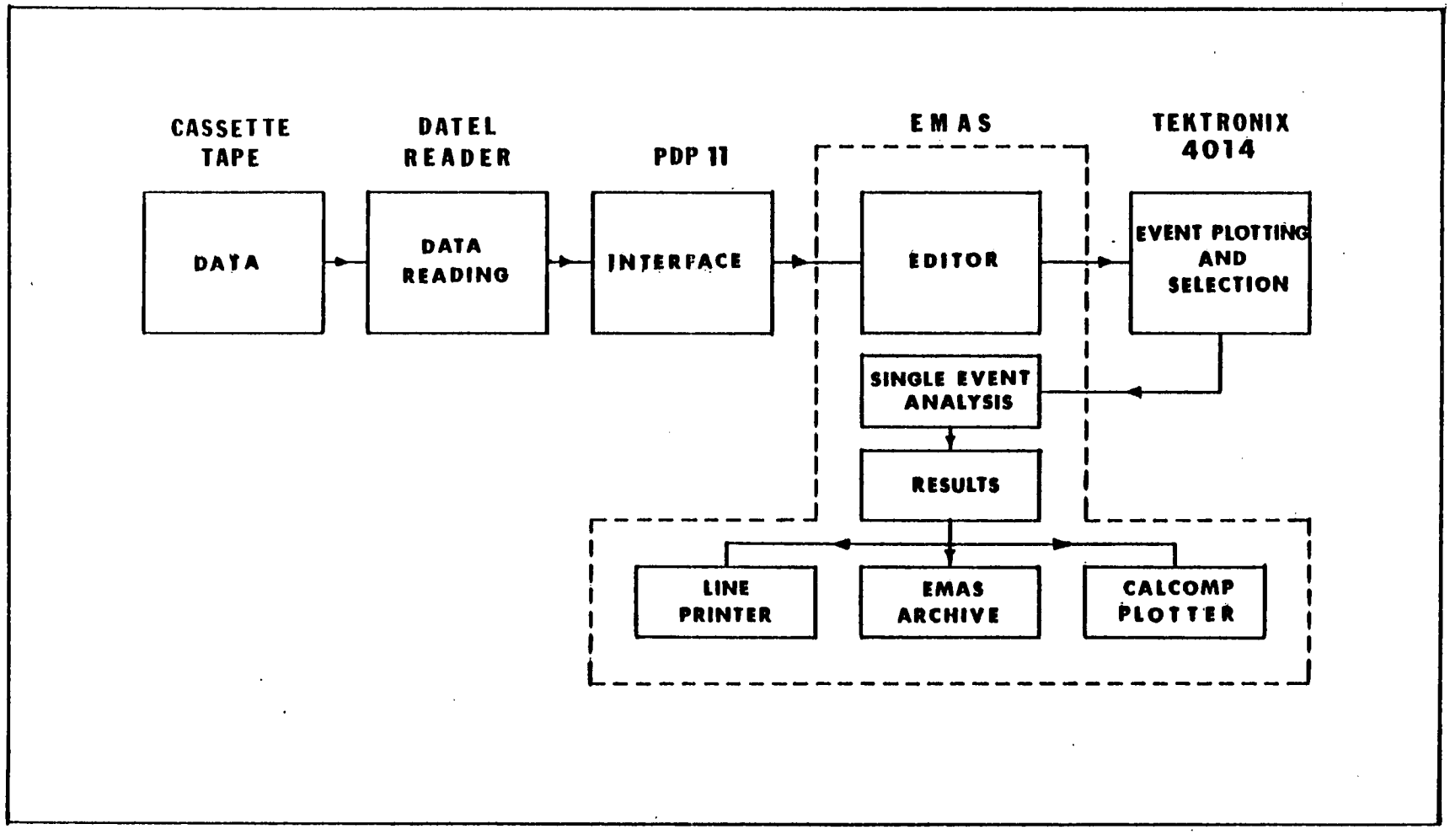

Fig.4.1 A block digram of the MT data editing and processing system.

ption. Before this transcription system was fully developed, transcription of the data to EMAS compatible 1/2" master tapes was done at the Geomagnetism Unit Laboratory,I.G.S.

4.1.1 Event Selection

An 'event' in this context means a section of the recorded signal that was considered suitable for analysis. In order to examine each cassette record before the selection of an event, a Tektronix 4014 console was necessary. The commands for the execution of the event selection Program are explained in the manual written by Dawes who also wrote the programs. The 'visual editing' and the qualifying factors which were considered before accepting a record section as an MT event in this study are discussed below.

For all data from a given site,the following procedure was adopted :

i) The first five channels of the record were replotted on the Tektronix in successive two-hour segments. A brief description of the data on each channel was made on a special event selection sheet and sections which were considered suitable as events were noted.

ii) The above procedure of 'visual editing' was repeated for all data files from the site.

iii) The suitable record sections were re-examined before final selection and filing. Usually, selection of about ten events was aimed at. The following factors determined their suitability.

a) Freedom from noise

From visual examination, it was possible to see sections which were contaminated by artificial variation due to extraneous

noise. See Fig.3.5d for example. Such sections were not selected for analysis.

b) Frequency Content

A balance between short and long period events was maintained as much as possible during the event selection so that mean response functions could be obtained later from a satisfactory number of estimates at all period within the period band of interest.

c) Occurrence Time Distribution

As far as was possible, events from different times of the day were selected. This was done so that any bias due to source field structure on calculated response functions would be minimised on averaging. Events were in general, fairly well distributed over different hours of the day at most sites as shown in Fig.4.2. Distribution was restricted at sites 19 and 21 by noise and at site 15 by limited mains power supply.

4.2 Single Event Analysis

Hermance(1973) has given an excellent review of the different methods for data analysis in electromagnetic induction studies. A description of the essential procedure adopted in this study has been given by Rooney (1976) and was published by Rooney and Hutton (1977). Only a brief outline of the procedure is therefore given in the sections that follow.

4.2.1 Spectral Analysis

The processing of event time series is usually done in the frequency domain. In this study, the fast-fourier transform (FFT), a high speed algorithm for calculating complex Fourier

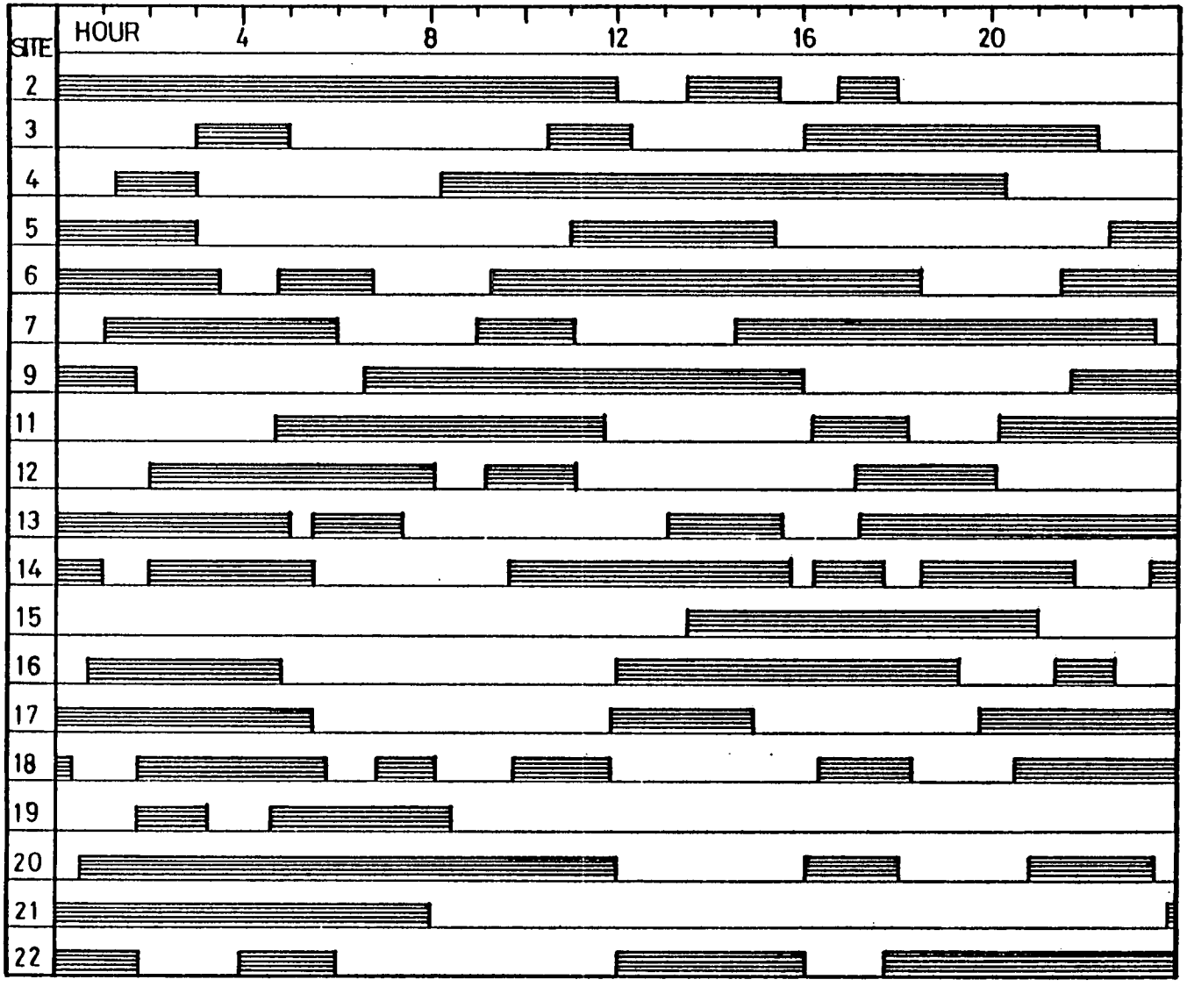

Fig.4.2 Event time distibution.

harmonic coefficients (Cooley and Tukey, 1965) was adopted.

For a signal s(t), defined over the interval $-\infty \leqslant t \leqslant \infty$, the function S(f) given by

$$S(f) = \int_{-\infty}^{\infty} s(t)\exp(-iwt)dt \qquad 4.1$$

is known as its Fourier transform, where $f=w/2\pi$ is the frequency.

However, the signal s (t) which represents an event in this study is a time series of finite length Ts with a sampling interval, Δt of 5s. From equation 4.1, the required Fourier transform in this case can be obtained from an estimate

$$S_T(f) = \int_{-T/2}^{T/2} s_T(t)\ \exp(-iwt)dt \qquad 4.2$$

Jenkins and Watts (1968, p.48) and Kanasewich (1973, p.91) have discussed the effect of data truncation on the evaluation of the spectra in equation 4.2 and have shown that

$$S_T(f) = \int_{-\infty}^{\infty} s(t)w_T(t)\exp(-iwt)dt \qquad 4.3$$

where $w_T = 0, |t| > T/2$

$= 1, |t| \leqslant T/2$ 4.4

is known as a data window and has a rectangular or box-car shape as shown in Fig.4.3a. Equation 4.3 indicates that the processing of a finite length signal, $S_T(t)$ is equivalent to operating on the product of an infinitely long signal s(t) and the data window $w_T(t)$. In the frequency domain, the operation is equivalent to the convolution of the transform S(f) and $W_T(f)$, the kernel or the Fourier transform of $w_T(t)$.

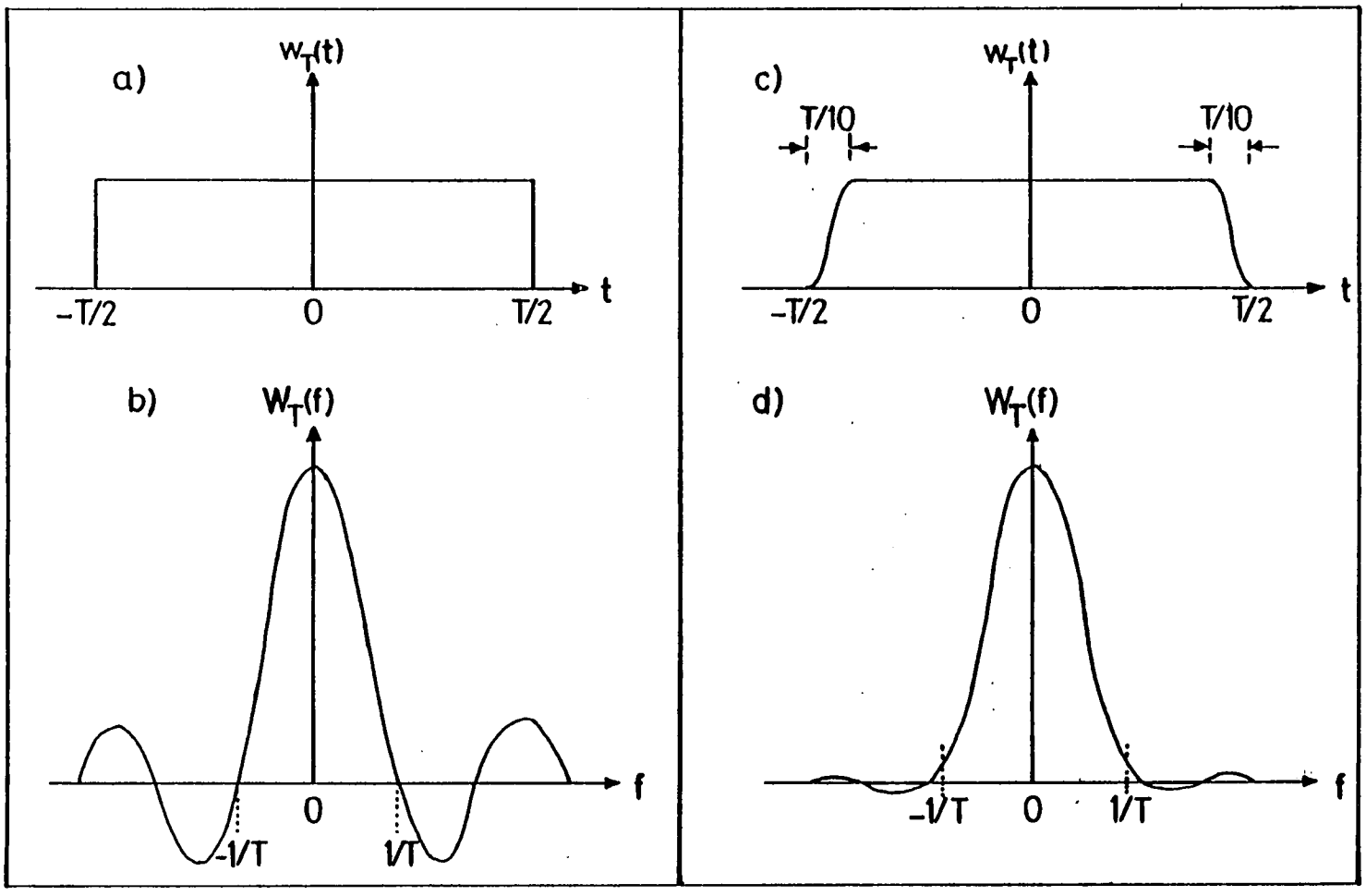

Fig.4.3 (a) The rectangular data window and (b) its spectral window. (c) The cosine taper data window and (d) its spectral window.

$$W_T(f) = \int_{-\infty}^{\infty} w_T(t)\exp(-iwt)dt$$

$$= T(\sin\pi fT/\pi fT) \qquad 4.5$$

A plot of $W_T(f)$ is shown in Fig.4.3b.

4.2.2 Precautions

i) The Nyquist Condition

In the brief discussion of spectral analysis outlined here, it has been assumed that signals of frequencies greater than $1/\Delta t$ have negligible amplitudes. The digitising interval was therefore chosen carefully to satisfy the condition

$$1/2\Delta t = f_N$$

where f_N is the Nyquist frequency or the highest frequency with appreciable power in the record section. If this condition is not satisfied, the spectral estimates are contaminated by high frequency power - an effect known as aliasing, Jenkins and Watts (1968, p.52). As a precaution, the sampling rate of 5s used in the data collection was less than halve the -3db low-pass filter cut-off periods and only averaged response functions at periods of 20s and above were used for interpretation in this study.

ii) Power Leakage Reduction

The raw filter shape in the frequency domain, Fig.4.3b, has large negative side lobes which can cause power leakage into the main lobe. In order to reduce this leakage, it is necessary to taper the time series with a cosine taper over one-tenth of the series length at each end (Bingham et al, 1967). The cosine taper data window and the corresponding spectral window are shown in Figs. 4.3c and d respectively. This window gives a satisfactory

compromise between frequency resolution and leakage reduction which are both essential in spectral analysis.

The spectral window tends to spread the power at any frequency to neighbouring frequencies and therefore spectral estimates can be distorted if power is not evenly distributed over all frequencies in the time series under analysis. As a precaution against such distortion, it is usual to pass the data through a filter in order to obtain a nearly flat spectrum and then to correct the final spectrum for this prewhitening operation (Kanasewich, 1973, p.106). For magnetotelluric analysis, Kurtz (1973) has shown that this operation has no noticeable effect on the response functions. In the present analysis, prewhitening was not therefore considered essential.

iii) Long Period Trends

Long period trends in the data imply the presence of frequency components with periods longer than the length of the time series. Such trends would be non-stationary and would produce large distortions in the computed spectra especially at low frequencies. In the MT data, such trends could be due to slow changes in D.C. levels at the electrodes and the effects of temperature variations on the instrumentation. Although such effects were not apparent in the record sections which were selected for processing in this analysis, the removal of the mean of the data set and its linear trend by the least squares method (Bendat and Piersol, 1971,p.291) formed part of the routine data preparation before Fourier transformation as a precaution against distortion due to trends.

iv) Augmentation of the Data Set

In the Cooley-Tukey fast Fourier transform method, it is

essential that the total number of points in the time series is a power of 2. Each data set was therefore extended to 2048 points by the addition of zeros before transformation into the frequency domain.

v) Smoothing of Spectral Estimates

Apart from the precautions which were taken to reduce leakage and improve frequency resolution, it is essential to have a stable spectrum. Fourier analysis assumes that the signal has a constant frequency and phase. MT signals in practice are not so ideal with the result that the corresponding raw FFT spectra are usually not smooth. Jenkins and Watts (1968, p.230) have discussed the distribution properties of spectral estimates for random signals and have shown that the distribution is chi-squared. The variance of the estimates can be reduced by averaging at each frequency over an ensemble of estimates from different events or by band averaging over a number of neighbouring frequencies (Bendat and Piersol, 1971,p.191). The second method of smoothing was adopted in the single event analysis.

4.2.3 Cross Spectra and Coherence Analysis

Let s(t) and u(t) be two time series and S(f) and U(f), their Fourier transforms. The smoothed autopower for s(t) is given by

$$P_{SS}(f) = \langle S(f)S^*(f) \rangle \qquad 4.6$$

where the asterisk implies the complex conjugate and the brackets the smoothed average.The smoothed crosspower estimate is given by

$$P_{SU}(f) = \langle S^*(f)U(f) \rangle \qquad 4.7$$

The coherence C_{su} between the two signals is defined by

$$C_{su}^2 = |P_{su}(f)|^2 / (P_{ss}(f) P_{uu}(f)) \qquad 4.8$$

where $0 \leqslant C_{su}^2(f) \leqslant 1$ for all frequencies (Bendat and Piersol, 1971, p.80 and p.141).

If $C_{su}^2 = 0$, s(t) and u(t) are uncorrelated; for $C_{su}^2 = 1$, the two signals are correlated.

For MT signals, C_{su}^2 is often greater than zero but less than one. In such a case, one or more of the following explanations are possible :

a) Noise is present in the measurements

b) The relationship between s(t) and u(t) is not linear

c) If u(t) is regarded as an output due to an input s(t), there are other unknown inputs in addition to s(t), the known input.

To illustrate noise effects on coherence, let

$$s(t) = i(t) + n_i(t)$$

$$u(t) = j(t) + n_j(t)$$

where i(t) and j(t) are desired input and out put and $n_i(t)$ and $n_j(t)$ are extraneous noise terms in the signals.

The desired coherence function from equation 4.8 is

$$C_{ij}^2 = |P_{ij}(f)|^2 / (P_{ii}(f) P_{jj}(f)) \qquad 4.9$$

The measured coherence, using equations 4.7 and 4.8 is

$$C_{su}^2 = |P_{ij}(f)|^2 / [P_{ii}(f) + P_{ni}(f)][P_{jj}(f) + P_{nj}(f)] \qquad 4.10$$

$$\therefore \; C_{su}^2 < C_{ij}^2$$

The measured coherence is less than the desired coherence in the absence of noise.

If s(t) is a linear combination of two signals, u(t) and v(t), in the frequency domain, their relationship can be expre-

ssed as

$$S(f) = Z_U(f)U(f) + Z_V(f)V(f) \qquad 4.11$$

In this case, a predicted value of S(f) is given by

$$\hat{S}(f) = \bar{Z}_U(f)U(f) + \bar{Z}_V(f)V(f) \qquad 4.12$$

where $\bar{Z}_U$ and $\bar{Z}_V$ are averaged values of the transfer functions in equation 4.11. The coherence between S(f) and $\hat{S}(f)$ is known as the predicted coherence and is defined by

$$C^2_{S\hat{S}} = |\bar{Z}_U P_{SU} + \bar{Z}_V P_{SV}|^2 / P_{SS}\{|\bar{Z}|^2_U P_{UU} + |\bar{Z}|^2_V P_{VV} + 2\text{Real}(\bar{Z}^*_U \bar{Z}_V P_{UV})\} \qquad 4.13$$

For MT analysis where the relationship between the electric field and the horizontal magnetic field components, equations 2.25 and 2.26 is similar to equation 4.11, Kurtz (1973) has shown that the predicted coherence is a better measure of the reliability of the transfer function estimates than the ordinary coherence. High predicted coherence indicates that the relationship in equation 4.11 is sufficiently accurate and distortion by random noise is negligible. This also applies to the relationship between the vertical component of the magnetic field, Hz and the horizontal components in the GDS analysis using equation 2.39 High predicted coherence was therefore one of the acceptance criteria as will be discussed later in this chapter.

4.2.4 Analysis Program for Single Events

The block diagram in Fig.4.4 summarises the main steps of the calculations carried out by the main program for single event analysis. The final results were stored on two files. One of the files was listed on the line printer for subsequent examination while the results in the second file could be listed as plots. Some of the results in the second file were used for further

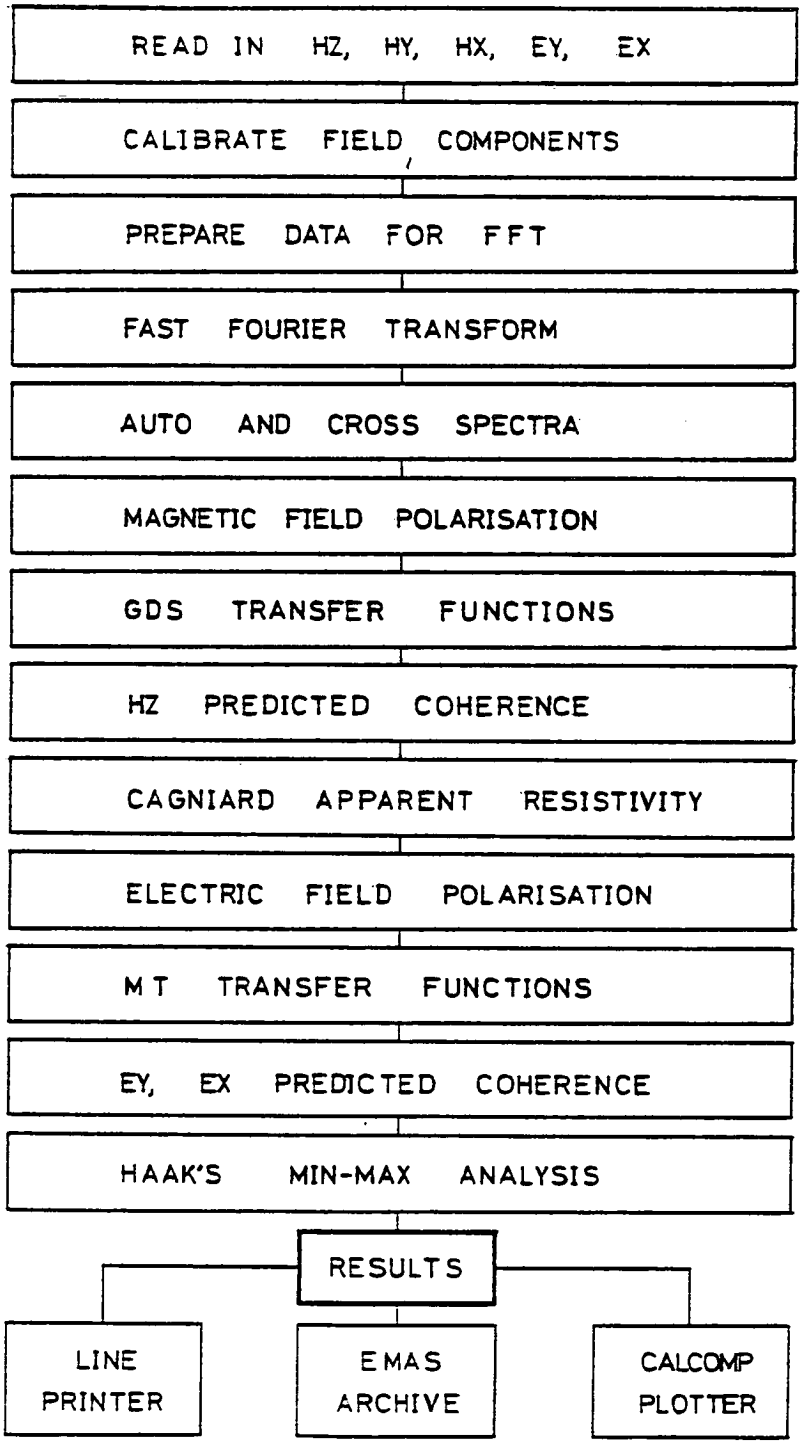

Fig.4.4 Scheme for single event analysis.

analysis by the event averaging program which will be described in the next section.

4.3 Mean Response Functions

In section 4.2.2, a number of precautions for reliable spectral and response function estimates were listed. In spite of such precautions, it is well known that induction response estimates tend to vary from event to event. Assuming that the effect of errors, which are due to measurement and computational noise, have been sufficiently minimised and that the electrical properties and structure of the earth at the recording site are independent of time, a possible explanation for the scatter in the response function is necessary. Source field studies have shown that the polarisation of the inducing field can vary between events at any given site (Green, 1978). The response function is also known to depend to some extent on the source field polarisation. Beamish (1979) has shown that the variance in the response functions can be minimised by averaging the estimates at each frequency over a number of events. In this study the response functions used for such averaging had to satisfy certain acceptance criteria which were based on high signal to noise ratio and predicted coherence. The algorithm used by Rooney and Hutton (1977) was adopted except for a few minor modifications considered necessary because of the introduction of digital recording.

4.3.1 The Averaging Program

The essential steps in the program for event averaging are shown in Fig.4.5. The main sources of random noise in the MT data

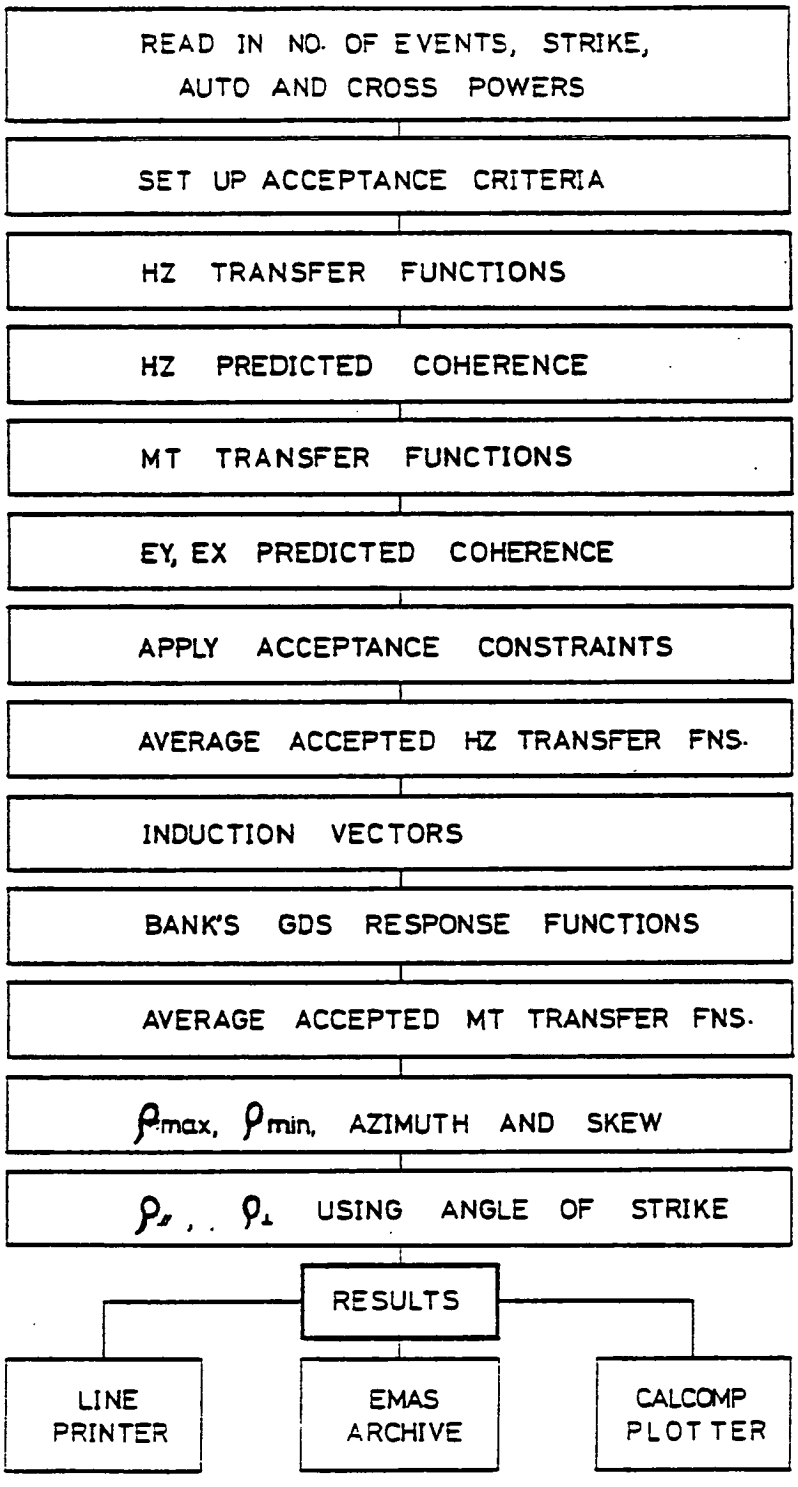

Fig.4.5 Scheme for the averaging program.

of Rooney (1976) was the digitiser noise which could be as high as 0.2% of the full -scale deflection. An acceptance criterion of a power level five times that of random noise in each series was considered necessary to minimise the effect of noise on the averaged transfer function. For digital records, an equivalent random noise component was estimated from the least significant bit in the Geologger tape records and was about 0.02% of the dynamic range. Many estimates therefore satisfied the signal to noise ratio requirement with the result that the scatter in the response functions was greatly reduced.

The second acceptance criterion required that the predicted coherence be more than 0.8 for Hz and 0.9 for either Ex or Ey. These high levels of required coherence were chosen so that reliable response functions could be obtained from the relationship in equation 4.11 as was discussed in section 4.2.3. From the results of similar analysis published in the last decade, coherence levels between 0.64 (Word et al, 1970) and 0.9 (Reddy et al, 1976) have been used by different workers.

Transfer functions which met the two acceptance requirements were averaged over events and also over period bands to obtain ten equispaced estimates per log decade.

The theory of error propagation was used for calculating errors in the transfer functions and tensor impedances. Log normal statistics was adopted for the calculation of principal apparent resistivities and their uncertainties in the manner discussed by Bentley (1973). Examples of plots of the results from this averaging program are presented for each site in Chapter Five.

4.3.2 Effect of Sequential Sampling

As was mentioned in Chapter Three, the input signals were sampled sequentially by the Geologger for which the manufacturer specified a time delay between adjacent channels of only 0.14s. Although it was felt that the effect of this delay on the response functions in the period band of measurement would be negligible, a check was made by allowing for the delay in a repeated analysis of the data from one of the MT sites. The simple theory which is given below indicates how the effect due to the frequency dependent phase shift introduced in the cross-spectral estimates by sequential sampling was calculated.

Consider the Fourier transform of a function $s_1(t)$ with a time shift Δt_1

$$S_1(f) = \int_{-\infty}^{\infty} s_1(t+\Delta t_1)\exp(-iwt)dt$$

$$= \exp(iw\Delta t_1)\int_{-\infty}^{\infty} s(t')\exp(-iwt')dt \qquad (t'=t+\Delta t_1)$$

$$= \exp(iw\Delta t_1)S_1'(f) \qquad 4.14$$

Similarly, for another function $s_2(t)$ with a time shift Δt_2,

$$S_2(f) = \exp(iw\Delta t_2)S_2'(f) \qquad 4.15$$

The desired cross-spectrum between the spectra of the functions without time shifts is

$$P_{S_1S_2}(f) = S_1^*(f)S_2(f)$$

$$= \exp(-iw\Delta t_1)S_1'(f)\exp(iw\Delta t_2)S_2'(f)$$

$$= S_1'(f)S_2'(f)\exp(iw(\Delta t_2-\Delta t_1)) \qquad 4.16$$

Equation 4.16 shows that every cross-spectrum estimate should be multiplied by the factor $\exp(iw(\Delta t_2-\Delta t_1))$ in order to

correct for the phase shift due to sequential sampling. Step 5 of the program for single event analysis (Section 4.2.4) was modified so that the cross-spectra were recalculated with the appropriate correction factor for time shifts between channels. Single event analysis and event averaging were repeated using data from Site 09. The results showed that the effect of sequential sampling on response functions in the period band of interest were not significant.

CHAPTER 5

RESULTS

The results of the data analysis will be presented in this chapter in two main sections. In the first section, the individual results of two-dimensional tensorial magnetotelluric analysis will be presented for each site. The results are presented as plots for each station and also tabulated for groups of stations under different regions. In the second section, Earth response functions will be presented for the region as a whole as it is hoped that this presentation will make the delineation of possible anomalous zones within the region easier. All results represent the average of about ten events at a given site.

5.1 Individual Station Results

A brief description of the location of each site is given. Plots of major and minor apparent resistivities and phases are shown for each site. The azimuth of the major impedance, the skew and NU, the number of degrees of freedom associated with each estimate are also presented.

5.1.1 The Lewisian Foreland (KLB, BAD,ACH,KIN)

The MT results for these sites are shown in Fig.5.1. Kinlochbervie(04) is on the western edge of the shield fragment. The Moine Thrust zone is about 30 km to the east of the site while the Minch, a fault-bounded basin containing sea water and conductive sediments lies to the west.

Badnabay (03) is on the eastern end of Loch Laxford, a sea lake. The surface geology of this part of the Foreland indicates

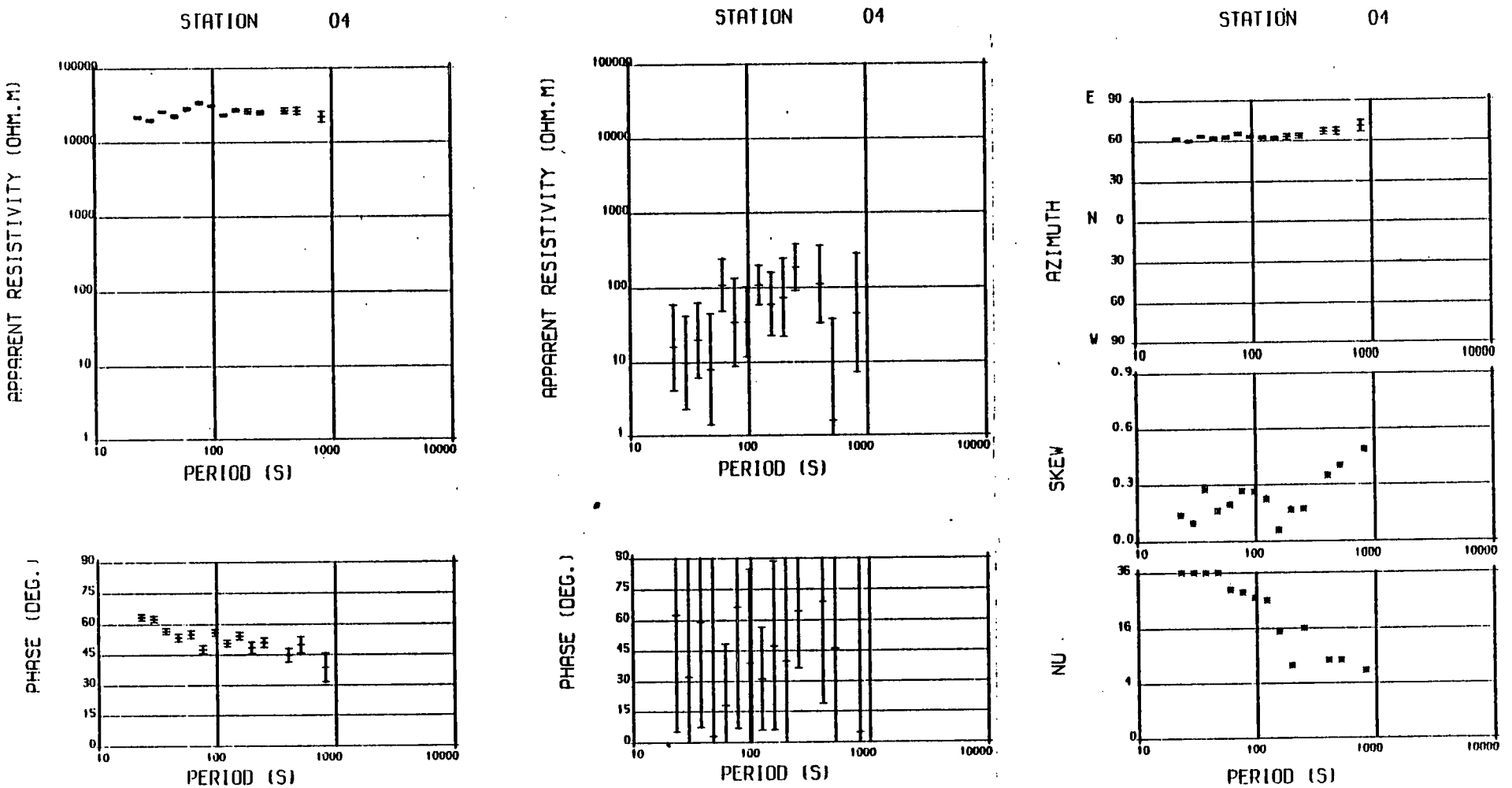

Fig.5.1a MT results for KLB.

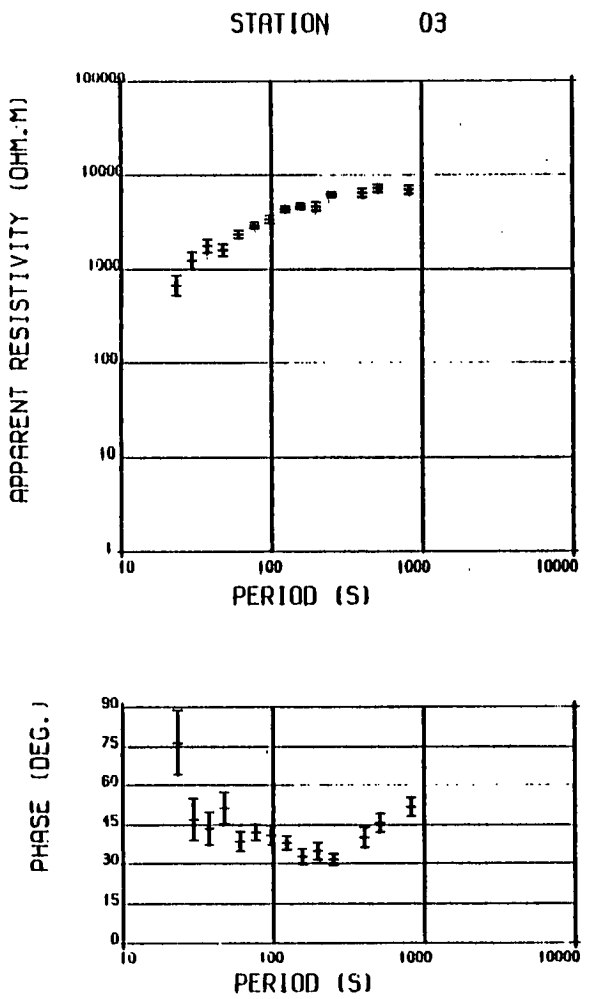

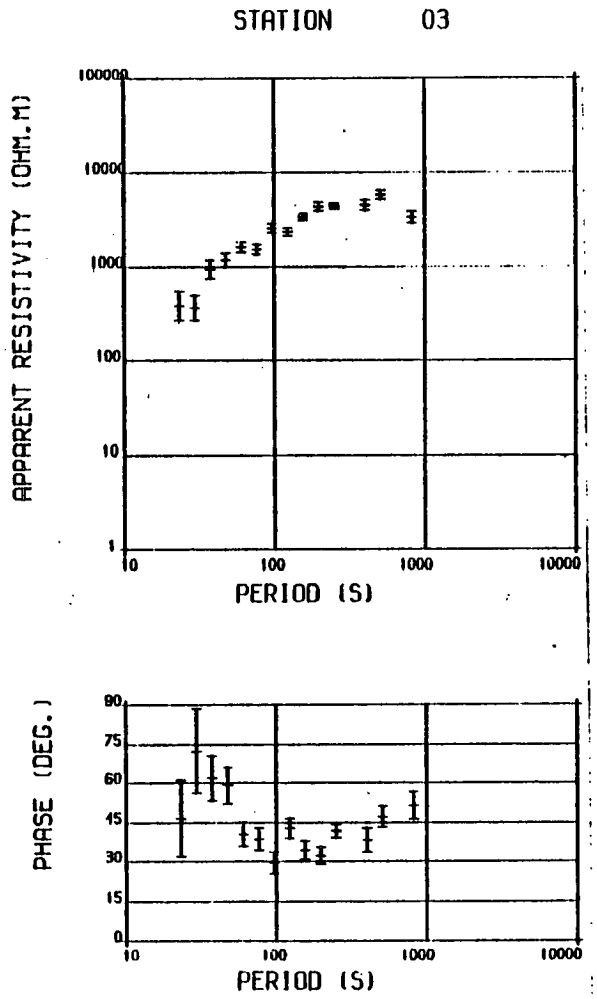

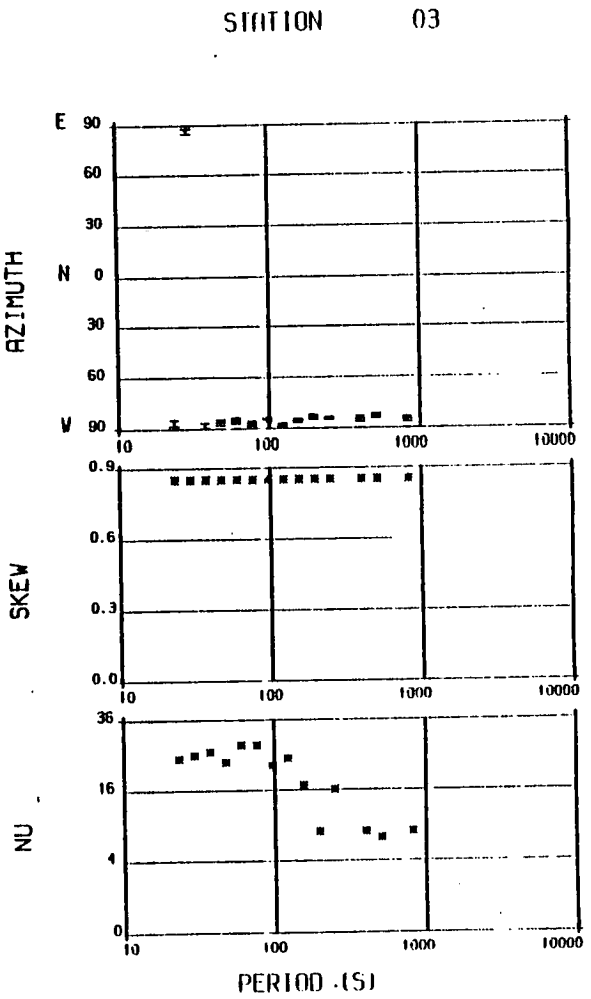

Fig.5.1b MT results for BAD.

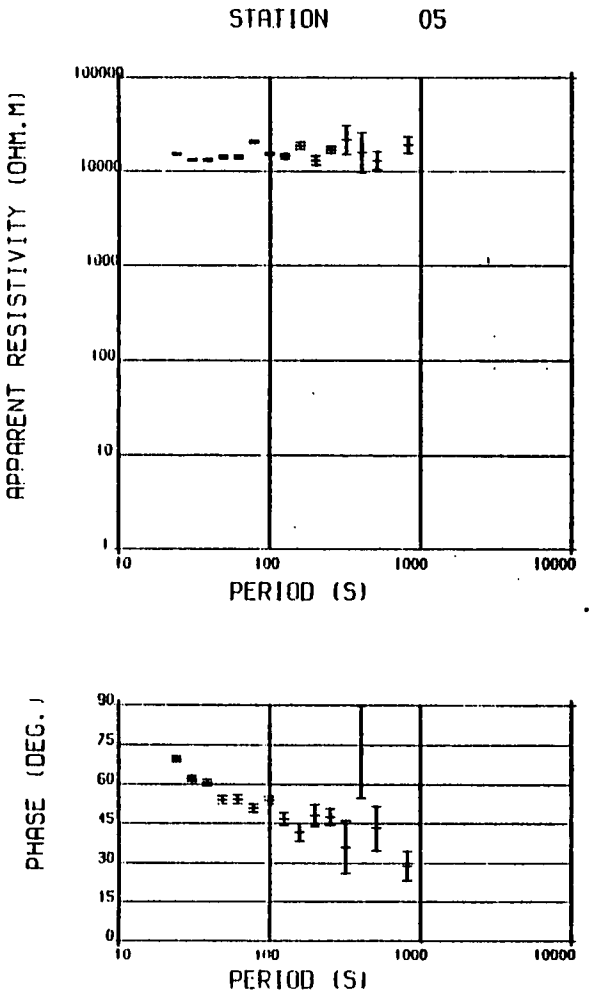

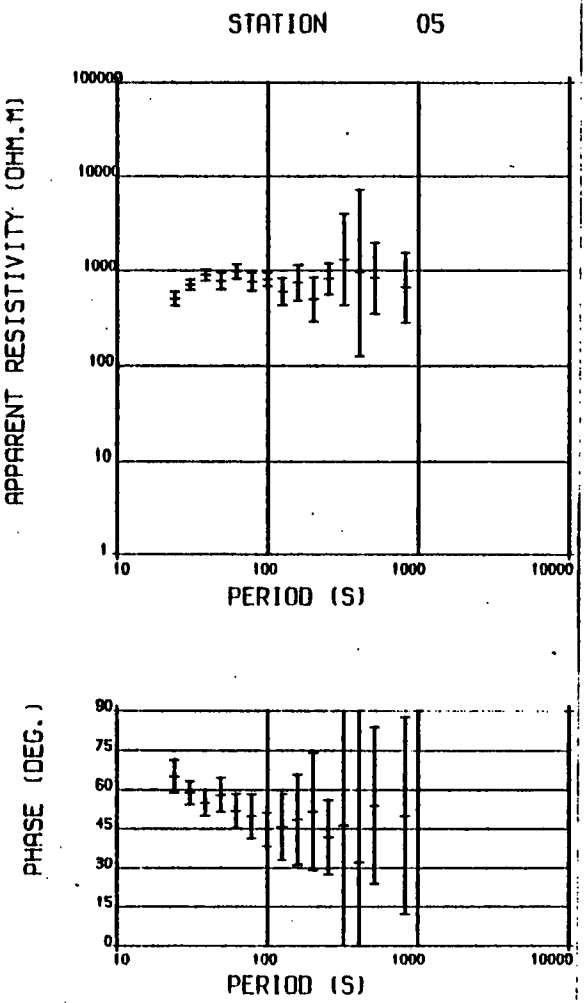

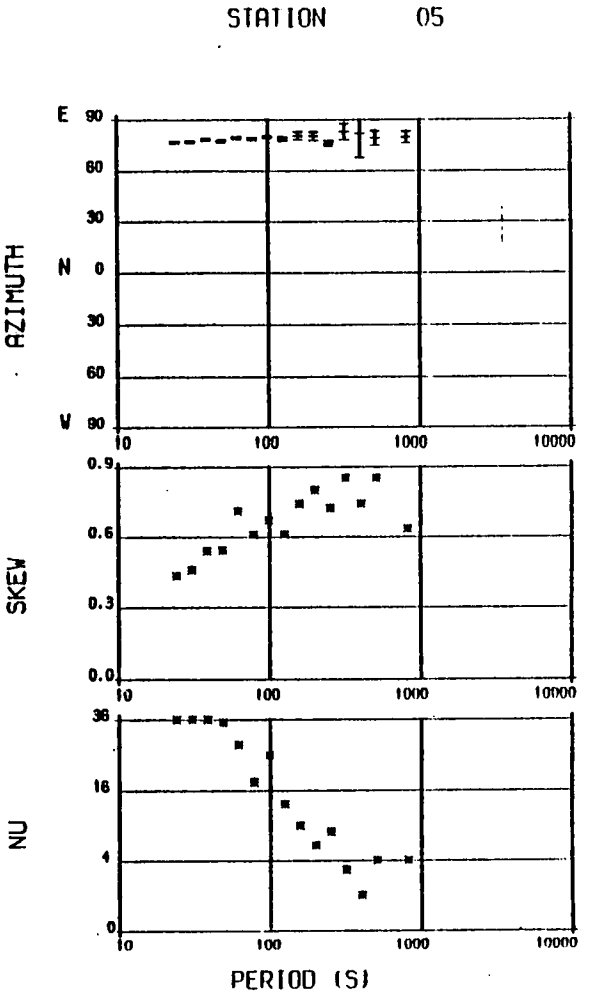

Fig.5.1c MT results for ACH.

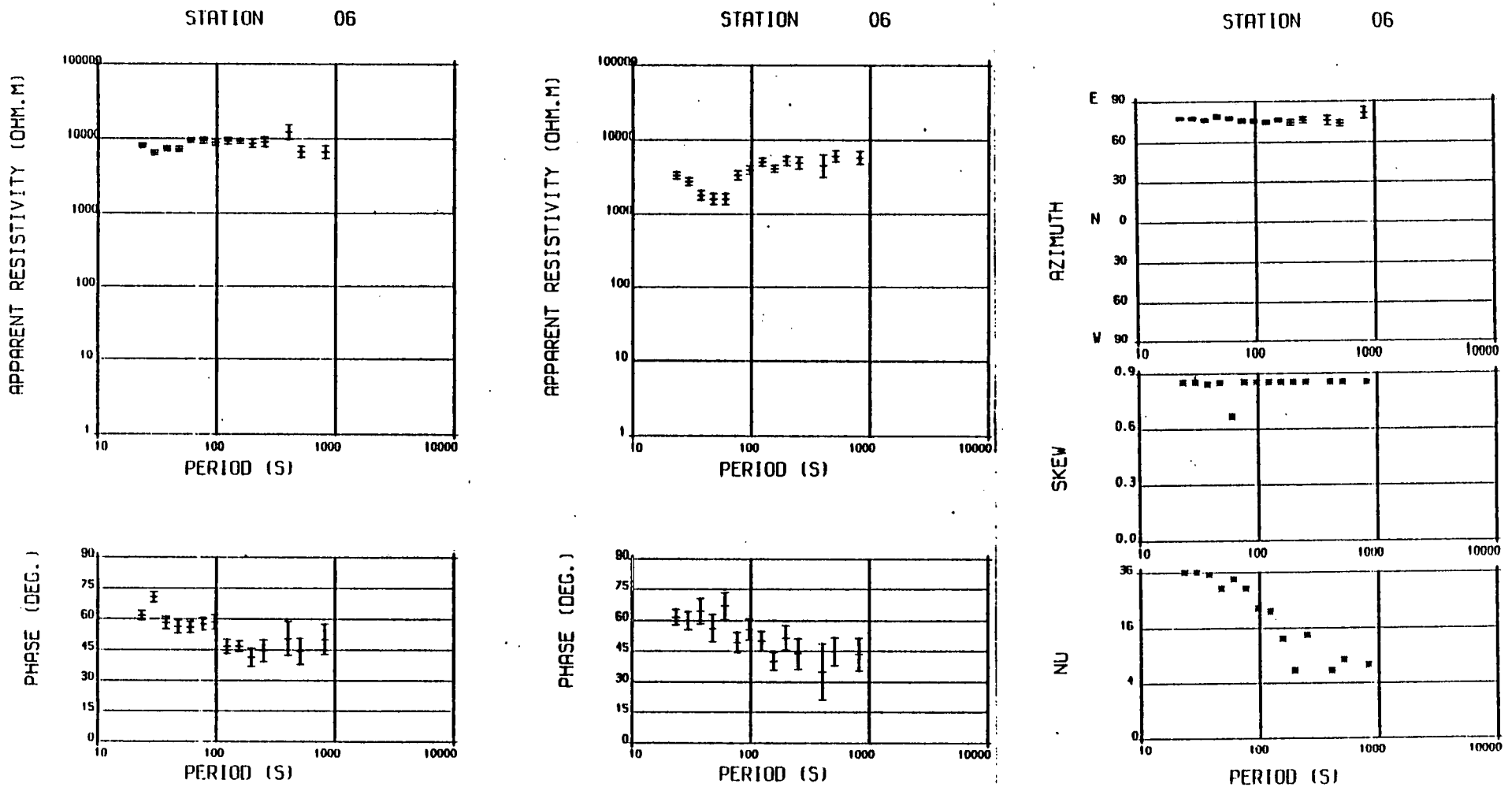

Fig.5.1d MT results for KIN.

that the shield fragment has been intruded into by numerous and extensive dykes which have west-north-west or north-west trends.

Achfary (05) is between Loch Stack and Loch More on the Westminster Estate and is near the western edge of the Moine thrust zone.

Kinloch (06) is near the eastern end of Loch More but lies within the Moine thrust zone. Kinloch is further inland than the other three sites on the Foreland. The positioning of the foreland sites at different distances from the coast should aid our understanding of the effect which the adjacent shallow seas has on the Earth electromagnetic response functions in the region. It is interesting to notice that the anisotropy between the maximum and the minimum apparent resistivity which is only about 2 at a period of about 100s increases to 19 at Achfary and 27 at Kinlochbervie which is very near the coast.

5.1.2 Lairg Region (SHN,TER,LAI,CIK,BNB)

The results for sites around Lairg are shown in Fig.5.2. West Shinness (19) is about 30 km east of the Moine thrust zone and therefore lies on the Caledonian metamorphic belt which extends over most of Scotland north of the Highland Boundary Fault. The east and the west coasts are each about 40 km away and the north coast is about 50 km from the site. After a day's recording at this site, an external noise source of an unknown origin developed especially during the daytime. On the analogue record, the noise appeared as a series of intermittent 'spikes' on the telluric channels. Since the noisy condition prevailed mostly at daytime, it was felt that the source was some artificial leakage current from a distant source. During the

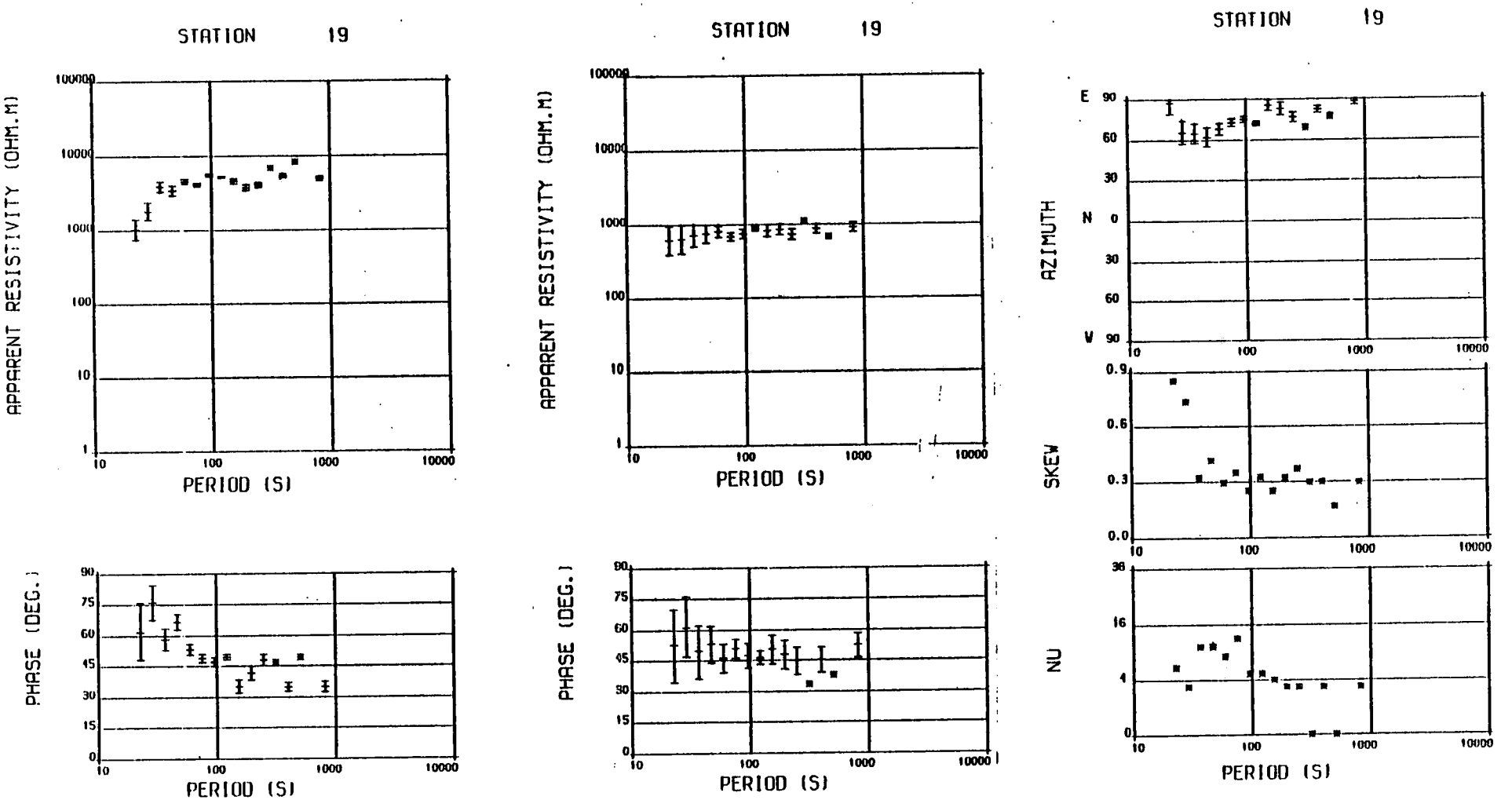

Fig.5.2a MT results for SHN.

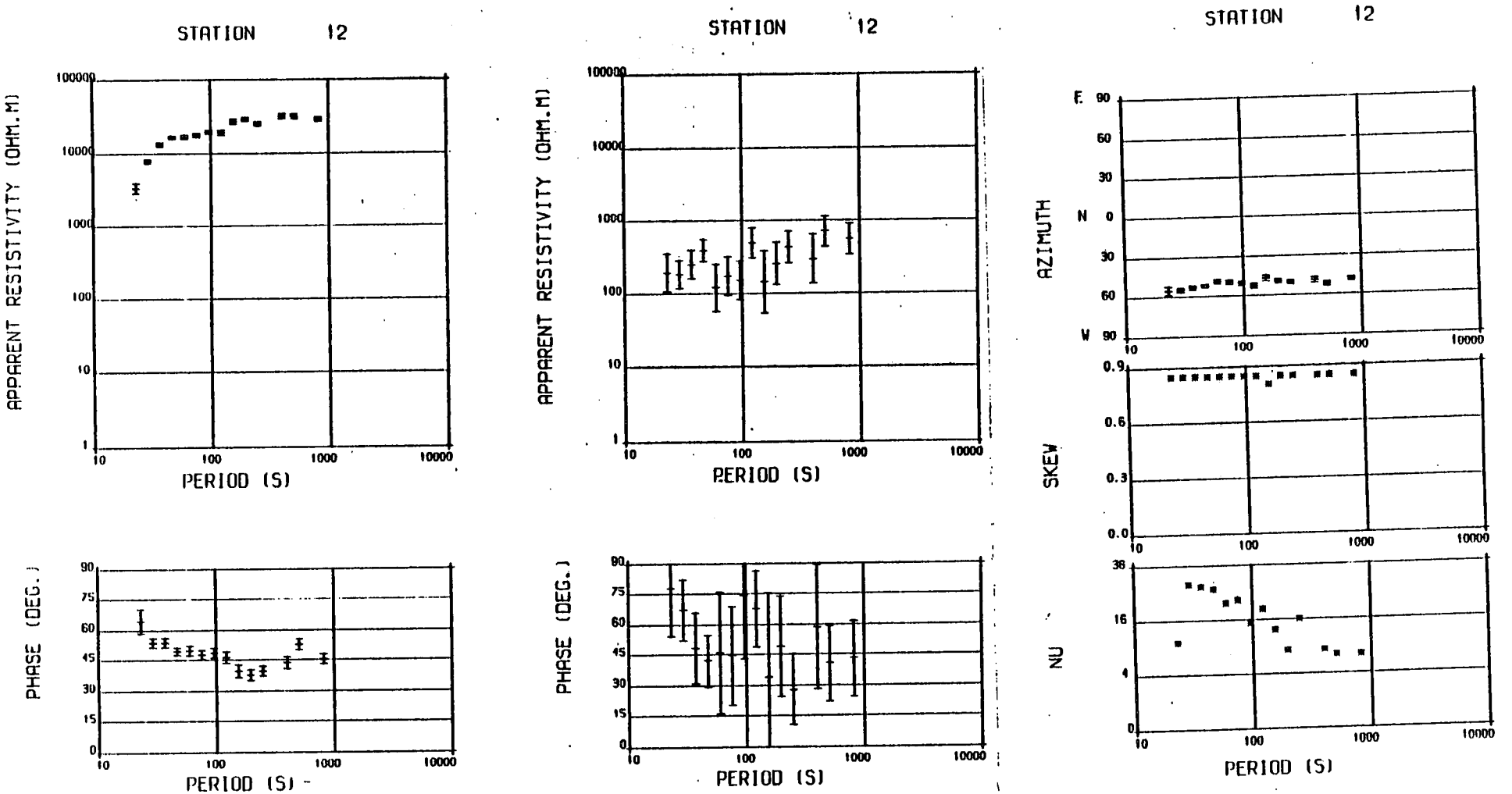

Fig.5.2b MT results for TER.

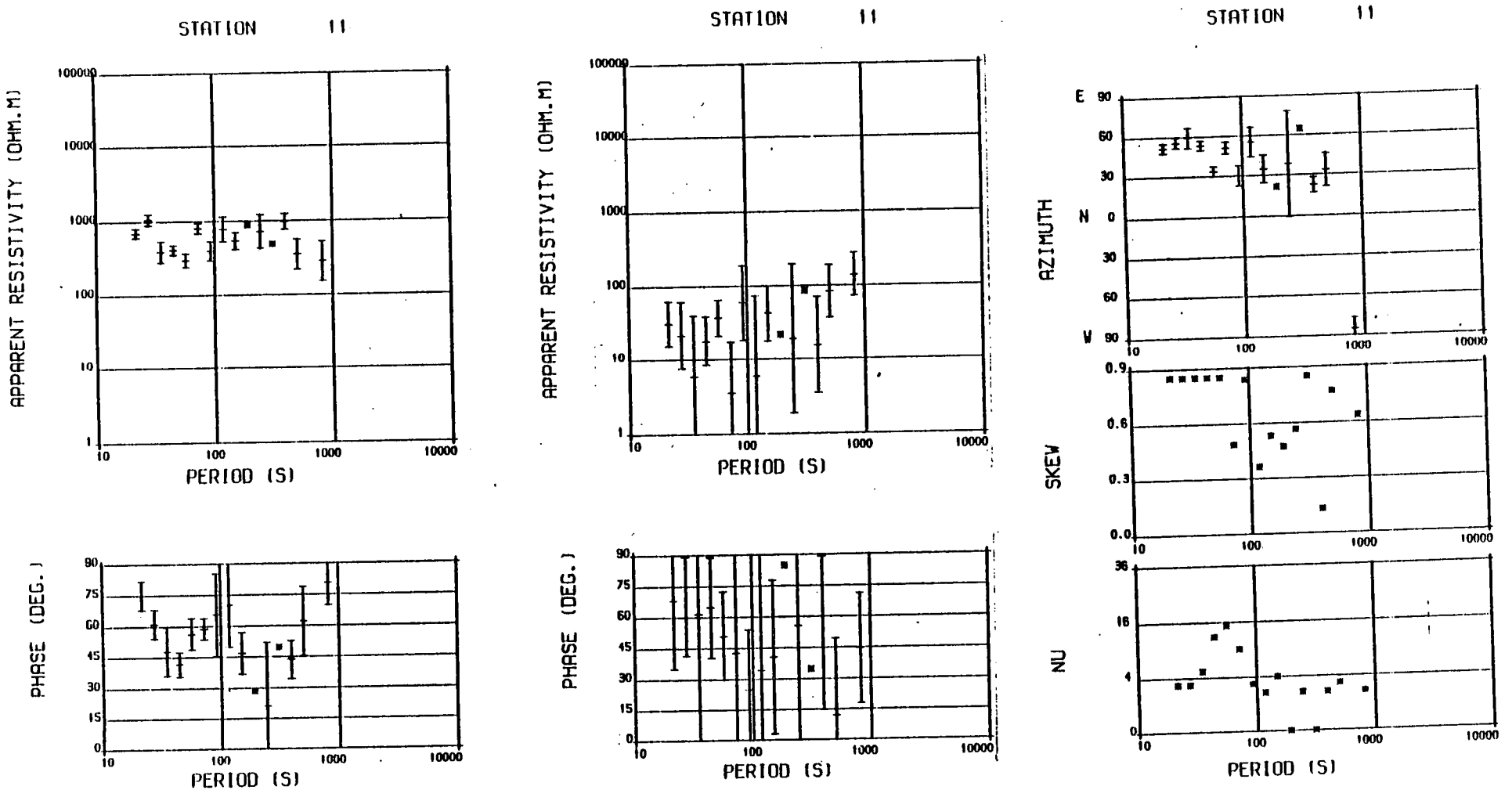

Fig.5.2o MT results for LAI.

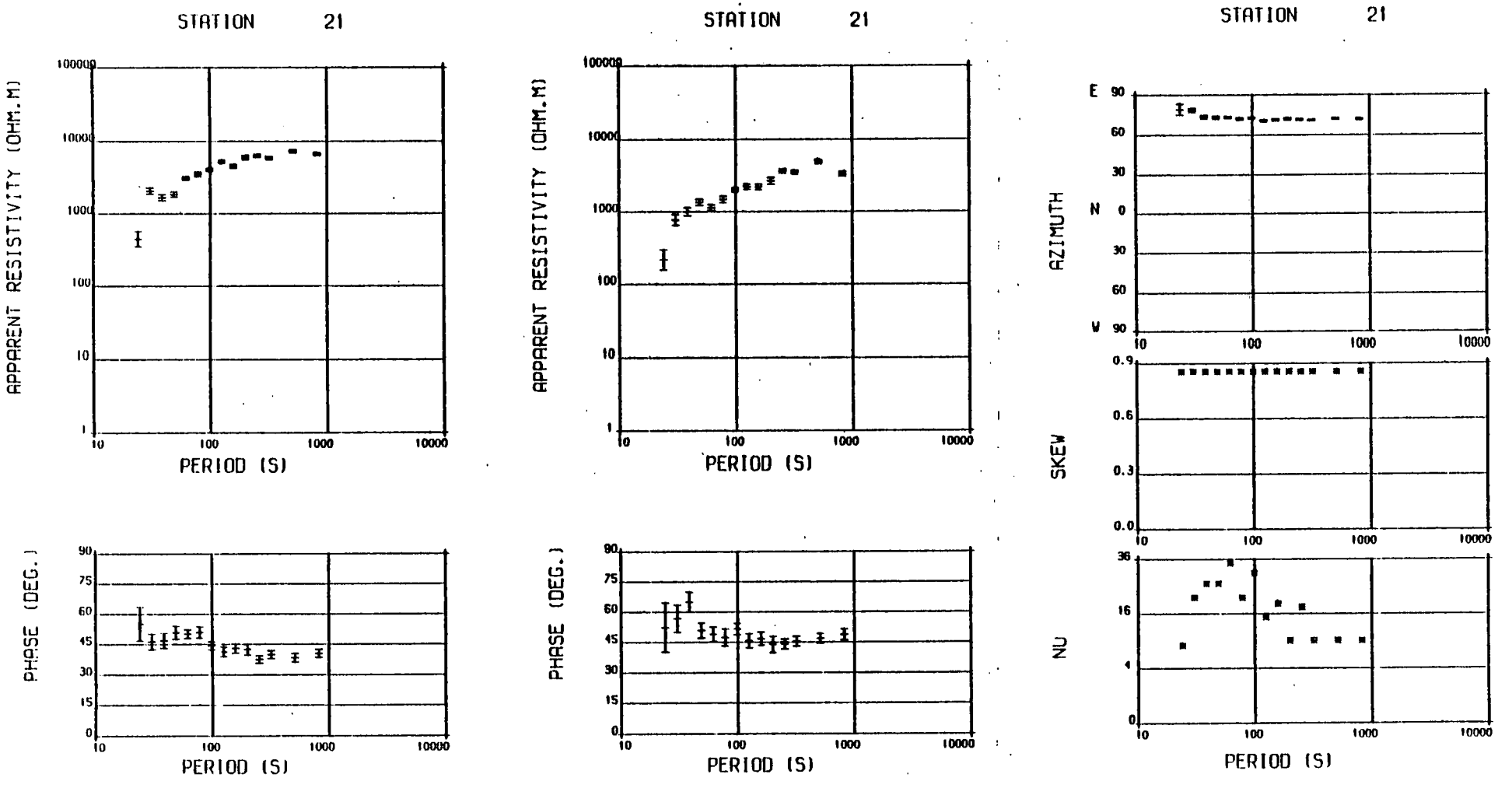

Fig.5.2d MT results for CIK.

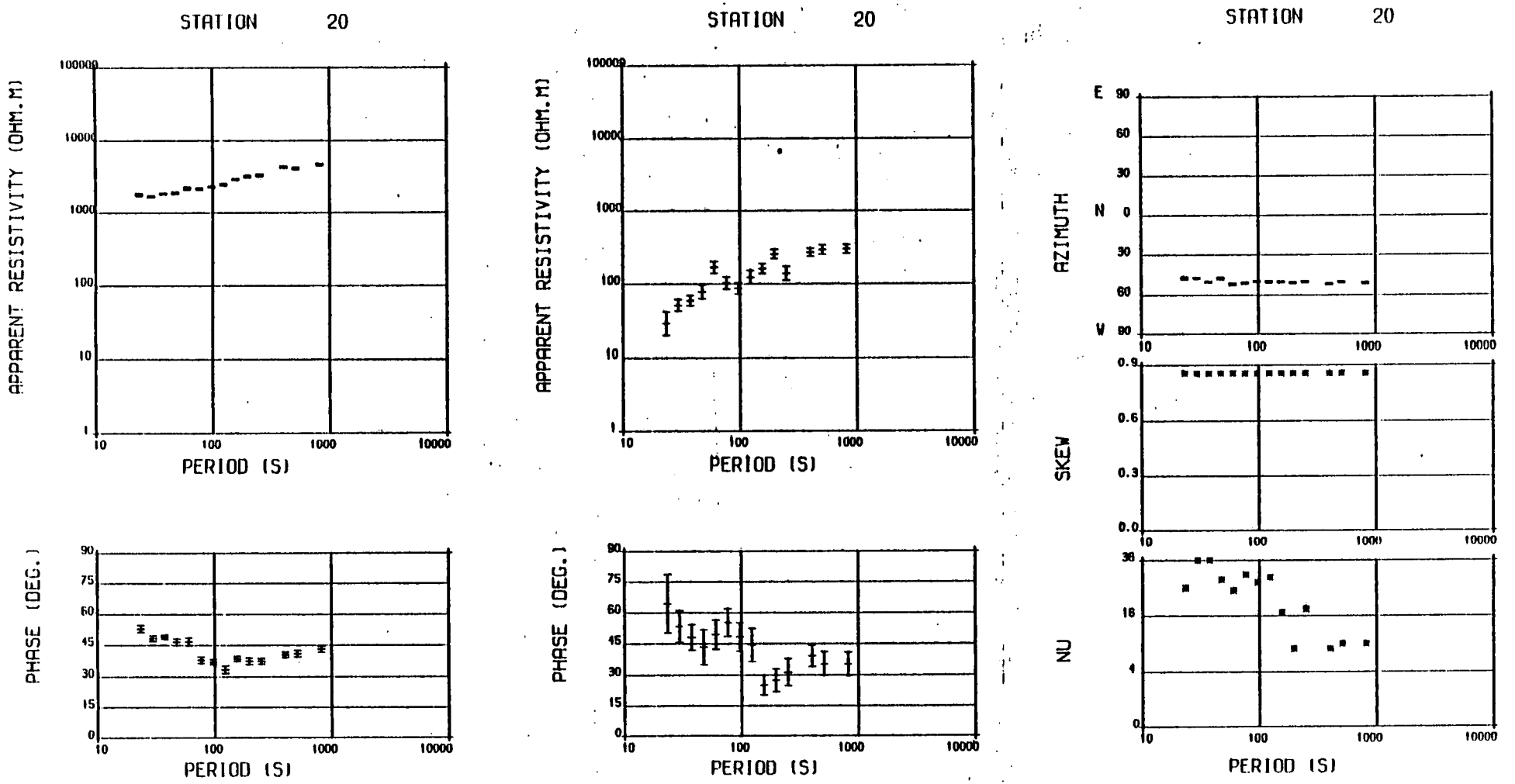

Fig.5.2b MT results for BNB.

initial visual editing of the tape data, only sections which were seen to be free from 'spikes' were filed away for analysis. Thus only four events were selected for analysis at this site and the events were from the early hours of the morning. Except for the first two short periods, the estimates for the MT parameters were relatively scatter-free.

Terryside (12) is only 5 km from West Shinness. It also lies within the Caledonian metamorphic zone north of Loch Shin. During the first two days of recording, the magnetic components were rather noisy. The source of the noise was traced to scrap fence wires which were then removed.

Lairg (11) is about 5 km south-east of Terryside and about 3 km from the eastern end of Loch Shin. Moine schists are the host country rock in the area but to the east of the site, there is a large granitic outcrop, the Lairg granite massive. The signal to noise ratio at this site was rather low inspite of a long period of recording of about one week. Hence most of the estimates could not pass the acceptance criteria and as a consequence, there are rather large uncertainties in the mean of the impedance estimates.

The 1977 preliminary results from Terryside and Lairg showed a marked change in the MT response at the two sites only about 5km apart. The sites West Shinness, Bonar Bridge (20) and Croick (21) were therefore occupied in the summer of 1978.

Croick (21) is in the central part of Ross-shire and about 15km west of Bonar Bridge. Thus it is about 30km from the east and the west coasts. The northern end of the Strathconon fault and the Cairn Chuinneag granite are about 5km from the site.

The other site, West Airdens farm in Bonar Bridge is about

15 km south-east of the Lairg granite but very near the Migdale granite, a smaller outcrop east of the MT site. The site is also about 15 km from Dornoch Firth and thus it is only about 10 km from the contact between the Devonian sediments in the Moray Firth basin and the more resistive country-rocks.

5.1.3 Great Glen Region (ALT,KIR,ALD,TOM,BOG,FTA)

The results for these sites are shown in Fig.5.3. Achanalt (18) is outside the Glen and on the central part of the Caledonian metamorphic zone of North-western Scotland. The site is about 50km from the west coast and also from the Moray Firth basin to the east . The Strathconon fault is about 6 km east of the site.

Most daytime records at the this site were contaminated by noise from vehicles. Another source of noise which could be identified twice during the daytime was ground vibration due to the local train. Hence most of the noise-free record sections used for the analysis were between 1600 and 0700 hours.

Kirkhill (02) is on Devonian sediments about 2km from Beauly Firth and thus the site lies within the Great Glen. There is a marked difference in the MT responses at this site - which is in the Glen - and responses at sites which are outside it. The apparent resistivities are low as expected for a site in a sedimentary basin.

Aldourie (07) is about 1 km from the northern end of Loch Ness and lies in the Great Glen between the eastern escarpment and the lake. The site is only 9 km from Kirkhill and is situated also on Devonian sediments which cover most of the Moray Firth region of the Great Glen. It is interesting that the apparent

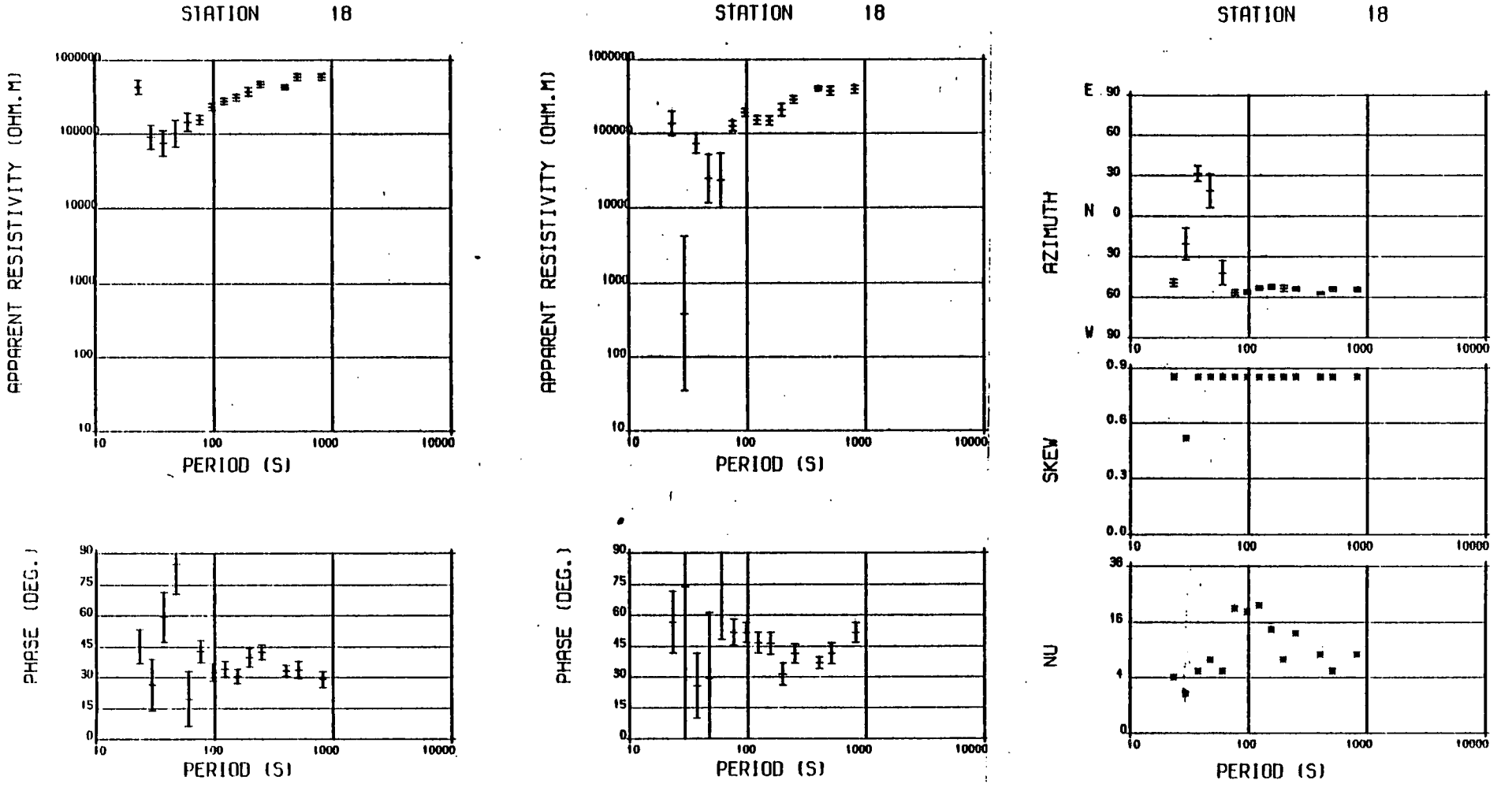

Fig.5.3a MT results for ALT.

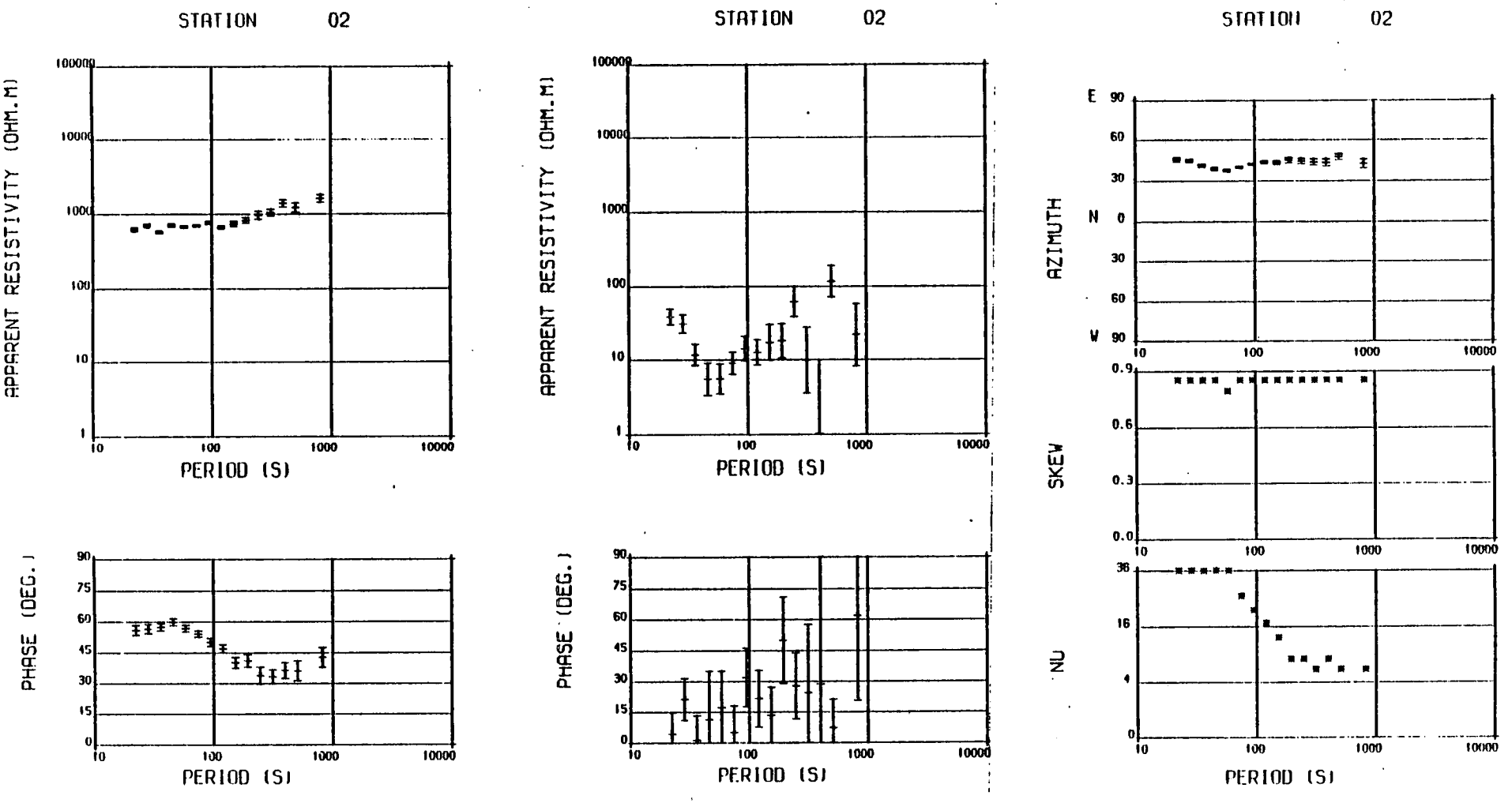

Fig.5.3b MT results for KIR.

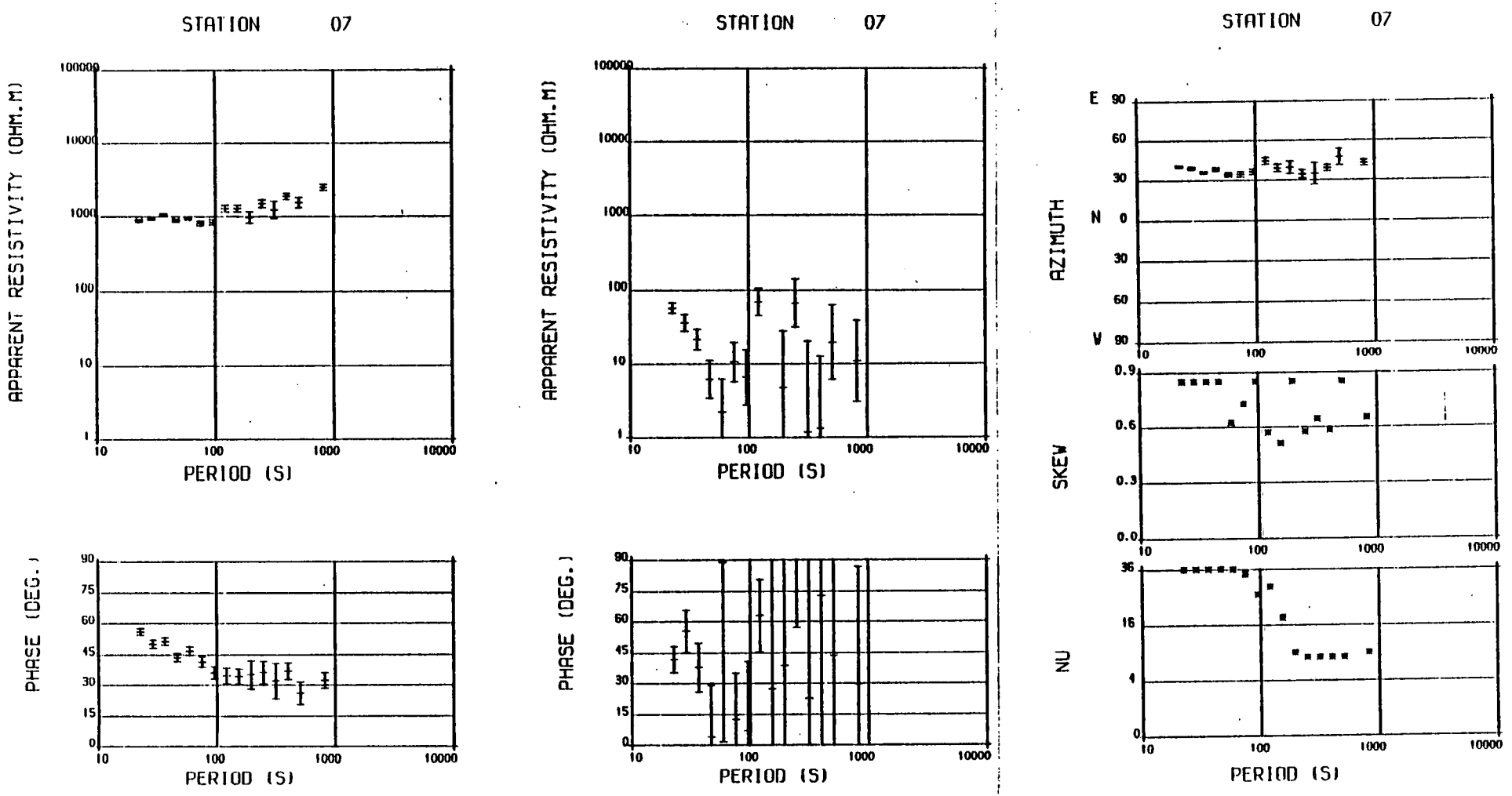

Fig.5.3o MT results for ALD.

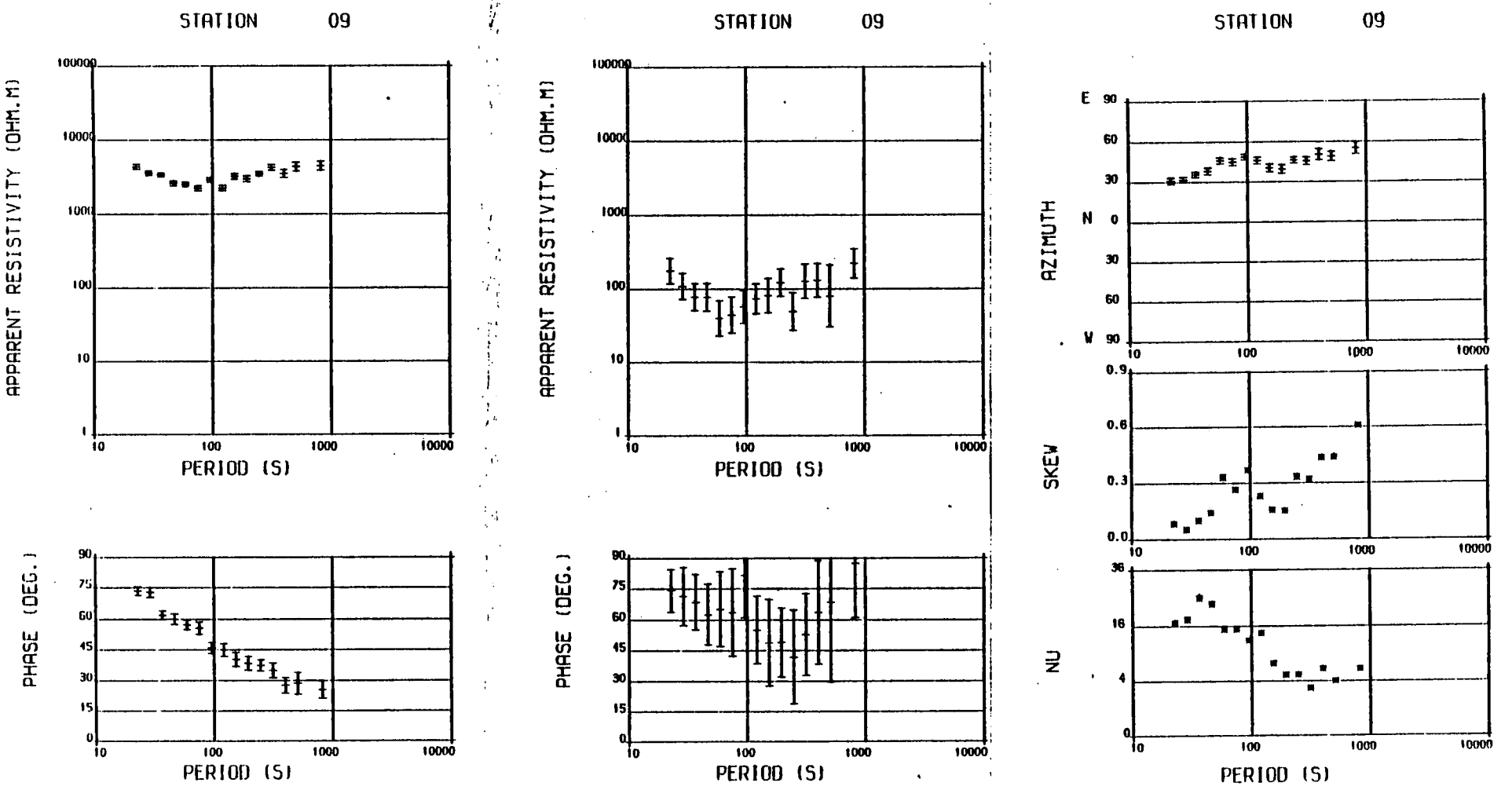

Fig.5.3d MT results for TOM.

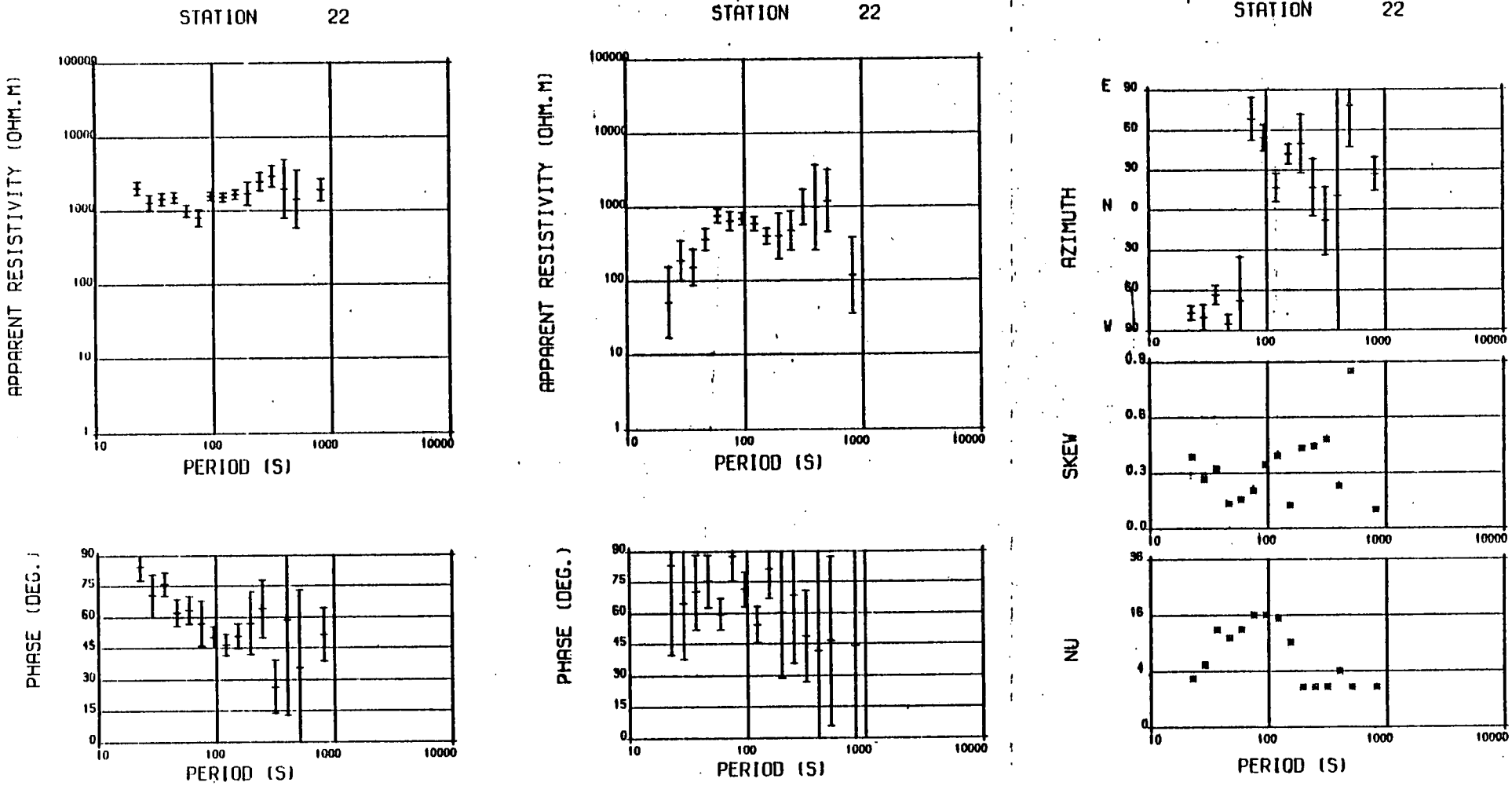

Fig.5.3e MT results for BOG.

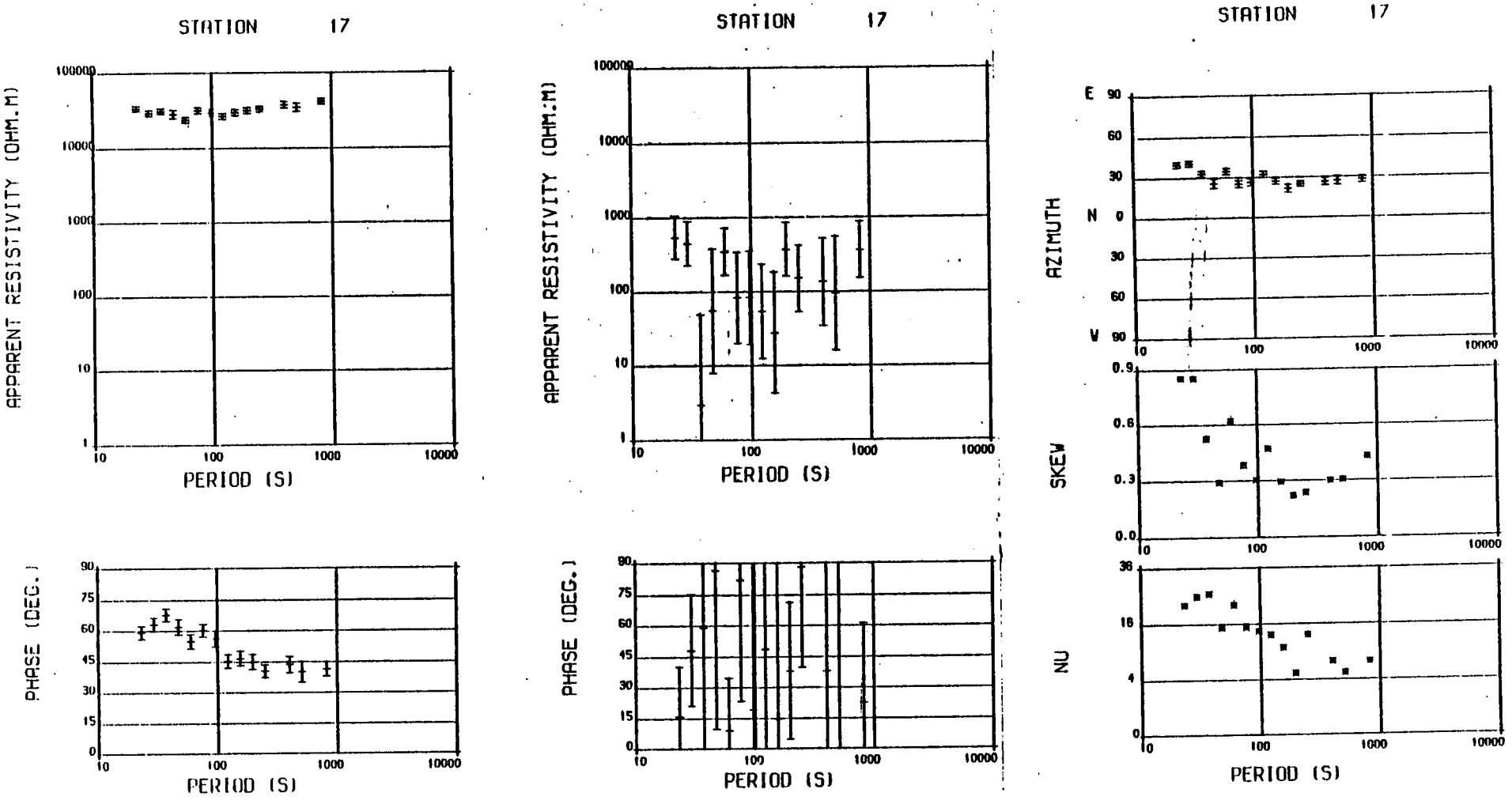

Fig.5.3f MT results for FTA.

resistivity data from this site and from Kirkhill are very similar both in value and period dependence. Hence the data from these sites can be taken to represent the Earth response function for the northern part of the Great Glen.

Tomatin (09) is over 300m above sea level and on the Grampian moine schists. The Moy and Findhorn granite complexes nearly surround the site.

Boat of Garten (22) is about 18km south-east of Tomatin but at a relatively lower altitude of 205m. To the south of the site lies one of the largest granite masses on the Grampians, the Cairngorm granitic pluton and to the west, the Monadhliadh granite.

The Great Glen Fault is thought to extend beyond the region of Northern Scotland. In order to study the conductivity structure of this feature along its length on land, measurements were made at Fort Augustus (17) and at Fort William (16). Fort Augustus is near the southern end of Loch Ness and the eastern escarpment of the Great Glen Fault. From surface geology, the site lies on undifferentiated moine rocks. The apparent resistivities at this site are higher than the corresponding values at Kirkhill and Aldourie which lie near the northern floor of the Great Glen. This is an interesting difference between the northern and the central part of the Glen.

5.1.4 Others (INV,KKM,FTW,KLE,CRO)

The MT results for these sites are shown in Fig.5.4. Inverey (13) is on Grampian moine schists between the Cairngorm and Lochnagar granite massives near Braemar. It is therefore not surprising that it also has the highest altitude of 356m on the

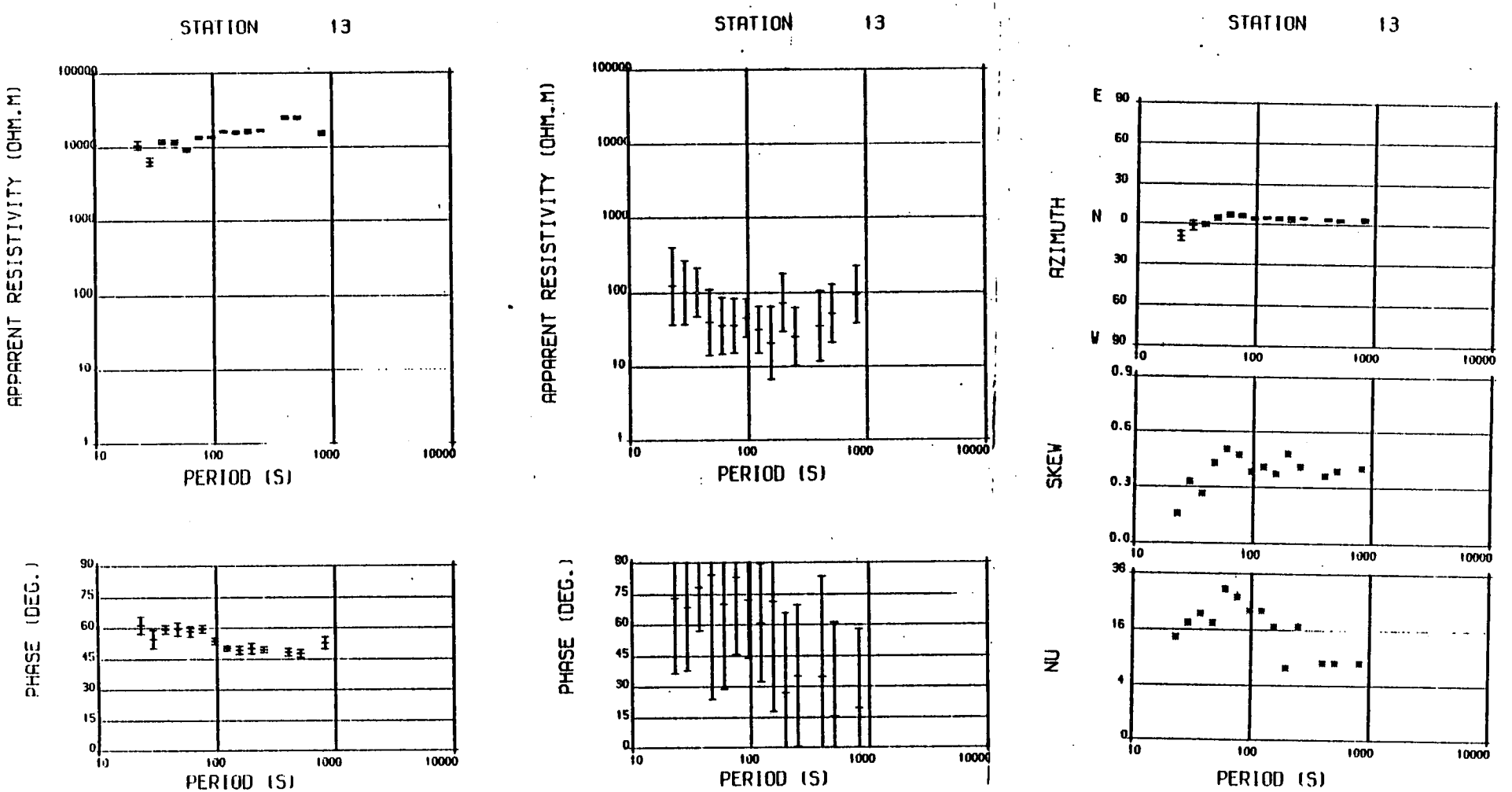

Fig.5.4a MT results for INV.

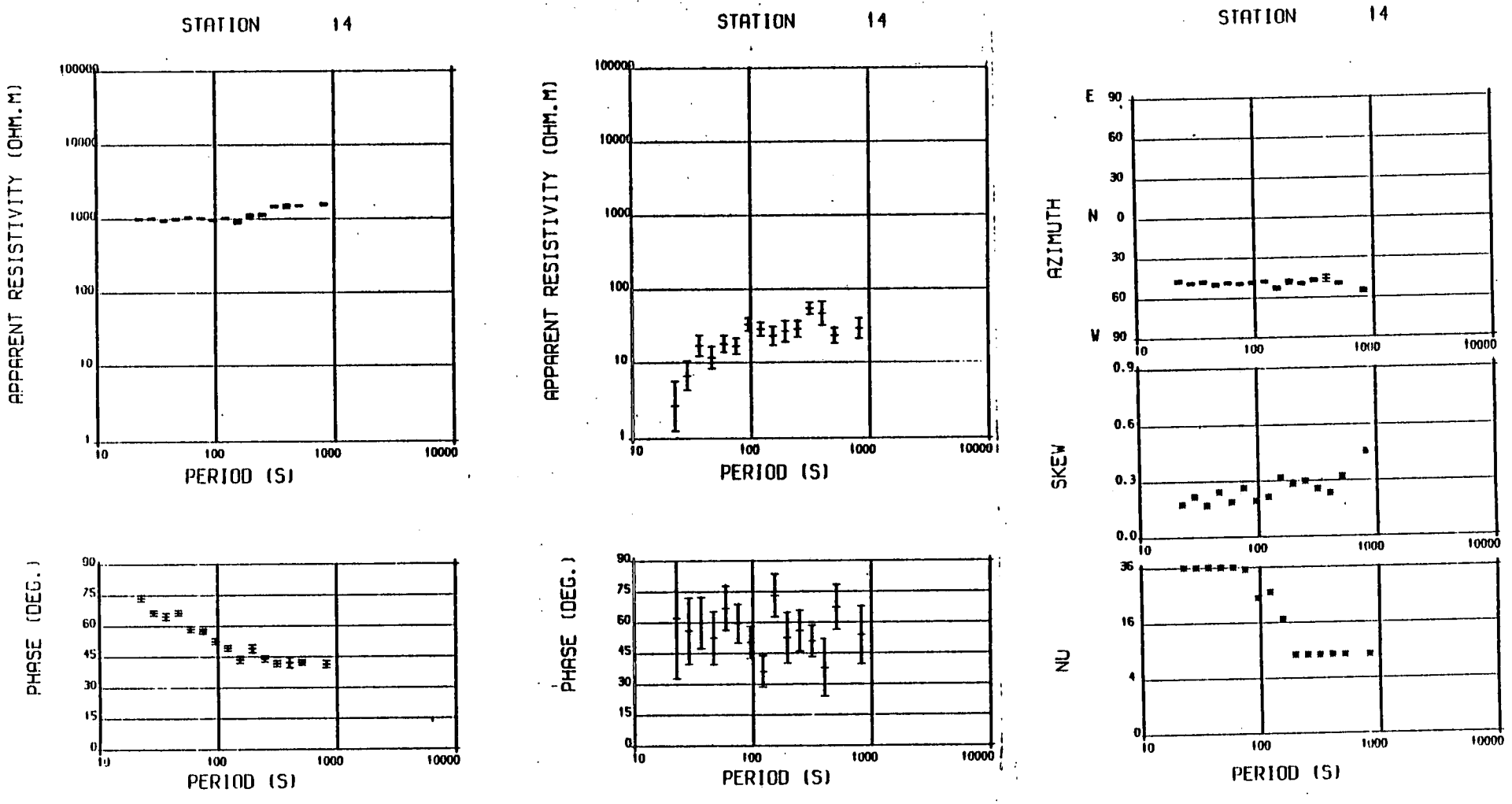

Fig.5.4b MT results for KKM.

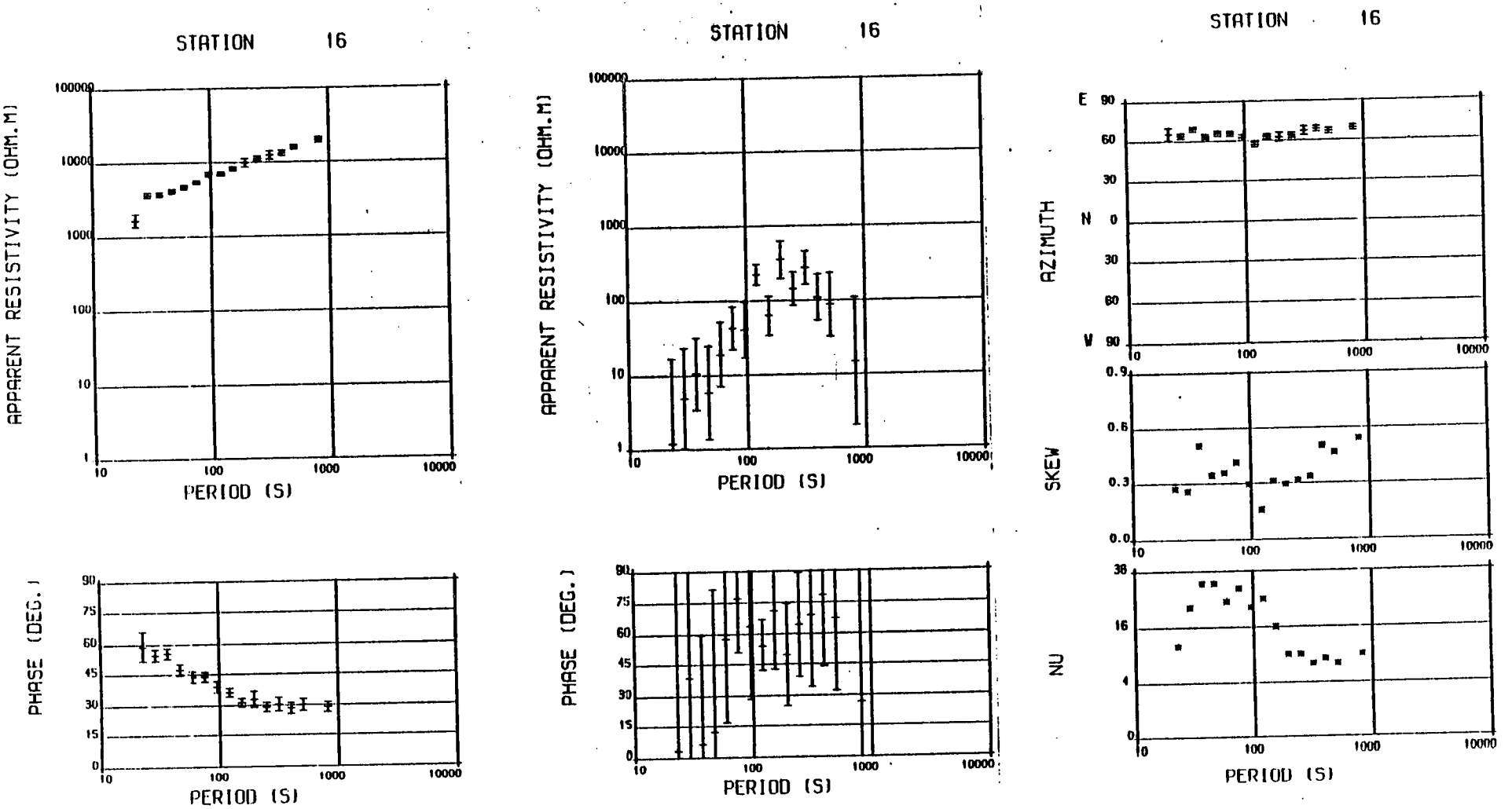

Fig.5.4c MT results for FTW.

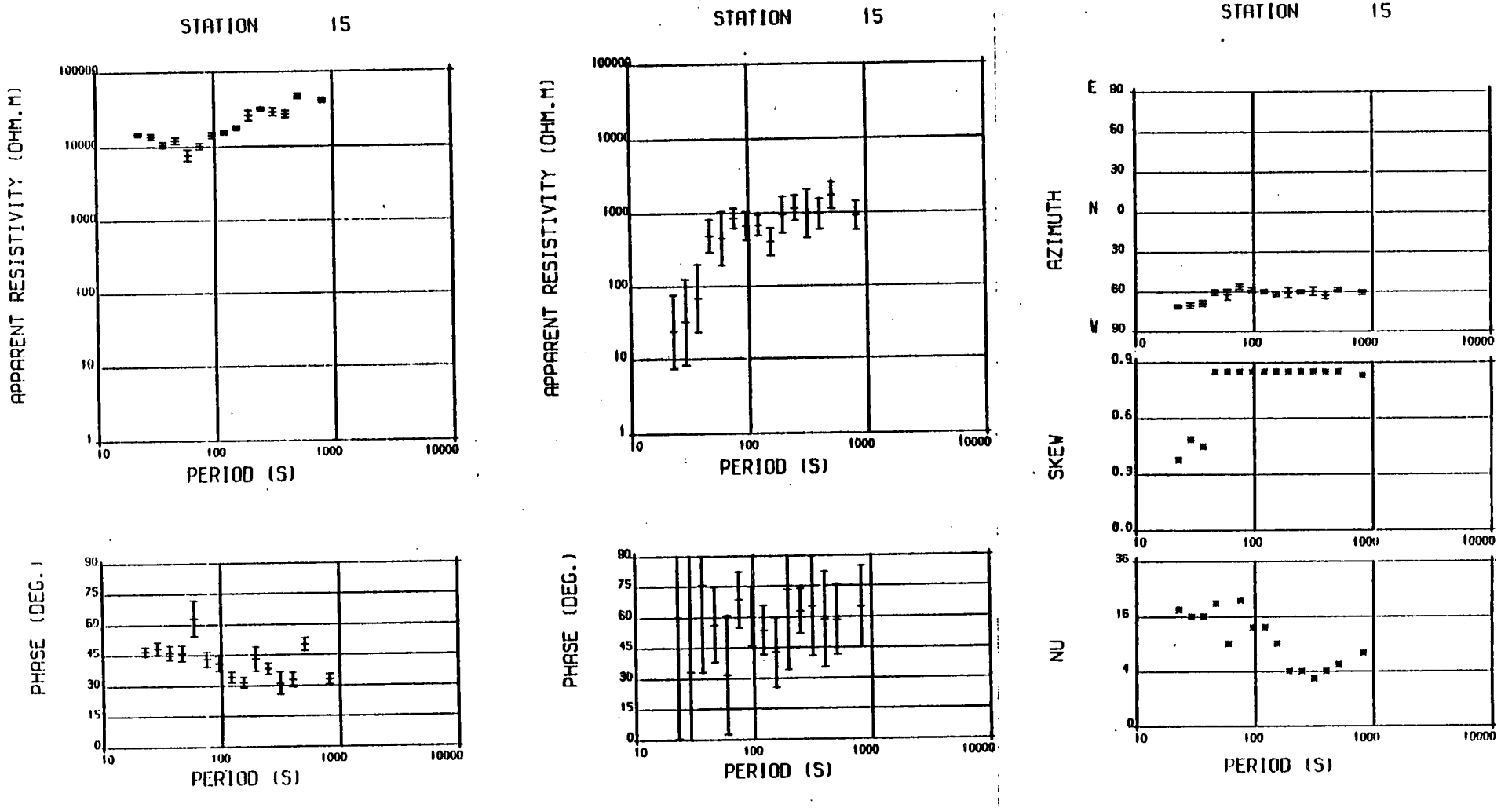

Fig.5.4d MT results for KLE.

MT traverse. It is interesting to see that the major apparent resistivity values at this site are very high when compared with values at other sites on the Grampian metamorphic zone. These high apparent resistivity values can be attributed to the presence of large granitic plutons in the area.

Kirkmichael (14) is about 20km south of Inverey and only about 10 km from the Highland Boundary fault. It was purposely chosen to lie outside the Grampian moine belt. The site is thus the only one on Dalradian schists and limestones in a belt of intense mineralisation north of the Highland Boundary fault. It is interesting to notice that apparent resistivity values obtained here are much lower than those at Inverey, the nearest site but one which is in a different geological setting.

Fort William (16) is the most southern site on the floor of the Great Glen. Ben Nevis, the highest mountain in Britain is about 4km away to the south-east. Both the eastern and the western escarpments of the fault can be seen from this site which is situated on one of the widest portions of the Glen. Surface geology indicates that the MT site here is on undifferentiated Moine rocks but to the east are the Ben Nevis granitic complex and outcrops of Moine limestones. The apparent resistivities here are lower than the values at Fort Augustus but considerably higher than the values at Kirkhill and Aldourie. There is therefore some indication here that the geoelectric structure is not uniform along the Great Glen.

Kinlocheil (15) is about 15 km west of Fort William and is situated on Moine schists. West of the area are outcrops of mica schists and the shallow sea which is only 25km away. It is interesting to see that the apparent resistivity values here are

higher than those on the Caledonian metamorphic zone but comparable with the values at sites on the shield fragment in Sutherland.

Croachy (08,10) was a problem site as there was artificial noise on the magnetic components. Part of this noise was traced to the electrical appliances in the cottage. It was therefore decided to try and record the magnetic field variation at another site nearby. While telluric recording continued at site 08, the Jolivet magnetometers were moved to site 10, about 1 km away. Unfortunately, recording had to be discontinued after a few hours as the mains power was switched off.

These results of single station analysis are summarised in Table 5.1.

5.2 Regional Results

In this section, results are presented for the North of Scotland as a whole. Attention is drawn to particular sub-regions or areas of the region where there is a fairly clear similarity in the behaviour or variation in the response functions within the area. It is felt that this presentation will help to highlight the differences, if any, between the tectonic and geological units in Northern Scotland.

5.2.1 Azimuth of the major impedance

The variation of the azimuths of the major apparent resistivity with period at each site has been shown in the previous section. In Fig.5.5, they are displayed on regional vector maps for three periods - 23, 95 and 819s. The plots are intended primarily to show at a glance the direction of the major apparent

Table 5.1

Summarised Results of Single Station Analysis

PARAMETERS	LEWISIAN FORELAND (KLB,BAD, ACH, KIN)	LAIRG (SHN, TER, LAI, CIK, BNB)	GREAT GLEN (ALT, KIR, ALD, TIM, BOG, FTA)	OTHERS (INV, KKM, FTW, KLE)
1. Azimuth of the major impedance	NE - SW direction except WNW at BAD - roughly normal to local coast	Depends on site	Parallel to geological strike of Great Glen Fault at KIR, ALD and TOM. Perpendicular to strike at ALT and BOG. Parallel to strike at BOG for periods over 95s.	Normal to Highland Boundary Fault at KKM. NE - SW at FTW and normal to Great Glen Fault at KLE.
2. Apparent Resistivity Anisotropy	Very anisotropic except at BAD and KIN. Anisotropy decreases by an order of magnitude between KLB and KIN.	Anisotropic except at CIK with a slight decrease at SHN.	Anisotropic except at BOG at long periods	Very anisotropic.

Table 5.1 continued

3. Skew	Generally high-over 0.8 except at KLB with values less than 0.3	High - over 0.8 except at SHN with values about 0.3	Comparatively low except at ALT, KIR and ALD.	Very low (<0.3) at KKM and comparatively low elsewhere except KLE.
4. Induction Vector				
a) Magnitude (Real) part	Very large	Large at the short periods except at LAI.	Large at the short periods except at KIR and TOM	Large at short periods
b) Direction	NW	Depends on site and period	SW or W except NW at FTA at the short periods. At 95s all point into the Glen except at FTA.	W or SW depending on site and period.

resistivity at each site. The magnitude can also be obtained by using the appropriate multiplification factor which is indicated at some sites. The azimuth also indicates roughly the mean or the persistent direction of the electric field at the site.

On the Foreland, the axis of the major impedance is confined between the north-east and the east-west direction for all sites except at Badnabay where the direction tends to be west-north-west. This is probably due to the bay-like shape of the local coastline. The directions are nearly all normal to the local coastline. They thus indicate the considerable influence the adjacent shallow seas and the ocean have on the magnetotelluric responses at those sites which are near to the coast.The results of two-dimensional numerical model studies which confirm these coastal effects in Northern Scotland are presented later.

Around Lairg region, the azimuth rotates through almost 180 deg. between West Shinness, Terryside and Lairg. There is also a marked decrease in the magnitude of the impedance at Lairg. It is interesting to note that the short period magnetic data also indicate an anomaly around this area. - (Section 6.2, Fig.6.8).

In Ross-shire, to the south of the Lairg region, the azimuth of the impedance again changes direction between Croick and Bonar Bridge. Both sites lie near the contact between the moine rocks of the metamorphic zone and the extensive Carn Chuinneag granitic pluton. Also Bonar Bridge is near the Dornoch Firth. Hence it appears that the sedimentary basin to the east and the resistive granitic massifs in the area have some influence on the direction of the maximum MT responses.

In the Great Glen region, Kirkhill and Aldourie are two sites within the Glen while Achanalt, to the north-west is

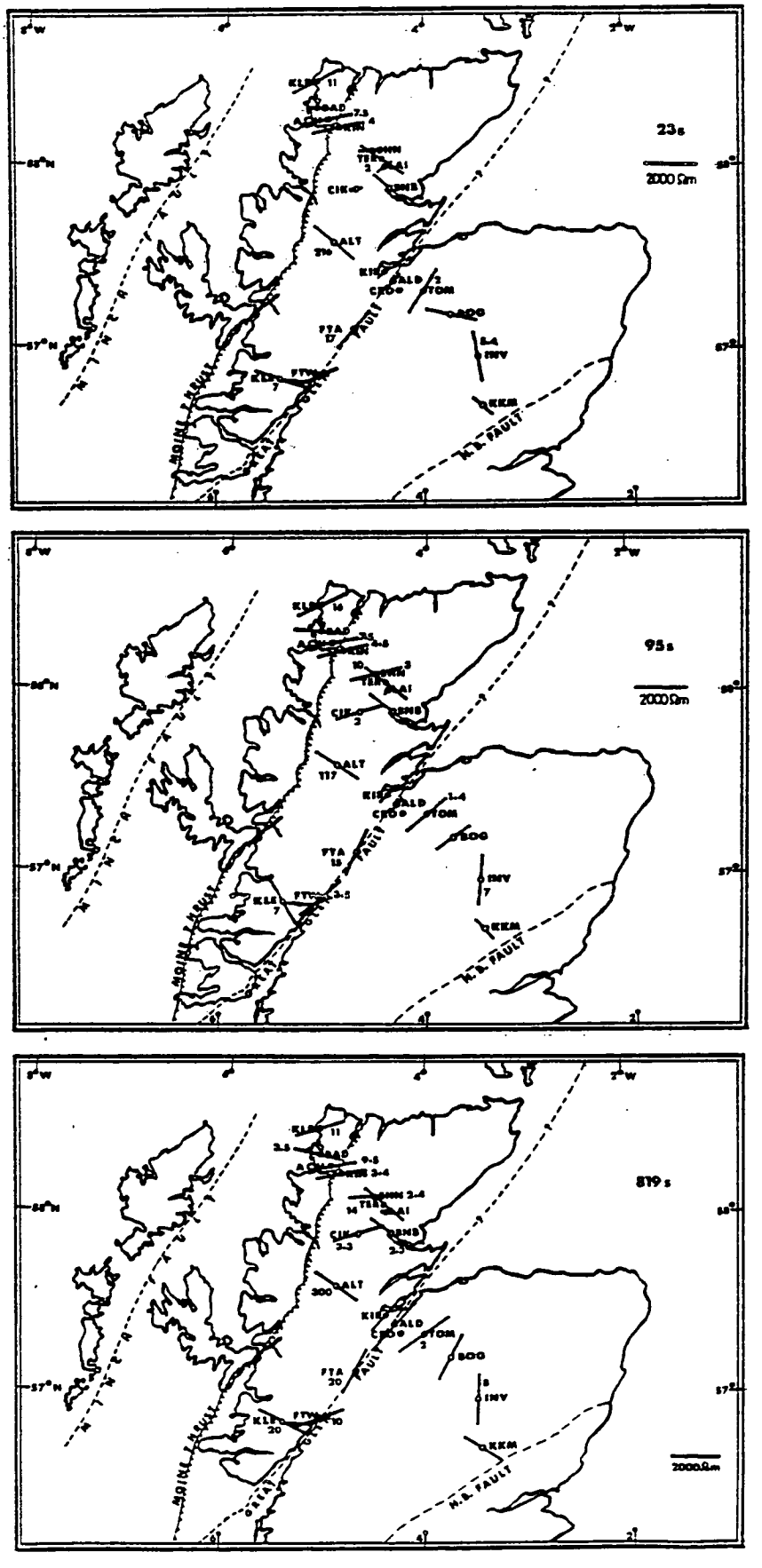

Fig.5.5 Maps of the azimuth of the major impedance.

outside it. The azimuths of the major impedances within the Glen are parallel to the strike of the fault but at Achanalt, the azimuth is perpendicular to the strike. This is the behaviour expected near a contact between resistive and conducting rocks. The sharp decrease in the magnitude of the impedance at all periods within the Glen also supports this simple explanation for the behaviour of the impedance azimuths in this region.

In the Central Highlands, the azimuths vary from site to site and are also period-dependent except at Kirkmichael. The azimuth at Kirkmichael is normal to the strike of the Highland Boundary fault at all periods. Hence as expected, the major impedance is in a direction perpendicular to the contact between the more resistive Dalradian rocks just north of the fault and the sediments in the Midland Valley. The azimuth at Inverey is probably influenced largely by the granitic plutons to the north-west and east of the site. At Tomatin which is 24 km from the Glen, the azimuth seems to be influenced by the presence of the Moy and Findhorn granite massifs as well as by the Devonian sediments nearby. At Boat of Garten, the azimuth rotates abruptly through about 90 deg. as the period increases. This suggests a marked difference between the crustal and the deeper geoelectric structure at the site.

Along the Great Glen, the direction of the maximum impedance changes at Fort Augustus to WNW at Kinlocheil which lies to the west of the Glen. The magnitude of the impedance at the southern sector is about twenty times its value at the northern sector of the Glen. These changes in the response parameters along the glen seem to suggest a significant irregularity in the geometry of the Great Glen conductivity structure. There is probably a conside-

rable sea effect on the response at Kinlocheil which is not far from the shallow Sea of the Hebrides.

5.2.2 Geoelectric Pseudosections

A pseudosection is a very useful way of presenting raw apparent resistivity data as a function of period as well as position on an MT traverse. In such a presentation , both the lateral variation of the resistivity and the variation of the resistivity with period (a measure of depth) is displayed in a convenient form for a general and qualitative information across the region under survey. Pseudosection presentation has been used recently by Breymann(1977), and Strangway and Koziar(1979) among others.

For the presentation which is reported here, the following procedure was adopted.

i) Most of the faults on the Highlands are approximately parallel to the Great Glen fault which has a geological strike direction of 40 deg. east of north - Section 1.5, Fig.1.10. The apparent resistivities in directions parallel ($\rho_{//}$) and perpendicular ($\rho_{\perp}$) to this strike was obtained by computer rotation of the impedance tensor for each site on the main MT traverse from Kinlochbervie to Kirkmichael.

ii) For each site, the matrix of $\rho_{//}$ and $\rho_{\perp}$ was assembled so that each column represents resistivities at a single site.

iii) Using an E.R.C.C. General Purpose Contouring Program (GPCP), a final grid was produced so that each column contained resistivity data with period increasing from the top row downwards in order to preserve the sense of depth in the pseudosection. The grid was then contoured and a plot of the pseudosection was

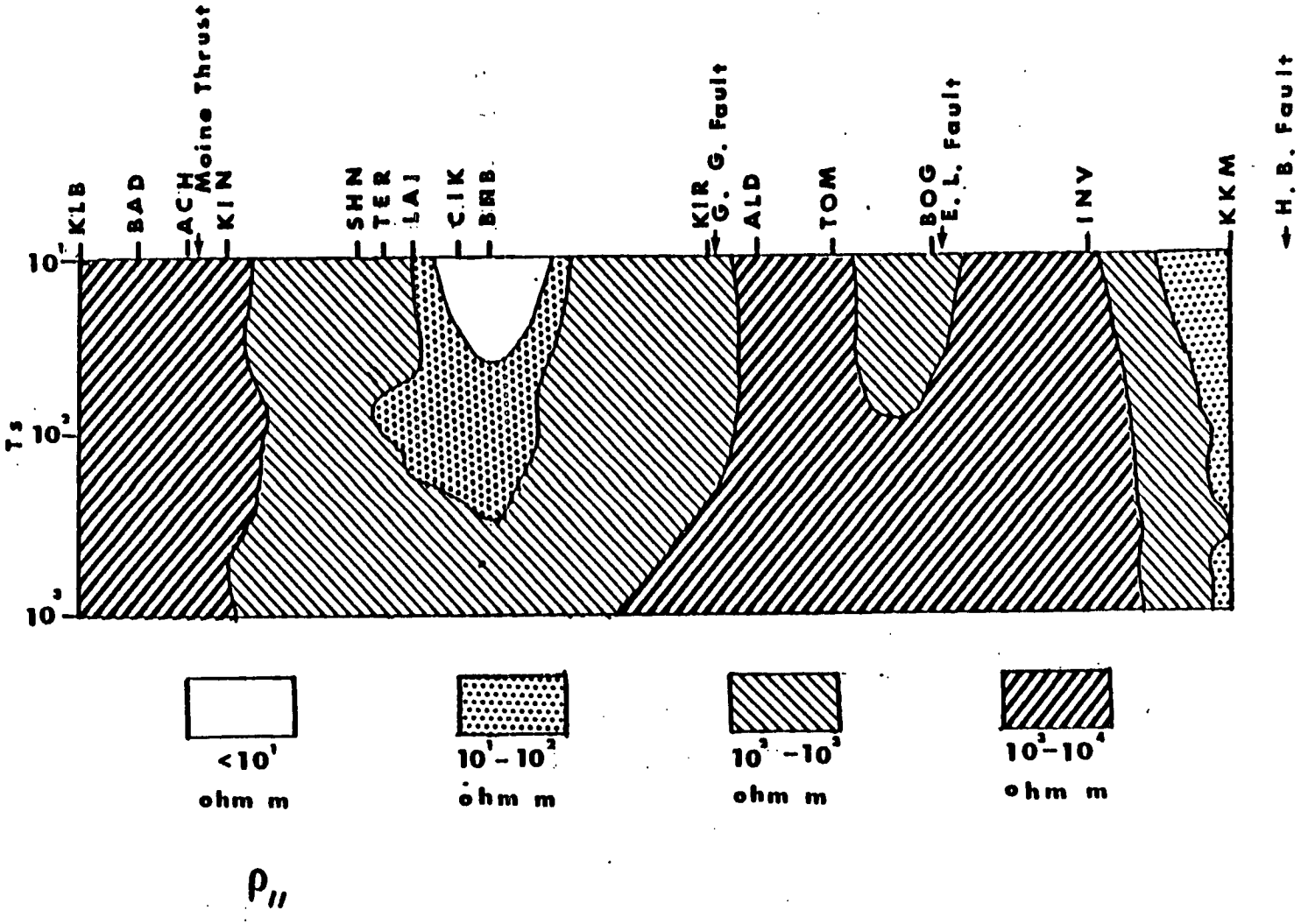

Fig.5.6a Geoelectric pseudo-section for $\rho_{//}$ (along a strike of N 40°E).

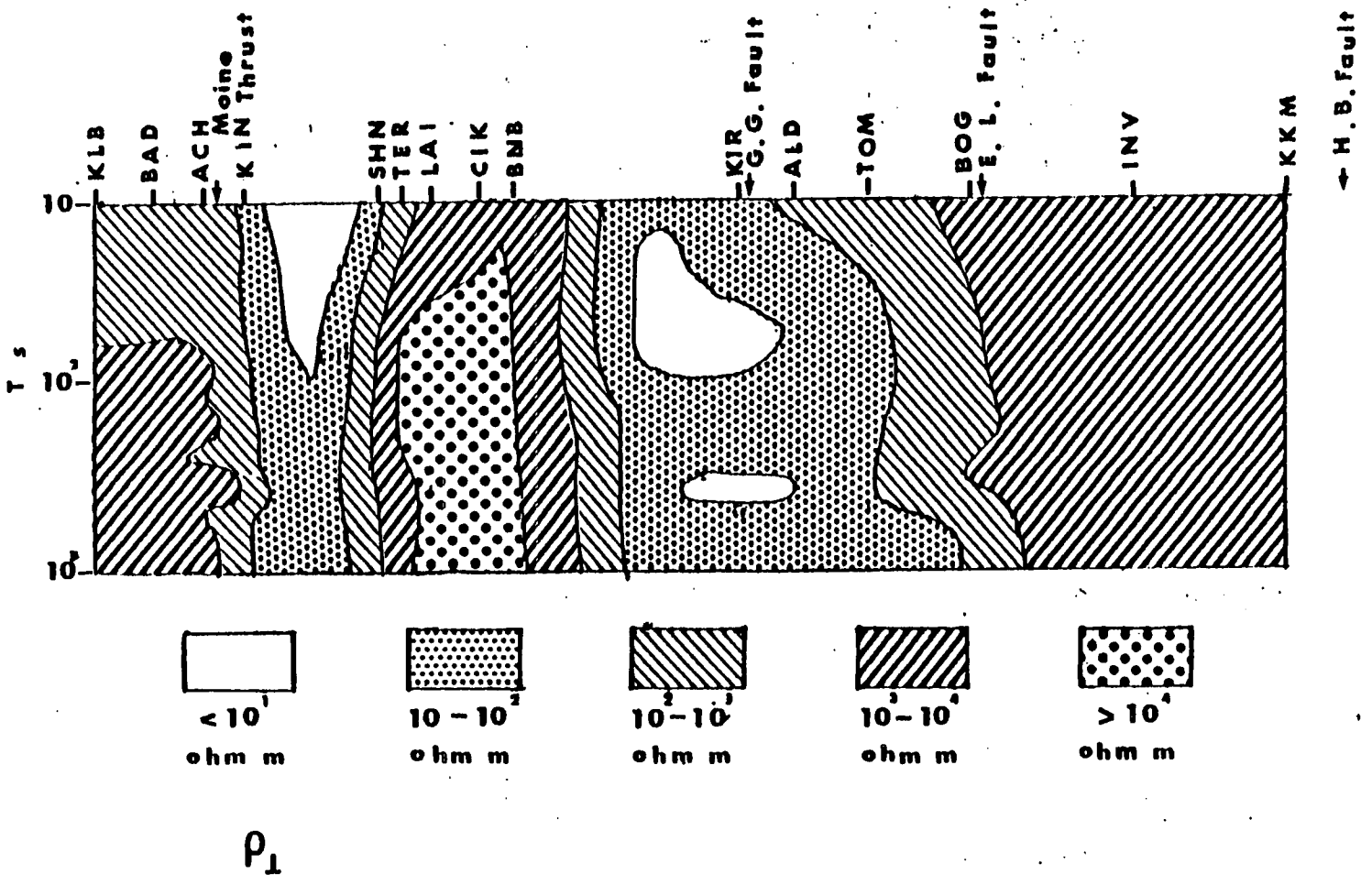

Fig.5.6b Geoelectric pseudo-section for $\rho_{\perp}$ (perpendicular to a strike of N40°E).

obtained from a Calcomp plotter output. For easy assessment, the contour intervals have been shaded in four decades as shown in Fig.5.6.

The two sections indicate the complexity of the geoelectric structure across Northern Scotland especially in the region north of the Great Glen where most of the sites showed three-dimensional characteristics. Inspite of this complexity, it is interesting to see that the sections together do delineate regions of high resistivity on the north-western shield fragment and around the major granitic intrusions on the Central Highlands as well as conducting zones around the Moray Firth region of the Great Glen and near the Highland Boundary Fault.

5.2.3 Induction Vector Maps

In Fig.5.7, maps (a) and (b) show plots of the real and imaginary induction vectors for 23 and 95s while (c) and (d) are maps of the vectors for 315 and 819s using all available data from both GDS and MT measurements. The station names for the GDS sites (1.4) are not shown for clarity.The centre periods for the GDS estimates are 5 and 13 minutes.

On the Foreland at short periods, the induction vectors are large and point to the surrounding shallow seas. This arises from the coast effect on short period magnetic induction data. Green (1974) found similar effects at periods between 20 and 500s at two of his coastal stations, Lerwick and Valentia during his induction study in the British Isles. For periods up to about 300s, the adjacent seas and the sediments in the Minch basin seem to be the dominating structures as can be seen in (c) where the arrows on the foreland and on the Isle of Lewis point to a

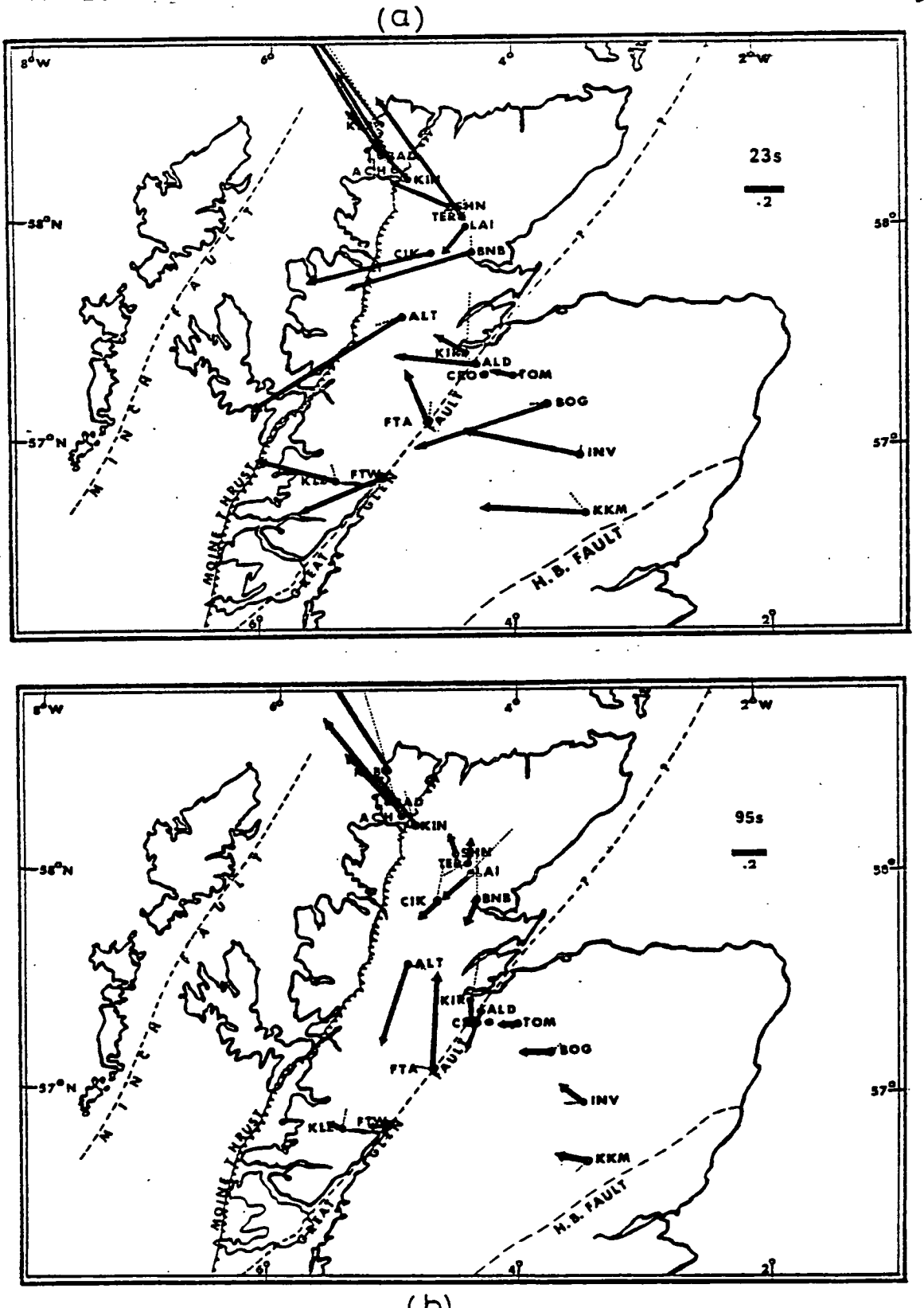

Fig.5.7a Induction vector maps (23 and 95s)

(c)

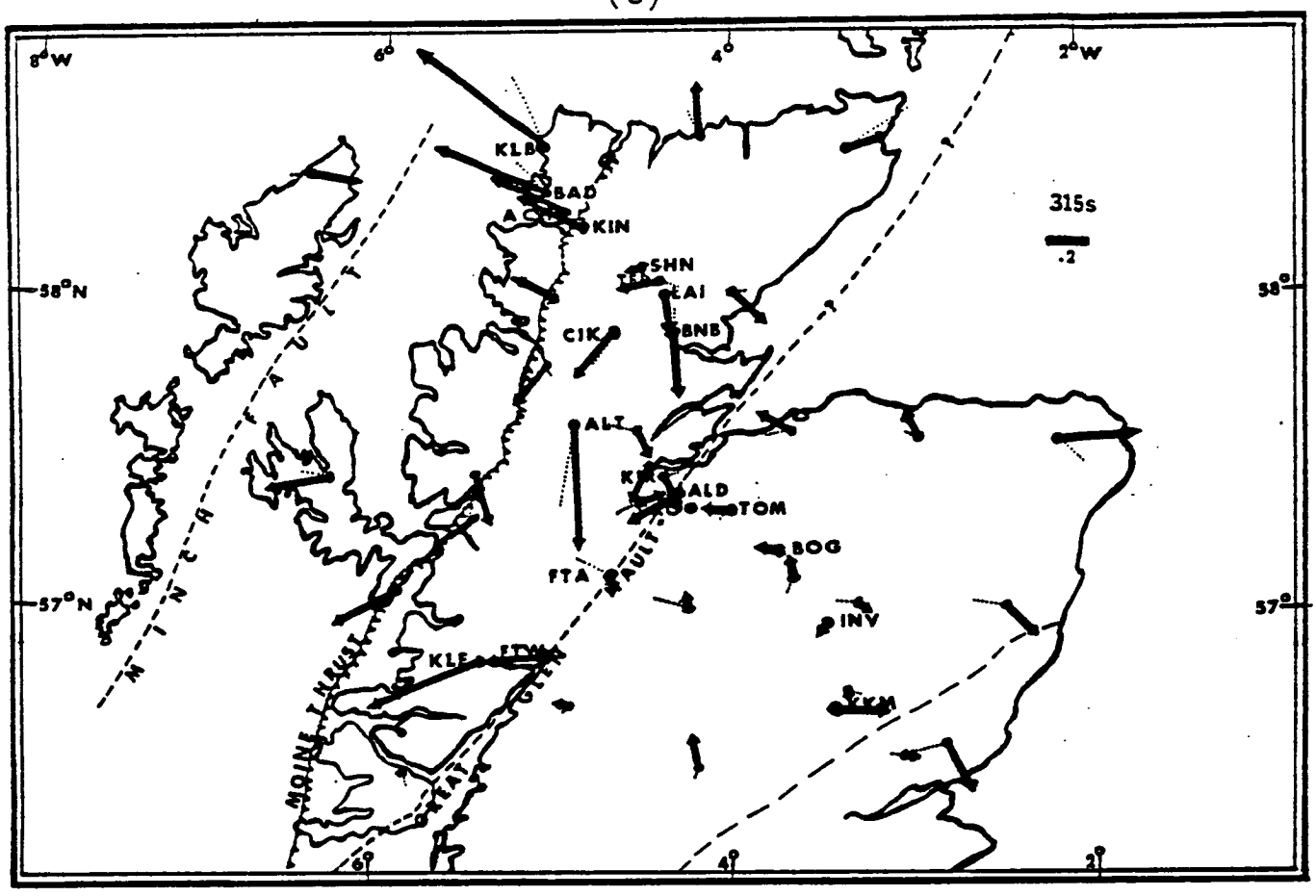

(d)

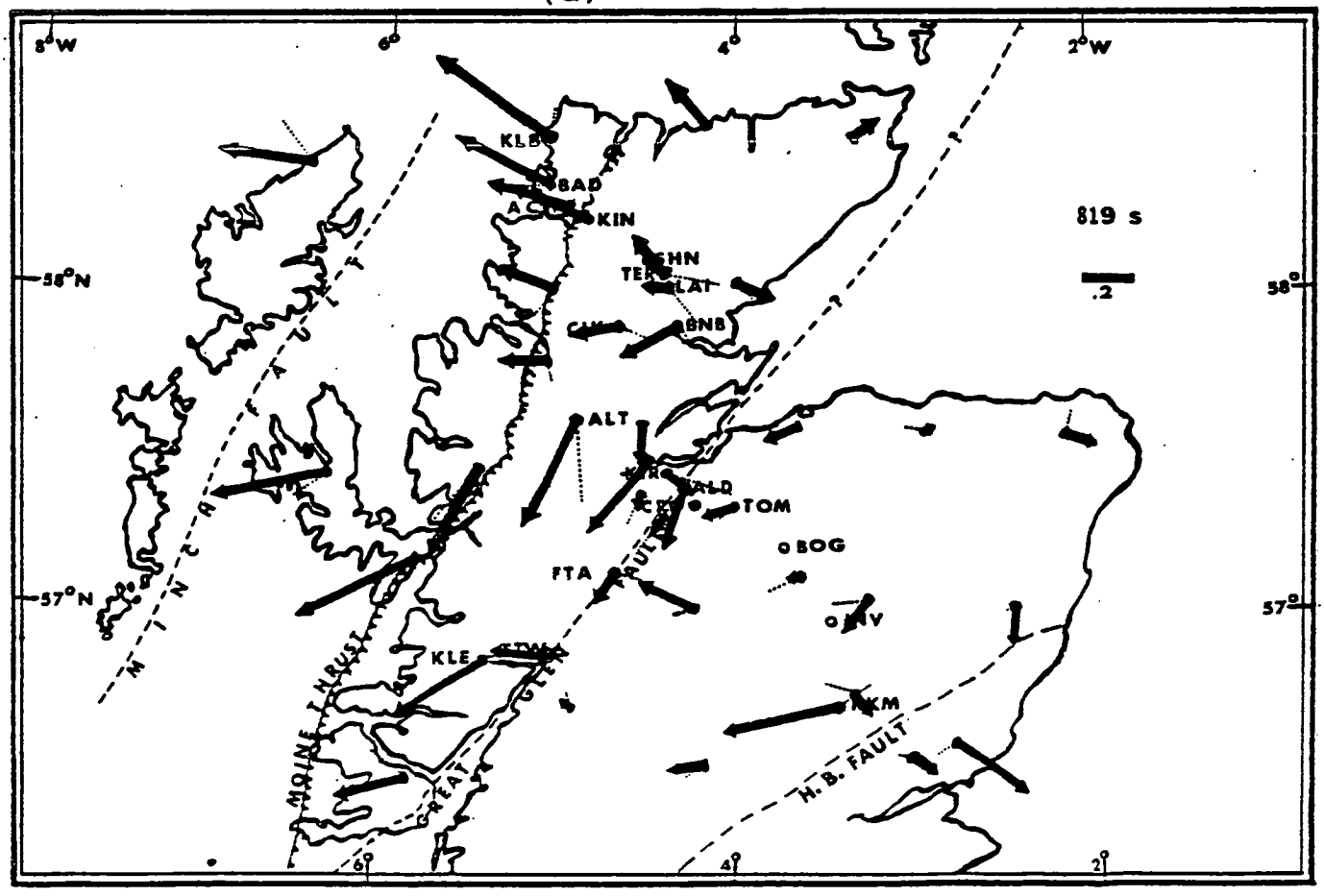

Fig.5.7b Induction vector maps (315 and 819s).

current concentration along the Minch.As the period increases to about 13 min, (d), the ocean seems to contribute to the response in the region. The magnitudes of both the real and the imaginary vectors are also considerably reduced. This observation is in very good agreement with the results of two-dimensional model responses for the region of Northern Scotland and its adjacent seas as will be shown later in 6.1.5. In the Lairg region, the behaviour of the vectors as the period increases is similar at West Shinness and Terryside while the vectors at Lairg, Bonar Bridge and Croick tend to rotate in the same sense.It is also interesting to see that the imaginary vector at Lairg tends to be large especially at short periods. This suggests that the anomaly which is also seen in the resistivity data is probably a shallow one.

In the north Great Glen area, the vectors at sites west of the fault rotate from a westerly direction to point to the Glen as the period increases to 95s. At this period, all real vectors in the Central Highlands also point to a current concentration in the Glen. However from the behaviour of the vectors at Fort Augustus, Fort William and Kinlocheil, most of the current appears to be diverted to the west near the central part of the Glen.

In the Central Highlands, the vectors in maps (c) and (d) reveal an additional complex pattern of current. The additional feature here may be due to the circulation of induced currents round the resistive granitic massifs in the area and the effect of the adjacent North Sea and the Atlantic Ocean which tends to become important at long periods.

5.2.4 Bank's GDS Response Functions

As discussed in Chapter Two, a presentation of GDS transfer function information in the form of Bank's maximum response arrows was carried out. The magnitudes of the maximum arrows were greater than those of the minimum response arrows as expected but the latter were often not negligibly small compared with the former at some sites especially at short periods.

Significant minimum response component implies that the strictly two-dimensional regional conductivity anomaly assumed in the maximum response function formalism is probably an over-simplification for a geologically complex region like Northern Scotland.

In Fig.5.8 only the maximum arrows for three periods are plotted for clarity but the azimuths of MT major impedance (Fig.5.5) are shown by broken lines. For a simple two-dimensional conductivity anomaly, the maximum arrow should be normal to the major impedance on the conductor and parallel to it away from the conducting region (Rooney and Hutton, 1977).

The plots in Fig.5.8 suggest that the situation in Northern Scotland is not so simple. Hence, the results of GDS maximum response analysis do not give information additional to the qualitative interpretation already provided by ordinary induction vectors.

5.3 Qualitative Conclusions from the Results

Having examined the primary results from both magnetotelluric and GDS analysis, it is helpful at this point to summarise the qualitative information which both techniques have provided so far about the region.

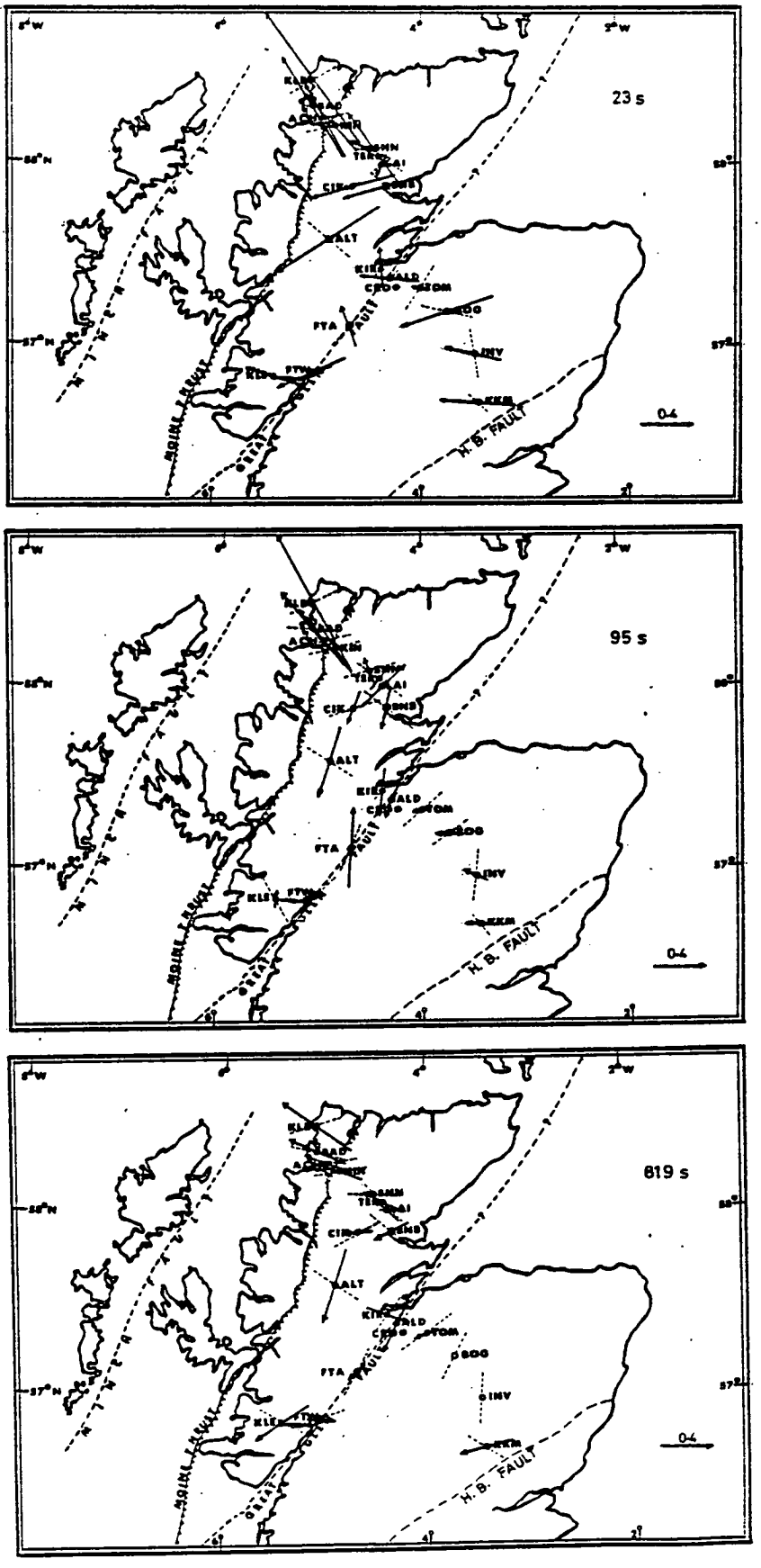

Fig.5.8 Bank's maximum response arrows.

(Broken lines - Azimuths of major impedance)

i) Complex Geology

MT response parameters like the azimuth and skewness and the magnitudes and directions of the induction vectors, especially in the region north of the Great Glen, confirm that the geology and the tectonic structure of Northern Scotland is not simple.

ii) The Effect of the adjacent Seas and Ocean

The azimuth of the major impedance and the induction vectors both reveal the considerable influence the seas and the ocean have on induction measurements in Northern Scotland. Induction in the shallow seas predominate at short periods and affect coastal stations most while the effect of the ocean is important across the whole region at long periods. In addition to these effects, strong local conductivity anomalies can be seen in some parts of the region.

iii) The Lairg Anomaly

The behaviour of the azimuth and the variation in the magnitude of the major apparent resistivity and the large imaginary part of short period induction vector around Lairg seem to point to a more localised anomaly in that area.

iv) The Great Glen Anomaly

Both the resistivity and the magnetic data indicate a non-uniform conductor in the Great Glen region.

v) Large Resistive Intrusions

High apparent resistivities at some sites indicate the

widespread granitic bodies in the Scottish Highlands. In the Grampian Highlands, the directions of the induction vectors at some of the sites suggest a complex diversion of induced currents round these resistive bodies supporting the deductions made from the apparent resistivity data.

In the next chapter, these conclusions are used as a qualitative introduction to a more quantitative study of the data.

CHAPTER 6

INTERPRETATION OF RESULTS

In the last chapter, the results of MT and GDS measurements in Northern Scotland were presented. Only a qualitative interpretation of the data was possible at that stage of analysis. In this chapter, a more quantitative analysis and discussion of the results are given. Various factors that can complicate data interpretation are considered and the different procedures adopted in order to minimise their effects are presented.

The results of one-dimensional inversion for typical sites in the regions identified qualitatively in Chapter Five are presented. Model geoelectric sections are constructed using the two-dimensional program described in Chapter Two and model responses are compared with experimental data. Both GDS Hz/Hy amplitude ratios and apparent resistivity and phase data are used in a complementary manner and these together provide some constraints on the range of acceptable models for the region.

The significance of the geoelectric structure obtained for the region is considered and some interpretation in terms of the geology, tectonic history, crustal and upper mantle constitution across the region are discussed. The deductions based on the geoelectric model are compared with conclusions from other geophysical studies in the region.

6.1 General Problems of Geoelectric Data Interpretation

In this section, the factors that can complicate the interpretation of induction data are reviewed briefly. These include the source field structure, regional geology, the distor-

tion of measured fields and the position of measurement sites relative to the conducting seas.

6.1.1 Source Field Effect

As was pointed out in Chapter Two, both the GDS and MT analysis assume that the source field has an infinite wavelength. A finite wavelength source would therefore introduce errors to Earth models based on the plane-wave theory (Price, 1962).

Most of the data used for interpretation in this study were in the period band 20 - 819s. The source field variations were therefore mostly in the micropulsation band and to a lesser extent, for periods greater than 600s, harmonics of substorm variation field. The morphology of micropulsation source fields have been studied for a number of years. Orr (1973) has presented a very comprehensive review of both theoretical and experimental results of world-wide micropulsation studies. In the British Isles, Orr and Webb (1975), Green (1974, 1978) and Stuart (1979) are among those who are continuing the study. From these and other reports, it is fairly well known that

a) micropulsation source fields are of magnetospheric origin

b) micropulsations at mid-latitudes have spatial wavelengths which are long compared to the depth of penetration of MT fields in the Earth.

c) pulsations with wavelengths less than the height of the ionosphere are strongly attenuated by the ionosphere.

For the British Isles, Green (1974) found that induction results based on the plane-wave assumption for the 20 - 600s period band for Lerwick (Lat. 60.13 deg.N) and Valentia (Lat. 51.93 deg.N), two coastal stations were similar. His observations

therefore imply that the assumption of a plane wave source field for micropulsation periods is a valid one for sites in the N. Scotland region (Lat. 56.72 - 58.48 deg.N) of this study.

Field variations in the period band 600 - 1000s are due to substorms and their harmonics and are associated with geomagnetic storms. The morphology of storm-time source field is complex. Hughes and Rostoker (1979) and Rostoker and Hughes (1979) have recently shown that source fields associated with magnetic activities at high latitudes (53.3 - 69.1 deg.N) have time-dependent dimensions and very complex structures.

The latitudinal variations of the field components X, Y and Z for moderate magnetic activity at five different times of day (Hughes and Rostoker, 1977) are shown in Fig.6.1a. Using these variations, Hutton et al (1980) have shown that there is a daily variation in the ratio $Z/(X^2+Y^2)^{\frac{1}{2}}$ with a maximum around dawn. They also pointed out that the space gradient in the ratio is greatest during the morning and evening hours for latitudes in the range 60 to 62 deg. as shown in Fig.6.1b.

Most source field studies often neglect the inevitable contribution by induction to the observed fields. The extent to which induction components contribute to reported spatial gradients in source fields is therefore difficult to quantify. Some of the scatter often observed in measured induction response functions at long periods is usually attributed to source field gradients. In this study, greater weight was therefore given to the data in the micropulsation band for which the plane wave assumption was considered valid.

6.1.2 Complex Geology

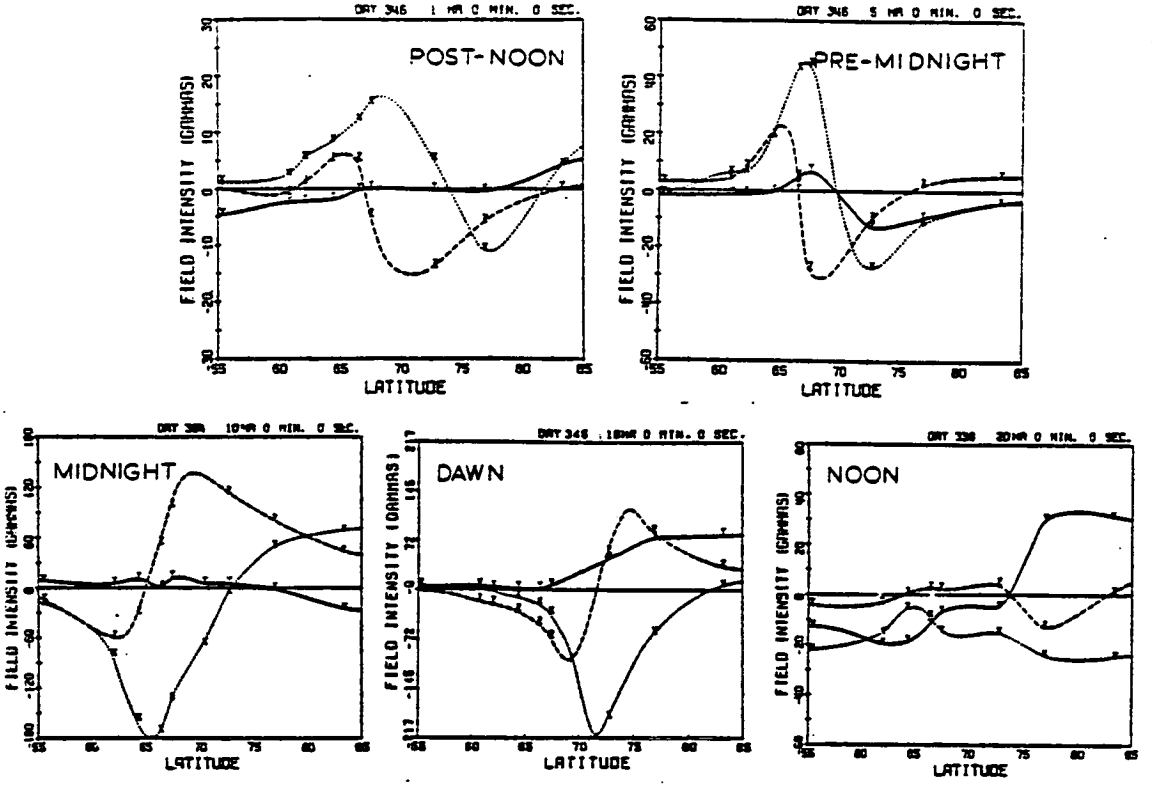

(a)

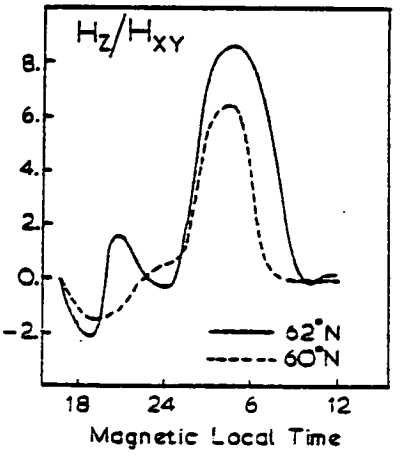

(b)

Fig.6.1a Latitudinal variations of D, H and Z at different times of day due to a typical steady-state auroral current system. (Hughes and Rostoker, 1977).

(b) Time variation of the ratio of vertical Hz to total horizontal Hxy magnetic field for geomagnetic latitudes relevant to N. Scotland.

Both the GDS and MT analysis assume idealised Earth structure of two-dimensional geometry. The few three-dimensional model studies also assume conveniently shaped anomalies in order to ease problem formulation and numerical solution as reviewed in Chapter Two. Although such studies have provided valuable information and interpretation of induction data, it is widely known that there are often problem sites within a region where the data cannot be satisfactorily interpreted in terms of two- or three-dimensional models. Complex geology at site or area of measurement can cause measured response parameters to differ considerably from idealised models.

A brief geological and tectonic description of Northern Scotland was presented in Chapter One. The geology of the region is complex. The complexity of the structures at certain sites was indicated by very high skew factors from conventional two-dimensional analysis results presented in Chapter Five.

In order to investigate these complexities further, the effect of the structures on the four tensor impedance elements were analysed by rotation. For each site, the averaged elements were rotated in steps of 5 deg. through 180 deg. and the result was displayed as plots using the Calcomp plotter. For a simple two-dimensional structure, the skews should be low and the diagonal elements Zxx and Zyy should be low compared to Zxy and Zyx. Further, Zxx or Zyy should exhibit two minima while Zxy or Zyx should have a single minimum on rotation (Rankin and Reddy, 1969; Hermance, 1973). It was found that for sites where low skews suggested a two-dimensional structure, the impedance elements were well-behaved. The behaviour of the rotated elements at sites with high skews was rather complex.

The region south of the Great Glen was generally two-dimensional. The region north-west of the Glen was rather complex except at site 19 (SHN) and site 4 (KLB) where both the skew and impedance rotation indicated simpler structures. Some typical results of the tensor impedance rotation analysis for both two-dimensional and complex sites are shown in Fig.6.2a and Fig.6.2b respectively.

Because of the obvious structural complexity of the region north of the Glen, there was need for caution in interpreting the data from the area strictly in terms of a regional two-dimensional model. As a precaution, the data from the two-dimensional sites identified in the rotational analysis and by relatively low skews were given more weight in the two-dimensional model studies and interpretation presented later. A comparison of results is also made with geological and other geophysical data from Northern Scotland.

6.1.3 Surface Distortion

In Chapter Two, it was pointed out that surface inhomogeneities at a given site can cause the distortion of measured MT fields and thereby complicate the interpretation of the data at a site within a general two-dimensional region. Berdischevsky and Dimitriev (1976) have reviewed the general problem of surface distortions in induction studies and have also suggested ways of identifying and minimising such effects. They pointed out that detailed information on the sedimentary cover in the region as well as simultaneous GDS and MT data were essential for a solution to the problem.

There is little geological information on the sedimentary

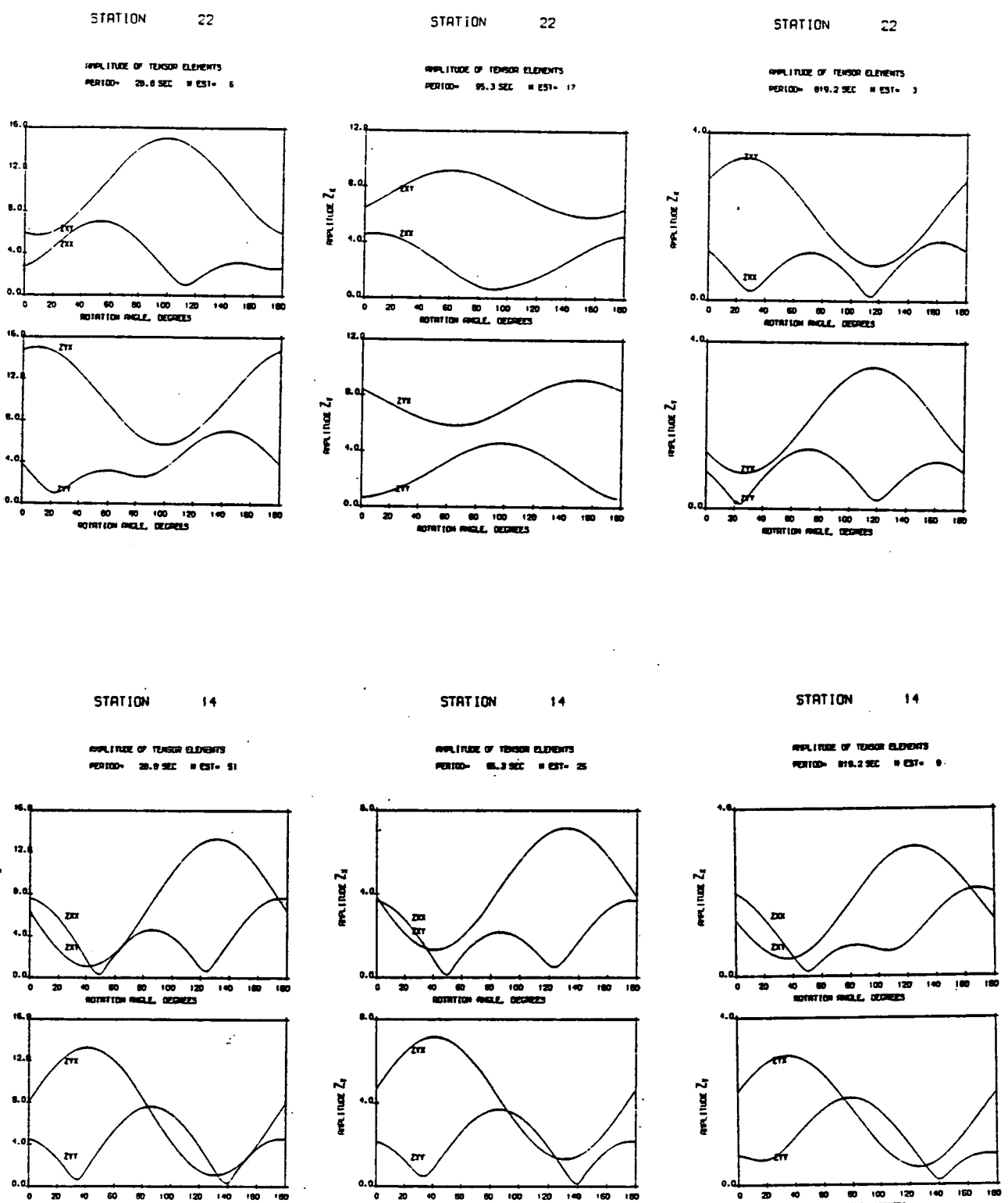

Fig.6.2 Results of impedance rotation analysis.

(a) Two-dimensional Sites.

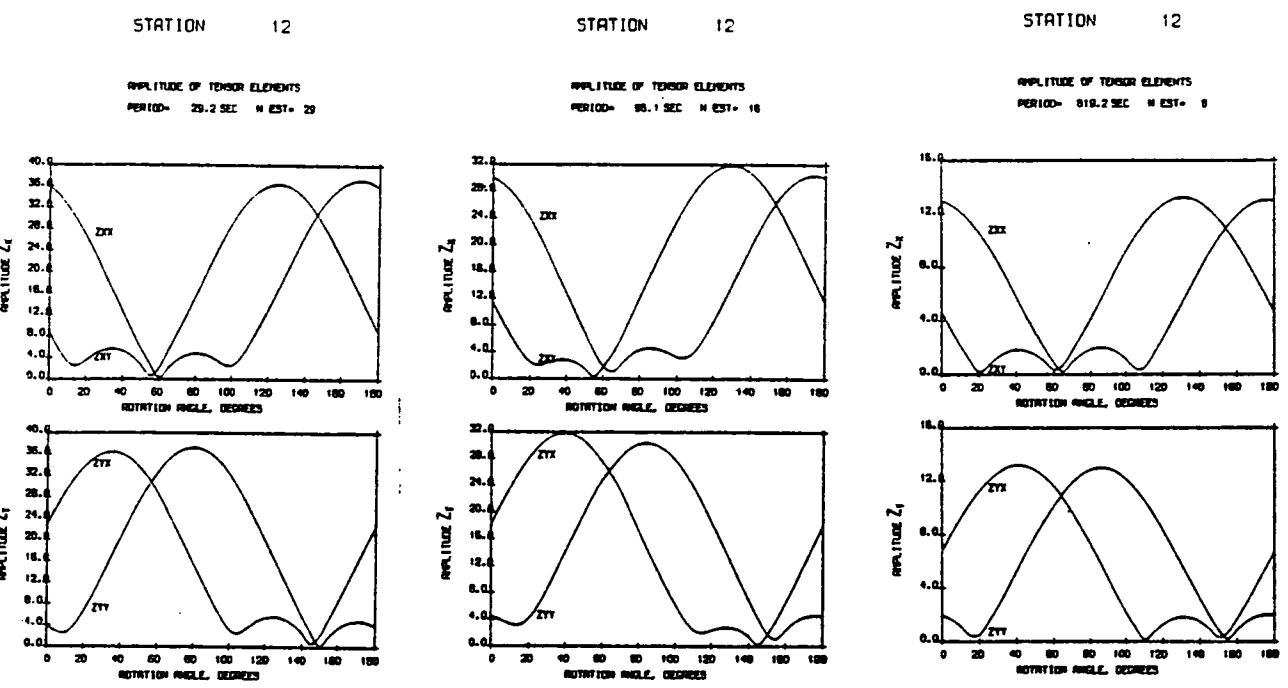

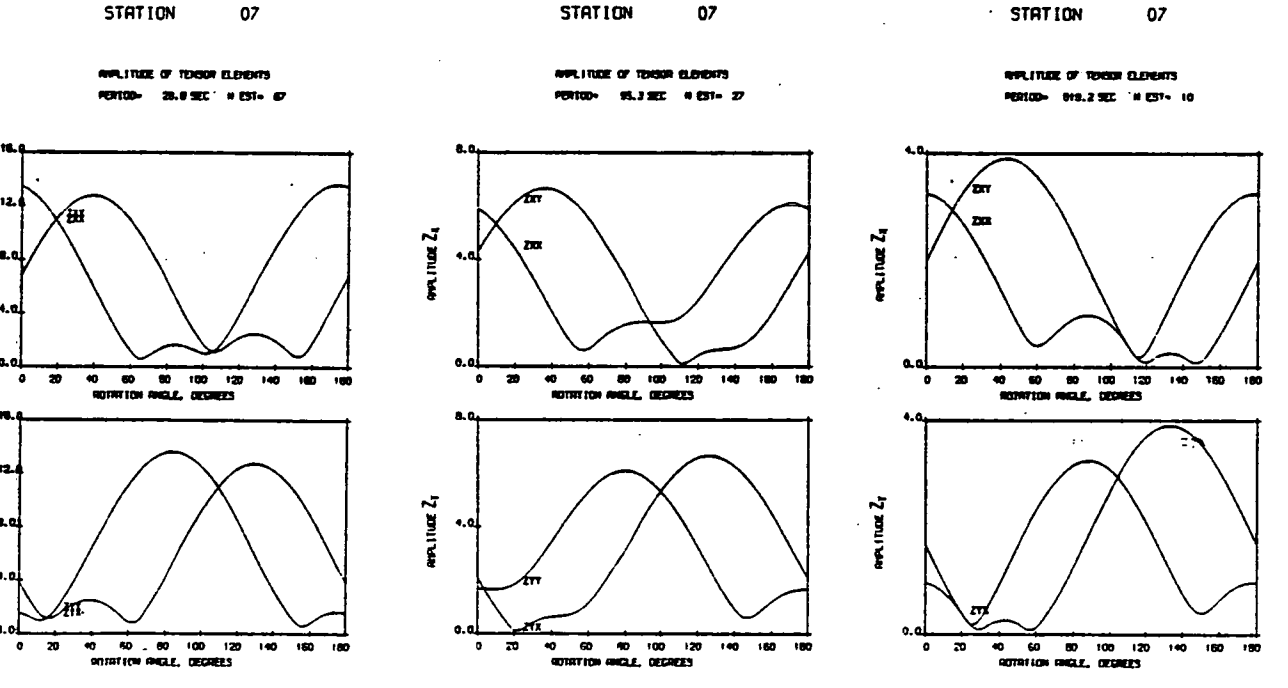

Fig.6.2(b) Complex Sites

cover in Northern Scotland apart from the area of Devonian sediments around the Moray Firth Basin. Simultaneous GDS and MT data are however available.

As discussed in Chapter Two, Haak's Min-max analysis should also provide some information on the perturbation of the measured response functions. The results of the analysis for sites in the Lairg region where short period magnetic and resistivity data indicated anomalous variation were examined. The azimuths of the rotated magnetic fields correlating with electric field components showed a high degree of period-dependence and scatter for the three sites SHN, TER and LAI. The results from two other sites, KLB and TOM outside the Lairg region were similarly unstable. It appears therefore that the Min-max method which was developed for identifying perturbations in a large two-dimensional conducting region can not be successfully applied to the situation in Northern Scotland which has a complex geology and adjacent conducting shallow seas.

The following procedures have therefore been adopted in order to minimise the effect of any surface distortion on the data.

i) For one-dimensional inversion, the mean apparent resistivity data calculated from rotated impedances Zxy and Zyx were used. This minimises the distortion of the data by three-dimensional surface inhomogeneities.

ii) Both MT and GDS responses were used together in the model studies as distortions of the magnetic fields by surface effects are thought to be considerably less.

6.1.4 Conductive Channelling of Induced Currents

Some conductivity anomalies indicated by magnetometer array studies (Gough, 1973; Vasseur et al, 1977) are difficult to explain by theories based on a local induction process. The explanation given for such anomalies often requires induction over a wider region far beyond the locality of measurements. The currents induced in the wider region are then thought to flow preferentially in the more conductive structures adjoining the region. Anomalous fields measured near such conducting structures would therefore be due to the current concentration in the conductors and not to currents due to a local induction in the structure itself.

Early reports of the phenomena were based on long period measurements from harmonics of the solar quiet time daily variation, Sq and storm time variation source fields. In the British Isles, Edwards et al (1971) and Bailey and Edwards (1976) have suggested current leakage between the Atlantic Ocean and the North Sea using long period magnetic data. They also postulated that a conducting path for the channelled currents was provided by the Eskdalemuir anomaly associated with a NE-SW crustal conductor at a depth of 10 - 12km. While it is less problematic to understand how the large potentials set up in the oceans and continents by long period variations could cause current leakage through suitable paths in the Earth, it is debatable whether the channelling phenomenon is relevant to short period measurements. For regional surveys using micropulsation variational fields, global Sq-type current loops can be excluded.

However, in order to allow for the effect of currents induced in structures outside the immediate boundary of the survey area, it is essential to include in models the regions

surrounding the survey sites. In practice, this implies extending the grid boundaries in numerical models by at least a few skin-depths beyond the model survey area. Lack of adequate knowledge about the conductivity structure of the surrounding region, limited computer storage and time are possible factors which may militate against this approach to the problem.

In this study, the two-dimensional models for Northern Scotland extended to ±500 km on either side of the Great Glen on a SE-SW traverse and included the shallow seas and the conducting sediments in the Midland Valley to the south.

6.1.5 Effect of Adjacent Seas

The effect of an ocean on long period induction measurements made near a coast - the coast effect, has been known for some time (Parkinson, 1959, 1962). A similar effect due to the adjacent seas and the Atlantic Ocean was found in Northern Scotland as pointed in Chapter Five.

A numerical study of the effect was therefore carried out with a view to finding a way of minimising its influence on the data from sites near the coast. A two-dimensional coast was assumed in the models which included the Atlantic Ocean to the west, Northern Scotland and the North Sea to the east. Model results of the effect of adjacent seas on induction responses for a half-space and a half-space with a buried conducting anomaly were studied as described below.

i) Half-space with adjacent Adjacent Seas and Island

A two-dimensional model of Northern Scotland along latitude 57.3 deg. N with the y-axis centered on Central Northern Scotland

and extending to ±1500 km was used. The model included the Atlantic Ocean and the Island of Skye to the west and the North Sea and Continental Europe to the east and corresponded in geophysical dimensions to the traverse T2 (Fig.2.13)in the laboratory analogue model (Dosso et al, 1980). The conductivities for land and sea water were 0.00063 and 3.6 S/m respectively as in the laboratory model.

The results for 23 and 95s are shown in Fig.6.3 where only the responses over mainland Scotland have been plotted. The following deductions can be made from the results.

a) The real and imaginary parts of Hz/Hy which should be zero in the absence of seas are very large near coasts.

b) the ratios are less than 0.1 over a distance of about ±10 km near the centre of the model.

c) the MT apparent resistivity and phase responses are also affected mostly near the coasts. For all periods, $\rho_{//}$ (E-polarisation case) is decreased while $\rho_{\perp}$ (H-polarisation case) is increased above the half-space value near the coast. The effect decreases rapidly inland from the coast and for these periods and conductivity contrasts, the effect is negligible after about 20 km from the model coast. This distance increases with period and for periods longer than about 1000s, the coast effect persists over greater distances across the region.

d) For periods below 1000s, a mean of the two resistivities gives a value which is close to the true resistivity of the model half-space without the seas. As this result also applies to points near the model coast, the coast effect can be minimised by interpreting averaged apparent resistivities using one-dimensional models.

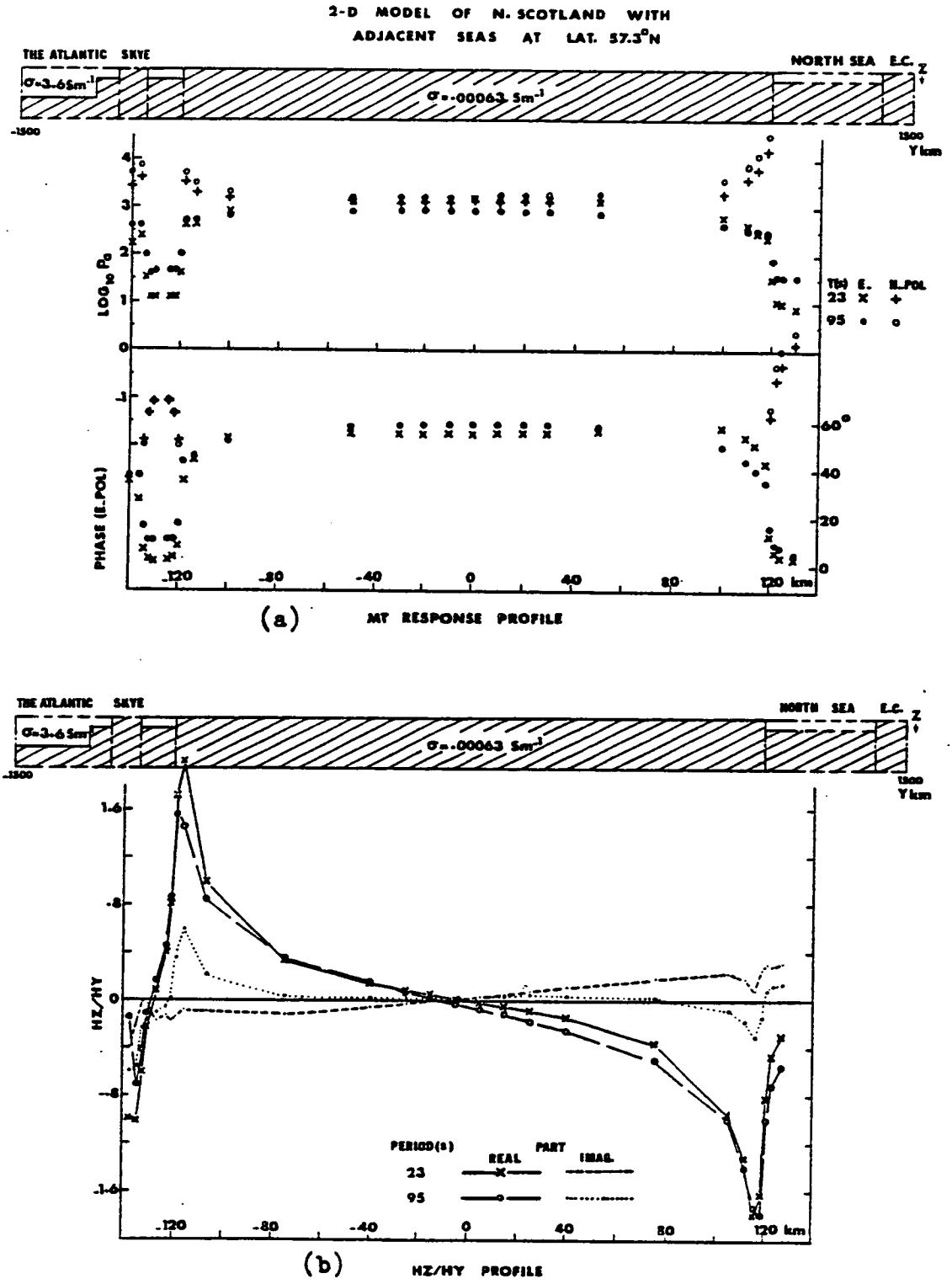

Fig.6.3 Results of numerical model coast effect studies.

(a) Apparent resistivity
(b) GDS amplitude ratio profile

The data from MT sites on the Lewisian Foreland provide an interesting example of the coast effect and how its effect on one-dimensional models can be minimised by the method suggested here. Fig.6.4a shows the plots of rotated major and minor apparent resistivities corresponding to $\rho_{\perp}$ and $\rho_{//}$ respectively. The marked decrease in anisotropy from KLB near the West Coast to KIN about 30 km inland supports the results of the numerical model study. For these sites, the effect of the east coast is negligible; the effect of the north coast, which is twice as far away as the west coast, is less than the effect of the latter but not negligible. The north coast is roughly at right angles to the west coast and will tend to cause an increase in $\rho_{//}$ and a decrease in $\rho_{\perp}$ from the results of the numerical studies. The suggested averaging therefore effectively minimises the combined effect of the two coasts.

The results of one-dimensional Monte-Carlo inversion of the mean MT responses for the three sites and the good agreement between the models obtained for the geoelectric structure of the Foreland are shown in Fig.6.4b. Interpretation based on either $\rho_{//}$ or $\rho_{\perp}$ from each site would have been contaminated by adjacent seas. The best fitting three-layer model is shown for each site by the solid line while the broken lines indicate the range of acceptable models. The best one-dimensional model has layer resistivities of $5*10^{5}$, $4*10^{3}$ and $7*10^{3}$ ohm m with interfaces at 28 km and 180 km. The one-dimensional models with their associated spaces of acceptable models provided satisfactory starting models for the more realistic two-dimensional studies, the results of which are shown later.

(a)

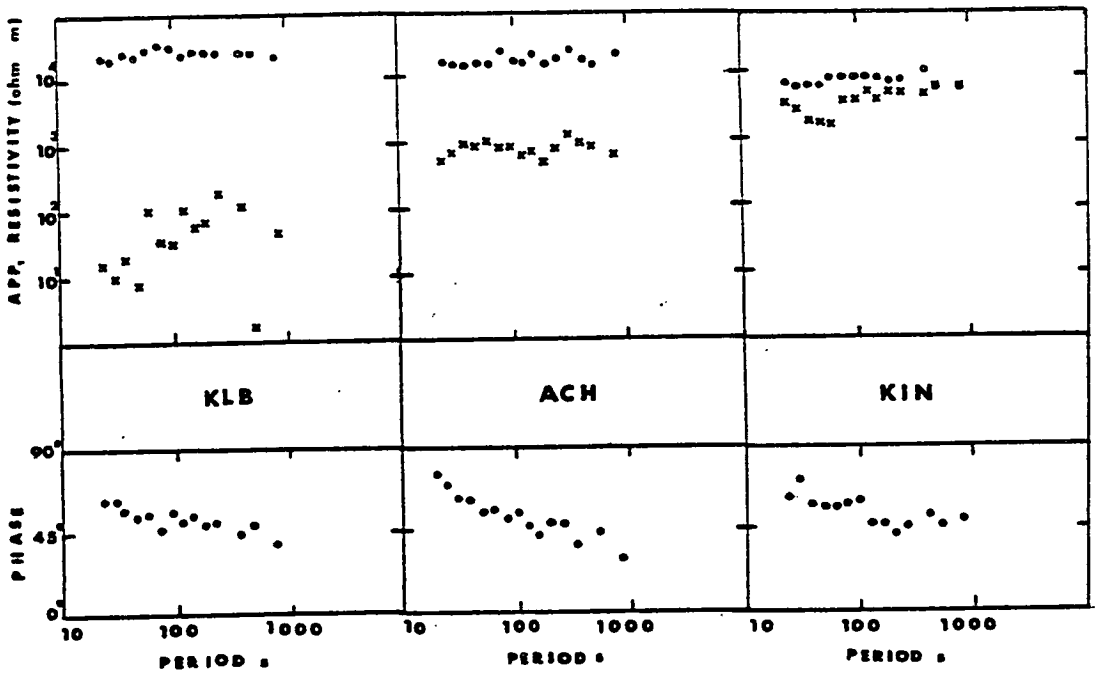

(b)

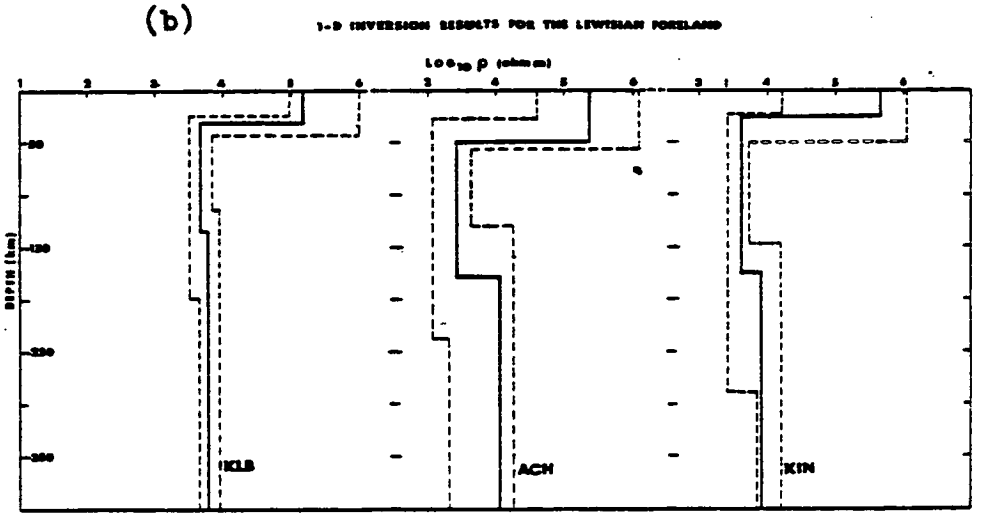

Fig.6.4 (a) MT response data for sites on the Foreland.
(b) One-dimensional resistivity models.

ii) Half-space with a Buried Conductor

In order to study the effect of adjacent seas on the response profile for a buried conductor, model responses were computed for a half-space with a buried conducting prism with and without adjacent seas. The prism had a section 50*40 km section and a conductivity of 0.02 S/m and was placed in a half-space of conductivity 0.00063 S/m. The depth to the top of the prism was 10 km and its axis was near y = 0. The response profiles are shown in Fig.6.5. The results show that

a) adjacent seas alter significantly the induction response for a buried conductor in an elongated island.

b) the inductive response of the buried conductor is superposed on the the coast effect profile. It is interesting to notice that on an island, the two turning points on the profile associated with the edges of the anomaly are more sharply defined than for burial in a half-space.

iii) Comparison of 2D Numerical and 3D Analogue Model Results

The results of laboratory analogue model study of the British Isles (Dosso et al, 1980) described in Chapter Two is shown in Fig.6.6 as a profile of Hz/Hy amplitude along latitude 57.3 deg.N which corresponds to traverse T2 in Fig.2.13. The period of the source field variation on the geophysical scale was 30 min. A two-dimensional numerical model of conductivity values of 0.00063 and 3.6 S/m for a uniform land and sea water as in the analogue model were assumed. The numerical model dimensions also corresponded to those of the laboratory model with the y-axis centered on central N. Scotland and extended to ±1500 km. The model included the Atlantic Ocean, the North Sea and part of the

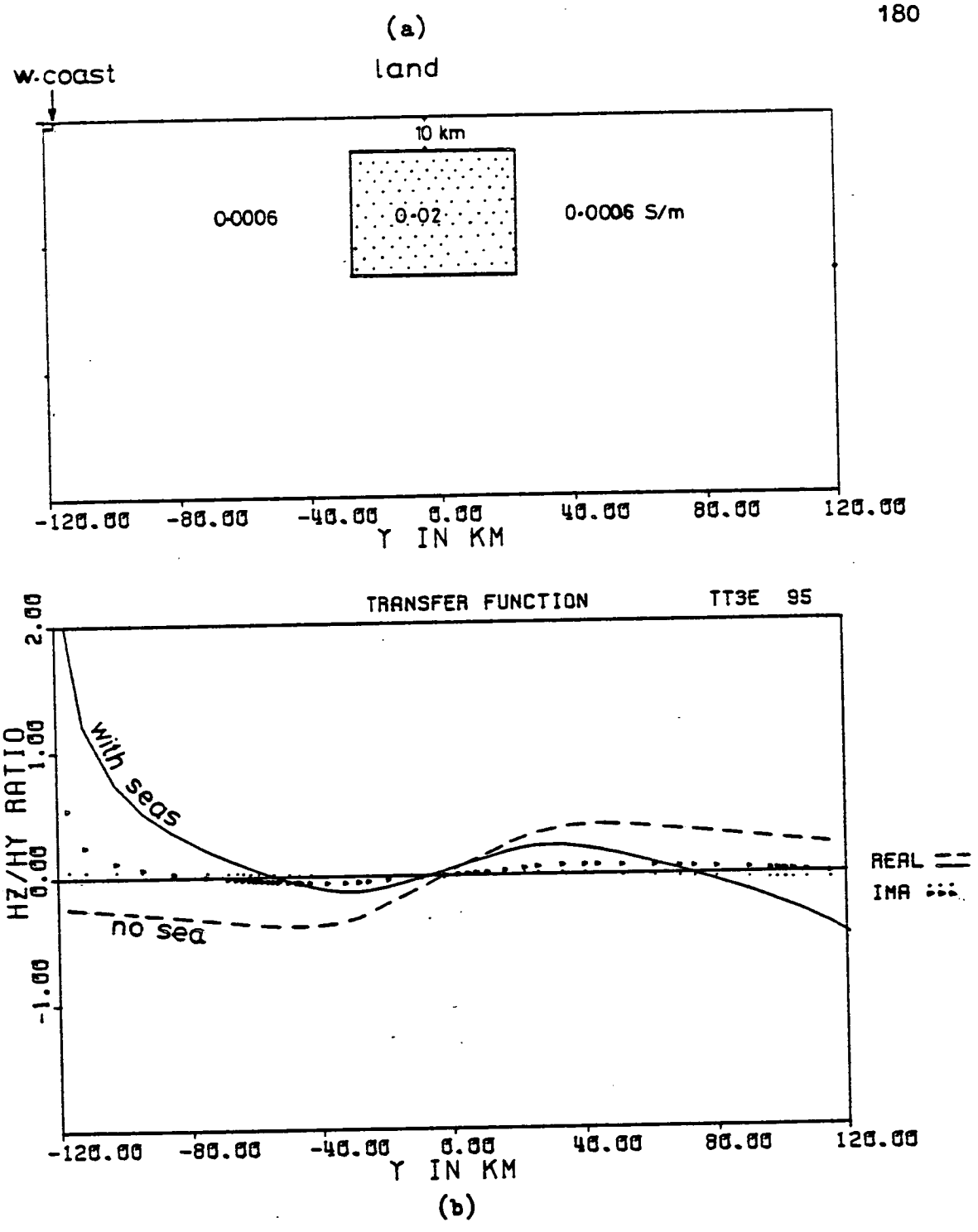

Fig.6.5 Two-dimensional GDS response for a buried conductor in an elongated island.

(a) The model

(b) The response

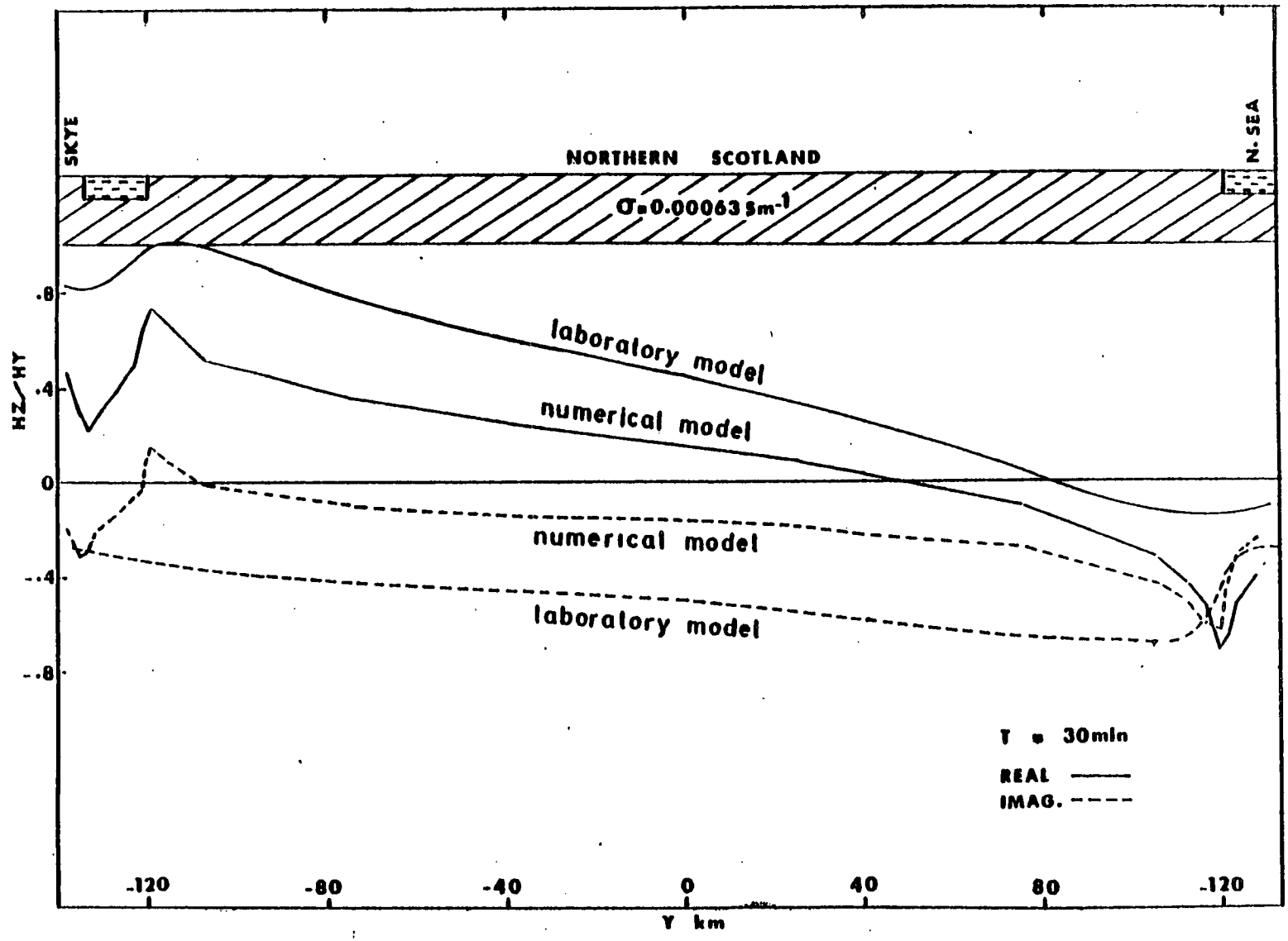

Fig.6.6 A comparison of three-dimensional analogue model with two-dimensional numerical results.

European continent as shown in the anologue model map in Fig.2.13. In Fig.6.6, only the response over N. Scotland have been plotted.

A comparison of the profiles shows a reasonable agreement in the slopes of the numerical and analogue plots of Hz/Hy due to the coast effect. However, the analogue values are about twice the numerical ones. Weaver (personal communication) has suggested that this may be due to the difference in the dimensionality of the models. Both models however, cannot give any quantitative information on the conductivity anomalies within the region as a uniform half-space was used assumed in each case.

iv) Comparison of Model Results with Data

From the GDS relation in equation 2.41, an estimate of the ratio Hz/Hy is given by the transfer function B for a hypothetical inducing field along the east-west direction. A profile of the real and imaginary parts of B from magnetic data from eleven sites along traverse T2 near latitude 57.3 deg. N was compared with a model Hz/Hy profile as shown in Fig.6.7.

The values of B are high near the east and the west coasts as in the model. There are interesting additional features superposed on the experimental profile near the central part of the traverse which corresponds to the position of the Great Glen. Therefore the coast effect alone cannot explain the observed induction response across the region. There are strong conductivity anomalies which may be associated with the geological units in Northern Scotland.

6.1.6 Conclusions on the General Problems of Interpretation

Fig.6.7 A comparison of two-dimensional numerical model with experimental data.

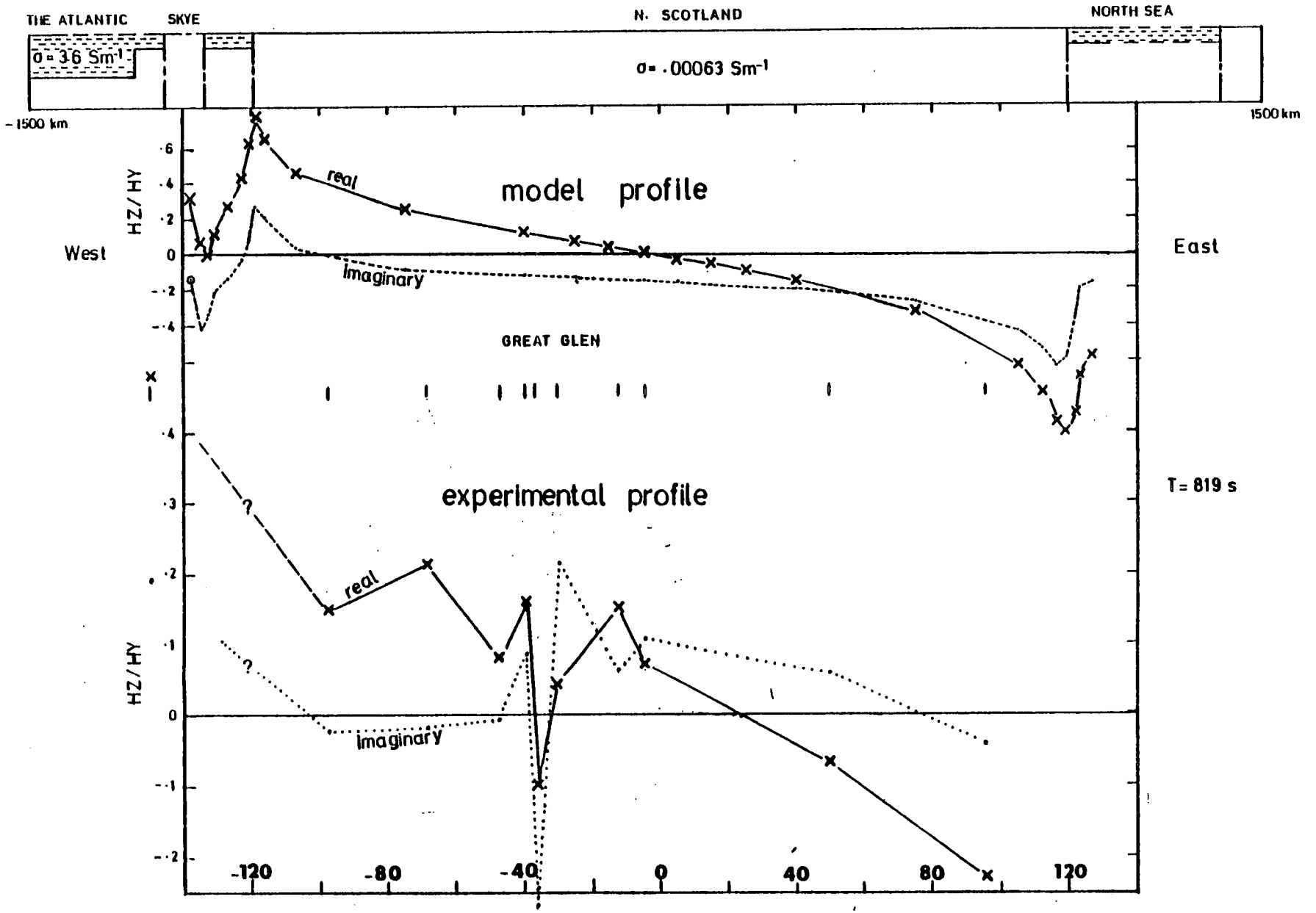

i) From reports of micropulsation source field studies and earlier induction studies on the British Isles at short periods (Green, 1974) source field effects on induction data at periods less than 600s are considered insignificant. As the non-uniformity of the source field for longer periods cannot be ruled out, less weight is given to the few data available in the long period band during modelling and interpretation.

ii) The geology of the region is complex. The combined use of the skew factor and the results of tensor impedance rotation analysis were used to identify less complex two-dimensional sites. Such sites were given more weight in the two-dimensional model studies.

iii) Little is known about the sedimentary cover which is essential for a detailed study of possible surface distortions of measured fields in the region. From surface geology, the main sedimentary cover is around the Moray Firth region. In order to minimise any surface effects, mean apparent resistivities were used for one-dimensional inversion and two-dimensional models were based on both GDS and MT data.

iv) Conductive channelling, as explained earlier, may be important at periods longer than those used in the this study. However, as a precaution, models which included regions a few skin-depths away from the measurement region were used for interpretation in order to simulate a realistic current flow in and around the region. It was therefore essential to include the

shallow seas adjacent to Northern Scotland for a realistic interpretation of the geolectric data.

v) The effect of the adjacent seas on the induction responses in of Northern Scotland were investigated by means of two-dimensional models. Results indicate that adjacent seas have a considerable influence on the geoelectric data. Inspite of the coast effect, strong conductivity anomalies associated with known geological units were apparent on comparing simple model responses with experimental data.

It was also found that the interpretation of mean apparent resistivities yielded realistic one-dimensional models for sites near the coast. For two-dimensional models, it was essential to include the seas otherwise model responses could not fit observed data.

6.2 GDS Hz/Hy Amplitude Ratio Profiles

The amplitude ratio profiles across the region on a NW-SE traverse are shown in Fig.6.8 for four periods. At all periods, there is an indication of a conductivity anomaly which can be associated with the Great Glen; the anomaly being more marked for periods greater than about 95s. At shorter periods, additional but shallower anomalies are apparent especially near Lairg.

It is interesting to notice that there is a fair agreement in the position for which the ratio is zero on the Grampian Highlands for 95 and 819s and the position of the zero contour in the in-phase hypothetical event contour plots (Hutton et al, 1980) shown in Fig.2.4 a,b,c,d.

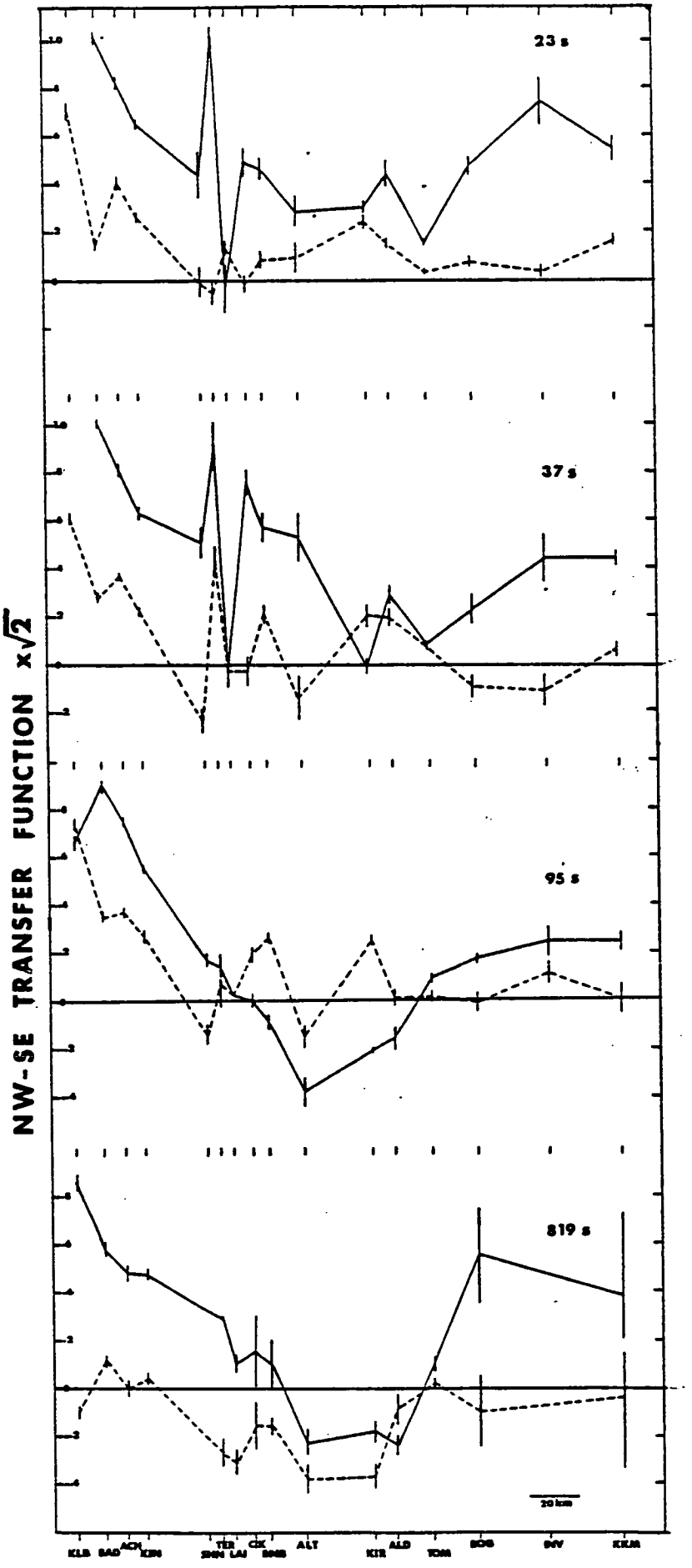

Fig.6.8 GDS Hz/Hy amplitude ratio profiles across Northern Scotland.

6.3 Resistivity Model for the Crust and Upper Mantle

Results of primary analysis of MT and GDS data were presented in Chapter Five and a qualitative interpretation in terms of lateral conductivity variations across the region was given. In this section, typical results of one-dimensional inversion of the MT data are presented for the different regions. As one-dimensional models for a complex region like Northern Scotland could be misleading, interpretations based on such models were considered tentative and were used as the basis for the more realistic two-dimensional modelling.

6.3.1 One-dimensional Models

The results of the Monte-Carlo inversion of mean apparent resistivity data for the Foreland is shown in Fig.6.4b. The results show that the resistivity of the crust decreases slightly at a depth of about 28 km with an increase in the upper mantle.

In the Lairg region, the one-dimensional model for site 19 (SHN) which was the most two-dimensional site in the area is shown in Fig.6.9c. The upper crust is resistive but the layer below it is about one order of magnitude less resistive than the corresponding layer under the Foreland. The upper mantle at a depth of about 45 km is resistive as on the Foreland.

Fig.6.9a shows the results for sites 2 (KIR) and 7 (ALD) which were located on the northern part of the Great Glen. The crust is less resistive than at the sites to west of the Glen and is underlain by a low resistivity layer of about 200 ohm m resistivity at a shallow depth of about 7 km. The upper mantle below 40 - 60 km depth is resistive.

As mentioned in Chapter Five, there is considerable varia-

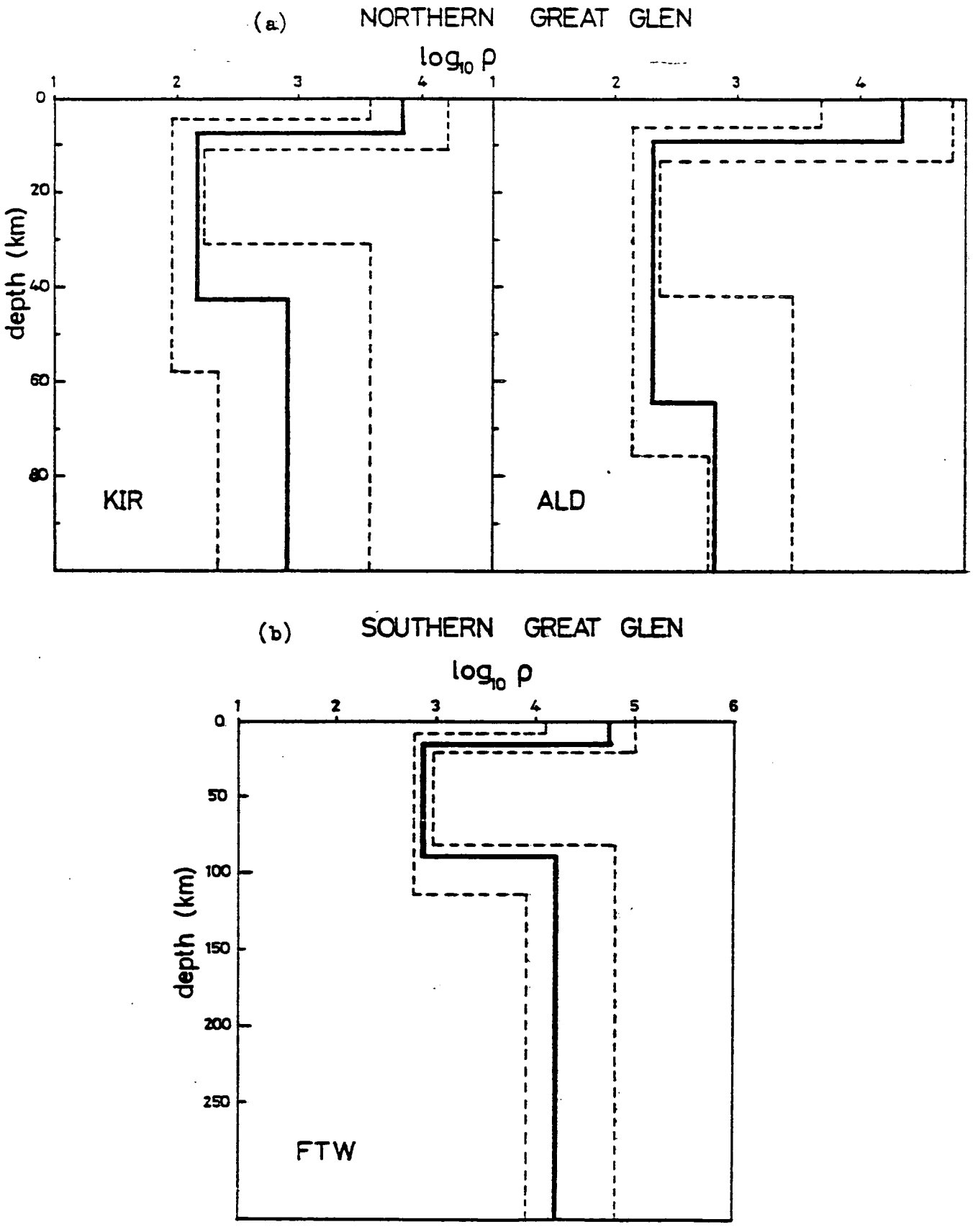

Fig.6.9 Regional one-dimensional models for the crust and upper mantle.

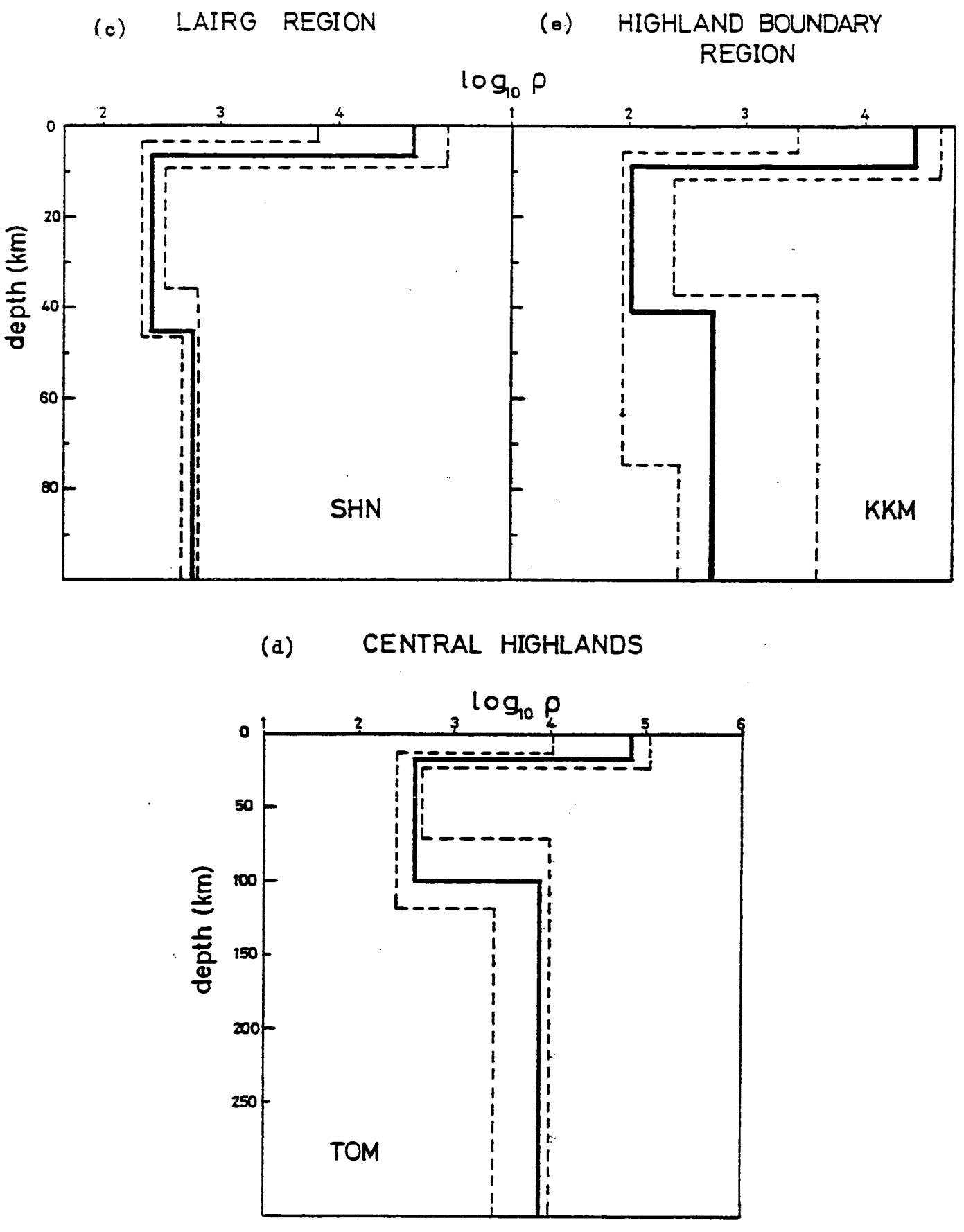

Fig.6.9 Regional one-dimensional models for the crust and upper mantle.

tion in the conductivity structure along the Glen. For site 16 (FTW), the southernmost station in the Glen, Fig.6.9b shows that the crust is more resistive than in the northern part and the lower crust is also more resistive by a factor of about three.

Fig.6.9d shows the model for site 9 (TOM) on the Grampian Highlands. The crust is more resistive than in the Glen and the lower crust is as conducting as under the Glen while the upper mantle is resitive.

Near the Highland Boundary Fault, the one-dimensional model for site 14 (KKM) indicates a crust that is less resistive than on the Grampian Highlands, a conducting lower crust and a resistive upper mantle as shown in Fig.6.9e.

From the one-dimensional models, the upper crust is very resistive except near the Great Glen area and there is considerable lateral variations in the resistivity of the crust across the region. The lower crust east of the Moine Thrust is conducting and the upper mantle is resistive. The results also show that there are irregularities in the conductivity structure along the Great Glen.

6.3.2 Two-dimensional Model

As discussed in section 6.1.5, a realistic two-dimensional model for Northern Scotland must include the adjacent seas to allow for the coast effect on measured induction parameters over the region. The reasonably good agreement between the results of the two-dimensional numerical model and the three-dimensional analogue model which both included the adjacent seas supports this and also indicates that inspite of the complexities already discussed, a two-dimensional model can give some useful informa-

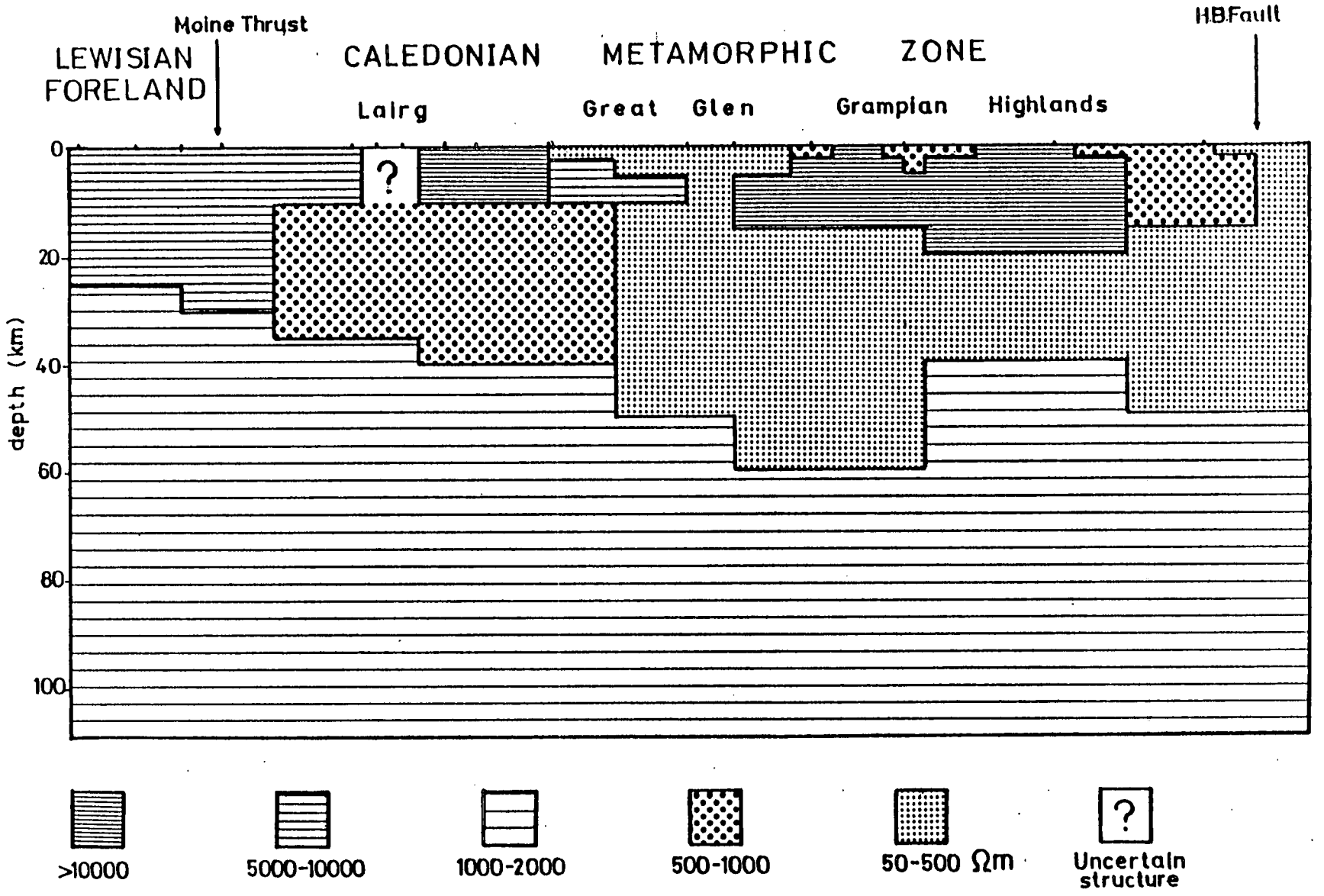

Fig.6.10 Two-dimensional resistivity model for Northern Scotland.

tion about the crust and the upper mantle in the region.

Starting with a simple three layer model based on one-dimensional inversion results, a satisfactory two-dimensional model which fitted most of the data is shown in Fig.6.10. The model responses are shown in Fig.6.11 and Fig.6.12. In the MT model response profiles, ρ_{max} (the continuous line in the figures) corresponds to $\rho_{//}$ while ρ_{min} correponds to $\rho_{\perp}$ in the Great Glen region in good agreement with experimental observation. It was very difficult to find a suitable model to satify the short period magnetic data for the Lairg region, therefore there is considerable uncertainty in the structure for the area. The two-dimensional model has the following features.

i) the Foreland crust (about 30 km thick) is very resistive and the resistivity is about 10000 ohm m. The upper mantle has a resistivity an order of magnitude less than the crust. The resistivity values are lower than those obtained directly from one-dimensional inversion for the region although the general form of the resistivity-depth variation for the two models are similar.

ii) On the metamorphic zone, east of the Foreland, the crustal resistivity (about 5000 ohm m) is less than the corresponding value on the Foreland except near Bonar Bridge, Tomatin and the Cairngorms where the crustal resistivities of about 20000 ohm m are higher than the values on the Foreland.The high crustal resistivity in the Grampian Highlands agrees very well with the value 19000 - 35000 ohm m for the top 200m of the crust from preliminary audio-magnetotelluric measurements near Tomatin (Hu-

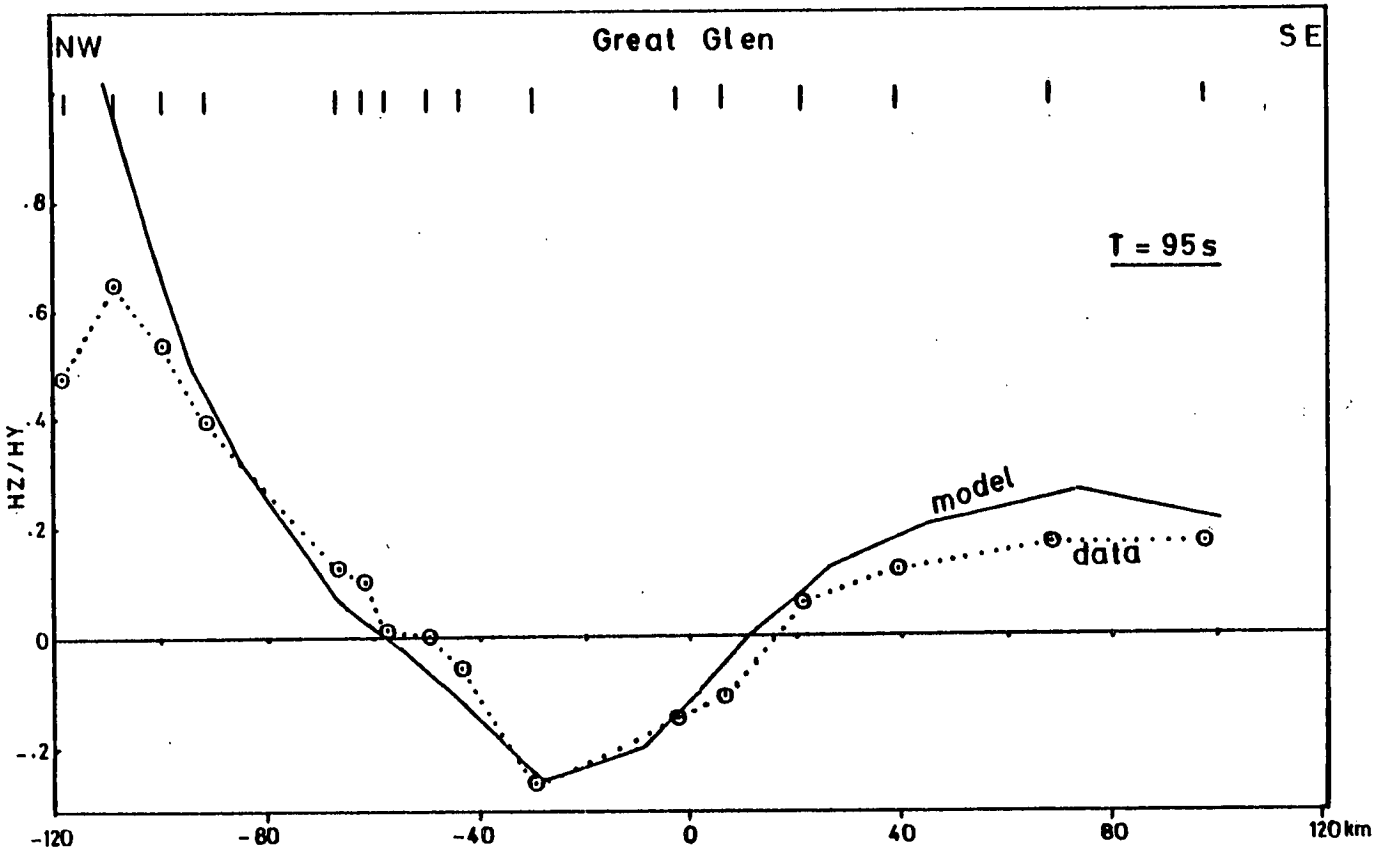

Fig.6.11a Two-dimensional model GDS responses and data compared for 95s.

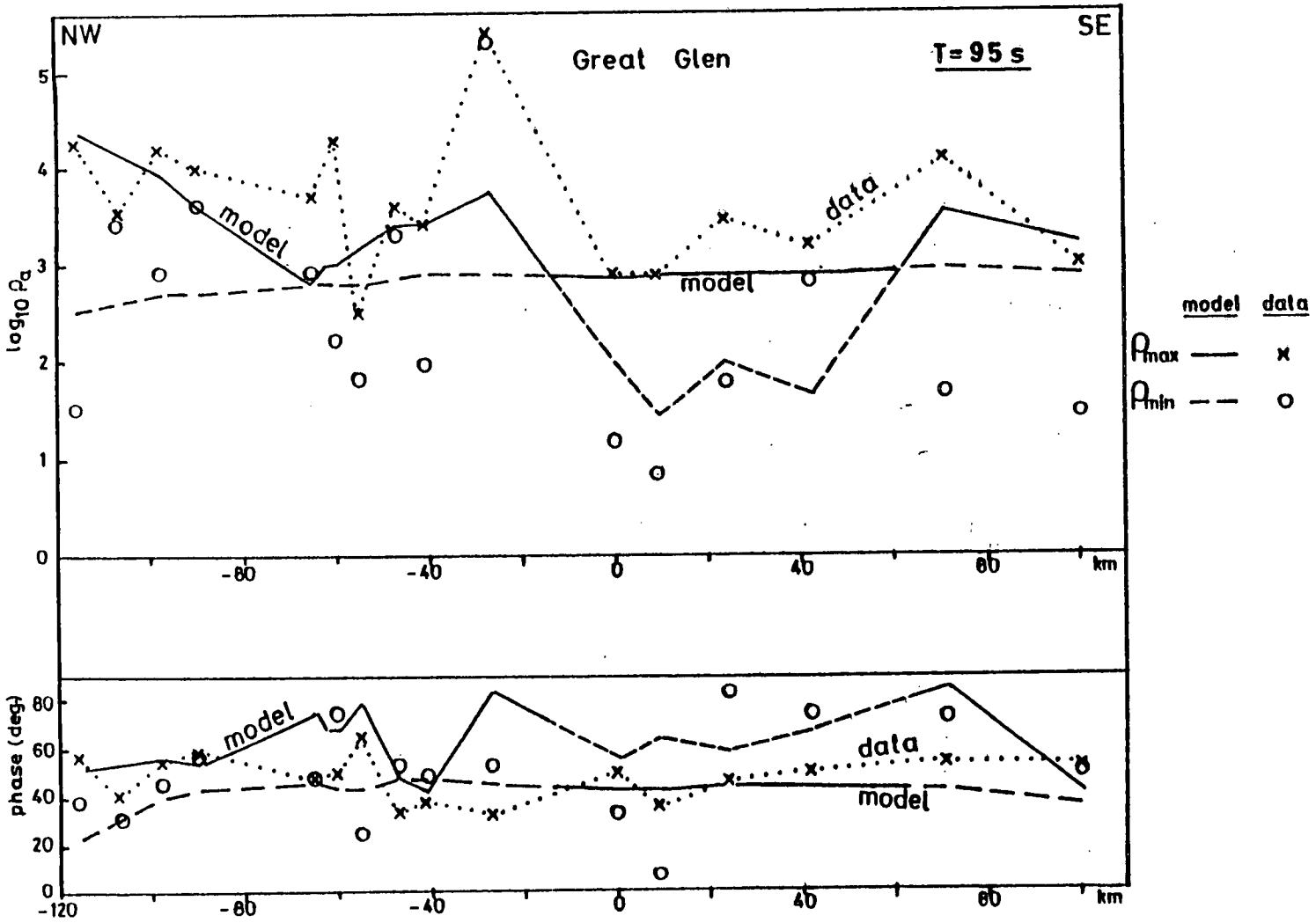

Fig.6.11b Two-dimensional model MT responses and data compared for 95s.

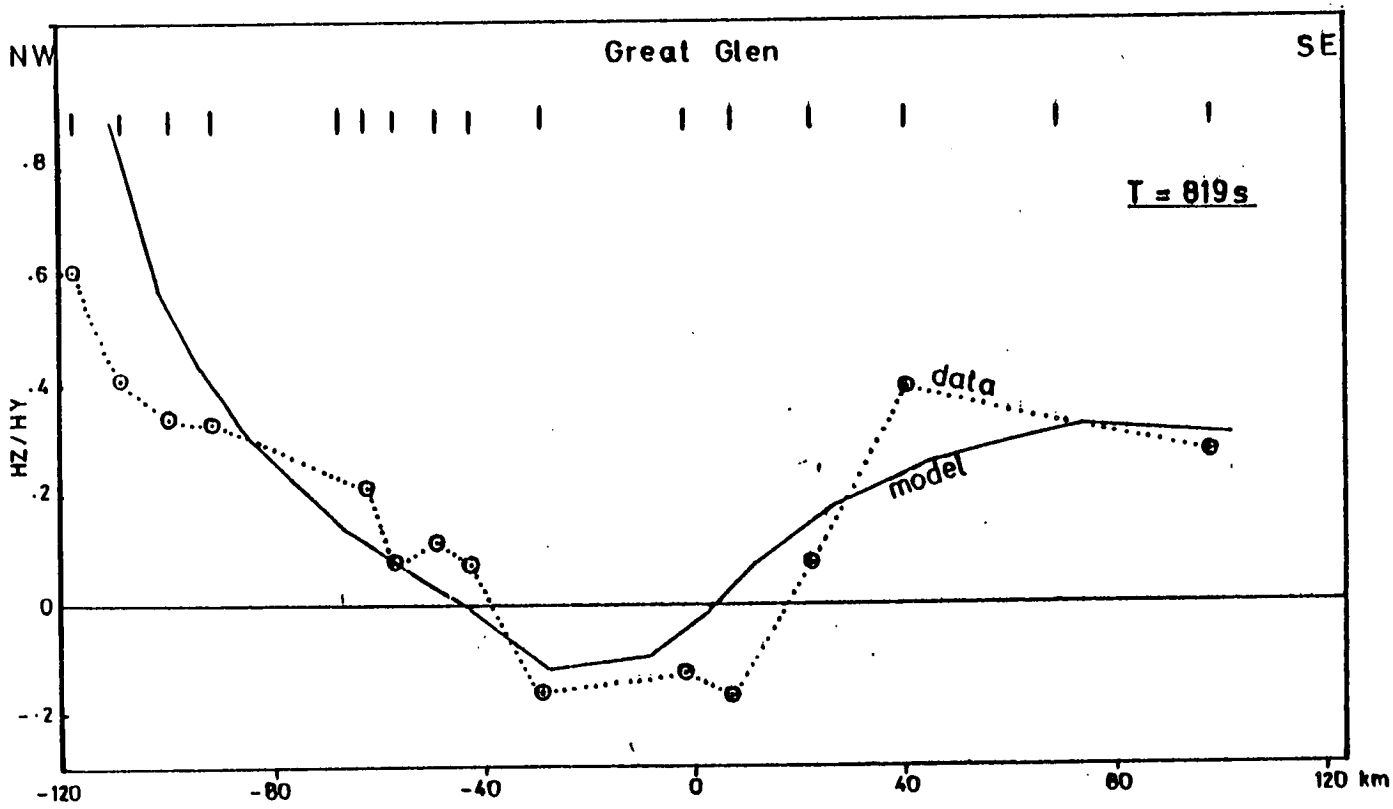

Fig.6.12a Two-dimensional model GDS responses and data compared for 819s.

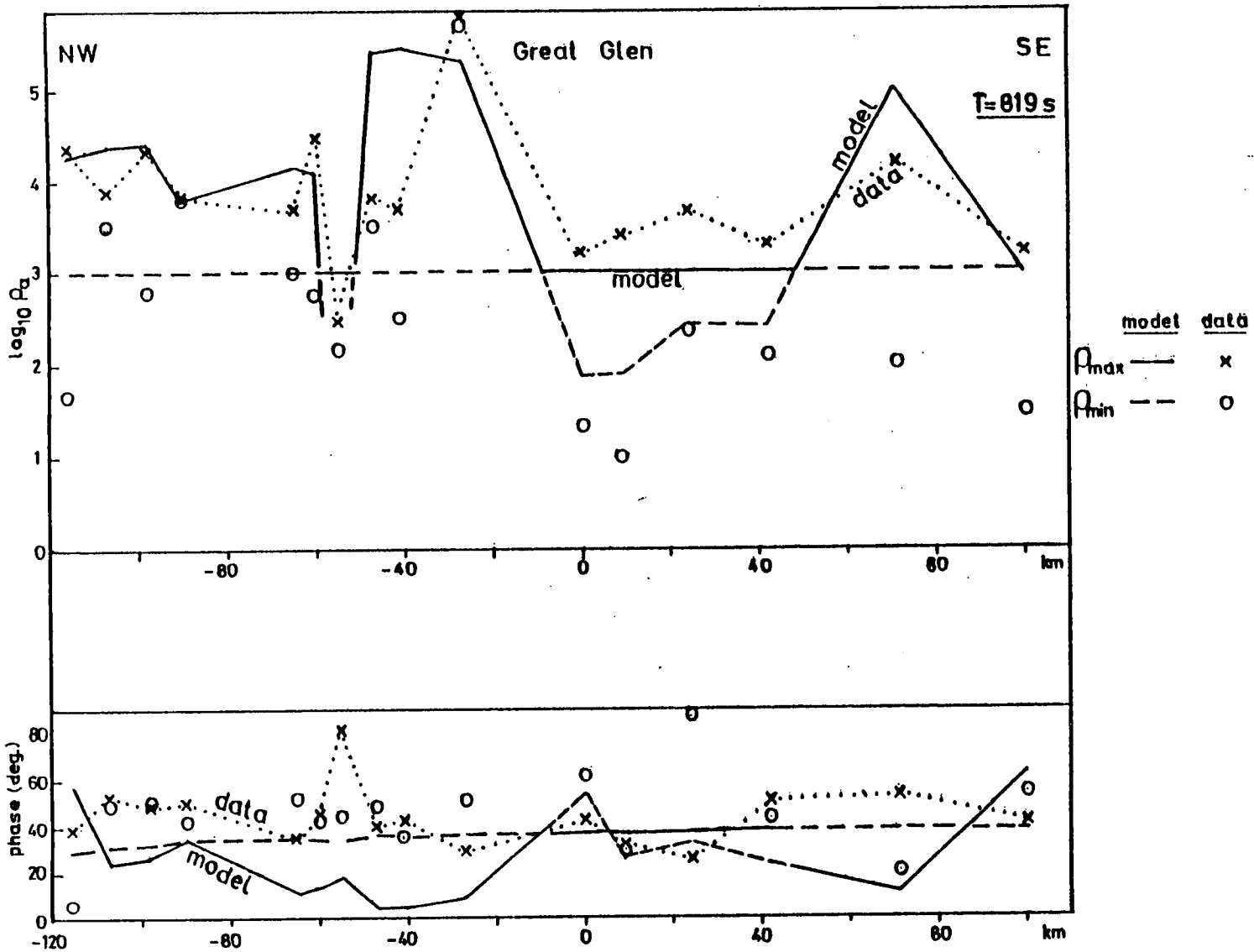

Fig.6.12b Two-dimensional model MT responses and data compared for 819s.

tton et al, personal communication).

iii) In the Great Glen region and near the Highland Boundary region, the crust is conducting. Both a surface and a deeper conductor which extends into the lower crust and upper mantle in the Great Glen region are needed for a satisfactory fit to the data. The magnetic data required the Great Glen conductor to have a resistivity about an order of magnitude lower than the value required by the apparent resistivity data for a good fit.

An upper mantle resistivity of about 2000 ohm m for the whole region as on the Foreland is acceptable in the model.

6.3.3 An Estimate of the Bounds of Acceptable Models

In seeking the bounds for acceptable models, a number of quantities can be varied in a two-dimensional numerical model of the type discussed here. For this study, resistivities and layer interfaces were considered more important in view of comparisons made later with the only available geophysical section from the LISPB seismic profile. Therefore resistivities and depths to layer interfaces were altered, model responses computed and compared with experimental results as before. The estimated bounds obtained are shown in Table 6.1.

As reviewed in Chapter One, resistivity measurements have shown that most stable Precambrian regions are marked by a very resistive upper crust, a conducting lower crust and a resistive upper mantle. It is interesting to notice that the results for Northern Scotland are similar to those from other Precambrian regions, except near the Great Glen where there are known sediments.

Table 6.1

Bounds of Acceptable Models

Layer	Depth to base (Km)	Resistivity, ρ (Ωm)
1. Upper crust	10 - 20	$2000 < \rho < 2.10^5$
2. Lower crust/uppermost mantle		
N.W. Highlands	30 - 60	50 - 1000
Great Glen	60 - 70	
Grampian Highlands	40 - 50	
3. Upper mantle	-	1000 - 2000

The resistivity values for the upper crust and the observed lateral variations along the traverse correlate fairly well with the surface geology. The high resistivities are associated with the highly granitized upper crust while the conducting region around the Great Glen is probably due to sediments with conducting interconnected pore fluids.

It is much more problematic to account for the low resistivity in a Precambrian lower crust. As discussed in Chapter One, the resistivity of a rock is sensitive to its free or bound water content. The effect of temperature and pressure may also be significant. Fig. 6.13 shows the plots of resistivity as a function of temperature for different rock types (Keller, 1971) used by Sternberg (1979) for his inference of the constitution of the lower crust in the Canadian Shield. Rocks of different composition at postulated temperatures of 300 - 400 deg.C at the lower crust could not explain the observed low resistivities. Only rocks with water of hydration could produce the observed low resistivities. Using the same procedure for the Scottish results, the resistivity values for the lower crust from the two-dimensional model are marked on the right hand side of Fig.6.13. Assuming normally used temperature of 300-500 deg.C in the lower crust in Northern Scotland, it can also be infered that hydrated rocks are responsible for the observed low resistivity in the region. It is probable that partial melting due to past tectonic activities near the Great Glen and the Grampian Highlands may also contribute to the observed low resistivity.

The upper mantle is believed to be mainly of olivine composition and the resistivities between 1000 to 10000 ohm m are reasonable for a stable continental upper mantle (Duba, 1972).

6.4 Evidence from Other Geophysical Models

Considerable geological data are available for the region. Seismic, gravity and some heat flow data have also been published as mentioned in Chapter One. It is therefore useful to see to what extent the resistivity model can contribute to our general understanding of some of the results from these other methods. However, there is need for caution in comparing geophysical results because there are many factors which can affect the correlation between Earth models from different geophysical methods.

There is a general agreement between surface geology and the resitivity model. The widespread granitic intrusions like Migdale, Moy, Findhorn and the Cairngorms within the metamorphic zone correlate very well with the zones of high resistivity in the upper crust. Resistivities over 5000 ohm m are usually associated with igneous rocks with low porosity such as granites although marbles and tight limestones can give similar results (Duba, private communication). The Devonian sediments in the Moray Firth region are also marked by the superficial and relatively conducting region around the Great Glen. The similarity of the resistivity model for Northern Scotland and some of the MT results from Eastern Canada provides some support for the common tectonic history of the North Atlantic terrains. The resistive upper and lower crust in the Foreland is believed to represent a North Atlantic shield fragment which was stabilised over 1600 million years ago and was unaffected by the Caledonian Orogeny which affected other parts of Scotland.

The lower crust east of the Moine thrust may represent a

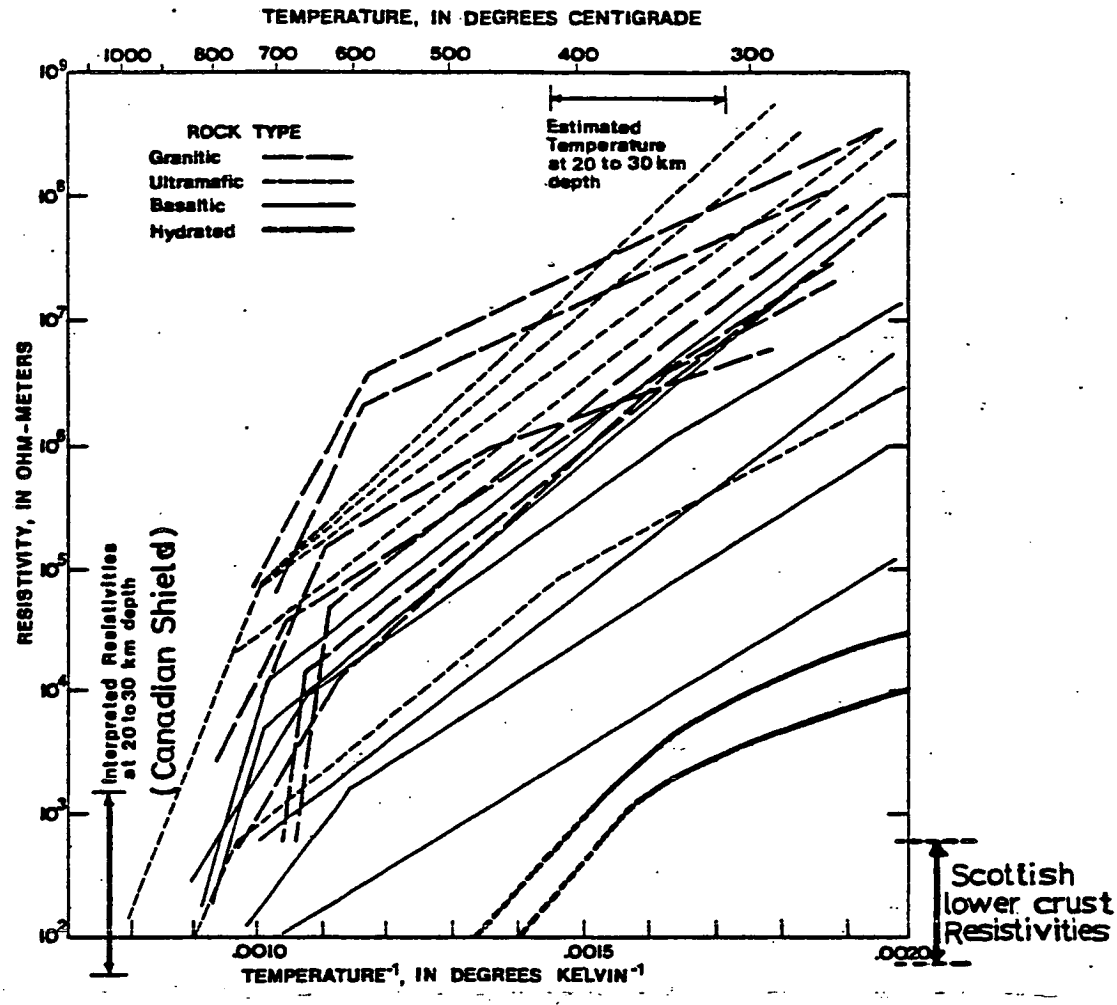

Fig.6.13 Resistivity as a function of temperature for samples of granitic rocks (from Sternberg, 1979) and showing the range of the Scottish lower crust resistivity.

Lewisian basement that has been reworked during the Grenville and the Caledonian Orogenies. The intensity of the reworking and migmatisation is believed to increase southwards towards the Highland Boundary Fault. The corresponding variation in the conductivity of the lower crust in the geoelectric model may therefore be partly related to the tectonic history of the region.

The few heat flow measurements (Fig.1.12) for the region (Pugh, 1977; Oxburgh et al, 1980) show that the values are within the range 40 - 83 mWm^{-2}. Pugh (1977) attributed the local high heat flow of 83 mWm^{-2} in the central part of Loch Ness to Foyer's granite about 10 km north-east of the MT site at Fort Augustus. High heat flow in Britain is generally associated with radiogenic elements in granitic bodies and from their heat flow data, Oxburgh et al (1980) estimate that the vertical extent of the bodies responsible for the heat production is about 16±4 km. This result is surprisingly in very good agreement with the thickness of the upper crust high resistivity zones associated with granites in the geoelectric model for Northern Scotland, as discussed in a letter submitted to 'Nature' recently by Hutton, Ingham and Mbipom.

It is also interesting to notice that the negative gravity anomally around Lairg and on the Grampian Highlands along the LISPB line have also been attributed to the abundance of granitic plutons which are about 7 - 19 km deep (Dimitripoulos and Donato, private communication).

The cross-section of the crust and upper mantle of Northern Britain obtained from p-wave velocities in the LISPB project (Bamford et al, 1978) was shown in Fig.1.11. The resistive upper

crust in the geoelectric model corresponds to the layer with p-wave velocities 6.1 - 6.2 km/s which was attributed to Caledonian metamorphic rocks. The pre-Caledonian basement layer with velocities greater tha 6.4 km/s cannot be resolved by the geoelectric data on the Foreland but elsewhere, this layer together with the LISPB model lower crust of velocity 7 km/s form the conducting layer in the geoelectric section.

The MT results from the Canadian Shield (Dowling, 1970) presented in Fig.1.3 showed that the conducting layer occured at depths which corresponded closely to the interface at which p-wave velocities changed from 6.11 to 6.51 km/s in good agreement with the Scottish seismic and MT results.

Hall and Simons (1979) have carried out laboratory measurements of p- and s-wave velocities for rocks from N.W. Scotland in order to infer the composition for the three seismic crustal layers in the region. Pressures of up to 8kb were used. From their measurements, they suggested that the upper crust was likely to be largely of mixed metamorphic rocks plus granites underlain by rocks of intermediate composition of mixed pyroxene--granulite facies. The lower crust was thought to be mainly basic in composition although the authors pointed out that there was a possibiltiy that hydrated rocks like mafic amphibolites and serpentinised peridotites could produce the apparent Poisson's ratios of 0.25 observed in the lower crust by Assumpcoa and Bamford (1978). The conducting layer in the geoelectric model favours the presence of hydrated rocks in the lower crust in the region.

The depth of 30 km to the resistivity interface on the Foreland agrees remarkably well with the crust-mantle boundary of

Fig.6.14 Geoelectric and seismic upper mantle structures around the Great Glen.

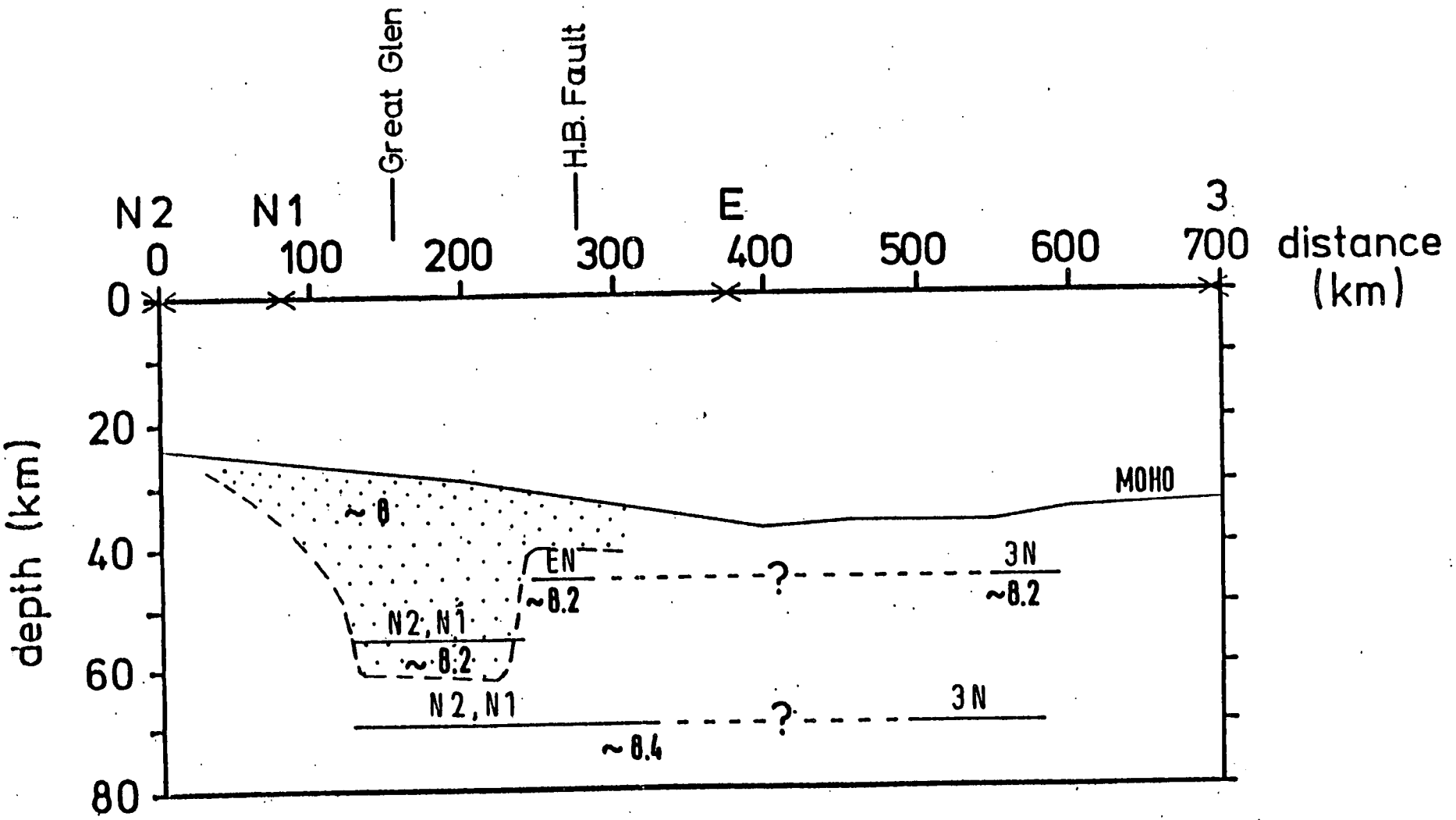

Geoelectric conductor - stippled; N2, N1, EN - mantle seismic velocity horizons, Faber and Bamford(1979).

sharp transition in p-wave velocity from 7 to 8 km/s. East of the Foreland, the corresponding resistivity interface occurs at depths between 40 - 60 km being deepest under the Great Glen region.

The significance of the difference between the LISPB moho and the corresponding resistivity interface was tested by constraining the resistivity model with a horizontal lower crust - upper mantle interface at 30 km, the mean seismic moho depth for the region. The fit of the model response was good to the north-west but rather poor near to and south of the Great Glen. The geoelectric interface at the upper mantle is therefore different from the seismic moho east of the Foreland. However, it is interesting to notice that mantle phases from some LISPB records (Faber and Bamford, 1979) qualitatively suggest lateral variations at depth ranges of 45 - 69 km compatible with the geoelectric interface under the Great Glen and the Grampian Highlands as illustrated in Fig.6.14.

CHAPTER 7

CONCLUSIONS AND SUGGESTIONS

7.1 Conclusions

The main conclusions that can be drawn from these studies are

i) The model of the deep geoelectric structure obtained for the first time for Northern Scotland is complex but there is good agreement with the known surface geology.

ii) The adjacent seas and ocean have a significant influence on the geoelectric response parameters in the region. From model studies, the coast effect on the apparent resistivity persists for about 20 km inland for periods less than about 100s and across the whole region for longer periods.

iii) The coast effect can be minimised by interpreting averaged apparent resistivities in one-dimensional models.

iv) A combined use of MT and GDS method in geoelectric studies is effective.

v) The zones of large resistive bodies delineated in the study correlate well with known granitic bodies. The resistive bodies extend to depths of 10-20 km in the geoelectric model.

vi) On the Lewisian Foreland, the whole crust is resistive and the depth to the first geoelectric interface is about 30 km in

good agreement with the depth to the Moho from seismic refraction studies.

vii) In the Great Glen region and near the Highland Boundary, the crust is conducting. The Great Glen conductor consists of a surface conductor as well as a deeper one.

There are significant lateral variations in the geoelectric structure of along the Glen.

viii) Under the metamorphic zone, the resistivity of the lower crust decreases from about 1000 ohm m north of the Great Glen to 500-50 ohm m in the Glen and under the Grampian Highlands.

Hydrated rocks and partial melting are the likely cause of the low resistivity layer in the lower crust and upper mantle across the region.

The geoelectric structure for the metamorphic zone is similar to the structure obtained by Jones and Hutton (1979b) for FTH and SAL, two sites in the Midland Valley.

ix) The good conductor in the Great Glen and the widespread resistive zones of large granitic bodies north of the Highland Boundary Fault are reminiscent of a region that has been subjected in the past to a major tectonic activity.

7.2 Suggestions for Future Studies

As the models presented here for the geoelectric structure of Northern Scotland is the first of its kind, there are still some interesting problems which merit further studies.

i) There is need to increase the short period (10-1000s) MT station density in the region for a better resolution of the complex geoelectric structures which this study has indicated. New sites could be added with advantage to those used for this study to reduce the station spacing to about 10 km or less.

ii) A second MT traverse parallel to the main traverse in this study but through Fort Augustus would also provide interesting results in view of the variation in the structure found along the Great Glen.

The north-western end of the traverse should reach Torridon to enable a study of the southern extension of the Scottish Shield fragment as well as the metamorphic zone.

iii) AMT measurements which require comparatively less effort should be made at least at every MT site for a control on the subsurface resistivity structure of the region.

iv) Experimental results should be compared with results from three-dimensional models which take into account the lateral conductivity variations as well as the lower crust conductor which has been detected in this study.

v) As regions of high heat flow in the U.K. are associated with large granitic bodies, heat flow measurements should be carried out in areas near the high resistivity zones indicated by the geoelectric model for possible future geothermal prospects.

APPENDIX

UNIVERSITY OF EDINBURGH

DEPARTMENT OF GEOPHYSICS

A check list for Geomagnetic Induction Measurement Systems

The Magneto-telluric System

In its present form, the filters, amplifiers and some power supply units which are needed for the magnetic (short period) and telluric measurements are rack-mounted together. However, for the purpose of a handy check list, the units and the requirements for each system will be listed separately.

1. The Magnetic System (short period variations)

Jolivet magnetometer	(3) + 1 spare
Wooden insulating box with polystyrene lids	(3)
Large protective fibreglass cisterns	(3)
Z sensor toflon support	(1)
Jolivet compensating magnet	(2) + spares
Non-magnetic screwdriver	(1)
Jolivet magnetometer fluid (carbon tetrachlorethylene)	(1 bottle)
Jolivet magnetometer spare bulb	(3)
Jolivet magnetometer spare photocell	(3)
Filter unit (for 3 components)	(1)
Amplifier unit (x1-100 for 3 components)	(1)
Keithley microvoltmeter (or x10 amplifier unit)	(3) + 1 spare
50 m power/signal leads (6 core)	(1)
Short (about 10 m) interconnecting power leads (3 core) fitted with red, green and blue plugs	(2)
Short interconnecting leads fitted with banana plugs for wiring up	(10)
Two core 10 m twisted leads for one-man "zeroing" of magnetometers	(1)
Syringe fitted with a small rubber tubing	(1)

2. The Telluric System

Lead electrodes	(4 + 1 earth)
1.2 mm SQ 3 core type cables:	
lengths - 200 m	(2)
100 m	(2)
50 m	(1)
Trigg amplifier/filter (10 s LPF) unit	(1)
1100 s (HPF), 300 s (HPF) and 200 s (LPF) unit	(1)
Telluric back off/amplifier (x1-100) unit	(1)
Short interconnecting leads fitted with banana plugs for wiring up	(8)
Lasotape roll	(6)
Small plastic junction boxes for cable interconnections	(12)

3. Recorders

(a) Multi-channel analogue recorder - 5 channel Watenabe type (1)

Accessories:

Input 2-core leads	(5)
Pens	(5)
Ink capsules	(5)
Bottles of different ink	(5)
Syringe (fitted with needle)	(1)
Syringe (fitted with rubber tubing)	(1)
Plastic wash-up cup	(1)
Methylated spirit (½ pint bottle)	(1)
Roll of tissue paper	(2)
20 m Watenabe charts per week at 7.5 mm/min	(4)

(b) Multi-channel digital recorder - 16 channel Geologger (1)

Accessories:

Main supply lead	(1)
Channels 1-3 special input lead	(1)
Multi-channel input lead/junction box	(1)
Data certified cassettes (type B) per week (at S.R. = 5 sec)	(9)
Paper labels for used cassettes per week	(9)
Bulk eraser for cassettes	(1)

4. Power Supply

At the moment, the system is run on mains supply. An independent power supply is possible using a generator, battery chargers, heavy duty batteries and an inverter.

The supply used currently is as follows:

Mains supply (250 V) point	(1)
50 m extension cable fitted with 4 socket distribution board and a 3-pin plug	(1)
50 m extension cable fitted with 4 socket distribution board and a lamp socket plug	(1)
±15 V power supply unit	(1)
3-core short power leads fitted with red, yellow and blue plugs	(5)
±6 V for Jolivet magnetometers (from 12 V battery with centre tap)	(2)
Battery charger	(1)
Distribution board (4 sockets) fitted with an earthing plug	(1)

5. Long Period Magnetic System

The following are required:

(a) The Fluxgate magnetometer unit -

3 component sensing head	(1)
3 component electronic control unit	(1)
Electronic control output lead	(2)
Electronic control mains lead	(1)
100 ft interconnecting cable	(1)
Toflon base for sensing head	(1)
Plastic basins for sensing head (one large, one small)	(2)
Plastic (waterproof) bag for sensing head	(1)

(b) Recorders

(i) Triple channel analogue recorder (Record Electric or Edgecumbe Peeble type) (1)

Accessories:

Pens with nib	(3)
Inkwells with ink	(3)
Syringe (fitted with needle)	(1)
Syringe (fitted with rubber tubing)	(1)
Plastic wash-up cup	(1)
Bottle of (spare) ink	(1)
Roll of tissue paper	(1)
Charts per week	(1)

(ii) Digital recorder:
(As in 3(b))

6. Tools

The following are necessary:

Compass	(1)
Set of watchmaker's screwdrivers	(1)
Set of star-head screwdrivers	(1)
Set of ordinary screwdrivers	(1)
100 m tape measure	(1)
Survey pole	(2)
Spirit level	(1)
Shovel	(1)
Auger	(1)
Pick	(1)
Crow bar	(1)
Wire stripper	(1)
Wire cutter	(1)
Long nose pliers	(1)
Penknife	(1)
Soldering iron	(1)
Solder (roll)	(1)
Mallet	(1)
Hammer	(1)
Plastic bucket	(1)
Large plastic pegs	(24)
Standard tool kit	(1)
ULF Signal generator	(1)
Multimeter	(1)
Portable radio receiver	(1)
Bar magnet	(1)

R E F E R E N C E S

Albouy, Y.,Godivier, R. and Perichon, P., 1971

Le sondages magnetotellurique, O.R.S.T.O.M.,Paris.

Assumpcao, M. and Bamford, D., 1978

LISPB-V. Studies of crustal shear waves. Geophys.J.R.astr.-Soc. v.54, 61-73.

Backus, G. and Gilbert, F., 1967

Numerical application of a formalism for geophysical inverse problems. Geophys.J.R.astr.Soc. v.13, 247-276.

Backus, G. and Gilbert, F., 1968

The resolving power of gross Earth data. Geophys.J.R.astr.-Soc. v.16, 169-205.

Backus, G. and Gilbert, F., 1970

Uniqueness in the inversion of inaccurate gross Earth data. Phil.Trans.R.Soc. A266, 123-192.

Bailey, R. C.,Edwards, R.N., Garland, G.D., Kurtz, R. and Pitcher, D.H., 1974

Electrical conductivity studies over a tectonically active area in Eastern Canada. J.Geomag. Geoelectr. v.26, 125-146.

Bailey, R.C. and Edwards, R.N., 1976

The effect of source field polarisation on geomagnetic variation anomaly in the British Isles. Geophys.J.R.astr.-Soc. v.44, 1-8.

Bamford, D.,Faber, S., Jacobs, B., Kaminski, W., Nunn, K., Prodehl, C., Fuchs, K., King, R. and Willmore, P., 1976

A lithospheric seismic profile in Britain-1. Preliminary results. Geophys.J.R.astr.Soc. v.44, 145-160.

Bamford, D., Nunn, K., Prodehl, C. and Jacob, B., 1978

LISPB-IV. Crustal structure of Northern Britain. Geophys.J.R-.astr.Soc. v.54, 43-60.

Banks, R.J., 1973

Data processing and interpretation in geomagnetic deep sounding. Phys.Earth Planet.Int. v.7, 339-348.

Banks, R.J. and Ottey, P., 1974

Geomagnetic deep sounding in and around the Kenyan Rift Valley. Geophys.J.R. astr.Soc. v.36, 321-335.

Beamish, D., 1979

Source field effects on transfer functions at mid-latitudes. Geophys.J.R.astr.Soc. v.58, 117-134.

Bendat, J.S. and Piersol, A.G., 1971

Random data: Analysis and measurement procedures. Wiley-Interscience, New York, U.S.A.

Bentley, C.R., 1973

Error estimation in two-dimensional magnetotelluric analysis. Phys.Earth Planet.Int. v.7, 423-430.

Berdichevsky, M.N., Van'yan, L.L., Fel'dman, I.S. and Porstendorfer, G.,1972

Conducting layers in the Earth's crust and upper mantle. Gerlands Beitr. Geophysik, Leipzig v.81, 187-196.

Berdischevsky, M.N. and Dmitriev, V.I., 1976

Distortion of magnetic and electrical fields by near-surface lateral inhomogeneities. Acta Geodaet.Geophys.Montanist. Hungary. Tomus11 (3-4), 447-483.

Bingham, C., Godfrey, M.D. and Tukey, J.W., 1967

Modern techniques for power spectrum estimation. I.E.E.E. Trans. Audio Electroacoust. v.AU15, 56-66.

Blohm, E.K., Worzyk, P. and Scriba, H., 1977

Geoelectric deep soundings in Southern Africa using the Cabora Bassa power line. J.Geophys. v.43, 665-679.

Brace, W., 1971

Resistivity of saturated crustal rocks to 40 km based on laboratory measurements. In The Structure and Physical Properties of the Earth's Crust, A.G.U. Geophys.Monogr.Ser. (ed. J.G.Heacock) v.14, 243-255.

Brewitt-Taylor, C.R. and Weaver, J.T., 1976

On the finite difference solution of two-dimensional induction problems. Geophys.J.R.astr.Soc. v.47, 375-396.

Brewitt-Taylor, C.R. and Johns, P.B., 1977

Diakoptic solution of induction problems. J.Geomag.Geoelectr. (in press,1980).

Breymann, U., 1977

Magnetotelluric investigation of a nearly circular saltdome in North Germany. J.Geophys. v.42, 391-397.

Brown, G.C. and Locke, C.A., 1979

Space-time variations in British Caledonian granites: Some geophysical correlations. Earth Planet.Sci.Lett. v.45, 69--79.

Cagniard, L., 1953.

Basic theory of the magnetotelluric method of geophysical prospecting. Geophys. v.18, 605-635.

Cooley, J.W. and Tukey, J.W., 1965

An algorithm for the machine calculations of complex Fourier series. Mathematics of Computation v.19, 297-307.

Dawes, G., 1978

Cassette processing programs. Internal Publication, Department of Geophysics, University of Edinburgh.

Dawson, T.W. and Weaver, J.T., 1979a

H-polarisation induction in two thin half-sheets. Geophys.J.-R.astr.Soc. v.56, 419-438.

Dawson, T.W. and Weaver, J.T., 1979b

Three-dimensional induction in a non-uniform thin sheet at the surface of a uniform conducting Earth. Geophys.J.R.astr-.Soc. v.59, 445-462.

Dosso, H.W., 1973

A review of analogue model studies of the coast effect. Phys.Earth Planet.Int. v.7, 294-302.

Dosso, H.W., Nienaber, W. and Hutton, V.R.S., 1980

An analogue model study of electromagnetic induction in the British Isles region. Phys.Earth Planet.Int. (in press).

Dowling, F.L., 1970

Magnetotelluric measurements across the Wisconsin Arch. J.-Geophys.Res. v.75, 2683-2698.

Duba, A., 1972

Electrical conductivity of olivine. J.Geophys.Res. v.77, 2483-2495.

Duba, A., 1976

Are laboratory electrical conductivity data relevant to the Earth ? Acta Geodaet.Geophys.Montanist. Hungary, Tomus 11(3--4), 485-495.

Edwards, R.N., Law, L.K. and White, A., 1971

Geomagnetic variations in the British Isles and their relation to electric currents in the ocean and shallow seas. Phil.Trans.R.Soc., London, A270, 289-323.

Everett, J.E. and Hyndman, R.D., 1967a

Magnetotelluric investigations in South-western Australia.

Phys.Earth Planet.Int. v.1, 49-54.

Everett, J.E. and Hyndman, R.D., 1967b

Geomagnetic variations and electrical conductivity structure in S.W. Australia. Phys.Earth Planet.Int. v.1, 24-34.

Faber, S. and Bamford, D., 1979

Lithospheric structural contrasts across the Caledonides of Northern Britain. Tectonophys. v.56, 17-30.

Fournier, H., 1978

Recent work in magnetotelluric soundings of the lower crust and uppermost mantle. Review paper, Fourth Workshop on EM induction in the Earth and Moon. Murnau, FRG.

Green, C., 1974

An induction study at micropulsation periods in the British Isles. Geophys.J.R.astr.Soc. v40, 225-240.

Green, C., 1978

Meridional characteristics of a Pc4 micropulsation event in the plasmasphere. Planet.Space Sci. v26, 955-967.

Gough, I.D., 1973

The interpretation of magnetometer array studies. Geophys.J.-R.astr.Soc. v.35, 83-98.

Haak, V., 1972

Magnetotelluric method - the determination of transfer functions in areas with lateral variation of conductivity. Zeitschrift fur Geophysik v.38, 85-102.

Haak, V., 1978

Interpretations - verfahren fur die magnetotellurik unter besonderer berucksichtigung lateral varrierender elektrischer leitfahigkeit im erdinnern und eines raumlich inhomogenen induzierenden magnetfelds. Muchen Ak.Abh.Math.nat.,

v.158.

Hall, J. and Simmons, G.,1979

Seismic velocities of Lewisian metamorphic rocks at pressures to 8 kbar : relationship to crustal layering in North Britain. Geophys.J.R.astr.Soc. v.58, 337-347.

Harland, W.B. and Gayer, R.A., 1972

The arctic Caledonides and earlier oceans. Geol.Mag. v.109, 289-314.

Harris, A.L., Johnson, M.R.W. and Powell, D., 1978

The orthotectonic Caledonides (Moines and Dalradians) of Scotland. In Caledonian-Appalachian Orogen of the North Atlantic Region. Geol.Surv.Canada, Paper 78-13, 82.

Hermance, J.F., 1973

Processing of magnetotelluric data. Phys. Earth Planet.Int. v.7, 349-364.

Hermance, J.F. and Grillot, L.R., 1974

Contraints on temperatures below Iceland from magnetotelluric data. Phys.Earth Planet.Int. v.8, 1-12.

Hobbs, B.A., 1975

Analytic solutions to global and local problems of electromagnetic induction in the Earth. Phys.Earth Planet.Int. v.10, 250-261.

Hughes, T.J. and Rostoker, G., 1977

Current flow in the ionosphere during period of moderate activity. J.Geophys.Res. v.82, 2271-2282.

Hughes, T.J. and Rostoker, G., 1979

A comprehensive model current system for high-latitude magnetic activity - 1. The steady state system. Geophys.J.R.astr.Soc. v.58, 525-569.

Hutton, V.R.S., 1976

Induction studies in rifts and other active regions. Acta.-Geodaet.Geophys.Montanist., Hungary, Tomus 11(3-4), 347-376.

Hutton, V.R.S., Sik, J.M. and Gough, D.I., 1977a

Electrical conductivity and tectonics of Scotland. Nature v.266, 617-620.

Hutton, V.R.S., Sik, J., Jones, A.G. and Rooney, D., 1977b

The interpretation of geomagnetic variation observations in Scotland using the hypothetcal event technique. Abstract. Geophys.J.astr. Soc. v.49, 275.

Hutton, V.R.S. and Jones, A.G., 1978

Magnetovariational and magnetotelluric investigations in S. Scotland. J.Geomag.Geoelectr. (in press,1980).

Hutton, V.R.S., Dawes, G., Ingham, M., Kirkwood, S., Mbipom, E.W. and Sik, J., 1980

Recent studies of time variations of natural electromagnetic fields in Scotland. Phys.Earth Planet.Int. (in press).

Jenkins, G.M. and Watt, D.G., 1968

Spectral analysis and its applications. Holden-Day Inc., San Francisco.

Jones, A.G., 1977

Geomagnetic induction studies in Southern Scotland. PhD Thesis, University of Edinburgh.

Jones, A.G. and Hutton, V.R.S., 1979a

A multi-station magnetotelluric study in Southern Scotland - 1. Fieldwork, data analysis and results. Geophys. J.R.astr.-Soc. v.56, 329-349.

Jones, A.G. and Hutton, V.R.S., 1979b

A multi-station magnetotelluric study in Southern Scotland -

2. Monte-Carlo inversion of the data and its geophysical and tectonic implications. Geophys.J.R.astr.Soc. v.56, 351-368.

Jones, F.W., 1973

Induction in laterally non-uniform conductors : theory and numerical models. Phys.Earth Planet.Int. v.7, 282-293.

Jones, F.W. and Price, A.T., 1970

The perturbation of alternating geomagnetic fields by conducting anomalies. Geophys.J.R.astr.Soc. v.20, 317-334.

Jones, F.W. and Pascoe, L.J., 1971

A general computer program to determine the perturbation of alternating electric currents in a two-dimensional model of a region of uniform conductivity with an embedded inhomogeneity. Geophys.J.R.astr.Soc. v.24, 3-30.

Jones, F.W. and Pascoe, L.J., 1972

The perturbation of alternating geomagnetic fields by three-dimensional conductivity inhomogeneities. Geophys.J.R.astr.-Soc. v.27, 479-485.

Jones, F.W. and Vozoff, K., 1978

The calculation of magnetotelluric quantities for three-dimensional conductivity inhomogeneities. Geophys. v.43, 1167-1-175.

Kaikkonen, P., 1977

A finite element program package for electromagnetic modelling. J.Geophys. v.41, 179-192.

Kanasewich, E.R., 1973

Time sequence analysis in Geophysics. University of Alberta Press, Edmonton, Alberta, Canada.

Keller, G.V., 1971

Electrical properties of the Earth's crust- a survey of

literature. ONR Contract, Colorado School of Mines, Golden.

Keller, G.V. and Frischknecht, F.C., 1966

Electrical methods in geophysical prospecting. Pergamon Press, New York.

Kennedy, W.Q., 1946

The Great Glen Fault. Q.J.Geol.Soc., Lond., v.102, 41-76.

Kennedy, G.C. and Higgins, G.H., 1972

Melting temperatures in the Earth's mantle. In The Upper Mantle (ed. A.R. Ritsema), Tectonophys. v.13, 221-232.

Kisak, E. and Silvester, P., 1975

A finite element package for magnetotelluric modelling. Compt.Phys.Comm., v.10, 421-433.

Kisak, E. Silvester, P. and Telford, W.M., 1977

A recursive method in the E-polarisation of magnetotelluric modelling by high-order finite elements. Acta Geodaet.Geophys.Montanist., Hungary, Tomus 12(1-3), 255-266.

Kovtun, A.A., 1976

Induction studies in stable shield and platform areas. Acta Geodaet.Geophys. Montanist., Hungary, Tomus 11(3-4), 333—346.

Kurtz, R.D., 1973

A magnetotelluric investigation of Eastern Canada. PhD Thesis, University of Toronto, Canada.

Kurtz, R.D. and Garland G.D., 1976

Magnetotelluric measurements in Eastern Canada. Geophys.J.R-.astr.Soc. v.45, 321-347.

Law, L.K. and Riddihough, R.P., 1971

A geographical relation between geomagnetic variation anomalies and tectonics. Can.J.Earth Sci., v.8, 1094-1106.

Lines, L.R. and Jones, F.W., 1973

The perturbation of alternating geomagnetic fields by three-dimensional island structures. Geophys.J.R.astr.Soc. v.32, 133-154.

Losecke, W. and Muller, W., 1975

Two-dimensional magnetotelluric model calculations for overhanging, high-resistivity structures. Zeitschrift fur Geophysik v.41, 311-319.

Madden, T. and Nelson, P., 1964

A defence of Cagniard's magnetotelluric method. Geophys.Lab. ONR Proj. NR-371-401, M.I.T., Cambridge, Mass.

Nienaber, W., Dosso, H.W., Law, L.K., Jones, F.W. and Ramaswamy, V., 1979

An analogue model study of electromagnetic induction in the Vancouver Island Region. J.Geomag.Geoelectr. v.31, 115-132.

Orr, D., 1973

Magnetic pulsations within the magnetosphere - A review. J. Atmos.Terr.Phys. v.35, 1-50.

Orr, D. and Webb, D.C., 1975

Statistical study of geomagnetic pulsations with periods between 10 and 70s and their relationship to the plasmapause region. Planet.Space Sci. v.23, 1169-1178.

Osememikan, J.E.A. and Everett, J.E., 1968

Anomalous magnetic variations in southwestern Scotland. Geophys.J.R.astr.Soc. v.15, 361-366.

Oxburgh, E.R., Richardson,S.W.,Wright, S.M., Jones, M.Q.W., Penny, S.R., Watson, S.A. and Bloomer, J.R., 1980

Heat flow pattern of the United Kingdom.

Second International Seminar on the Results of E.C. Geothe-

rmal Energy Research, Strassbourg, 149-152.

Parkinson, W.D., 1959

Directions of geomagnetic fluctuations, Geophys.J.R.astr.-Soc. v.2, 1-14.

Parkinson, W.D.,1962

The influence of continents and oceans on geomagnetic variations. Geophys.J.R.astr.Soc. v.6, 441-449.

Peeples, W.J. and Rankin, D., 1973

A magnetotelluric study in the western Canadian sedimentary basin. Pure Appl. Geophys. v.102, 134-147.

Peltier, W.R. and Hermance, J.F. 1971

Magnetotelluric fields of a Gaussian electrojet. Can.J.Earth Sci. v.8, 338-346.

Phillips, W.E.A., Stillman, C.J. and Murphy, T., 1976

A Caledonian plate tectonic model. J.Geol.Soc.Lond. v.132, 579-609.

Praus, O., 1975

Numerical and analogue modelling of induction effects in laterally non-uniform conductors. Phys.Earth Planet.Int. v.10, 262-270.

Praus, O., 1976

Numerical solutions of the magnetotelluric field in inhomogeneous structures. In Geoelectric and Geothermal Studies, K.A.P.G. Geophysical Monograph (ed. A. Adam), Hungary, 231-244.

Price, A.T., 1949

The induction of electric currents in non-uniform thin sheets and shells. Quart.J.Mech.Appl. Math. v.2, 283-310.

Price, A.T., 1962

The theory of magnetotelluric fields when the source field is considered. J.Geophys.Res. v.67, 1907-1918.

Pugh, D.T., 1977

Geothermal gradients in the British lake sediments. Limnol. and Oceanogr. v.22, 581-596.

Raiche, A.P. 1974

An integral equation approach to three-dimensional modelling. Geophys.J.R.astr.Soc. v.36, 363-376.

Rankin, D. and Reddy, I.K. 1969

A magnetotelluric study resisitivity anisotropy. Geophysics v.34, 438-449.

Ranganayaki, R.P. and Madden, T.R., 1980

Generalised thin sheet analysis in magnetotellurics : an extension of Price's analysis. Geophys.J.R.astr.Soc. v.60, 445-457.

Read, H.H. and Watson, J. 1975

Introduction to Geology Vol.2, Partl - Early Stages of Earth History.

Reddy, I.K. and Rankin, D. 1973

Magnetotelluric response of a two-dimensional sloping contact by finite element method. Pure Appl.Geophys. v.105, 847-857.

Reddy, I.K., Phillips,R.J., Whitcombe, J.H., Cole, D.M. and Taylor, R.A. 1976

Monitoring of time-dependent electrical resistivity by magnetotellurics. J.Geomag.Geoelectr. v.28, 165-178.

Ringwood, A.E., 1969

Composition and evolution of the upper mantle. In The Earth's Crust and Upper Mantle (ed. P.J. Hart) A.G.U. v.13, 1-17.

Robinson, B., 1977

Electromagnetic induction in the seas around the Orkney Islands. Acta Geodaet.Geophys.Montanist., Hungary, Tomus 11(1-3), 191-194.

Rooney, D. 1976

Magnetotelluric measurements across the Kenyan Rift Valley. PhD Thesis, University of Edinburgh.

Rooney, D. and Hutton, V.R.S., 1977

Magnetotelluric and magnetovariational study of the Gregory Rift Valley. Geophys.J.R.astr.Soc. v.51, 91-119.

Rostoker, G. and Hughes, J.T., 1979

A comprehensive model current system for high-latitude magnetic activity - 2. The substorm component. Geophys.J.R.astr.Soc. v.58, 571-581.

Schmucker, U., 1964

Anomalies of geomagnetic variations in the South-western United States. J.Geomag.Geoelectr. v.15, 193-221.

Schmucker, U., 1970

Anomalies of geomagnetic variations in the South-western United States. Bull.Scripps Inst.Ocean., Univ. of Calif., San Diego, v.13, 165pp.

Sik, J. and Hutton, V.R.S., 1977

A magnetometer array study in Scotland. Acta Geodaet.Geophys-.Montanist., Hungary, Tomus 11(1-3), 139-143.

Singh, B.P., 1978

Geomagnetic sounding of conductivity anomalies in the lower crust and uppermost mantle. Review paper, The Fourth Workshop on EM Induction in the Earth and Moon, Murnau, FRG.

Stanley, W.D., Boehl, J.E., Bostick, F.M. and Smith, H.W., 1977

Geothermal significance of magnetotelluric sounding in the

Eastern Snake River Plain - Yellowstone Region. J.Geophys.-Res. v.82, 2501-2514.

Stegena, L., 1977

Electrical conductivity structure and geothermal reservoirs. Acta Geodaet.Geophys.Montanist., Hungary, Tomus 11(3-4), 377-397.

Sternberg, B.K., 1979

Electrical resistivity structure of the crust in the Southern Extension of the Canadian Shield - Layered Earth models. J.Geophys.Res. v.84, 212-228.

Strangway, D.W. and Koziar, A., 1979

Audio-frequency magnetotelluric sounding - a case history at the Cavendish Geophysical Test Range. Geophysics v.44, 1429-1446.

Srivastava, S.P., 1965

Method of interpretation of magnetotelluric data when source field is considered. J.Geophys.Res. v.70, 945-954.

Srivastava, S.P., 1967

Magnetotelluric two- and three-layer master curves. Dom.Obs-.Publ. v.35, No.7, Canada Dept. of Energy, Ottawa.

Stuart, W.F., 1979

On the arrival of the initial movements of Pi2s at conjugate stations. J.Atmos.Terr.Phys. v.41, 1223-1232.

Summers, D.McN., 1976

The inversion of geomagnetic data. PhD Thesis, University of Edinburgh.

Swift, C.M., 1967

A magnetotelluric investigation of an electrical conductivity anomaly in the South-western United States. PhD Thesis,

Dept. of Geol.and Geophys., M.I.T., Cambridge, Mass.

Tikhonov, A.V., 1950

Determination of the electrical characteristics of the deep strata of the Earth's crust. Dokl.Akad.Nauk., U.S.S.R., v.73, 295-297.

Trigg, D.F., 1972

An amplifier ad filter system for telluric signals. Publ. Earth Phys.Branch, Canada, v.41, 66.

Valiant, M.J., 1976

N.E.R.C. Geologger technical handbook, I.G.S., Magnetic Observatory, Hartland.

Van Zijl, J.S.V. and Joubert, S.J., 1975

A crustal geoelectric model for South African Precambrian granitic terrains based on deep Schlumberger soundings. Geophysics v.40, 657-663.

Vasseur, G., Babour, K., Menvielle, M. and Rossignol, J.C., 1977

The geomagnetic variation anomaly in the northern Pyrenees : study of the temporal variation. Geophys.J.R.astr.Soc. v.49, 593-607.

Vasseur, G. and Weidelt, P., 1977

Bimodal electromagnetic induction in non-uniform thin sheets with an application to the northern Pyrenean induction anomaly. Geophys.J.R.astr.Soc. v.51, 669-690.

Wait, J.R., 1954

On the relationship between telluric currents and the Earth's magnetic field. Geophysics v.19, 281-289.

Wait, J.R., 1962

Theory of magnetotelluric fields. J.Res., N.B.S., v.66D,

No.5, 509-541.

Watson, J., 1978

The basement of the Caledonide Orogen in Britain. In Caledonian-Appalachian Orogen of the North Atlantic Region. Geol.-Surv. Canada, Paper 78-13, 75-77.

Weaver, J.T., 1979

Electromagnetic induction in the thin sheet conductivity anomalies at the surface of the Earth. Proc.I.E.E. v.67, 1044-1050.

Weidelt, P., 1972

The inverse problem of geomagnetic induction. Zeitschrift fur Geophysik, v.38, 257-289.

Weidelt, P., 1975

Electromagnetic induction in three-dimensional structures. J.Geophys. v.41, 85-109.

Wilson, J.T., 1966

Did the Atlantic close and then re-open ? Nature v.211, 676-681.

Williamson, K., Hawlett, C. and Tammemagi, H.Y., 1974

Computer modelling of electrical conductivity structures. Geophys.J.R.astr.Soc. v.37, 533-536.

Word, D.R., Smith, H.W. and Bostick, F.W., 1970

An investigation of the magnetotelluric tensor impedance method. Tech. Report No.82, Elec. Geophys. Lab., University of Texas at Austin, U.S.A.

Wright, J.A., 1969

The electromagnetic response of two-dimensional structures. Gamma, 7, Inst. Geophysik Meteorologie, Tech. Univ., Braunschweig.

Wright, J.A., 1970

Anisotropic apparent resistivities arising from non-homogeneous two-dimensional structures. Can.J.Earth Sci. v.7, 517-531.

Wyllie, P.J., 1971

A discussion of water in the crust. A.G.U. Monogr. v.14, 257-260.

Yungul, S.H., 1961

Magnetotelluric sounding three-layer interpretation curves. Geophysics v.26, 465-473.

Zablocki, C.I., 1964

Electrical properties of serpentinite from Mayaguez, Puerto Rico - a study of serpentinite, Washington, 1964.